Immobilization of Diastase α-amylase on to synthetic and natural polymers

Thesis submitted to

Cochin University of Science and Technology

in partial fulfilment of the requirements for

the award of the degree of

Doctor of Philosophy

in

Chemistry

Under the Faculty of Science

by

Navya Antony

Under the Supervision of

Dr. P. V. Mohanan

DEPARTMENT OF APPLIED CHEMISTRY

COCHIN UNIVERSITY OF SCIENCE AND TECHNOLOGY

KOCHI – 682022

March 2014

Department of Applied Chemistry
Cochin University of Science and Technology
Kochi – 682022

Certificate

*This is to certify that the thesis entitled "**Immobilization of diastase α–amylase on to synthetic and natural polymers**" submitted for the award of the Degree of Doctor of Philosophy of the Cochin University of Science and Technology, is a record of original research work carried out by **Mrs. Navya Antony** under my supervision and guidance in the Department of Applied Chemistry and further that it has not formed the part of any other thesis previously.*

Kochi – 22
25-03-2014

Dr. P.V. Mohanan
Assistant Professor
Department of Applied Chemistry
Cochin University of Science and Technology
Kochi – 682 022

Declaration

*I hereby declare that the thesis entitled "**Immobilization of diastase α – amylase on to synthetic and natural polymers**" submitted for the award of Ph.D. Degree of the Cochin University of Science and Technology, is based on original research work done by me under the guidance of Dr. P.V. Mohanan, Assistant Professor, Department of Applied Chemistry, Cochin University of Science and Technology and further that it has not previously formed the basis for the award of any other degree.*

Kochi – 22
25-03-2014

Navya Antony

Acknowledgement .....

"Sometimes our light goes out but is blown into flame by another human being. Each of us owes deepest thanks to those who have rekindled this light."

Albert Schweitzer

First and foremost, I would like to thank God, who is the greatest teacher of all.

This thesis has been kept on track and been seen through to completion with the support and encouragement of numerous people. On the completion of my thesis, it is a pleasant task to express my sincere gratitude and appreciation to all those who contributed in many ways to the success of this study and made it an unforgettable experience for me. It will remain as one of the most cherished moments in my life.

At this moment of accomplishment, my first debt of heart-felt gratitude must go to my supervising guide Dr. P.V. Mohanan for introducing me to this exciting field of science. I have been fortunate to have an advisor who gave me the freedom to explore on my own, and at the same time provided me the guidance to recover when my steps faltered. His patience and support helped me to overcome many crisis situations and finish this thesis work. I am also thankful to him for carefully reading and commenting on countless revisions of this manuscript. Throughout my thesis-writing period, he provided encouragement, sound advice, and lots of good ideas.

I express my deepest gratitude to Dr. N. Manoj, Head of the department of Applied Chemistry, for all the support and also for providing all the facilities needed for completion of my thesis.

I express my sincere thanks to Dr. K. Girish Kumar, my doctoral committee member and former H.O.D, Applied Chemistry; for all his support and encouragement during my research work. I really enjoyed doing the departmental activities under his guidance. He is really a wonderful model in the role of a teacher who makes learning an enlightening experience.

I am also truly grateful to Dr. K. Sreekumar, former H.O.D, Applied Chemistry for his valuable suggestions and clearing many of my doubts regarding the work. His constant support and guidance during the course of my Ph.D and enabling me to overcome the hurdles encountered thereof, will be always remembered with gratitude.

I extend my immense thanks to all faculty members, administrative staff and librarians who were always ready to give their timely help whenever required.

My special regards to my teachers because of whose teaching at different stages of education has made it possible for me to reach this pinnacle where I could complete this thesis successfully.

I am extremely indebted to Dr. S. Velmathi, Associate Professor, Dept of Chemistry, NIT, Trichy for providing permission to carry out BET analysis at their institution. I express my gratitude to Sanjini for spending her precious time, in midst of her hectic work schedule, for carrying out my analysis. I also extend my special thanks to Seles Sebastian for his constant support and help for carrying out several analyses.

I take this opportunity to thank Shibu Eapen, Adarsh, Melbin and Saji of SAIF, STIC, CUSAT for the technical help extended in carrying out several analyses.

I gratefully acknowledge CUSAT and UGC-BSR for providing me financial support.

The cheerful moments shared with Gibi, Smitha, Sinija, Soumya, Anjali, Sherly Miss, Divya, Teresa, Leena, Litha, Mahesh, Anoop, Rajesh and all my friends in other labs are unforgettable and etched forever in my memory. I would like to extend my special thanks to my senior Ashly for many comments and advices. I would also like to extend my thanks to all my labmates; Priya, Divya, Remya, Jessica, Shanty, Sneha, Bindhu and Maria for their love and companionship.

I would like to express my heartfelt gratitude to my parents-in-law for their unfailing emotional support. Words cannot express how grateful I am to you both for all of the sacrifices that you have made on my behalf. Your prayers for me was what sustained me this far. I also thank for the heart-warming kindness, support and care from my brother's -in-law, Mr. Saju Jos, Dr. Sajeev Jos and their family.

It is hard for me to find words to express my gratitude to my parents. I express my profound gratitude to you both, for your constant and unwavering support, timely encouragement and endless patience. I am also grateful to my sister Nidhi for her emotional support during my work and for the love and care shown to my kids. I also thank my sister Niji and her family for giving the motivation to complete my thesis work soon.

Last but not the least; I am greatly indebted to my husband Sanu Jos. He was always around at times I thought that it is impossible to continue, and helped me to keep things in perspective. Words are inadequate when I wish to express my appreciation towards him without whose constant support I could not have completed my research work successfully. He was always ready to face any difficulties for the completion of my Ph. D work. I remember with gratitude the hours he spent in helping me in computers, for his university visits etc., in spite of all the domestic affairs. He is certainly the main contributor of all the best in my life for the last seven years; I thank God for giving him as my husband, friend and companion. He has seen me through the ups and downs of the entire Ph.D and has shared this entire amazing journey with me, so it only seems right that I dedicate this thesis to him.

I owe very much to my dear son shaan and my sweet daughter shreya for the bundle of joy they gave me, which helped me in draining out all the stress related to my research work.

Finally, once again my greatest regards to the Almighty for bestowing upon me the courage to face the complexities of life and complete this thesis successfully.

Thank You

Navya Antony

Preface

Emerging community concerns and growing environmental awareness throughout the world has forced the researchers to synthesize new green materials and processes that enhance the environmental quality of products. In this perspective biocatalysis has now become a central part of green chemistry. The use of enzymes can easily turn a chemical process green, as enzymes are nature's catalysts. They are present in every living organism and are designed to accelerate specific reactions taking place in cell and its immediate surroundings without itself undergoing any change. They have been widely accepted in diverse sectors owing to their high selectivity, ability to operate under mild conditions and green chemistry.

However for large extent of commercialization of these bio-derived catalysts, recovery yield, costs and reusability factor becomes mandatory, failing which hamper their use in industrial processes. Thus there is an increased demand among world's biotechnological industries to enhance enzyme productivity by developing novel techniques for increasing their shelf life. These requirements are inevitable to facilitate large-scale and economic formulation.

Enzyme immobilization provides an excellent base for increasing availability of enzyme to the substrate with greater turnover over a considerable period of time. Nowadays, immobilized enzymes are preferred over their free counterpart due to their prolonged availability that curtails redundant downstream and purification processes. Immobilization generates continuous economic operations, automation, high investment/capacity ratio and recovery of product with greater purity. Immobilized enzymes have biomedical and industrial applications and for this reason, this area has continued to develop into an ever-expanding and multidisciplinary field during the last couple of decades. The success of the vast usage of immobilized enzymes lies in the fact

that they prove to be environmental friendly, cheaper and easy to use when compared to other parallel technologies.

Several natural and synthetic supports have been assessed for their efficiency for enzyme immobilization. Synthetic polymer materials are prepared by chemical polymerization using various monomers. As a kind of important carrier, synthetic polymer materials exhibit the advantages of good mechanical rigidity, high specific surface area, inertness to microbial attack, easy to change their surface characteristics, and their potential for bringing specific functional group according to actual needs. Hence, they have been widely investigated and used for enzyme immobilization.

When it comes to the natural polymer materials, much attention has been paid to cellulose and other natural polymer materials owing to their wide range of sources, easy modification, nontoxic, and pollution-free, with a possibility of introducing wide variety of functional groups and good biocompatible properties.

In our work, we report the use of synthetic polymer, polypyrrole and its derivatives and natural polymers coconut fiber and sugarcane bagasse as supports for Diastase α- amylase immobilization. An attempt was also made to functionalize both synthetic and natural polymers using Amino-propyl triethoxysilane. Supports and their immobilized forms were characterized via FT-IR, TG, SEM, XRD, BET and EDS techniques. Immobilization parameters were also optimized so as to prepare stable immobilized biocatalyst for starch hydrolysis.

Thesis is divided into five chapters

Chapter 1: Biocatalysis- relevance and applications

This chapter gives a brief overview about biocatalysis, importance of enzymes as biocatalyst, need for enzyme immobilization, different immobilization methods available, advantages and disadvantages of immobilization of enzymes, different

supports available etc. The supports and methods adopted for our study are also depicted here in nutshell. Finally objectives of the present study are also summarized towards the end of the chapter.

Chapter 2: Experimental techniques

In this chapter steps adopted to prepare immobilized enzymes were discussed. The methods adopted to determine the activity of α- amylase is also described. In addition to these topics general discussions about biochemical and physico-chemical characterization have also been carried out.

Chapter 3: Immobilization of Diastase α- amylase on to synthetic polymers

This chapter deals with immobilization studies of diastase α- amylase on to polypyrrole and its derivatives. Synthesis procedures adopted for the preparation of polymeric supports and its characterization via FT-IR spectroscopy, TG, BET and SEM analysis were also explained in detail.

Chapter 4: Immobilization of Diastase α-amylase on to natural polymers

Use of natural fibers from coconut and sugarcane bagasse as support for immobilization of diastase α- amylase has been depicted in this chapter. Evidences supporting the functionalization and immobilization of enzyme on to these supports were also given based on the FT-IR, TG, SEM, EDS and XRD analysis.

Chapter 5: Summary and Conclusions.

This chapter presents the summary and important findings of the work done.

References are given at the end of each chapter.

Contents

Chapter 1

Biocatalysis-Relevance and Application

Contents

1.1 Biocatalysis

In conventional chemical processes, catalysis comes to the lime light as it sculpts the chemical precursors into precise molecular shapes by lowering the activation energy without itself undergoing any transformation. An ideal catalyst should have all the desirable features like high turnover number, cost-effectiveness, chemo-selectivity, stereo-selectivity, regio-selectivity, good stability, sustainable productivity, non-toxicity, bio-degradability or eco-friendliness and must be broadly useful [1].

Conventional catalysts which have many advantages do not possess all the qualities of an ideal catalyst. Most of them, being quite toxic, may require special handling or inert atmospheres. And, depending on the further use of the product, some catalysts may not be able to be used. A catalyst that is suitable for a particular reaction may not be suitable if that reaction is used to make a drug for people, as catalyst-derived impurities may be toxic. Removing them from the products is quite difficult. And here comes the importance of bio-catalysis.

Bio-catalysis is a fascinating and challenging field in the current global arena where there is more demand for the applications that have biological impact

and is of great importance in chemical and pharmaceutical industries. It can be defined as the use of natural substances, which vary in complexity from single enzyme to whole cells, to promote the inter-conversion of chemical species by speeding up the chemical reaction.

Enzymes have been naturally tailored to perform under physiological conditions. However, bio-catalysis refers to use of "enzymes as process catalysts under artificial conditions (in vitro), so that a major challenge in bio-catalysis is to transform these physiological catalysts into process catalysts which are able to perform under the usually tough reaction conditions of an industrial process"[2]. They differ from conventional processes not only by featuring a different type of catalyst but also constitute a new technology base [3].

Modern bio-catalysis is developing new and precise tools to achieve green chemistry goals and to improve wide range of production processes through short process routes which thus reduces costs and generates less waste and toxic side products and thereby reduces the environmental footprints. It also offers increased selectivity, lower temperature and pressure and complete renewability so that it may not pose any harm to humans and animals and is emerging as a boon to sustainable environment. Biocatalysts are being used extensively in the industrial production of bulk chemicals, pharmaceuticals, medical diagnostics [4,5], agro chemical products, cosmetic applications [6,7] and food ingredients [8].

1.1.1 Enzymes, Nature's catalysts

Enzymes are proteins, sometimes with prosthetic groups, sugars or lipids bound to them. They are biodegradable and can meet all requirements of an ideal catalyst. They have high turnover numbers and when produced efficiently by modern genetic engineering methods, enzymes are highly cost effective. They are catalytically active in presence of water as well as various organic solvents. As selective catalysts, both chemo selective and stereo selective, enzymes are often

unequalled. Their extreme specificity and activity under moderate conditions are also widely appreciated by different production sectors [9-12].

1.1.2 Enzyme Structure

Enzymes were called as catalysts by the Swedish chemist Berzelius. The simplest enzymes are proteins of molecular weight ranging from 10,000 to 40,000, whereas, others are very large molecules with molecular weights of 150,000 to 2 million.

At physiological pH, the protein's positive charge are due to the amino-acid residues lysine and arginine and to a lesser degree, histidine, whereas, negative charges are due to glutamic acid and aspartic acid residues. When the pH is acidic, glutamic acid and aspartic acid residues have little charges while lysine and arginine have stronger positive charges. However, when the pH of the protein solution is raised, the converse occurs. Glutamic and aspartic acids both release a proton each and turn negatively charged while lysine and arginine residues tend toward the uncharged. The above descriptions are illustrated in the figure: 1.1 [13].

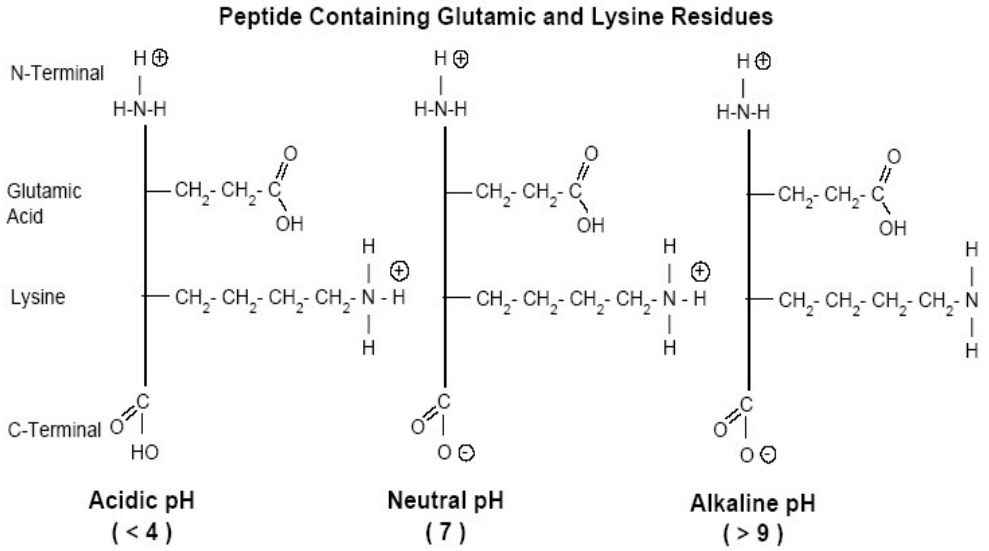

Figure: 1.1 Structure of Amino Acids at Different pH [13]

To a very considerable extent the conformation assumed by an enzyme protein and the stabilization of its structure is the result of competition and co-operation of various factors [14]. The interaction of the amino acid via their close proximity to one another in the primary structure creates the secondary structure.

In order for a protein to exert specific enzymatic action at least some regions in each polypeptide chain must have a certain typical spatial conformation. This feature is responsible for the enzyme's characteristic form and activity. This spatial structure assumed by an enzyme as a result of interaction between the amino acid side chains too far from one another in the primary structure is termed the tertiary structure. It is stabilized partly by disulphide bridges that form between cysteine residues of near lying portions of the chain. Some enzymes consist of several, often two or four, identical or different polypeptide sub-chains spatially arranged to give a specific structure called quaternary structure [15,16]. Such a structure is held together by non-covalent bonds, particularly ionic bridges, hydrogen bonds, or hydrophobic interactions. All these structures are depicted in the figure: 1.2.

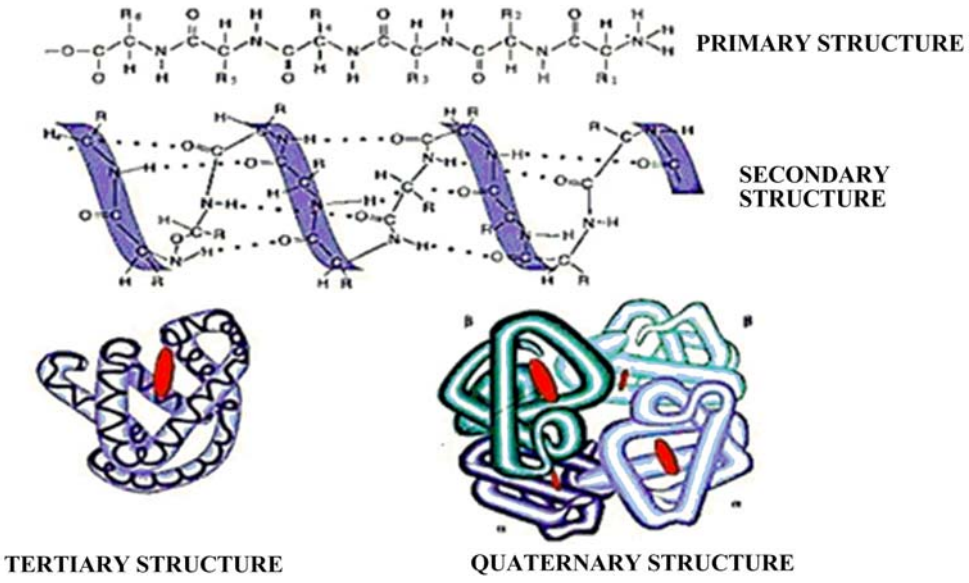

Figure: 1.2 Structure of protein

In a certain region of enzyme the amino-acids are arranged in a specific sequence and spatial conformation that are responsible for the catalytic function. This region is known as active site or catalytic center. Enzymes are distinguished from each other by this geometric area into which will fit only one or a very limited number of compounds called substrates. It is in the active site where catalysis actually occurs. Many enzymes require the presence of a metal ion, or a co-enzyme (co-factor), in order to be active catalysts.

1.1.3 Classification of enzymes and their applications

Enzymes are classified according to the guidelines of the Nomenclature Committee of the International Union of Biochemistry and Molecular Biology (IUBMB) (Anonymous 1984) into six families, based on the type of chemical reaction catalyzed. A four digit number is assigned to each enzyme by the Enzyme Commission (EC) of the IUBMB: the first one denotes the family, the second denotes the subclass within a family and is related to the type of chemical group upon which it acts, the third denotes a subgroup within a subclass and is related to the particular chemical groups involved in the reaction and the forth is the correlative number of identification within a subgroup.

The six families are: Oxidoreductases which catalyze redox reactions, Transferases which catalyze transfer of groups such as methylenes or phosphates, Hydrolases which catalyze hydrolysis, Lyases which catalyze the addition of groups to double bonds or vice versa, Isomerases which catalyze molecular isomerization, Ligases which catalyses synthesis reactions involving families of enzymes.

Among these classes, hydrolases have had technological significance. The reason underlying is that these enzymes are well endowed to perform as biocatalysts since they are robust, rather simple proteins not requiring coenzymes, many of them being extracellular. Production is, therefore, rather simple, enzyme costs are low and they perform well under harsh process conditions.

Industrial applications represent more than 80% of the global market of enzymes. Food enzymes are by far the most widely used [17,18]. Beyond industrial applications, there is an ever-increasing use of enzymes in other fields, like chemical and clinical analysis, biomedicine and research [19-22].

1.1.4 Enzyme catalysis

In 1860 Emil Fischer postulated the mechanism by which the active site takes part in the reaction of an enzyme and its substrate. In fact the molecular structure serves two functions: Firstly the substrate molecule of interest gets adsorbed on to the complementary surface of the enzyme, and secondly catalytic action occurs, converting substrate to product which is then released back to solution leaving the enzyme catalyst unaltered. This process has been described as similar to the fitting of a key into a lock, the active site of the enzyme forming a lock specific for only one substrate. During this conversion of substrate to product, there is an intermediate stage where substrate and enzyme forms a complex. This complex enters a transition state in which the activation energy for the specific reaction is significantly lower compared to that in the free state. Thus reaction proceeds more rapidly, provided they are energetically feasible. Even though recent reports provide evidence in favour of this theory [23], this rigid model hardly explains many experimental evidences of enzyme biocatalysis.

Later on, the induced-fit theory was proposed [24] according to which the substrate induces a change in the enzyme conformation after binding that may orient the catalytic groups in a way prone for the subsequent reaction; this theory has been extensively used to explain enzyme catalysis [25].

Based on the transition-state theory, enzyme catalysis has been explained according to the hypothesis of enzyme transition state complementariness, which considers the preferential binding of the transition state rather than the substrate or product [26]. The reaction profile showing trend of uncatalyzed and enzyme catalyzed reaction is shown in the figure: 1.3.

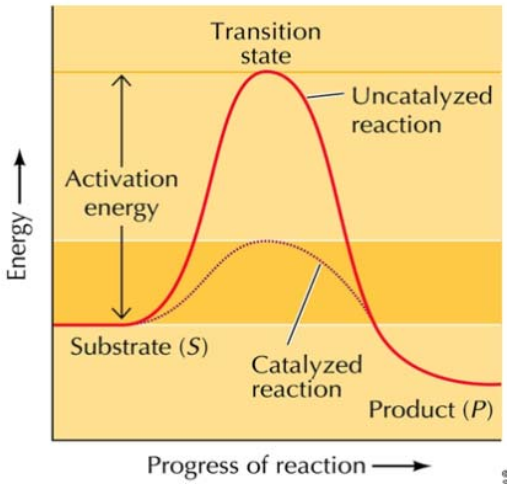

Figure: 1.3: Reaction Profile: uncatalyzed and enzyme catalyzed

1.1.5 Enzyme kinetics

Enzyme kinetics refers to the quantitative analysis of all factors that determine the catalytic potential of an enzyme. Knowledge of enzyme kinetics is important because it is necessary for the understanding of the analytical aspects of enzyme behaviour, formulation of molecular models for enzyme action, and also for technological reasons, it allows the formulation of kinetic models for the design and evaluation of reactor performance [27]. It is also a powerful tool for the understanding of properties of enzymes and the mechanism of enzyme action.

The basic equations for enzyme kinetics were developed by Michaelis and Menten. According to the mechanism:

$$E + S \underset{k_{-1}}{\overset{k1}{\rightleftharpoons}} ES \xrightarrow{k_2} E + P \qquad 1.1$$

Substrate S combines with the enzyme E to form an enzyme-substrate complex ES which breaks down into product P and liberates the enzyme. The constants k_1, k_{-1} and k_2 are the rate constants for the reaction in the direction

indicated by the associated arrow. This kinetics of a simple enzyme reaction can be better explained by the equation attributed to Michaelis-Menten where velocity of the reaction V at a particular substrate concentration S is given by

$$V = \frac{Vmax\ [S]}{K_m + [S]} \qquad 1.2$$

Where V_{max} is the maximum rate at which the reaction proceeds at the infinite substrate levels. It measures the maximum catalytic potential of the enzyme, while K_m is a constant which is normally seen as substrate concentration needed to give a reaction rate of half V_{max}. It provides a measure of the affinity of the enzyme active site for its substrate. K_m, the Michaelis constant and V_{max} are the two most important parameters used to characterize the kinetic properties of the enzyme.

From the Michaelis -Menten plot it was pointed out that when [S] is very much greater than the dissociation constant for the enzyme- substrate complex, the enzyme becomes saturated with the substrate. V is the maximum velocity and is independent of substrate concentration. Such a reaction is having zero order, since the rate is proportional to the zeroeth power of the substrate concentration. This means adding more substrate to the solution will not increase the rate of the reaction. The other extreme form occur when [S] is very much less than K_m. Since the rate of the reaction under these conditions is directly proportional to the substrate concentration raised to the first power, the reaction is the first-order in substrate. In the region between zero order and first order the complete equation is required and the reaction order is mixed. However, it is difficult to measure V_{max} at higher substrate concentration since the graph tails off. The measurement then obtained introduces considerable error of judgment on both the values of V_{max} and K_m. Hence chemists prefer to plot data in such a way that the points lie on a straight line.

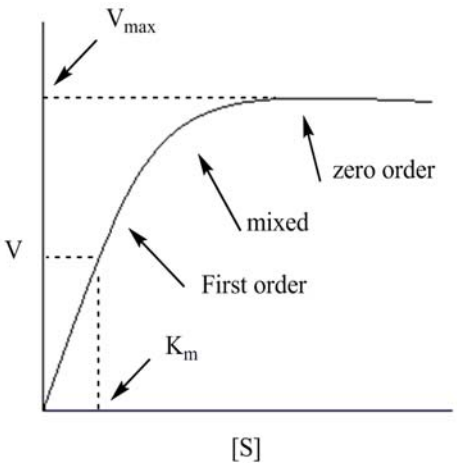

Figure: 1.4 Graphical representation of velocity against substrate concentration in an enzyme catalyzed reaction.

It is pointed out by Lineweaver and Burk in 1934 that taking reciprocals of both sides of linear equation can solve the problem. Thus the most widely used linear transformation of the Michaelis-Menten equation is the Lineweaver-Burk equation.

$$\frac{1}{V} = \frac{K_m}{V_{max}} \frac{1}{[S]} + \frac{1}{V_{max}} \qquad 1.3$$

A plot of 1/v versus 1/S is a straight line with a slope of K_m/V and intercept of 1/V on the 1/V axis $-1/K_m$ on the 1/S axis as shown in the figure: 1.5.

The Hanes-Woolf plot is also a graphical representation of enzyme kinetics in which the ratio of the initial substrate concentration [S] to the reaction velocity V is plotted against [S].The equation was obtained by rearranging the Michaelis-Menten equation.

$$\frac{[S]}{V} = [S] \frac{1}{V_{max}} + \frac{K_m}{V_{max}} \qquad 1.4$$

From the equation it is clear that perfect data will yield a straight line of slope $1/V_{max}$, a y-intercept of K_m/V_{max} and an x-intercept of -Km.

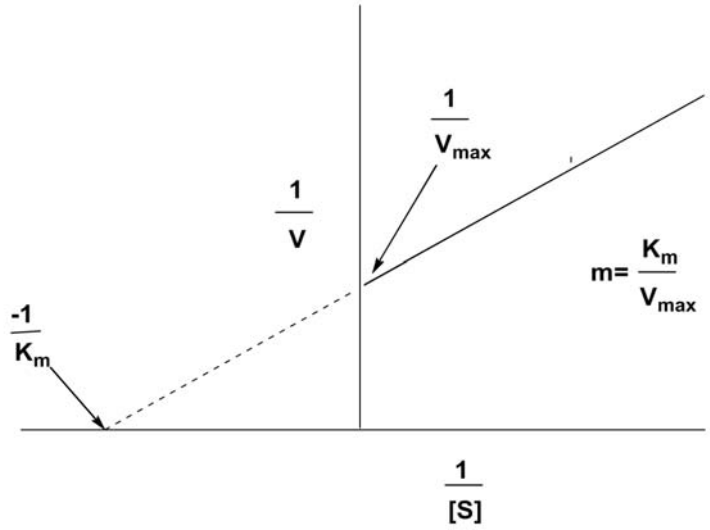

Figure: 1.5: Lineweaver - Burk plot for determination of substrate kinetic constants

The method of Hanes (Hanes 1932) and Eaddie-Hofstee (Hofstee 1959) have been the most used alternatives.

1.2 Enzyme immobilization

The term 'immobilized enzyme' was adopted at the first Enzyme Engineering Conference, held at Henniker New Hampshire, in 1971. Immobilized enzymes are defined as biocatalysts that are restrained or localized in a microenvironment yet retain their catalytic properties for a much longer time than the free enzyme and can be used continuously for many analyses [28]. It thus improves the handling properties of the catalyst and thus enhances the efficiency with which it is used in bioconversions. This technology unites the disciplines of chemistry, biochemistry and cell biology on one hand with biochemical and process engineering on the other [29].

Immobilization is the application of heterogeneous catalysis to biological systems. At first glance, the practical development of protocols for immobilization

of enzymes is intimately related to simplicity, cost-effectiveness, and stabilization of enzymes. Moreover, if properly designed, immobilization may also improve enzyme properties as substrate specificity and selectivity and the effect of inhibitors can be reduced.

The ideal immobilization procedure for a given enzyme is one which permits a high turnover rate of the enzyme yet also retains a high catalytic activity over time. However, regardless of its nature or preparation, an immobilized enzyme, by definition, has to perform two essential functions: namely, the non-catalytic functions (NCFs) that are designed to aid separation (e.g. isolation of catalysts from the application environment, reuse of the catalysts and particularly control of the process); and the catalytic functions (CFs) that are designed to convert the targeting compounds (or substrates) within a desired time and space [30]. As a result, an immobilized enzyme can be labeled as 'robust', when both the catalytic and the non-catalytic functions can meet the requirements of a specific application.

1.2.1 Need for immobilization

For the industrial production of sugars, amino acids and pharmaceuticals immobilized enzymes are highly economical [31]. Besides industrial application immobilized enzymes are widely used in synthesis of number of biotechnological products with applications in diagnostics, biosensors etc. [32,33]. Thus in order to extend the use of immobilized enzymes to other fields of science, development of new methodologies and a better understanding of current techniques are inevitable.

1.2.2 Choice of support

The characteristics of the matrix are of paramount importance in determining the performance of the immobilized enzyme system. The support material can have a critical effect on the stability of the enzyme and the efficiency

of enzyme immobilization, although it is difficult to predict in advance which support will be most suitable for a particular enzyme.

Ideal support properties include physical resistance to compression, hydrophilicity, inertness toward enzymes, ease of derivatization, biocompatibility, high surface area, resistance to microbial attack, and availability at low cost [34-36].

Supports can be classified as inorganic and organic according to their chemical composition. The organic supports can be subdivided into natural and synthetic polymers [37]. In spite of many advantages of inorganic carriers (e.g., high stability against physical, chemical, and microbial degradation), most of the industrial applications are performed with organic matrices.

There is also a trend toward the utilization of polymer based supports. These are known to be more stable under alkaline conditions, resulting in reduced band broadening effects compared with silica and glass phases. The versatile chemical compositions and physical properties coupled with widely available structural forms of polymers have made them excellent candidates as supports for enzyme immobilization.

Natural polymers including polysaccharides (cellulose, cellulose derivatives, dextran and chitosan) as well as synthetic polymers, such as polystyrene and polyacrylates, polypyrrole, polyaniline, polytoluidine etc. have been studied to immobilize enzymes [38]. With most polymers, the major barrier is the lack of highly reactive functional groups on the surfaces for direct covalent bonding. Often, surface modifications are needed to fulfill this particular task.

Due to the often conflicting requirements of a good support, various materials have been used. At present there is no universally recommended support, the final choice being a compromise for each particular enzyme and experimental system.

1.2.3 Methods of enzyme immobilization

The enzymes can be attached to the support via interactions ranging from reversible physical adsorption and ionic linkages to stable covalent bonds. One way of classifying the various approaches to immobilizing enzymes is in two broad categories: irreversible and reversible methods [39].

The strength of the binding is usually inversely related to the ease with which it can be reversed. These two conflicting objectives-stability and reversibility-are difficult to fulfill simultaneously. The main task is to select a suitable carrier (defined as the non-catalytic part of an immobilized enzyme, on which the catalytic part is constructed), condition (pH, temperature, and nature of medium) and enzyme itself (source, nature and purity) to design an immobilized biocatalyst.

The stability of an immobilized enzyme is dictated by many factors such as the number of bonds formed between the enzyme and carrier, the nature of the bonds, the degree of confinement of enzyme molecules in the carrier, the microenvironment of the enzyme and carrier, and the immobilization conditions. From an industrial perspective, simplicity and cost-effectiveness are key properties of immobilization techniques, but a long term industrial re-use of immobilized enzymes also requires the preparation of very stable derivatives having the right functional properties (activity, selectivity) for a given reaction [40,41] .

1.2.3.1 Adsorption

Protein adsorption is the net result of the various interactions between and within the system components; the sorbent surface, the protein molecules, the solvent (water) and any other solutes present such as low molecular mass ions [42].

The forces causing the interactions comprise of Van der Waals forces, Lewis acid-base forces (including hydrogen bond forces), electrostatic forces (including ion pairing) and more entropically based effects such as the hydrophobic

effect (at least under ambient conditions) and internal packing (steric/excluded-volume) restrictions.

Depending on the surface charge characteristics of the adsorbates, the surface properties of the adsorbent play a key role in the removal or separation of the various macromolecules of environmental and biological importance. One of the developments in recent years has been focused on looking for novel adsorbents that have better performance for macromolecule removal and separation [43]. Protein adsorption is of great importance in the chemical and pharmaceutical industries [44,45].

The simplest immobilization method is nonspecific adsorption, which is mainly based on physical adsorption or ionic binding [46,47]. The advantages of choosing adsorption as the immobilization technique are that usually no reagents are required and the process involves minimal preparation and cleanup work. Nearly full activity of the enzyme is retained since the active site of the adsorbed enzyme is unaffected.

Such methods are therefore economically attractive, but may suffer from problems such as enzyme leakage from matrix when the interactions are relatively weak. Despite its simplicity, adsorbed enzymes are susceptible to ambient conditions such as pH, temperature, ionic strength, polarity etc., which will cause leakage of enzymes from supports. Another disadvantage is that there is no specific binding by substrate or contaminants to the carrier which may result in diffusion limitations and mass transfer problems.

1.2.3.2 Covalent binding

Immobilization of proteins by methods based on the formation of covalent bonds is one among the most widely used. Because of the stable nature of bond, the leakage of enzyme from the support upon use is minimized. However, in order to achieve high levels of bound activity the covalent binding should involve

functional groups on the enzyme that are not required for catalytic activity and do not lie near the active site.

In general, binding is achieved by a nucleophilic group on the enzyme reacting with an activated functional group on the support material. The activation processes are generally designed to generate electrophilic groups on the support which, in the coupling step, react with the strong nucleophiles on the proteins. Glutaraldehyde is a bifunctional reagent quite useful for developing protocols for covalent immobilization to solid supports [48,49]. Enzyme immobilization on amine-activated supports activated with glutaraldehyde is a simple process [50-52].

However, because of the covalent nature of the bond, the matrix has to be discarded together with the enzyme once the enzymatic activity decays. The benefit of obtaining a leak-proof binding between enzyme and matrix resulting from these reactions is partially offset by the cost, in terms of generally low yield of immobilized activity and by the nonreversible character of this binding [53-55].

1.2.3.3 Entrapment

The entrapment method is based on the occlusion of an enzyme within a polymeric network that allows the substrate and products to pass through but retains the enzyme [56]. In membrane retention the enzyme is retained by a semi-permeable membrane that allows free-passage of the substrates and products of reaction. More than one enzyme can be retained so that cascade reactions can be performed. Retention can be attained by microencapsulation and by containment in ultra-filtration membranes

1.2.3.4 Cross-linking

The cross-linking method is based on the formation of covalent bonds between the enzyme, by means of bi- or multifunctional reagents. The individual biocatalytic units (enzymes, organelles, whole cells) are joined to one another with the help of bi-or multifunctional reagents (e.g. glutaraldehyde, glyoxal,

diisocyanates, hexamethylenediisocyanate etc.) [57,58]. Main disadvantages include severe diffusion limitations and poor mechanical strength or rigidity.

1.2.4 Characteristics of immobilized enzyme

1.2.4.1 pH profile

All enzymes have an optimal pH at which they show a maximum reaction rate. The pH of the medium has a similar effect on both free and immobilized enzymes but the pH stability relationship is of even greater concern with immobilized enzymes which have to undergo adverse conditions during coupling. The pH at which enzymes bind to a support is a critical parameter to be determined for any method of immobilization. When the enzyme is immobilized, the optimal pH may shift, depending on the nature of the carrier and charged groups on the enzyme surface and the active site. Thus the optimum pH for binding may be a complex function and usually has to be determined empirically, taking into account of enzyme's stability and the known protein binding character of the support.

Goldstein and co-workers studied this phenomenon in detail [59]. In a nut shell, they report that if a carrier is negatively charged, then a high concentration of positively charged ions (H^+) will accumulate at the boundary layer between the carrier and the surrounding solution. This accumulation of hydrogen ions will cause the pH at the carrier surface to drop below that of the bulk solution. The enzyme therefore sees a pH below that of the bulk solution. In this manner apparent pH of the immobilized enzyme may be increased. If the carrier is positively charged, the opposite may occur.

1.2.4.2 Temperature

During immobilization, the reaction temperature can affect those methods where chemical reactions are involved. It is normal practice to keep the temperature low at 4°C or an ice bath at 0°C to minimize protein denaturation. This obviously retards reaction rate and room temperature may be adequate in practice.

Thermal inactivation of the enzyme is found to be dependent on the immobilization method.

Adsorption is found to possess a lower inactivation rate in comparison to covalent coupling or cross-linking [60]. The surface on which the enzyme is immobilized is responsible for retaining the structure in the enzyme through hydrogen bonding or the formation of electron transition complexes. These links will prevent vibration of the enzyme and thus increase thermal stability.

1.2.4.3 Kinetics:

The basic kinetics of enzymes is similar whether they are free in solution or held in matrix. However, matrix can significantly change the apparent kinetics. The majority of these changes can be attributed to 1) diffusional limitation caused by the substrate to the active site within the matrix 2) interactions of enzyme with the matrix as a result of mass transfer limitations 3) partitioning of components between the stationary and mobile phases. For convenience these phenomena will be divided into those resulting from direct effects on the enzyme itself and those caused by the interactions between the substrate or product and the matrix.

Although some of these changes may be due to perturbations in the structure and hence affect the catalytic performance of the enzyme, the bulk of these differences can be interpreted as a consequence of moving from homogeneous to heterogeneous catalysis as a result of immobilization.

1.2.4.4. Stability

It is important to distinguish between stability of enzyme during immobilization and the stability of the enzyme once immobilized either during storage or more importantly under operational conditions. Like all other proteins enzymes are susceptible to thermal denaturation, whether they are immobilized or in the free state. In many cases, however, the rate of inactivation and denaturation of an immobilized enzyme is less than that of free enzyme.

Enzyme which shows excellent thermal stability does not necessarily show excellent operational stability because the operational stability of immobilized enzymes is not only a function of thermal stability, but of such factors as carrier durability, nature of interaction with the carrier, binding position and number of bonds, the freedom of the conformation change in the matrix, the microenvironment in which the enzyme molecule is located, the chemical and physical structure of the carrier, the properties of the spacer linking enzyme to the carrier, and the conditions under which enzyme is immobilized.

1.2.5 Benefits and limitations of enzyme immobilization

The immobilized enzymes offer several advantages over the soluble enzymes. They include:

1.2.5.1 Retention of catalyst

Immobilized enzymes can be exploited for their full life time under ideal conditions without loss or unnecessary deactivation, which is achieved by passing the substrate through a reactor containing the bound enzyme or by repeatedly transferring the active catalyst to fresh batches of substrate. The product separation is thus easier as, no toxic byproduct reaches product. Thus immobilization makes the provision for maximum use with the biocatalyst.

1.2.5.2 Micro-environmental control

The environment around an immobilized catalyst differs significantly from the homogeneous equivalent. Surface charge or hydrophobic regions on the matrix will interact specifically with the catalyst. These effects can substantially increase the thermo-stability of the enzyme thus reducing the degrees of freedom for the protein chain. The apparent pH optimum of a biocatalyst can be altered by immobilization on a charged matrix.

1.2.5.3 Less interference

The immobilized enzyme appears to be less susceptible to the normal activators and inhibitors that affect the soluble enzyme. Only strongest inhibitor will decrease the activity and only strongest activator will boost its catalytic power.

1.2.5.4 Limitations

The success of immobilization technology illustrates that, in general, the benefits of the technique far outweigh any disadvantages. The limitations mainly result from loss of catalyst activity during immobilization, mass transfer problems, physical discrimination between catalysts and the fluid, prolonged operation, and empirical nature of immobilization technology.

1.3 Synthetic polymer-polypyrrole, as support for enzyme immobilization

Polypyrrole (PPY) is an especially promising, inherently conducting polymer (ICP), as it is highly conducting, environmentally stable, and relatively easy to synthesize. It is believed to be a cross-linked polymer because it is insoluble in every solvent. This is due to the strong inter-chain interactions [61]. As a consequence, its exact chemical structure is still a matter of debate.

1.3.1 Synthesis of Polypyrrole

Polypyrrole was first synthesized in 1916; the oxidation of pyrrole using acidified hydrogen peroxide oxidant gave an amorphous polymeric product which became known as “pyrrole black” [62]. Pyrrole can be polymerized by oxidation in solution, either chemically or electrochemically.

Water is the most commonly used polymerization solvent but organic solvents such as aliphatic alcohols, ethers and esters also provide high conductivity polymer. PPY synthesis might be performed from water solution at neutral pH, since it opens the ways for entrapment and/or doping of polypyrrole by various biomaterials like small organic molecules, proteins, DNA and even living cells.

Some of the oxidizing agents include metal transition salts [63], halogens [64,65], and persulphates [66,67]. On the basis of oxido-reduction potential oxidant affects the polymerization kinetics and hence the morphology and conductivity also varies [68]. Among the oxidants, most widely used are $FeCl_3$ and ammonium peroxydisulphate) (APS). $FeCl_3$ have redox potential lower than APS and hence can induce slower and more controlled reactions (APS-2.01eV; $FeCl_3$-0.77eV)[69].

Methods of electrochemical PPY deposition have some limitations: the polymerization reaction should be conducted in oxygen free solution, and more-or-less stable analytical parameters can be observed only after a PPY swelling period, which can usually be up to several days [70]. Such limitations significantly reduce the applicability of PPY-based systems in the design of amperometric biosensors. Moreover electrochemical synthesis of polymers is a complex process and various factors such as the nature and concentration of monomer/electrolyte, cell conditions, the solvent, electrode, applied potential and temperature, pH affects the yield and the quality of the film. Thus, optimization of all of the parameters in one experiment is difficult.

In contrast, chemical polymerization does not require any special instruments [71]. It can be used to synthesize bulk quantities of polypyrrole in a fast and easy way. The chemical method of polypyrrole synthesis is based on the initiation of polymerization by oxidative compounds [72]. In this way, Angeli firstly synthesized polypyrrole in 1916. The chemical polymerization is a precipitation polymerization which forms a black, intractable powder or flakes in the reaction vessel. These powdered samples have a much larger specific surface than the electrochemically polymerized PPY film. All polypyrrole samples reported, consisted of spherical particles in the size range from ~100-400 nm in diameter.

1.3.1.1 Mechanism

The chemical oxidative doping of polypyrrole proceeds via radical cationic mechanism. It is the only way allowing the production of high quality massive

conducting polymer and the most promising for industrial applications. According to Colin Pratt, in the initial step, electron is removed from the pi system of the pyrrole backbone producing free radical and a spinless positive charge [73]. These radical species couple through deprotonation forming soluble bipyrroles. The polymer has resonance structures that resemble the aromatic or quinoid forms. Then in the propagation step bipyrroles are oxidized again and oligomers with radical cations are produced. The coupling of these bipyrroles results in the formation of an extended conjugated chain. Water was found to be trapped in the PPY with formation of pyrrolidinone rings at chain terminations. The hydroxypyrrole units are formed by nucleophilic attack of water during the preparation [74]. The hydroxyl groups introduced in the ring by this attack would finally produce carbonyl groups by keto-enol tautomerism [75].

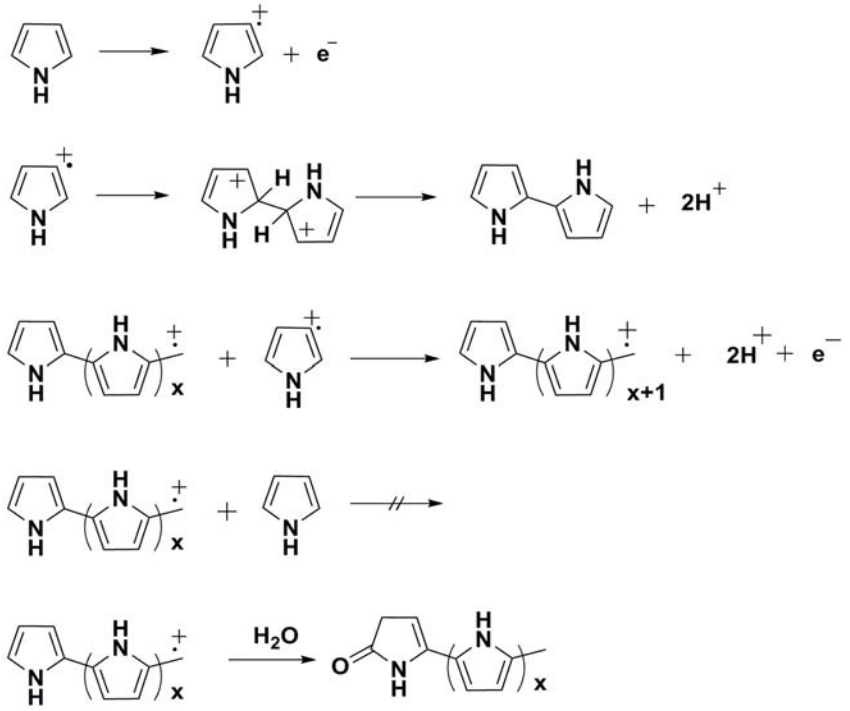

Figure: 1.6: Chemical oxidative doping of polypyrrole via radical cationic mechanism

1.3.1.2 Molecular Weight

The molecular weight of polypyrrole is effectively infinite as it is believed to be highly cross-linked. The cross-link induced insolubility of the polymer, has precluded the determination of molecular weight by the conventional methods, namely GPC, viscosity measurements or colligative methods.

A variety of possible configurations of the pyrrole rings in neutral polypyrrole are theoretically possible, these include rings, helices and linear chains. It seems most probable that the preferred conformation is the linear chain structure shown in Figure: 1.7.

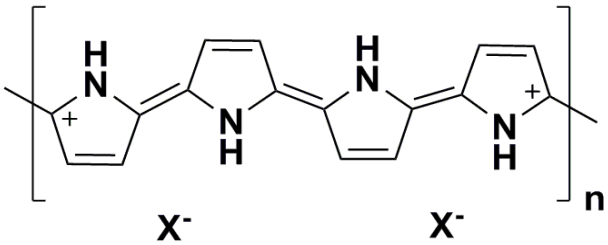

Figure: 1.7 Linear chain structure of Polypyrrole

1.4 Natural polymers-as support for enzyme immobilization

Natural polymers are increasingly being studied and used for applications in which synthetic polymers have traditionally been the materials of choice. For the last few years, many researchers have sought for inexpensive support matrixes for enzyme immobilization. The high cost of some available commercial support is promoting a search for cheaper substitutes.

Lignocellulosic agro-industrial waste supports, such as saw dust, straw, wood chips/shavings, rice husk [76], bagasse [77], spent grains [78] and coconut fiber [79,80] are suitable raw material sources for immobilization matrixes. The unique morphologies of the natural substances afforded by the hierarchical self-assembly of the polymer chains give superior type properties which are not seen in synthetic polymers [81].

The impetus for the heightened interest in this new technology is the need to increase the use of biodegradable and recyclable materials to limit the volume of material sent to landfills, and the desire to use renewable raw materials sources instead of nonrenewable sources [82]. Natural macromolecular polymers have been widely applied to many fields including food, fermentation, clinical diagnoses, environmental protection, and power production.

The main natural polymers that have been used are cellulose, cross-linked dextrans, starch, tannin, agarose, chitin, chitosan, collagen, gelatin, albumin, and lipid bodies [83]. Cellulose materials have been widely used as carriers for enzyme immobilization. Their advantages are accessibility, cheapness, hydrophilic character and great number of hydroxyl groups on the surface capable of chemical reaction [84].

The name cellulose was coined by Anselme Payen in 1838, and he suggested that cell walls of a large number of plants were constructed of mainly this cellulose unit [85]. In addition to cellulose, natural plant fibers are comprised of hemicelluloses, lignins, aromatics, waxes, other lipids, ash and water soluble compounds. A proper description of the structure and properties of cellulose requires the application of the principles of both the carbohydrate and polymer chemistry.

Chemical evidence for the structure of cellulose has been admirably summarized by Purves [86]. It is thus generally accepted that cellulose is a linear condensation polymer consisting of D-anhydroglucopyranose units joined together by β-1,4-glycosidic bonds. Cellulose is thus a 1,4-β-D-glucan whose basic repeating unit is the dimmer cellobiose, which comprises two glucose units bound by the β-1,4 linkage as well as intermolecular hydrogen bonds. The pyranose rings are in the $^4C_1$ conformation which means that the -CH_2OH and OH groups, as well as the glycosidic bonds, are all equatorial with respect to the mean planes of the rings [87].

When the cellulose molecule is fully extended it takes the form of a flat ribbon with hydroxyl groups protruding laterally and capable of forming both inter

and intra-molecular hydrogen bonds. The surface of the ribbon consists mainly of hydrogen atoms linked directly to carbon and is therefore hydrophobic. These two features of the molecular structure of cellulose are responsible for its supra-molecular structure and this, in turn, determines many of its chemical and physical properties.

Cellulose can take many forms, a phenomenon that is the basis for numerous in-depth reviews of this important natural polymer. In its native form, cellulose is typically called cellulose-I. This cellulose-I crystal form has also two allomorphs, cellulose Iα and Iβ. The ratio of these allomorphous forms depends on the plant species used to isolate the cellulose fibers. Cellulose II is formed irreversibly when native cellulose is mercerized or regenerated from solution [88].

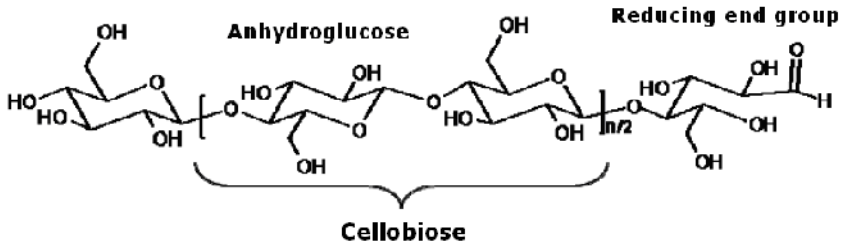

Figure: 1.8 Structure of cellulose

The structure and the morphology of cellulose have been the subject of a large amount of work. Their chief monomer units are various ring substituted phenyl propane's linked together in ways still only partially understood. Their detailed structures differ from one source to another. They are all very inert and have yet been put to relatively little industrial use.

1.4.1 Fiber chemical treatment

The development of pretreatment processes strong enough as to separate the cell wall arrangement and mild enough as to avoid a significant chemical degradation of biomass components is a challenge for today's chemical industry [89]. For the novel pretreatment methods, it is advisable to use cheap and easily

recoverable chemicals and low-cost equipment. The use of environmentally friendly and low energy-intensive approaches is highly desired.

Most mentioned method to clean fibers found in literature is distilled water cleaning. A.K. Mohanty et al. [90] soaked coir with hot water and found an increase of the flexural strength. The chemical cooking process is the most efficient and most used to perform the separation of ligno-cellulosic components of vegetal biomass [91]. It results in enlargement of the inner surface area of substrate particles, accomplished by solubilization and/or degradation of hemi-cellulose and lignin [92,93].

The chemical treatment not only removes the lignin, hemicelluloses, silica and pith from the fiber but also improves the surface roughness, so as to have a better interaction between the cellulose parts of fiber with other matrices of interest [94].

1.4.1.1 Acid hydrolysis

Acid hydrolysis of the biomass has concentrated on the use of low mineral acids like H_2SO_4, HCl, HNO_3, and H_3PO_4. The most utilized one is sulphuric acid [95-98]. Depending on the acidic media there will be variation in percentage removal of each structural component of lignin and hemicelluloses. During acid hydrolysis the amorphous hemicelluloses are hydrolyzed much more rapidly thus yielding surface rich in cellulose [99]. Most often degradation occurs via substitution reactions and broken links followed by condensation reaction and consequently lignin and hemicelluloses are removed in smaller proportions.

1.4.1.2 Alkaline hydrolysis

Of all chemical treatments applied to natural fibers, the most widely used method is alkaline treatment. It results in disruption of hydrogen bonding in the network structure. Alkaline treatment promotes the removal of partially amorphous constituents such as hemicelluloses, lignin, waxes and oils soluble in alkaline solution and therefore reduces the level of fiber aggregation, making the surface

rougher [100]. During the alkaline treatment, OH groups present in the fibers react with sodium hydroxide according to the equation [101].

$$\text{Fiber-OH} + \text{NaOH} \rightarrow \text{Fiber-O-Na}^{+} + \text{H}_2\text{O} \qquad 1.5$$

Thus alkaline hydrolysis determines the partial separation of the cellulose fibers from the cell wall and an improvement of the physical and chemical characteristics of cellulose, particularly its reactivity to other chemical agents. These treatments are usually made using diluted solutions of NaOH (1-10%) at low or high temperatures and concentrated NaOH solutions over 10% only at low temperatures [102].

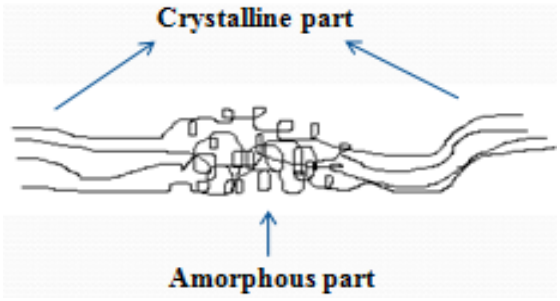

Figure: 1.9 Schematic representation of crystalline and amorphous part of cellulose

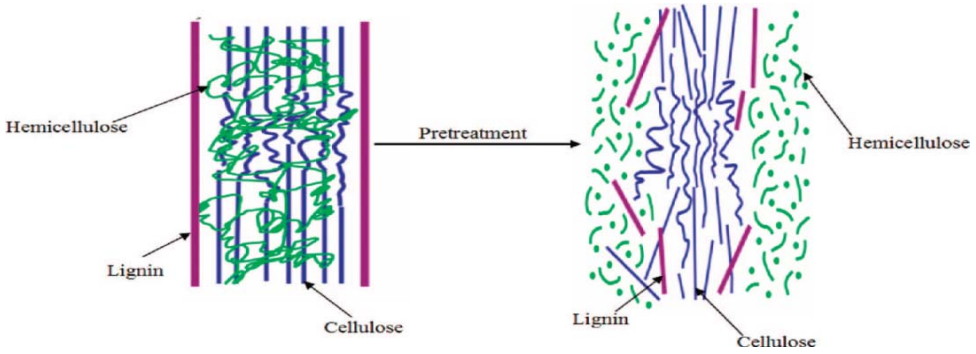

Figure: 1.10 Schematic representation of the role of pretreatment in the conversion of biomass to fuel [103].

Alkali treatment is recognized to hydrolyze the amorphous parts of cellulose present in fibers so that after treatment the material contains more crystalline cellulose

[100]. Therefore, alkaline pretreatment can play a significant role in exposing the cellulose by increasing the number of reaction sites. Lignin removal increases effective surface area by eliminating nonproductive adsorption sites and by increasing access to cellulose and hemicelluloses.

1.4.1.3 Chemical modification

In this method, the fiber surface is treated with a chemical compound that forms chemical bonds between the fiber and the matrix. An example of chemical modification is the reaction of cellulose fibers with silane. The reactive silanol groups have a high affinity for each other, forming -Si-O-Si- bonds and also for the hydroxyl sites of fibers which are thus linked via hydrogen bonds.

Herrera-Franco et al. deposited a silane coupling agent on henequen fibers and have found that adhesion between the natural fibers and the matrix plays an important role in the final mechanical properties of the composite [104]. Gwong et al. have reported that chemical modifications of wood fibers were expected to enhance adhesion between wood fibers and base polymers for final wood-composite applications with increasing compatibility [105].

The primary aspect of all these studies is the introduction of functional groups on fiber surfaces with specific focus on synthetic approaches to regulate surface architecture.

1.4.2 Advantages and disadvantages

Cellulose is a relatively stable polymer, due to the hydrogen bond network; it does not dissolve in common aqueous solvents. In contrast with mineral fibers (glass, carbon fibers), the cellulose fibers have good flexibility and elasticity, properties that help them to maintain a high aspect ratio in the process of manufacturing.

The fact that almost any cellulose material could be considered as a potential source for isolation of nano-cellulose structures, represent another important advantage in using cellulose elements as a reinforcing phase in polymeric matrix composites.

Plant fibers can be attractive as engineering materials due to their low costs [106], very high strength-to-weight ratio [107,108], light weight and easy to process state. Other considerations include their renewable nature, insulation from skin irritation, and biodegradability.

Disadvantages include fluctuations in supply and demand cycles based on product availability and harvest yields, moisture absorption, and quality variations depending upon growing sites and various seasonal factors.

1.4.3 Cellulose fibers of our choice are Sugarcane Bagasse and Coconut fibers as the supports for enzyme immobilization

With the realization of the value of ecofriendly natural products, the world is progressively moving towards the increased use of renewable natural resources. Easy extraction methods, modern machinery introduced over decades and new and versatile application of these fibers as a result of technological advances, which include enzyme immobilization, have been the main milestones enabling this industry to progress from its humble beginnings.

1.5 α - amylase- the model enzyme of our study

α-Amylases (E.C. 3.2.1.1.) are extra cellular endoenzymes that randomly cleave α -1,4 linkages between adjacent glucose units in the linear amylose chain and ultimately generate glucose, maltose and maltotriose units. [109]. Most of the α-amylases are metallo-enzymes, which require calcium ions (Ca^{2+}) for their activity, structural integrity and stability [110].

These enzymes are of great significance in present day biotechnology with applications ranging from baking, brewing, fermentation, detergent applications, textile designing, and paper industries to analysis in medicinal and clinical chemistry

[111,112]. Amylases are ubiquitous enzymes produced by plants, animals and microbes, where they play a dominant role in carbohydrate metabolism.

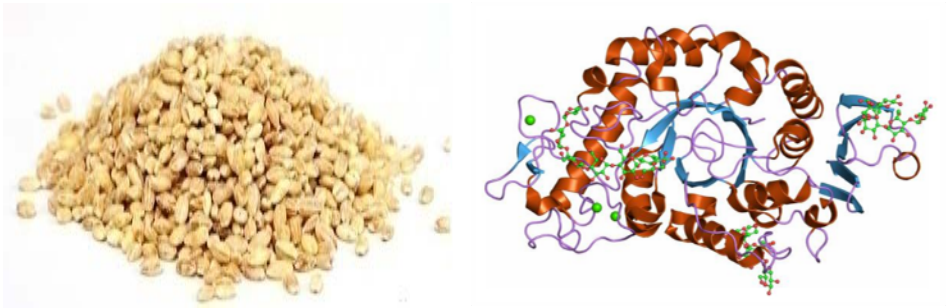

Figure: 1.11 Diastase α-amylase from barley seeds

1.6 Objectives of the present work

The major objective of present work is to immobilize diastase α-amylase on to synthetic polymer- polypyrrole, its derivatives and natural polymers- coconut fiber and sugarcane bagasse- followed by their biochemical and physico-chemical characterization. Diastase α-amylase was chosen as the model enzyme of our study, as it is very cheap and performs simple hydrolysis reaction. They are also an industrially important class of enzymes especially in food, pharmaceutical, detergent, paper industries etc.

Adsorption is used as the method of immobilization as it is simple and can be carried out with ease providing high catalytic activity and efficiency. The covalent binding method was also applied for functionalized support so as to compare the efficiency with adsorption method. In order to ensure the efficiency of immobilization, the influence of several parameters were optimized. The kinetic parameters, reusability and, storage stability were also investigated. The main objectives of the study are:

- Synthesis of polypyrrole in presence of different oxidizing agents and different methods.

- Synthesis of polypyrrole using surfactants as template.
- Synthesis of polypyrroles functionalized using glutaraldehyde and APTES.
- Synthesis of polypyrrole copolymers.
- Synthesis of polypyrrole composites.
- Preparation of chemically modified natural fibers.
- Immobilization of diastase α-amylase via adsorption on to these polymers synthesized.
- Physico-chemical and biochemical characterization of these polymers.
- Optimization of immobilization parameters such as pH of immobilization medium, time for immobilization, amount of protein adsorbed on supports and activity variation with respect to each optimized parameters.
- Study on the effect of reaction pH, temperature, pre-incubation time, thermal stability on the activity of immobilized enzyme.
- Evaluating kinetic parameters K_m and V_{max} and comparing with the native enzyme kinetic parameters.
- Estimating the efficiency of immobilization on the basis of immobilization yield and activity yield.
- Study on reusability, and storage stability of immobilized enzymes prepared.

1.7 References

[1] P.W.N.M. van Leeuwen, Homogeneous Catalysis: Understanding the Art University of Amsterdam, The Netherlands (2004) 408.

[2] A. Illanes, Enzyme Biocatalysis : Principle and application, springer New York, (2008) 391.

[3] A.S. Bommarius, B.R. Riebel, Biocatalysis : Fundamentals and applications, Wiley-VCH, Weinheim, (2004) 611.

[4] C.C. Xiang, Y. Chen, cDNA microarray technology and its applications, Biotechnol. Adv. 18 (2000) 35-46.

[5] P. D'Orazio, Biosensors in clinical chemistry, Clin. Chim. Acta. 334 (2003) 41 - 69.

[6] S.J. Benkovic, A. Ballesteros, Biocatalysts - the next generation, TIBTECH 15 (1997) 385-86.

[7] M.A. Wegman, M.H.A. Janssen, F. van Rantwijk , R.A. Sheldon, Towards biocatalytic synthesis of β-lactam antibiotics, Adv. Synth. Catal. 343 (2001) 559-576.

[8] M. Gavrilescu, Y. Chisti, Biotechnology-a sustainable alternative for chemical industry, Biotech. Adv. 23 (2005) 471 - 499.

[9] A. Schmid, J.S. Dordick, B. Hauer, A. Kiener, M. Wubbolts, B. Witholt, Industrial biocatalysis today and tomorrow, Nature 409 (2001) 258-268.

[10] S.M. Thomas, R. DiCosimo, V. Nagarajan, Biocatalysis: applications and potentials for the chemical industry, TIBTECH 20 (2002) 238-242.

[11] H. Zhao, K. Chockalingam, Z. Chen, Directed evolution of enzymes and pathways for industrial biocatalysis, Curr. Opin. Biotechnol. 13 (2002) 104-10.

[12] A. Bruggink, A.J.J. Straathof, L.A.M. van der Wielen, Fine chemical industry for life science products: Green Solutions to Chemical Challenges, Adv. Biochem. Eng./ Biotechnol. 80 (2003) 69-113.

[13] P.M. Claesson, E. Blomberg, J.C. Froberg, T. Nylander, T. Arnebrant, Protein interactions at solid surfaces, Adv. Colloid Interface Sci. 57 (1995) 161-227.

[14] R.H. Haschemeyer, A.E.V. Haschemeyer, Proteins: a guide to study by physical and chemical methods, John Wiley, New York, (1973) 358.

[15] M. Dixon, E.C. Webb, Enzymes 3rd edn. Academic Press, New York, (1979) 1116.

[16] T.E. Creighton, Proteins (2nd edn). W.H Freeman and Co., New York, (1993) 507.

[17] D.W.S. Wong, Food enzymes: Structure and mechanisms, Chapman Hall, New York, (1995) 390.

[18] R.J. Whitehurst, B.A. Law, Enzymes in food technology, CRC Press, Boca Raton, USA, (2002) 255.

[19] K.M. Koeller, C.H. Wong, Enzymes for chemical synthesis, Nature. 409 (2001) 232-240.

[20] J. Van Brunt, Biosensors for bioprocesses, Biotechnol. 5 (1987) 437-440.

[21] R.B. Christie, The medical use of proteolytic enzymes. In: Topics in Enzyme and Fermentation Biotechnology, (Wiseman A (ed)) 4 Ellis Horwood Ltd., Chichester, England (1980) 25-84.

[22] C. Polisson, Type II restriction endonuclease obtainable from Pseudomonas alcaligenes and a process for producing the same. US Patent 5098839, 1992.

[23] S. Sonkaria, G. Boucher, J. -O. Flórez, B. Said, S. Hussain, E. L. Ostler, S. Gul, E. W. Thomas, M. Resmini, G. Gallacher, K. Brocklehurst, Evidence for 'lock and key' character in an anti-phosphonate hydrolytic antibody catalytic site augmented by non-reaction centre recognition: variation in substrate selectivity between an anti-phosphonate antibody, an anti-phosphate antibody and two hydrolytic enzymes, Biochem J. 381 (Pt 1) (2004) 125-30.

[24] D.E. Koshland, Application of a theory of enzyme specificity to protein synthesis, Proc. Natl. Acad. Sci. USA, 44 (1958) 98-104.

[25] M.S. Yousef, S.A. Clark, P.K. Pruett, T. Somasundaram, W.R. Ellington, M.S. Chapman, Induced fit in guanidino kinases - comparison of substrate-free and transition state analog structures of arginine kinase, Protein Sci. 12 (2003) 103-111.

[26] S.J. Benkovi´c, S.-S. Hammes, A perspective on enzyme catalysis, Science 301 (2003) 1196-1202.

[27] M.F. Chaplin, C. Bucke, Enzyme Technology, Science Cambridge University Press, Cambridge (1990) 264.

[28] T.O. Rourke, in T. Godfrey, S. West (eds), Industrial Enzymology 2nd edn, Macmillan Press Ltd, U.K. (1996) 103-131.

[29] J.M. Guisan, Methods in biotechnology; Immobilization of enzymes and cells 2nd edn. 2006.

[30] L. Cao, Carrier-bound immobilized enzymes. Principles, application and design, Wiley-VCH, Weinheim, (2005b) 563.

[31] A. Tanaka, T. Tosa, T. Kobayashi, Industrial Application of Immobilized Biocatalysts, Marcel Dekker, New York (1993) 185-207.

[32] G.G. Guibault, J.M. Kauffmann, G.J. Patriarche, Immobilized Enzyme Electrodes as Biosensors. In: Protein Immobilization. Fundamentals and Applications (R.F. Taylor, ed.), Marcel Dekker, New York, NT, (1991) 209-262.

[33] R.F. Taylor, Immobilized Antibody and Receptor Based Biosensors. In: Protein Immobilization. Fundamentals and Applications (R.F. Taylor, ed.), Marcel Dekker, New York, (1991) 263-303.

[34] M. Trevan, Techniques of Immobilization. In: Immobilized Enzymes. An Introduction and Applications in Biotechnology (M. Trevan, ed.), Wiley, Chichester-New York, (1980) 1-9.

[35] P. Brodelius, K. Mosbach, Immobilization Techniques for Cells/Organelles In: Methods in Enzymology, (K. Mosbach, ed.), Academic Press, London, 135 (1987) 173-454.

[36] K. Buchholz, J. Klein, Characterization of Immobilized Biocatalysts, In: Methods in Enzymology, (K. Mosbach, ed.), Academic Press, London, 135 (1987) 3-30.

[37] J.M.S. Cabral, J.F. Kennedy, Covalent and coordination immobilization of proteins. In: Protein immobilization. Fundamentals and Applications, (R.F. Taylor, ed.), Marcel Dekker, New York, (1991) 73-138.

[38] S. Datta, L.R. Christena, Y.R.S. Rajaram, Enzyme immobilization: an overview on techniques and support materials, Biotech. 3 (2013) 1-9.

[39] M. Gupta, B. Mattiasson, Unique applications of immobilized proteins in bioanalytical systems. In: Methods of Biochemical Analysis, (C.H. Suelter, ed.), Wiley, New York 36 (1992) 1-34.

[40] L. Gianfreda, M.R. Scarfi, Enzyme stabilization: state of the art, J. Mol. Cell Biochem. 100 (1991) 97-128.

[41] L. Cao, Carrier-bound immobilized enzymes. Principles, application and design, Wiley-VCH, Weinheim, (2005a) 563.

[42] W. Norde, J. Lyklema, The absorption of human plasma albumin and bovin pancrease ribonuclease at negatively charged polystyrene surface IV, J. Colloid Interface Sci. 66 (1978) 295.

[43] Y. Seida, Y. Nakano, Removal of humic substances by layered double hydroxide containing iron, Water Res. 34 (2000) 1487-1494.

[44] M.J.-G. Mura, J.C. Voegel, S. Behr, E.F. Bres, P. Schaaf, Adsorption / desorption of human serum albumin on hydroxylapatite: A critical analysis of the Langmuir model, Proc. Natl. Acad. Sci. USA, 88 (1991) 5557-5561.

[45] C.A. Haynes, W. Norde, Globular proteins at solid/liquid interfaces, Colloids Surf. B 2 (1994) 517-566.

[46] R. A. Messing, Adsorption and inorganic bridge formations. In: Methods in Enzymology, (K. Mosbach, ed.), Academic Press, New York, XLIV (1976) 148-169.

[47] J. Woodward, Immobilized enzymes: adsorption and covalent coupling. In: Immobilized Cells and Enzymes: A Practical Approach, (J. Woodward, ed.), IRL, Oxford, UK, (1985) 3-17.

[48] L. Betancor, F.-G. L´opez, A. Hidalgo, N.-M. Alonso, G.D.C. Mateo, R.-L. Fernández, J.M. Guisán, Different mechanisms of protein immobilization on glutaraldehyde activated supports: Effect of support activation and immobilization conditions, Enzyme and Microb. Technol. 39 (2006) 877-882.

[49] A.-D. Hamerska, J. Bryjak, A.W. Trochimczuk, Novel method of enzymes stabilization on crosslinked thermosensitive carriers, Enzyme Microb. Technol. 38 (2006) 921-925.

[50] P. Monsan, G. Puzo, H. Mazarguil, On the mechanism of the formation of glutaraldehyde protein bonds, Biochimie. 57 (1975) 1281-1292.

[51] N. Alonso, F.-G. L´opez, L. Betancor, A. Hidalgo, C. Mateo, J.M. Guisan,. Immobilization and stabilization of glutaryl acylase on aminated sepabeads supports by the glutaraldehyde crosslinking method, J. Mol. Catal. B Enzym. 35 (2005) 57-61.

[52] F.-G. L´opez, L. Betancor, A. Hidalgo, N. Alonso, G.-L. Fernández, J.M. Guisán, R.-L. Fernández, Preparation of a robust biocatalyst of D amino acid oxidase on Sepabeads supports using the glutaraldehyde crosslinking method, Enzyme Microb. Technol. 37 (2005) 750-756.

[53] O. Zaborsky, Immobilized enzymes, CRC Press, Cleveland, Ohio (1973) 176.

[54] L. Cao, Carrier-bound immobilized enzymes, Principles, application and design, Wiley-VCH, Weinheim, (2005b) 563.

[55] J.M. Guisan Methods in biotechnology: Immobilization of enzymes and cells, 2nd edn. Humana Press, Totowa, NJ (2006) 500.

[56] K.F. O'Driscoll, Techniques of enzyme entrapment in gels, In: Methods in Enzymology, (K. Mosbach, ed.), Academic Press, New York, XLIV (1976) 169-183.

[57] M.S.M. Eldin, C.G.P.H. Schroen, A.E.M. Janssen , D.G. Mita, J. Tramper, Immobilization of *pencillin G acylase* onto chemically grafted nylon particles, J. Mol. Catal.B Enzym. 10 (2000) 445-51.

[58] N. Albayrak, S.T. Yang, Immobilization of beta-galactosidase on fibrous matrix by polyethyleneimine for production of galacto-oligosaccharides from lactose, Biotechnol. Prog. 18 (2002) 240-51.

[59] L. Goldstein, Microenvironmental effects on enzyme catalysis. A kinetic study of polyanionic and polycationic derivatives of chymotrypsin, Biochem. 11 (1972) 4072-4084.

[60] P. Vrabel, M. Polakovic, V. Stefuca, V. Bales, Analysis of mechanisms and kinetics of thermal inactivation of enzymes: evaluation of multi temperature data applied to inactivation of yeast invertase, Enzyme Microb. Technol. 20 (1997) 348-354.

[61] E.J. Oh, K. S. Jang, Synthesis and characterization of high molecular weight highly soluble polypyrrole in organic solvents, Synth. Met. 119 (2007) 107.

[62] G.B. Street, T.C. Clarke, R.H. Geiss, V.Y. Lee, A. Nazzal, P. Pfluger, J.C. Scott, Characterization of Polypyrrole, Journal De Physique, Colloque C3, supplement aun6, Tome 44, juin 1983.

[63] T.H. Chao, J. March, A Study of polypyrrole synthesized with oxidative transition metal ions, J. Polym. Sci. A: Polym. Chem. 26 (1988) 743-753.

[64] K. G. Neoh, E. T. Kang, T. C. Tan, Effects of acceptor level on chemically synthesized polypyrrole-halogen complexes, J. Appl. Polym. Sci. 37 (1989) 2169-2180.

[65] E.T. Kang, K.G. Neoh, H.C. Ti, Electrical properties of chemically synthesized polypyrrole-halogen charge transfer complexes, Solid State Commun. 60 (1986) 457-459.

[66] K.C. Khulbe, R.S. Mann, C.P. Khulbe, Polymerization of Pyrrole by Potassium Persulfate, J. Polym.Sci.: Poly. Chem. 20 (1982) 1089-1095.

[67] A. Malinauskas, "Chemical Deposition of Conducting Polymers," Polymer 42 (2001) 3957-3972.

[68] S. Xing, G. Zhao, Morphology, structure and conductivity of polypyrrole prepared in the presence of mixed surfactants in aqueous solutions, J. Appl. Polym. Sci. 104 (2007) 1987-1996.

[69] T.K. Mandal, B.M. Mandal, Dispersion polymerization of pyrrole using ethylhydroxyethylcellulose as a stabilizer, J. Polym. Sci. A: Polym. Chem. 37 (1999) 3723-3729.

[70] A. Ramanavicius, K. Habermuller, E. Csoregi, V. Laurinavicius, W. Schuhmann, Polypyrrole entrapped quinohemoprotein alcohol dehydrogenase. Evidence for direct electron transfer via conducting - polymer chains, Anal. Chem. 71 (1999) 3581-3586.

[71] A. Ramanvicius, A. Kausaite, A. Ramanaviciene, J. Acaite, A. Malinauskas, Redox enzyme glucose oxidase initiated synthesis of polypyrrole, Synth. Met. 156 (2006b) 409 - 413.

[72] M.C. Henry, C.C. Hsueh, B.P. Timko and M.S. Freund, Reaction of pyrrole and chloroauric acid. A new route to composite colloids, J. Electrochem. Soc. 148 (2001) 155- 162.

[73] C. Pratt, Essay on conducting polymers Interdisciplinary material Science 22.2.96.

[74] G. Maia, E.A. Ticianelli, F.C. Nart, FTIR Investigation of the polypyrrole oxidation in Na_2SO_4 and $NANO_3$ aqueous solutions, Zeitschrift Phys. Chem. 186 (1994) 245-257.

[75] W. Prissanaroon, L. Ruangchuay, A. Sirivat, J. Schwank, Electrical conductivity response of dodecylbenzene sulfonic acid-doped polypyrrole films to SO_2-N_2 mixtures, Synth. Met. 114 (2000) 65-72.

[76] S. F. D'Souza, S. S. Godbole, Immobilization of invertase on rice husk using polyethylenimine, J. Biochem. Biophys. Methods 52 (2002) 59-62

[77] S. Varavinit, N. Chaokasem, S. Shobsngob, Covalent immobilization of a glucoamylase to bagasse dialdehyde cellulose, World J. Microbiol. Biotechnol. 17 (2001) 721-725.

[78] C. Rocha, L. Ducso, M. P. Gonçalves, J. A. Teixeira, Spent-grains and zeolites as potencial carriers for trypsin immobilization, 4 Mercosur Congress on Process Systems Engineering Proceedings (CD-ROM), Costa Verde, Brazil (2005).

[79] G. Dey, V. Nagpal, R. Banerjee, Immobilization of α-amylase from *Bacillus circulans GRS 313* on coconut fiber, Appl. Biochem. Biotechnol. 102-103 (2002) 303-313.

[80] A.I.S. Brigida, A.D.T. Pinheiro, A.L.O. Ferreira, G.A.S. Pinto, L.R.B. Gonçalves, Appl. Biochem. Biotechnol. 136-140 (2007) 67-80.

[81] J. Huang, T. Kunitake, Nano-precision replication of natural cellulosic substances by metal oxides, J. Am. Chem. Soc. 125 (2003) 11834-5.

[82] D.R. Coffin, M.L. Fishman, "Physical and mechanical properties of highly plasticized pectin /starch films", J. Appl. Polym. Sci. 54 (1994) 1311-1320.

[83] Y.-Q. Zhang, Natural silk fibroin as a support for enzyme immobilization, Biotechnol. Adv. (1998) 961-971.

[84] S. Varavinit, N. Chaokasem, S. Shobsngob, Immobilization of a thermostable α- amylase, Science Asia 28 (2002) 247-251.

[85] A. Payen, "Mémoire sur la composition du tissu propre des plantes et du ligneux" (Memoir on the composition of the tissue of plants and of woody material), Comptes rendus, 7 (1838) 1052-1056.

[86] C.B. Purves, In Cellulose and Cellulose Derivatives, I. Pt, E. Ott, H. M. Spurlin, M. W. Graffline, Eds., Interscience, New York, (1954) 29.

[87] W.N. Haworth," The constitution of sugars", E. Arnold and Co., London, (1929) 24.

[88] A.N. Frone, D.M. Panaitescu, D. Donescu, Some aspects concerning the isolation of cellulose micro and nano fibers, U.P.B. Sci. Bull. Series B 73 (2011) 1454-2331.

[89] E. Canetieri, G.J.M. Rocha, J.R. de Carvalho, J.B.A. Silva, Optimization of acid hydrolysis from the hemicellulosic fraction of Eucalyptus grand is residue using response surface methodology, Bioresour. Technol. (2007) 422-8.

[90] A.K. Mohanty, M. Misra, L.T. Drzal, Sustainable bio - composites from renewable resources: opportunities and challenges in green materials world, J. Polym. Environ. 10 (2002) 19-26.

[91] N. Fernandez, Pulp and paper development from sugarcane bagasse. In: Third Internacional Non-wood Fiber Pulping and Papermaking Conference, Proceedings, Pequim, 1 (1996) 231-240.

[92] G. Marton, J. Dencs, L. Szokonya, Principles of biomass refining. In: Handbook of heat and mass transfer. Houston: Gulf Publishing, (1989) 609-52.

[93] K. Youssef, M. Ghareib, M. Nour El Dein, Improvement of the biodegredation of some cellulosic wastes by acid pretreatment, Acta Microbiol. Pol. (1991) 187-95.

[94] S.V. Prasad, C. Pavithran, P.K. Rohatgi, Alkali treatment for coir fibers for coir-polyester composites, Research regional laboratory, India, (1983) 1443-1454.

[95] R. Torget, P. Werdene, M. Himmel, K. Grohmann, Dilute acid pretreatment of short rotation woody and herbaceous crops, Appl. Biochem. Biotechnol. (1990) 115-26.

[96] Springer, Hydrolysis of aspenwood xylan with aqueous solutions of hydrochloric acid. TAPPI Journal, (1966) 102-6.

[97] M. El-Taaboulsi,. M. Nassar, E .-R. Abd El,. A modified method of nitric acid pulping of bagasse, J. Chem. Technol. Biotechnol. (1983) 87-96.

[98] J. Fontana, J. Corea, J. Duarte, A. Barbosa, M. Blumel, Aqueous phosphoric acid hydrolysis of hemicelluloses from sugarcane and sorghum bagasses, Biotechnol. Bioeng. Symposium No. 14, (1984) 175-85.

[99] D. Fengel, G. Wegener, Wood Chemistry, Ultrastructure, Reactions, Berlin: Walter de Gruyter, 1989.

[100] M. Le Troedec, D. Sedan, C. Peyratout, J.P. Bonnet, A. Smith, R. Guinebretiere, V. Gloaguen, P. Krausz, Influence of various chemical treatments on the composition and structure of hemp fibers, Compos. Part A: Appl. S, 39 (2008) 514-522.

[101] I.A.T. Razera,"Firas lignocelulosicas como agente de refrco de compositos de matriz fenolica e lignofenolica,"Ph. D Thesis, Universidade de Sao PAULO. 2006.

[102] S.K. Nayak, S.S. Tripahy, J. Rout, A.K. Mohanty, Coir-Polyester composites: Effect on fiber surface treatment on mechanical properties of composite, International Plastics Engineering and Technology, 04 (2000) 79-86.

[103] T.A. Hsu, M.R. Ladisch, G.T. Tsao, Alcohol from cellulose, Chem. Technol. 10 (1980) 315-319.

[104] A.-G. Valadez, J.M.-U. Cervantes, R. Olayo, P.J.-F. Herrera, Chemical modification of henequen fibers with an organosilane coupling agent, Composites Part B 30 (1999) 321-331.

[105] J.G. Gwon, S.Y. Lee, G.H. Doh, J.H. Kim, Characterization of Chemically Modified Wood Fibers Using FTIR Spectroscopy for Biocomposites, J. Appl. Polym. Sci. 116 (2010) 3212-3219

[106] S.P. Carruthers, S.P. Carruthers, F.A. Miller, C.M.A. Vaughan, Editors , Crops for Industry and Energy, CAS Report 15 (1994) 93-108.

[107] A.J. Bolton, Natural fibers for plastic reinforcement, Mat. Tech.9 (1994) 12.

[108] A.J. Bolton, The potential of plant fibers as crops for industrial use, Outlook on Agriculture 24 (1995) 85.

[109] K.K. Kiran, T.S. Chandra, Production of surfactant and detergent-stable, halophilic, and alkali tolerant α- amylase by a moderately halophilic *Bacillus sp.*, Strain TSCVKK Appl. Microbiol. Biotechnol. 77 (2008) 1023-1031.

[110] R.V. de Carvalho, T.L.R. Côrrea, J.C.M. de Silva, L.R.C. de Oliveira Mansur, M. Lelis L. Martins, Properties of an amylase from thermophilic bacillus sp., Braz. J. Microbiol. 39 (2008) 102-107.

[111] P.H. Pandya, R.V. Jarsa, B.L. Newalkar, P.N. Bhalt, Studies on the activity and stability of immobilized α-amylase in ordered mesoporous silicas, Microporous Mesoporous Mater. 77 (2005) 67-77.

[112] S. Alva, J. Anupama, J. Savla, Y.Y. Chiu, P. Vyshali, M. Shruti, B.S. Yogeetha, D. Bhavya, J. Puri, K. Ruchi, B. Kumudini, K.N. Varalakshmi, Production and characterization of fungal amylase enzyme isolated from *Aspergillus sp. JGl12* in solid state culture, Afr. J. Biotechnol. 6 (2007) 576-581.

****

Chapter 2

Experimental Techniques

Contents

2.1 Introduction

An important aspect of materials science is the characterization of the materials that we use or study in order to learn more about them. The proper designing of materials under study is essential so as to make them available for variety of applications. The characterization typically has a goal to improve the performance of the material. Characterization techniques are typically used to determine molecular structure, morphology, thermal properties etc.

Today, there is a vast array of scientific techniques available to the materials scientist that enables this characterization. The methods and techniques adopted for biochemical and physico-chemical characterization of supports taken for our study will be explained briefly in this section. The characterization of a support and its immobilized forms involves the determination of its characteristic physical and chemical properties following established experimental techniques under known conditions.

This chapter also describes the various strategies that have to be considered while preparing the immobilized enzyme. By the careful investigation of each of

these parameters efficiency of immobilization can be found out. Again it should be emphasized that in this short research work not all of those aspects can be discussed, but the techniques we adopted have elegant ways to focus on particular aspects or to overcome some of the shortages.

2.2 Methods adopted

2.2.1 Physical adsorption

This is one of the simplest and oldest methods of preparing an immobilized enzyme and it does not directly affect the active sites [1]. The interaction between the enzyme and the surface of support occurs through weak interactions such as hydrogen bonding, hydrophobic and Van der Waals attraction. The immobilization of large proteins would be favourable using this approach because of many additive interactions. Based on the charges of the support and the protein conformation the strongly bound immobilized enzymes can be prepared [2]. Thus, immobilization of complex proteins of multiple units would be possible without the disruption of subunits. The solid supports make the enzyme molecules more robust. So the catalysts can be reused for several times after easy separation from the reaction media.

2.2.2 Preparation of Immobilized α-amylase

Enzyme immobilization involves the interaction of two species, the enzyme and the carrier. The polar groups like amino groups on lysine and carboxyl groups on glutamic acid, apolar surface areas or sugar moieties are found to have impact on properties of the enzyme surface. There is no general method available that can be commonly used as method of immobilization. Only way is to carry out trial and error, until a satisfactory system has been developed. During this process of selecting a method, proper conditions should be maintained so that enzyme is stable to and during the immobilization process. There are several different polymeric supports where immobilization can be carried out, but there is no

particular one that prevails over the others. This suggests that none fulfill all the requirements for any particular application. Reactive functional groups can be introduced in the matrix of polymeric supports by choosing appropriate organic monomers.

In order to immobilize the enzyme, the 0.1g polymer was weighed in an electronic balance and to that a definite volume of enzyme solution prepared in buffer solution of desired pH was added. It was then shaken in a water bath shaker at room temperature for two hours and then centrifuged. It was washed several times with the same buffer that was used for immobilization, in order to remove the unbound enzyme. The immobilized enzyme thus obtained was filtered using a sintered glass filter or filter paper and dried in airflow. It was stored in a refrigerator at 4°C and used for further studies. The supernatant and washings collected were tested for unbound enzymes that get leached from the support.

2.2.3 Optimization of immobilization parameters

The adsorption of enzymes onto carriers can proceed via different types of interactions which include hydrophobic interactions, Van der Waals forces and entropy changes. Sugar residues of glycosylated enzymes can ensure adsorption via hydrogen bonds; large hydrophilic surface areas of the enzyme will interact with a hydrophilic carrier. Depending on the pH of the solution and the isoelectric point, the surface of the enzyme may possess charges [3]. Proteins can exist as neutral, positively or negatively charged state. At a pH below their pI, proteins carry net positive charge; and above their pI, they carry net negative charge. Thus, the attraction and repulsion of the enzyme molecules and polymer surface can be regulated by the change of pH value. When the pH is below the pI, the electrostatic attractions between the positive charges of enzyme molecules and negative charge of polymer surface induce more loadings. The above situations demand proper immobilization methods tailored for particular needs. Efficient immobilization protocols should take into account all these factors so

that the best compromise between stability, activity, easy handling and cost is reached. Also the surface properties of both enzyme and carrier can be used to advantage, obtaining enzyme preparations that outperform the native enzyme. Hence the influence of pH, temperature, time of pre incubation, and enzyme concentration during immobilization of α-amylase on both synthetic and natural polymers were investigated.

The pH was varied in the range 3-9 and effect of pH during immobilization thus determined is evaluated so as to obtain the best pH for immobilization of enzyme on corresponding support taken. The contact time was varied between 1-4 hours and enzyme concentration chosen from the range 10-500 mg depending on the surface area of support. The immobilized polymers were analyzed for enzyme activity under optimized conditions. Sodium acetate-acetic acid (0.2M, pH 3-5.5) and sodium phosphate (0.2M, pH 5.6-8) were used as buffers for optimization studies.

2.2.4 Estimation of protein

In order to determine the amount of enzyme adsorbed on polymer support, protein estimation in the solution before and after immobilization and also in washings has to be carried. This was achieved by performing the protein determination according to method proposed by Lowry et al., using Folin & Ciocalteus Phenol reagent and measuring absorption at 750 nm in Spectro UV-Vis Double beam UVD-3500 spectrophotometer [4]. The amount of immobilized protein was calculated from the difference between the amount of protein introduced into the reaction mixture and the protein present in the filtrate and washing solutions after immobilization.

2.2.5 Immobilization efficiency

Immobilization yield (IY) was calculated by measuring concentration of protein in supernatants before and after immobilization, according to equation 2.1 below.

$$IY\ (\%) = \frac{C_1 - C_2}{C_1} \times 100 \qquad 2.1$$

Where C_1 was the concentration of protein taken for immobilization and C_2 was the concentration of protein present in supernatant after immobilization. And the activity yield was determined by the equation 2.2.

$$AY\ (\%) = \frac{\text{Activity of immobilized enzyme}}{\text{Activity of free enzyme}} \times 100 \qquad 2.2$$

The immobilization efficiency,

$$IE = \frac{AY}{IY}\ (\%) \qquad 2.3$$

2.2.6. Activity of α-amylase

The activity of both soluble and immobilized α-amylase was determined by the hydrolysis of starch with the enzyme and subsequent determination of the residual starch with iodine-potassium iodide reagent. 1% potato starch solution was prepared by boiling the starch powder in distilled water. The solution was then cooled to 40°C. To a known amount of free and immobilized enzyme in buffer, 1ml starch solution was added and incubated at optimum temperature in a water bath with constant shaking for fixed time interval. After the time is attained whole set up is immersed in ice bath for 10 minutes and the reaction mixture was soon arrested by the addition of 0.3ml 1M HCl. To the 0.5ml of above solution, 0.1ml of iodine-potassium iodide reagent was added and then diluted with distilled water to a known volume. The blue colour developed was measured at 650 nm in a UV-Vis spectrophotometer. The results were correlated with the absorbance of standard starch solution and amount of starch converted was calculated. All tests were performed in triplicate and results are presented in average and standard deviation. One enzyme unit (EU) of α- amylase activity was defined as the amount of

enzyme, which converts 1mg/ml of starch in 1minute at optimum temperature and pH.

2.3 Biochemical characterization

2.3.1 Effect of pH on activity

Enzyme molecules are amphoteric containing large number of acidic and basic groups at their active site and on their surfaces. The charges on these groups vary with the pH of the environment. In a solution of low pH value amylase has positive value because any basic groups such as Nitrogen groups in protein would be protonated. If the environment was too basic the acid groups would be deprotonated. This would alter electrical attractions between polar groups.

Every enzyme has an optimum pH range outside which the enzyme is inhibited. The charge on the carrier surface changes the microenvironment of the enzyme bound to it [5]. The pH optimum for maintaining maximum stability may differ considerably from that for maximum activity. The stability optimum is much broader than activity optimum. Stability to pH changes caused by acid and alkali is as a rule improved by immobilization, although it may occasionally be lowered.

The activity of immobilized α-amylase was compared with that of soluble α- amylase at different pH values (4.0-8.0) using 0.2 M acetate buffer (pH 4 - 5.5) and 0.2 M phosphate buffer (pH 5.6 - 8).

2.3.2 Effect of temperature on activity and stability

The effect of temperature on the activity of free and immobilized α-amylase was tested by performing the reaction in such a way that reaction was carried out at various temperature ranging from 30-70°C at optimum pH and 1% starch solution as substrate. In order to compare the thermal stability of immobilized enzyme with respect to free enzyme, both are subjected to various temperatures ranging from 30-70°C for 1hour in a water bath.

After 1hour of pre-incubation both free and immobilized enzymes in buffer was cooled to optimum temperature and enzymatic reaction was carried out with subsequent addition of definite amount of 1% starch solution to each reaction medium for a known time interval.

Thermal inactivation studies of both free and immobilized enzymes at optimum temperature with respect to time were carried out by pre-incubating the respective enzyme in buffer solution of optimum pH at its optimum temperature for definite time intervals. After each time interval definite amount of enzyme preparation is withdrawn from the water bath and activity was tested by standard assay procedure done before. All the results are presented as if the highest value obtained during each reaction was assigned the value of 100% activity.

2.3.3 Determination of Kinetic parameters

The kinetic parameters of the adsorbed α-amylase and free amylase were determined in a batch reactor by measuring the rates of the reaction at various substrate concentrations ranging from 0.8mg/ml - 2mg/ml at optimum temperature and pH. K_m and V_{max} were calculated from the Lineweaver - Burk plots and Hanes-Woolf plots.

2.3.4 Storage stability of free and immobilized enzymes

The storage stability of soluble and immobilized enzymes was measured by calculating their activities after being stored at 4°C in buffer solution for a required period. The measurement was conducted at regular intervals of time. The activity was compared with initial activity and was represented as percentage initial activity retained.

2.3.5 Reusability study of immobilized enzyme

The reusability of the immobilized enzyme was tested by repeated batch experiments by measuring the residual activity of immobilized enzyme at its

optimum conditions at fixed time intervals. After each run, the immobilized enzyme was removed, washed with buffer solution and mixed with fresh substrate solution.

2.4 Physico-Chemical characterization

2.4.1 FT-IR Spectroscopy

The vibrational spectrum of a molecule is considered to be a fundamental tool that helps to understand characteristic of the molecule. It thus serves as a fingerprint for identification by the comparison of the spectrum from an ''unknown'' with previously recorded reference spectra.

In the case of polymeric materials and their additives Fourier Transform Infrared Spectroscopy is a popular tool for identification and characterization of polymer backbone and the effect of functionalization or copolymerization that have been conducted. The complexity of infrared spectra in the 1450 to 600 cm^{-1} region makes it difficult to assign all the absorption bands, and because of the unique patterns found there, it is often called the fingerprint region. Absorption bands in the 4000 to 1450 cm^{-1} region are usually due to stretching vibrations of diatomic units, and this is sometimes called the group frequency region [6].

The FT-IR spectra of polymers and enzyme immobilized polymers were obtained using Thermo Nicolet, Avatar 370 FT-IR spectrophotometer in the wavelength region 400-4000cm^{-1} using KBr pellet method at room temperature and the resolution applied was 4cm^{-1}.The spectra were corrected for the H_2O and CO_2 content in the optical path.

2.4.2 Thermo-Gravimetric Analysis (TGA)

Thermogravimetric analysis is a type of testing performed on samples that determines changes in weight in relation to a temperature program in a controlled

atmosphere. In order to determine accurately the point where weight loss is most apparent, derivative weight loss is plotted.

TGA is commonly employed in research and testing to determine characteristics of materials such as polymers, to determine degradation temperatures, absorbed moisture content of materials, the level of inorganic and organic components in materials, decomposition points of solvent residues. Analysis is carried out by raising the temperature of the sample gradually and plotting weight (percentage) against temperature. The temperature in many testing methods routinely reaches 1000°C or greater in either inert or reactive atmospheres. After the data are obtained, curve smoothing and other operations may be done to find the exact points of inflection. Linear heating rates of 5-10°C/min are typical.

Thermal studies were performed on Perkin Elmer Pyris Diamond 6 Thermogravimetric Analyzer in nitrogen atmosphere in the temperature range of 50-800°C and heating rate of 10°C per minute. Powdered samples of about 3mg were sealed in standard platinum pans. The instrument was calibrated using indium and tin as standards. Sample residual weight (TG curves) and its derivative (DTG curves) versus temperature were automatically generated by Pyris software.

2.4.3 Scanning Electron Microscopy

A scanning electron microscope (SEM) is a type of electron microscope that images a sample by scanning it with a beam of electrons in a raster scan pattern. The interaction of electrons with atoms in the sample produces signals that contain information about sample surface topography. The types of signals produced by a SEM include secondary electrons, back-scattered electrons (BSE), characteristic X-rays, light (cathodoluminescence), specimen current and transmitted electrons. Due to the very narrow electron beam, SEM micrographs have a large depth of field yielding a characteristic three-dimensional appearance useful for understanding the surface structure of a sample.

SEM images were performed using the JEOL Model JSM -6390LV scanning electron microscope.

2.4.4 Surface area measurement

Surface area is a critical parameter for supports used for enzyme immobilization. It is more beneficial when supports with high specific surface area are used when it comes to the case of industrial application. Although the catalytic activity may be only indirectly related to this surface area, its determination is generally considered as an important requirement in characterization of support [7].

The BET theory which is widely used for obtaining adsorption isotherm was developed by Stephen Brunauer, Paul Emmett, and Edward Teller in 1938. The BET theory was an extension of the Langmuir theory, developed by Irving Langmuir in 1916. Adsorption is defined as the adhesion of atoms or molecules of gas to a surface. The amount of gas adsorbed depends not only on the exposed surface but also on the temperature, gas pressure and strength of interaction between the gas and solid.

The BET equation, equation 2.4, uses the information from the isotherm to determine the surface area of the sample, where X is the weight of nitrogen adsorbed at a given relative pressure (P/Po), X_m is monolayer capacity, which is the volume of gas adsorbed at standard temperature and pressure (STP), and C is constant. STP is defined as 273 K and 1 atm.

$$\frac{1}{X[(P_0/P)-1]} = \frac{1}{X_m C} + \frac{C-1}{X_m C}\left[\frac{P}{P_0}\right] \qquad 2.4$$

Prior to the measurement all samples were degassed at room temperature for 8-10 hours in nitrogen flow. Protein adsorption on various adsorbents has been extensively studied in the literature [8-13]. Generally, proteins have shown to give Type I isotherm (Langmuir isotherm). However, numerous studies have shown that these isotherms cannot be fundamentally described with the Langmuir model [14-16].

Nitrogen adsorption measurements were performed at liquid nitrogen temperature with a Micromeritics Tristar 3000 surface area and porosity analyzer. From this specific surface area was determined. All samples were degassed at room temperature for 10 hours in nitrogen flow.

2.4.5 X-ray powder diffraction

In order to identify phase of crystalline material and to get information on unit cell dimensions X-ray powder diffraction (XRD) is widely used analytical technique. X-ray diffraction is based on constructive interference of monochromatic X-rays and a crystalline sample when conditions satisfy Bragg's Law ($n\lambda=2d \sin\theta$). By scanning the sample through a range of 2θ angles, all possible diffraction directions of the lattice should be attained due to the random orientation of the powdered material. Conversion of the diffraction peaks to d-spacing allows identification of the mineral because each mineral has a set of unique d-spacing. Typically, this is achieved by comparison of d-spacing with standard reference patterns.

In the case of natural fibers in order to detect the effect of chemical pretreatment XRD is widely used. For example Ray et al. reported that after treatment of cellulose with NaOH there was increase in the intensity of peaks when compared with the untreated ones. This is explained due to the formation of new hydrogen bonds between certain of the cellulose chains as a result of the removal of hemicelluloses, which normally separates the cellulose [17].

Crystallinity index were determined using Bruker AXS D8 Advance X-ray Powder Diffractometer.

2.4.6 Energy Dispersive X-ray Spectrometry (EDS)

In order to carry out localized chemical analysis energy dispersive X-ray spectrometry is widely used. The principle of this technique makes use of X-ray spectrum emitted by a solid sample bombarded with a focused beam of electrons to obtain a qualitative and quantitative analysis of the sample. By scanning the beam

in a television-like raster and displaying the intensity of a selected X-ray line, element distribution images or maps are obtained. The images produced reveals surface topography of the sample.

The fundamental principle that each element has a unique atomic structure allows unique set of peaks on its X-ray spectrum [18]. Qualitative analysis identifies the lines in the spectrum so as to find what elements are present in an unknown specimen. Quantitative analysis involves measuring line intensities for each element in the sample by counting pulses generated in the detector by X-ray photons.

Energy dispersive spectrometers employ pulse height analysis: a detector giving output pulses proportional in height to the X-ray photon energy is used in conjunction with a pulse height analyzer. The resolution of an EDS is good enough to separate the K lines of neighbouring elements.

EDS spectra were recorded using JEOL Model JED- 2300 make spectrometer.

2.5 Conclusion

The techniques discussed makes it easier to analyze and differentiate between the products formed via different synthesis procedures, to make sure the desired functionalization has occurred during the functionalization process and finally to confirm the immobilization of enzymes on to the supports. Also by proper preparation of immobilized enzyme and optimizing the parameters governing the immobilization, it is possible to prepare a stable biocatalyst that serves many applications for industrial purposes.

2.6 References

[1] D. Tanyolac, B.I. Yuruksoy, A.R. Ozdural, Immobilization of a thermostable α-amylase, termamyl, onto nitrocellulose membrane by Cibacron Blue F3GA dye binding, Biochem. Eng. J. 2 (1998) 179-186.

[2] T. Tosa, T. Mori, N. Fuse, I. Chibata, Studies on continuous enzyme reactions. I. Screening of carriers for preparation of water-insoluble aminoacylase, Enzymologia. 31 (1966) 214-224.

[3] U. Hanefeld, L. Gardossi, E. Magner, Understanding enzyme immobilization, Chem. Soc. Rev. 38 (2009) 453-468.

[4] O.H. Lowry, N.J. Rosebrough, A.L. Farr, R.J. Randall, Protein measurement with the Folin phenol reagent, J. Biol. Chem. 193 (1951) 265-275.

[5] W. Hartmeier, Immobilized Biocatalysts, Springer-Verlag, Berlin (1988).

[6] J. Coates, Interpretation of Infrared Spectra, A Practical Approach, Encyclopedia of Analytical Chemistry R.A. Meyers (Ed.) John Wiley & Sons Ltd, Chichester (2000) 10815-10837.

[7] J. Haber, Manual on catalyst characterization, Pure & Appl. Chem. 63 (1991) 1227-1246.

[8] J. Deere, E. Magner, J.G. Wall, K. Hodnett, Mechanistic and Structural Features of Protein Adsorption onto Mesoporous Silicates, J. Phys. Chem. B 106 (2002) 7340-7347.

[9] S.J. Sofia, V. Premnath, E.W. Merrill, Poly (ethylene oxide) Grafted to Silicon Surfaces: Grafting Density and Protein adsorption, Macromolecules 31 (1998) 5059-1070.

[10] E. Ostuni, B.A. Grybowski, M. Mrksich, C.S. Roberts, G.M. Whitesides, Adsorption of Proteins to Hydrophobic Sites on Mixed Self-Assembles Monolayers, Langmuir 19 (2003) 1861-1972.

[11] A. Vinu, V. Murugesan, M. Hartmann, Adsorption of Lysozyme over Mesoporous Molecular Sieves MCM-41 and SBA-15: Influence of pH and Aluminum Incorporation, J. Phys. Chem. B 108 (2004) 7273-7330.

[12] L.M. Karlsson, P. Tengvall, I. Lundström, H. Arwin, Penetration and loading of human serum albumin in porous silicon layers with different pore sizes and thickness, J. Colloid Interface Sci. 266 (2003) 40-47.

[13] Y. Nakashimada, Synthesis and Characterization of Conducting Polymers for use in Protein Chromatography on a MEMS Fabricated Micro Open Parallel Plate Separators (μOPPS), A thesis submitted to the Division of Graduate Studies and Research of the University of Cincinnati 2005.

[14] H.N. Öztop, D. Saraydın, D. Şolpan, O. Güven, Adsorption of BSA onto radiation-crosslinked poly (AAm/HPMA/MA) terpolymers, Polym. Bull. 50 (2003) 183 - 190.

[15] K. Hamada, K. Yamashita, T. Serizawa, T. Kitayama, M. Akashi, Adsorption of Bovine Serum Albumin onto Poly (methyl methacrylate) Stereocomplex Films with a Molecularly Regulated Nanostructure, J. Polym. Sci. Part A: Polym. Chem. 41 (2003) 1807-1812.

[16] H. Tsai, C. Chen, W. Lee, Influence of Surface Hydrophobic Groups on the Adsorption of Proteins onto Nonporous Polymeric Particles with Immobilized Metal Ions, J. Colloid Interface Sci. 240 (2001) 379-383.

[17] D. Ray, B.K. Sarkar, A.K. Rana, N.R. Bose, Effect of alkali treated jute fibers on composite properties, Bull. Mater. Sci. 24 (2001) 129-135.

[18] J. Goldstein, Scanning Electron Microscopy and X-ray Microanalysis, Springer, 2012.

****

Chapter 3

Immobilization of Diastase α-amylase on to Synthetic Polymers

Contents

3.1 Significance of polypyrrole as support for enzyme immobilization

The incorporation of enzymes into conducting polymer matrices provides very convenient and stable biocatalyst interfaces that have important practical applications. Among the conducting polymers, polypyrrole has attractive applications as one of fundamental building materials in the design of various analytical tools [1].

Polypyrrole (PPY) is one of the most promising polymers suited for technological and biomedical applications because of its stability under environmental conditions [2], thermal stability [3], bio-compatibility [4,5] bio-degradability [6], and

resistance to microbial attack [7]. The possibility of PPY synthesis in aqueous media and modification of its surface with various functionalizing agents makes this polymer a promising support for anchoring many enzymes and proteins [8,9].

The oxidation potential of polypyrrole is lower than that of pyrrole monomer; the polymer will be oxidized concurrently with pyrrole monomer during the polymerization reaction. Consequently, polypyrrole, will exist frequently in its oxidation state, carrying charges in the polymer, since a small amount of nitrogen atoms present in polypyrrole are positively charged. Although some of the counter anions present in the polymerization solution are integrated into the emergent polymer during the polymerization reaction to sustain neutrality of charge, yet the presence of the positive charges in the form of nitrogen atoms in the structure of the polypyrrole is beneficial in its applications in adsorption or filtration separation [223].

PPY is found to be promising, especially as an immobilization matrix in the design of various catalytic biosensors based on the catalytic action of enzymes, also, it is often used in the design of immunosensors and DNA sensors. Successful application of conducting polymers modified by enzymes in catalytic biosensors started by entrapment of glucose oxidase within polypyrrole [11], and employed for glucose sensing. S. Cete et al. have successfully immobilized uricase upon polypyrrole - ferrocenium film [12]. Moreover, PPY nanoparticles can be used for biosensor design. Self-encapsulation of redox enzyme- glucose oxidase E.C. 1.1.3.4 from *Penecillum vitale* (GOX) within conducting polymer polypyrrole was reported by Arunas Ramanavicius [10].

Recently, T. Sandu et al. reported immobilization of polyphenol oxidase on to polypyrrole functionalized with glutaraldehyde. The authors observed that peaks corresponding to C=O bonds seen in IR spectrum were characteristic of carbonyl and carboxyl groups which are formed through oxidative polymerization. These peaks were missing from IR spectrum of enzyme immobilized PPY which they reported as due to consumption during enzyme immobilization by the reaction with COOH or NH_2

groups from the enzyme. As per their conclusion enzyme immobilization could be done directly on pure PPY, without previous functionalization.

In order to perform as bioactive platform for the immobilization of biomolecules, it is necessary to carry out chemical modification of PPY. This can be achieved either by forming copolymers, conductive polymeric composites or blends with commercially available polymers or inorganic materials which offer better mechanical and optical properties, stability and processability [31].

3.2 Significance of Diastase α-amylase as the model enzyme for immobilization.

The Diastase α-amylase (EC 3.2.1.1; 1,4 α-D-glucan glucanohydrolase) enzyme which hydrolyzes starch to malto oligosaccharide is of great importance in present day biotechnology [13]. It was the first type of enzyme discovered in 1833, by Anselme Payen, who found it in malt solution. This enzyme catalyses the hydrolysis of α-1,4-glucosidic linkages in amylose, amylopectin and glycogen in an endofashion. It does not hydrolyse the α-1,6 linkages or any other branch points and so produces maltose and limit dextrins; the precise action pattern depends on the source of the amylase. Amylase is known to attack both insoluble starch and starch granules held in aqueous suspension.

Today diastase means α-, β-,γ-amylase (all of them hydrolases which differ in the way they attack the bonds of the starch molecules) that can break down carbohydrates. This starch degrading enzyme has received a great deal of attention because of its perceived technological significance and economic benefits.

Several methods have been developed for immobilization of α-amylase with each having its own advantages and disadvantages. α-amylase (Diastase) was immobilized on calcium alginate gel beads [14]. V. Singh et al. reported Silver nanoparticle (AgNPs) doped gum acacia-gelatin-silica nanohybrid as effective support for diastase amylase immobilization [15]. α-amylase was also found to be immobilized

onto poly (styrene-2-hydroxyethyl methacrylate) microspheres activated using epichlorohydrin [16].

Saville et al. have reported that amylase uptake on silaceous support was in the range 20-60% [17]. Aksoy et al. reported that α-amylase was covalently bound on poly (methyl methacrylate-acrylic acid) activated microspheres [18]. Kubrak et al. reported the immobilization of α-amylase via entrapment on Ca^{2+}-alginate beads [19]. Siso et al. immobilized α-amylase from *Aspergillus oryzae* onto corn grits and porous silica [20]. α-amylase was immobilized on celite by Ertan et al. via adsorption [21].

Bajpai et al. used semi-interpenetrating polymer network of poly (ethylene glycol), poly (vinyl alcohol) and polyacrylamide as support for immobilization of α-amylase [22]. P.C Ashly et al. immobilized α-amylase on poly (o-toluidine) [23] and polyaniline [24] which were prepared in both acidic and basic forms and functionalized with glutaraldehyde and ascorbic acid. Y. Ohtsuka et al. reported the immobilization of α-amylase on polymeric carriers having different structures and have found out that the amount of immobilized α-amylase mainly depended on the surface area of carriers, while the enzymatic activity depended on the texture of carrier surface [25].

In our study we carried out the immobilization of diastase α-amylase on to polypyrrole prepared using different strategies. The synthesis procedures adopted for the preparation of polymeric supports, biochemical and physico-chemical methods used for characterization of immobilized enzymes, optimization of immobilization parameters, estimation of protein and immobilization efficiency, are discussed in detail in this chapter. Finally the properties of immobilized enzymes are compared with that of free enzyme and kinetic parameters of both are evaluated.

3.3 Supports selected for our study

The supports prepared by different methods are designated as follows:

- Polypyrrole prepared by different oxidizing agents $FeCl_3$ and ammonium persulphate will be represented as PF and PA whereas PPY prepared via

interfacial polymerization will be represented as PI. Corresponding immobilized forms are represented as PFE, PAE and PIE.

- Polypyrrole prepared using surfactants SDS, CTAB and TWEEN 80 as the templates will be designated as PS, PC and PT respectively. Immobilized forms will be represented as PSE, PCE and PTE.
- Polypyrrole functionalized using glutaraldehyde as the spacer is designated as PG. Polypyrrole functionalized via coupling agent APTES is named as PN. Immobilized forms as PGE and PNE.
- Polypyrrole composites with silica and their functionalized form with APTES will be designated as PSi and PSiA respectively. The composite prepared by polymerization of pyrrole and 1-(3-aminopropyl pyrrole silica) nanocomposites will be named as PAM. Polypyrrole prepared using colloidal silica sol as templates will be designated as PM. The corresponding immobilized forms will be designated as PSiE, PSiAE, PAME and PME.
- Copolymers of polypyrrole and polyaniline will be named as PYPA. Copolymer of pyrrole and 1-(2-aminophenyl pyrrole) will be represented as PYPH. Immobilized forms are PYPAE and PYPHE.

3.4 Materials Used

Diastase α-amylase	Hi Media Laboratories Pvt. Ltd. Mumbai
Starch soluble (potato)	s.d fiNE chem. Ltd. Mumbai
Albumin Bovine	Sisco Research Laboratories Pvt. Ltd. Mumbai
Folin &Ciocalteu's Phenol Reagent	Sisco Research Laboratories Pvt. Ltd.
Chlorodimethyl vinyl silane 25ml (97%)	Sigma Aldrich

1-2 cyanoethyl pyrrole (99%)	Sigma Aldrich
1-2 aminophenyl pyrrole (98%)	Sigma Aldrich
Pottasium iodide	Universal laboratories
I_2 resublimed AR	s.d fiNE CHEM. Ltd
Ludox SM-30 colloidal silica 30wt% suspension in water	Sigma Aldrich
Glutaraldehyde	LOBA CHEMIE Pvt. Ltd .Mumbai
Aminopropyl triethoxy silane (APTES)	Sigma Aldrich
Ammonium persulphate	s.d fiNE CHEM. Ltd
Ferric chloride	s.d fiNE CHEM. Ltd
Glacial acetic acid	s.d fiNE CHEM. Ltd
HCl	s.d fiNE CHEM. Ltd
NaOH	Universal Laboratories
Pyrrole	Sigma Aldrich
Acetone	s.d fiNE CHEM. Ltd
$CHCl_3$	Spectrochem

3.5. Immobilization of α-amylase on polypyrrole prepared in presence of different oxidizing agents and different methods

In this section we have discussed the preparation of polypyrroles and investigated the effect of different oxidizing agents and different methods on the morphology of polypyrroles and compared their efficiency as support for enzyme immobilization.

3.5.1 Preparation of Polypyrrole using APS as oxidizing agent

Preparation of polypyrrole has been carried out based on the IUPAC technical report prepared for publication by J. Stejskal in collaboration with R.G. Gilbert [26]. Pyrrole (extra pure) was first distilled under reduced pressure prior to the reaction. All other reagents and solvents were of reagent grade and were used as received.

The Polypyrrole was prepared using chemical polymerization method. An acidic environment is paramount to successful polymerization because it considerably inhibits the formation of simple dimmers and other oligomers which would otherwise occur [27]. Peroxydisulphate is the most commonly used oxidant, and its ammonium salt is preferred to potassium counterpart because of its better solubility in water. The mole ratio of monomer to oxidant affects the quality of the polymer formed. Hence the recommended stoichiometric ratio of peroxodisulphate to pyrrole, 1.25:1 was used for the polymerization reaction. The polymerization was completed within 1 hour at 0-2°C. Since the reaction was exothermic, low temperature was preferred.

The main disadvantage of using APS as the oxidant is that it is stoichiometrically consumed in the reaction, which means that the reaction requires a large amount of the chemical for mass production, resulting in a troublesome treatment of the acidic by-products of the oxidant [30].

Distilled pyrrole (40 mmol, 2.8 ml) was dissolved in 100 ml 1M HCl taken in a volumetric flask. Ammonium persulphate (50 mmol, 11.4095g) was also dissolved in 100 ml 1M HCl taken in another volumetric flask. Both solutions were kept for 1 hour in an ice bath, mixed in a beaker, stirred and was kept un-agitated for 24 hours at room temperature. The next day precipitated polypyrrole was filtered out under vacuum and washed with distilled water several times to remove any impurities present. The precipitate was then washed with three 100 ml portions of 0.2 M HCl to remove the residual monomer, oxidant and its decomposition

products. PPY thus formed was uniformly protonated with chloride counter ions. In addition to this sulphate or hydrogensulphate anions from the decomposition of peroxydisulphate also participated as counter anions.

The precipitate was finally washed with acetone in order to remove low molecular weight organic intermediates and oligomers. This prevented aggregation of PPY during drying and finely powdered samples were obtained, which was dried at room temperature for 2 days and further in an oven at 60°C for 3 hours. The equation is shown below [28]:

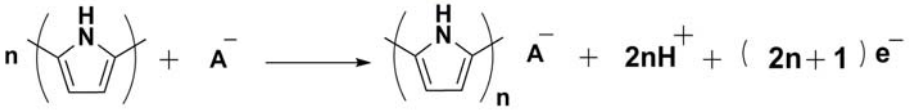

Scheme: 3.1 Preparation of polypyrrole in the presence of APS

3.5.2 Preparation of polypyrrole using $FeCl_3$ as oxidizing agent

Synthesis of polypyrrole nanoparticles was achieved using micro emulsion polymerization system by oxidation of pyrrole monomer with iron (III) chloride hexahydrate. As the oxidant was added, the colour of the solution changed to deep greenish black which was an indication of oxidation of conducting polypyrrole. The reaction product polypyrrole was obtained in the form of a black powder. The black colouration is characteristic of polypyrrole and is due to the extended system of conjugated double bonds along the polymer backbone.

In most of the published papers on the chemical polymerization of pyrrole, usually, $FeCl_3$ was used as the oxidant because a much higher conversion was obtained than with APS. The oxygen may enter the PPY structure during the polymerization process itself as a consequence of the water presence in polymerization solution, as well as by reaction of the prepared polymer with atmospheric oxygen. These facts can explain the higher yield of polymerization reaction using $FeCl_3$ as oxidant. The reaction is represented as shown below [29].

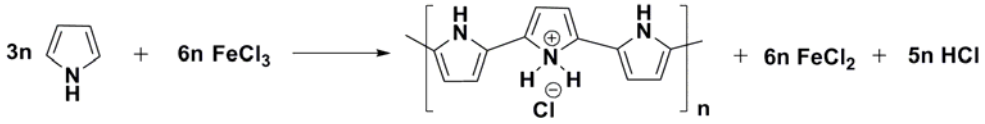

Scheme 3.2: Preparation of polypyrrole in presence of $FeCl_3$

The optimum $FeCl_3$ / pyrrole molar ratio is 2:3 and it can vary in the range 0.5 to 4 [31] and we have chosen a mole fraction of 2 for our studies. Polypyrrole (PPY) was chemically synthesized in distilled water (100 ml) by mixing pyrrole (Py) 0.18 M (1.21 ml) with an oxidizing solution of $FeCl_3$ (0.36 M). The synthesis was allowed to proceed at 5-7°C. The pyrrole solution was kept in the ice bath before adding $FeCl_3$ (5.8 g). Since this is an exothermic reaction, the addition was done slowly and at low temperature. The synthesis was performed without agitation and kept for 24 hours. The precipitate was collected by filtration, rinsed first with distilled water, then with acetone and dried at 60°C in an oven [32].

3.5.3 Preparation of polypyrrole by interfacial polymerization.

Polypyrrole were synthesized based on already reported interfacial oxidative polymerization of pyrrole monomer. Pure pyrrole was distilled just prior to the reaction. Pyrrole (12.8 mmol, 0.9 ml) was dissolved in 40 ml of pure chloroform (spectroscopic grade). An oxidizing solution, comprising of 3.2 mmol (0.73 g) of ammonium persulphate dissolved in 40 ml of 2 M HCl was gently added to the monomer solution obtained above. The mixture was left undisturbed for 24 hours and a thin layer of the polymer was obtained at the interface. Sample was isolated by centrifuging the aqueous layer, washed with de-ionized water and was dried under vacuum [33].

3.5.4 Physico-chemical characterization

3.5.4.1 FT-IR Spectrum of Polypyrrole prepared by different oxidizing agents and different methods.

Polypyrrole consists of five-membered rings linked together to form a conjugated chain. FT-IR spectra of the PPY samples synthesized at different polymerization conditions indicate the typical characteristics of PPY which were consistent with literatures.

The FT-IR spectra are of good quality and the infrared bands are well defined. The FT-IR spectrum of PPY samples were plotted with the percentage transmittance as a function of wave number (cm^{-1}). The main absorption peaks of all samples were in the same region but with variations in their relative intensities depending on the method of preparation. The unique characteristics include nitrogen-hydrogen bonds which can participate in hydrogen bonding, and both C-N and C-H ring stretching.

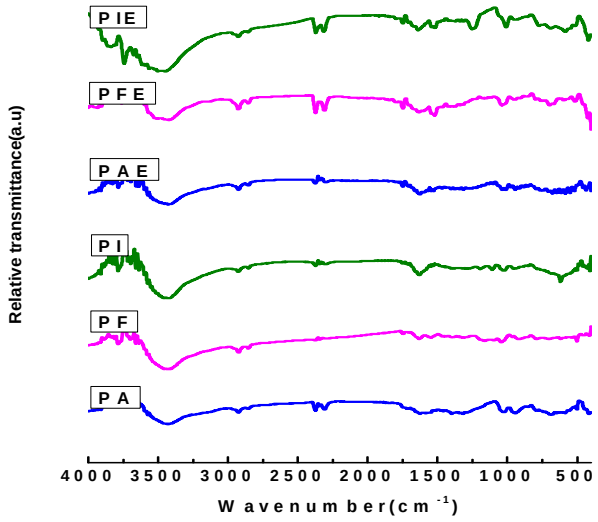

Figure: 3.1 FT- IR Spectrum of polypyrrole prepared in presence of different oxidizing agents and their immobilized forms

The oxidized PPY are characterized by a very large absorption band located in the spectral domain between 4000 and 2500 cm^{-1}, which is characteristic of the

OH groups belonging to residual water molecules trapped in the polymer matrix [34]. The spectrum of the polypyrrole powder showed that the N-H stretching band of pyrrole ring also appeared at 3433 cm^{-1}. The small peaks at 2925 and 2851 cm^{-1}, are due to aromatic five-membered ring C-H ring stretching.

Table 3.1 Assignment of main peaks in the spectra of PPY prepared in presence of different oxidizing agents (w-weak, vw- very weak, s-strong)

Peak assignments (cm^{-1})	PA	PAE	PF	PFE	PI	PIE
N-H stretch	3433	3428	3428	3424	3435	3446
C-H stretch	2929m, 2856w	2926m, 2849w	2924, 2856w	2926, 2852w	2924w 2856vw	2926w 2856vw
C=O	1710vw	1745w	1702w	1753w	1708w	1705, 1748vw
C-C-N inter ring bending	1630bm	1656, 1596,	1633.6s	1644 1596,	1640s	1656, 1644,
C=C stretch,C-H ring inplane bending	1549	1542	1544	1542	1547	1542
C-N stretch	1116	1110	1109	1108	1112m	1110
N-H ring out of plane bending (vs)	1045	1040	1044	1035	1027m	1009
Ring deformation	947	948	963	944	947	939
C=C-N in plane deformation	856	859	856	862	856	852

The intensity of the sharp bands located at 1710 cm^{-1} depends on the oxidation degree of the polymer. Indeed, this band is weak in the reduced form and is intensified in the oxidized form [34]. According to Lei and Martin polypyrrole is actually a copolymer of pyrrole and hydroxypyrrole [35].

The hydroxyl bands in the IR spectrum had been obscured by a broad absorption from 1600 cm^{-1} upwards due to the conductivity of polypyrrole. Reduction of the polymer had failed to completely eliminate this broad absorption because of partial oxidation by traces of oxygen. On the basis of these data, the band can be attributed to carbonyl groups fixed in the position of some pyrrole

rings which is the consequence of the nucleophilic attack of water molecules on pyrrole during preparation [36]. The hydroxyl groups introduced in the ring by this attack would finally produce carbonyl groups by keto-enol tautomerism [37].

The literature lists, a band at 1458 cm^{-1}, due to the conjugated C-N bond stretching vibration in the ring. The bands located around 900 cm^{-1}, 1200 cm^{-1} and 1550 cm^{-1} are characteristic of the oxidized PPY that have been associated by Zerbi with the effective conjugation coordination and show sensitivity to the oxidation level and to the conjugation length of the chain [38]. The band located at 1550 cm^{-1} in the spectrum is attributed to C=C / C-C stretching vibrations of the PPY chain.

The very weak peaks around 1384 cm^{-1} appear in most PPY spectra. These peaks are assigned to C=O bond from carboxyl groups which are formed through oxidative polymerization. These peaks are missing from PPY-E spectrum because they are consumed during enzyme immobilization, by reaction with COOH or NH_2 groups from the enzyme. Similar results were also reported by T. Sandu et al. [39].

The peaks at 1344 cm^{-1} and 1315 cm^{-1} arise as a result of C-C in ring stretching. The peak near 1300 cm^{-1} is due to C-N stretching of the polymer and peak at 1380 cm^{-1} is because of $C\text{-}N^{+}$ stretching and C-C vibration [40].

The band at 1296 cm^{-1} corresponds to C-H deformation. The IR spectra for pyrrole in water display intense narrow bands of plane vibrations of deformation at 1019 cm^{-1}, 1045 cm^{-1}, 1075 cm^{-1} respectively. The C=C stretching of aromatic compounds generally occur in the range of 1000-1100 cm^{-1}.

The band observed near 950 cm^{-1} is due to the C-H out of plane bending. The peak at 750-780 cm^{-1} inferred the presence of polypyrrole indicating C-H, -N-H ring out of plane bending and peak near 800 cm^{-1} is due to the C-N stretch [28].

The spectra of all of the samples displayed the characteristic peaks of polypyrrole with noticeable differences due to shifts to either higher or lower frequencies, depending on the experimental conditions [41]. These shifts in the

frequencies could be interpreted in terms of the nature of the dopant and its influence on the ring vibrations of polypyrrole [38].

Various IR bands and their assignments are given in table 3.1. The IR studies reflect difference in molecular orientation and crystallinity of each PPY sample. Similar spectral differences have been attributed to the changes in conformation, molecular ordering, and packing of the polymers as in previously reported IR studies [42].

When α-amylase was immobilized on to these samples characteristic additional peaks corresponding to enzyme structure was observed around 1650 cm^{-1}. This can be ascribed to the amide I band that represents the stretching vibrations of C=O bonds in the backbone of the protein [43].

FT-IR spectra shows bands centered at 1648 and 1544 cm^{-1} that can be attributed to amide I and amide II, respectively. The amide II band arises from the combination of C-N stretching and N-H bending vibrations of the protein backbone [44], which confirms the incorporation of enzyme into the polymers [45].

The spectra also indicate an amide group at 3424 cm^{-1} (N-H stretching) for PFE, 3428 cm^{-1} for PAE and 3446 cm^{-1} for PIE. The bands at 1596 cm^{-1} (N-H bending), and 1656 cm^{-1} corresponds to C=O stretching. α-amylase contains a major percentage of aspartic and glutamic acids along with other amino acids [46]. The spectrum clearly indicates the presence of carboxylate ion groups at 1646 cm^{-1} a broad strong band [asymmetrical $(C\text{-}O)_2$ stretch] and 1398 cm^{-1} [symmetrical $(C\text{-}O)_2$ stretch], respectively. In addition to these bands, the other observed peaks are the asymmetrical $(\text{-}NH_3)^+$ N-H band at 1317 cm^{-1}, and the symmetrical ($\text{-}NH_3^+$) N-H band at 1510 cm^{-1}[22].

A band at 2932 cm^{-1} in all immobilized samples is due to CH_2 groups of α-amylase [47]. Almost all bands get broadened after immobilization of α-amylase. Thus the peaks observed in the spectrum match well with the ones available in the literature confirming the formation of polypyrrole and its immobilized forms.

3.5.4.2 Thermogram of α-amylase

The TG and DTG curves for free amylase were characterized by several weight loss peaks. The first weight loss in TG was at temperature range from 90°C to 140°C, which might be due to dehydration of the interstitial water that gets adsorbed in the free α-amylase sample. From 200 to 360°C, continuous weight loss was observed indicating a complete decomposition of the organic structure of the enzyme as it could not withstand such elevated temperatures. The DTG curve shows two major peaks at 140 and 235°C and three minor peaks at 200, 292 and 362°C. The peak at 140°C corresponds to loss of water molecules that are trapped in the enzyme molecule. The other peaks might be the result of gradual decomposition of enzyme's organic structure.

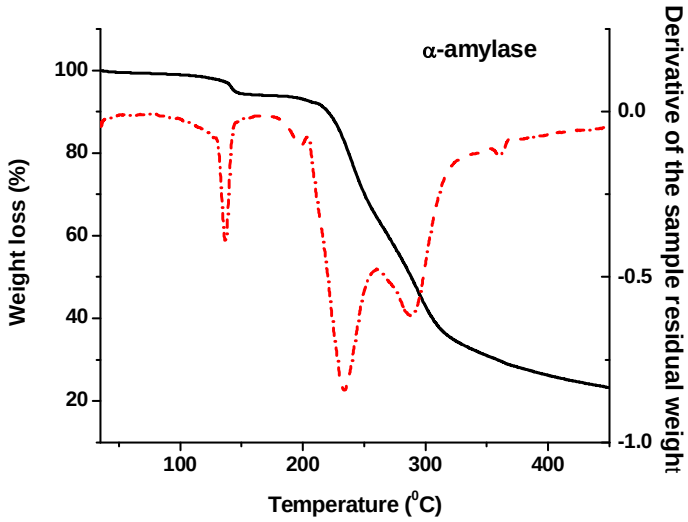

Figure: 3.2 Thermogram of α-amylase

3.5.4.3 Thermogram of polypyrrole prepared in presence of different oxidizing agents and via different methods

The TG curves of polpyrrole prepared in the presence of different oxidizing agents and different methods are shown in the figure: 3.3. From the figure it is clear that the thermal stability of polypyrroles differ significantly as the oxidants and methods was varied. In all cases the initial weight loss was attributed to loss of water, the second weight loss was assigned to loss of any dopants and solvent molecules that get adsorbed on the surface of polymer backbone. Finally the third weight loss will be the decomposition of polymer structure.

The first significant weight loss occurs already at temperature between 30 and 100°C. It is known, that PPY is hygroscopic and during the heating to 100°C the residual water evaporates. For PA the main mass loss, which corresponds to polymer degradation, starts at about 187°C. The second minor weight losses corresponding to polymer decomposition starts at 336°C which continues up to 800°C.

But after immobilization PAE showed major weight loss at 157°C due to protein degradation after which weight loss occurred at 309°C, and is continuous till 800°C which corresponds to polymer decomposition.

For PF the main weight loss starts with a broad peak at 234°C and minor weight loss at 577°C. After immobilization of α-amylase the weight loss starts at 226°C which might be the result of protein degradation of α-amylase. The major weight loss at 277°C & 302°C corresponds to polypyrrole decomposition which is continuous till 800°C.

In the case of PI the major decomposition due to polypyrrole degradation starts at 255°C and minor weight loss starts at 415°C which continues upto 800°C. When α-amylase was immobilized the major decomposition peak starts at 194°C which is attributed to degradation of organic structure of enzyme. The weight loss corresponding to that of polymer backbone was observed at 296°C which continues up to 800°C.

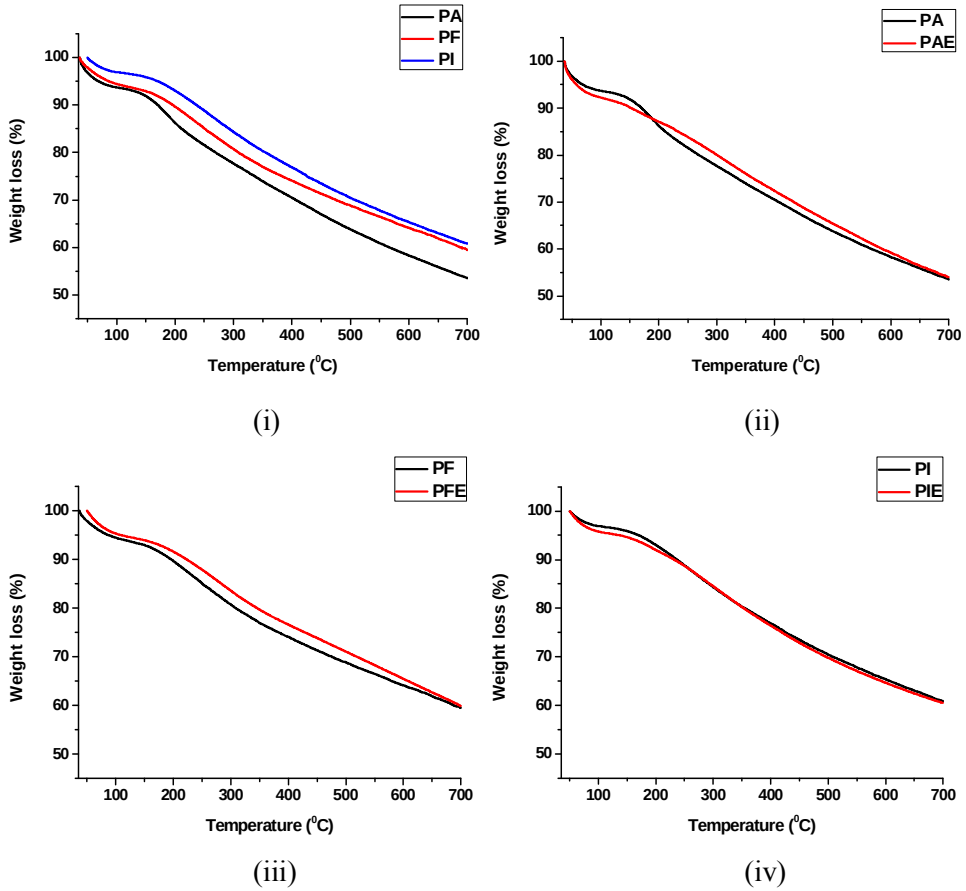

Figure: 3.3: Thermograms of (i) PA, PF and PI (ii) PA and PAE (iii) PF and PFE (iv) PI and PIE

3.5.4.4 Surface Area analysis

BET surface area of polymers before and after immobilization of α-amylase is given in the table 3.2. For all polymers prepared by conventional chemical polymerization method in the presence of oxidizing agents APS and $FeCl_3$, the surface areas obtained were too low. The polymer prepared using APS as oxidizing agent was found to have higher surface area than that prepared with $FeCl_3$ as the oxidant. For interfacial polymerization method the surface area was slightly more than that produced using $FeCl_3$ via bulk polymerization method.

Table: 3.2 Surface areas of PPY polymers

Polymers	Surface area (m^2/g)
PA	15.6
PF	4.6
PI	8.7
PAE	4.8
PFE	1.39
PIE	3.39

3.5.4.5 Scanning electron microscopy

The scanning electron microscopy was performed in order to investigate the dimensions and the surface morphology of polypyrrole samples.

Polypyrrole prepared in presence of ammonium persulphate as the oxidizing agent (PA) showed globular structure with particle size ranging from 116 nm-228 nm. Literature studies revealed that dopant anion has a profound influence on the morphology of PPY formed [48]. In the case of persulphate as the oxidant sulphate anions played the role of dopant anion in the synthesis medium. As persulphates are relatively strong oxidants (E_0=2.1V) it has much faster polymerization rate. The higher nucleation speed in the system increases the aggregation of nuclei and the stabilization is less effective which results to larger particles in the final dispersion.

The SEM micrographs of polypyrrole prepared in presence of $FeCl_3$ as oxidizing agent (PF) exhibited globular sized particles which have a distribution of dimensions between 120-440nm.

The SEM images of polypyrrole prepared by interfacial polymerization (PI) also showed globular structures with particle size ranging between 200-440 nm. It is because the reaction time and method of polymerization has significant impact on the resulting polymer morphology.

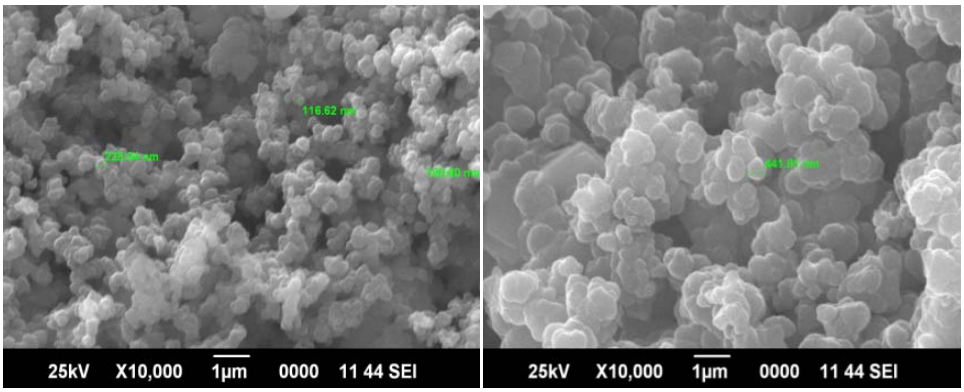

(i) (ii)

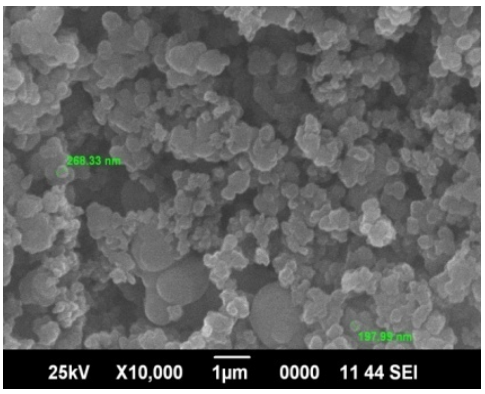

(iii)

Figure: 3.4: SEM images of (i) PA (ii) PF (iii) PI

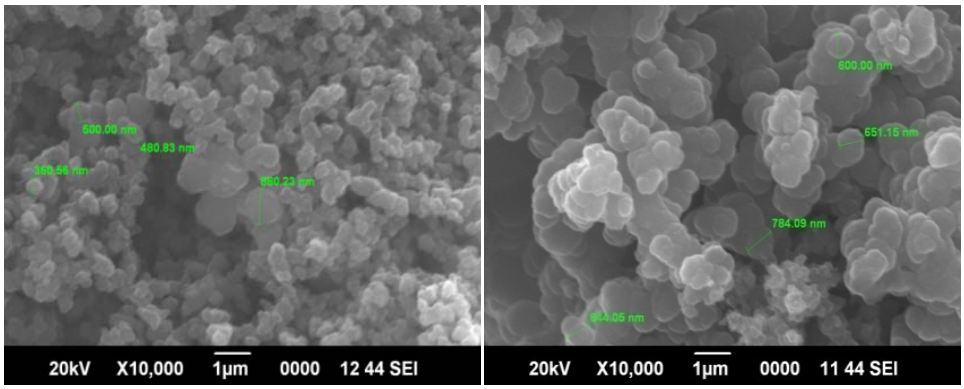

(iv) (v)

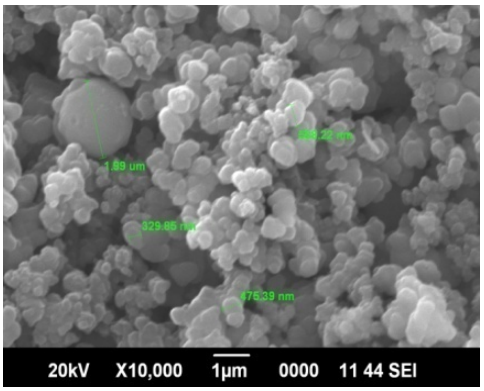

(vi)

Figure: 3.5: SEM images of (iv) PAE (v) PFE (vi) PIE

3.5.5 Biochemical characterization

3.5.5.1 Coupling of α-amylase on polymer supports and their immobilization efficiency

The pH of the medium has a similar effect on both free and immobilized enzymes, but the pH stability relationship is of even greater concern with immobilized enzymes which have to undergo adverse conditions during coupling. Thus pH at which enzymes bind to a support is a critical parameter to be determined for any method of immobilization. It is enzyme activity which is of great concern and this is the product of total bound protein, which generally increases at a particular range of pH depending on the support and enzyme surface charges, and retains activity, which falls as the pH of coupling solution becomes more extreme.

Thus the optimum pH for binding may be a complex function and usually has to be determined empirically, taking into account of the enzyme's stability and the known protein binding character of the support [49]. Amino, thiol, carboxyl, phenolic, guanidine, imidazole, disulphide, indole, thioether and hydroxyl groups of the aminoacid chain are responsible for linking to a support matrix [50]. The amount

of enzyme adsorbed depends on nature of support, type of enzyme, concentration of enzyme, medium used for immobilization, contact time, temperature, pH etc.

So the inevitable part of every immobilization study is the investigation of each of these parameters. The effect of pH of medium in which the enzyme is dissolved during immobilization on to polymeric supports is shown in the figure: 3.6.

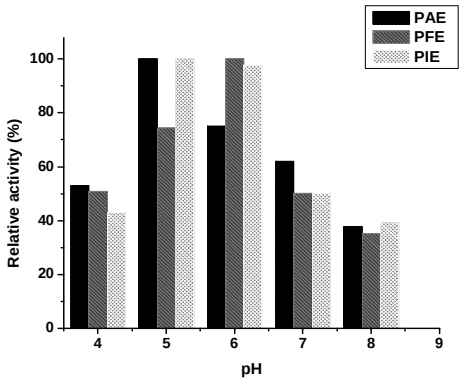

Figure: 3.6: Effect of pH of immobilization medium on the relative activity of immobilized α-amylase

Amylase adsorption was investigated in different pH's of buffer solutions that are in the range 4-8, because amylase becomes unstable above pH 9.0 as its isoelectric point is around 4.6. The pH range for activity of diastase α-amylase is in the range 5-8 with optimum pH between 5 and 5.5. PPY has an isoelectric point around 7 [51]. Both polypyrrole and amylase does not have a strong charge at pH close to its isoelectric point. Above isoelectric point both are positively charged and below isoelectric point both are negatively charged.

The maximum activity of the immobilized enzyme was observed in the range 5-6. The optimum pH is that which favours the interaction between the enzyme and support in such a way that maximum activity of biocatalyst can be retained with better immobilization efficiency. It was found that pH 5 was best for immobilization of α-amylase on PA and PI and pH 6 for PF.

At pH 4 PPY have overall net positive charge and lysine and arginine amino acid residues on the protein surface of amylase have slight positive charge as it is close to its isoelectric point. Hence PPY should repel amylase. However, the results were different from what was expected. Hydrophobic interactions appear to dominate amylase adsorption at pH 4 for the polypyrrole adsorbent. This is because PPY is hydrophobic as it has large aromatic rings in the polymer backbone. Therefore, for these adsorbents, hydrophobic interactions dominate and the effect of pH is minimized. The small adsorption difference due to pH might originate from ionic effects, as a result of secondary amino groups of the pyrrole rings.

At pH 5, the secondary amino group possesses positive charge and it attracts α-amylase, which has a net negative charge. At pH 6 also the secondary amino group of PPY has net positive charge and these amino groups in polypyrrole are accessible to face to protein molecules without steric hindrance. Hence it attracts net negatively charged amylase molecules. At pH 7 PPY has no charge and hence hydrophobic interaction dominates over electrostatic attraction.

When the immobilization is carried out at higher pH, the same amount of enzyme is immobilized, however the activity of the immobilized enzyme is lower than when the immobilization process is carried out at pH 5 and 6. This is because at higher pH PPY adsorbents have overall net negative charge and amylase is also having net negative charge which results in electrostatic repulsion.

Thus the strength of the electrostatic interaction between the enzyme and the adsorbent is very important in maintaining the overall activity of the enzyme. The variation of activity with pH, within a range of 2-3 units each side of the pI, is normally a reversible process [52]. The curve profile became much broader between pH 5 and 7 although optimum pH of free enzyme was at pH 5.

The native enzyme could not survive with increase in pH towards alkalinity. This shows that the stability of the enzyme against pH was significantly improved upon immobilization. This is possible due to the stabilization of enzyme

molecules resulting from multipoint attachment on the surface of support and due to the charge effects of the support.

The difference in adsorption encountered among different adsorbents on immobilization pH can be explained based on their morphological difference as a result of their difference in preparation conditions. This was also evident from their characterization studies conducted via SEM and BET analysis. PA has smaller particle size compared to other two which correspondingly resulted in increase in surface area and hence increase in adsorbed amount of enzyme on it than the other two.

3.5.5.1.1 Effect of contact time on the activity of α-amylase

The contact time needed for enzyme to get adsorbed on PPY adsorbents is shown in the figure: 3.7.

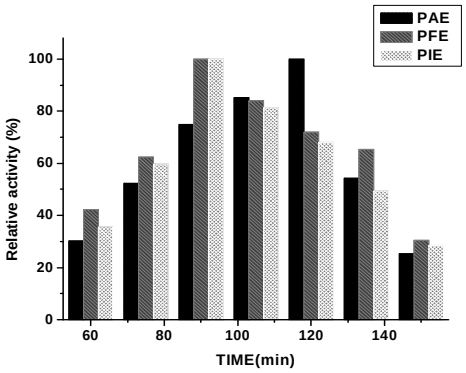

Figure: 3.7: Optimization of immobilization time needed for effective coupling of α-amylase.

Adsorption occurs at the moment of contact when enzyme solution in a particular pH is added to PPY. Enzyme activity and adsorption first increases with increase in contact time and after that even if adsorption of enzyme increases, activity is found to decrease which might be due to lower accessibility of substrate as a result of multilayer adsorption of enzyme [53]. For all adsorbents optimum activity was obtained at 120 minutes of contact time.

Ball and Ramsden also mentioned that the amount of enzyme adsorbed increases with increase in enzyme concentration indicating that the electrostatic interactions between the molecules promote further adsorption [54]. This means that when the enzyme concentration is high, protein aggregation increases the surface adsorption capacity. But the active sites that are exposed to substrate get decreased as several of these sites get blocked due to overlaid protein layer one above other.

3.5.5.1.2 Effect of initial protein concentration on protein loading on to supports

The amount of protein bound to PPY adsorbents was analyzed based on the optimized conditions obtained.

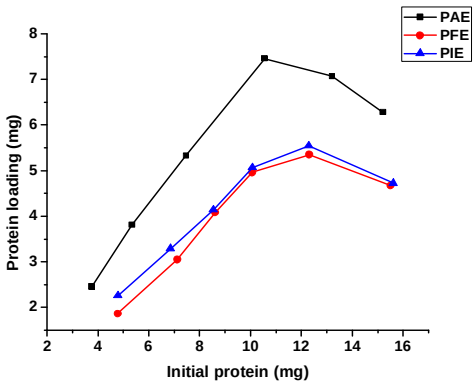

Figure: 3.8: Change in protein loading with respect to initial amount of protein added to support

The effect of initial protein concentration on protein loading is depicted in the figure: 3.8. Apparently, adsorbed amount of enzyme increases with increase in enzyme concentration. But after a particular concentration no further increase in adsorption occurs, instead a saturation point is reached and enzyme starts desorbed from the surface if loaded heavily. The amount of adsorbed protein depends on the strength of interaction between enzyme and the support and method of immobilization.

Even if maximum amount of enzyme get adsorbed at higher concentrations, optimum concentration was selected based on the optimum activity shown by the

immobilized enzyme at a particular concentration. As a result of this baseline kept throughout the study, many of the results were contradictory than expected. Usually we expect an increase in activity with increase in enzyme loading. Shift from this usual trend occurred as a result of the fact that during the immobilization process, the multipoint attachment to support unavoidably hampers the free conformation of enzymes and sometimes non-biospecific interactions of enzyme with the support results in the denaturation of enzyme protein, and thus resulting in its activity and stability losses [55]. It is thus important that the properties of support and immobilization processes should be well understood in order to improve activity retention of the immobilized enzyme [56].

3.5.5.1.3 Effect of initial protein concentration on the immobilization yield and activity of loaded enzyme.

Immobilization yield obtained for all adsorbents at various concentration taken are shown in the figure: 3.9.

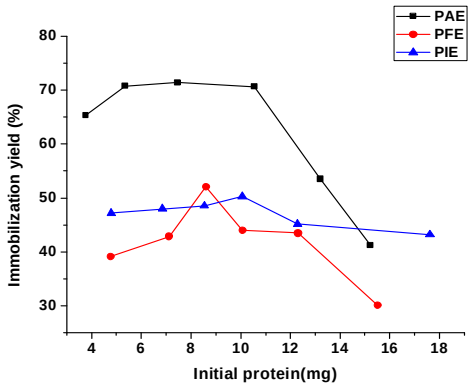

Figure: 3.9: Effect of initial protein concentration on immobilization yield of enzyme

From the figure: 3.9 it is clear that on addition of protein to the support, protein loading increases which then reaches a saturation point and then starts decreasing, which might be due to desorption at high loading due to weak interaction between enzyme and the support. Thus the optimum intake of protein

with maximum retention of its activity on PA, PF, and PI are 7.5 mg/g, 4.4 mg/g and 4.7 mg/g respectively. The corresponding immobilization yield was 71%, 44%, and 43% respectively.

Immobilization yield was not the prime parameter in optimizing protein loading in all cases; instead it is the activity of immobilized enzyme that played the key role in deciding the effectiveness of adsorption at a particular concentration. Because in the case of PA upon the addition of 7.5 mg of initial protein, optimum immobilization yield of about 71.4% was obtained. But maximum protein loading obtained at initial protein amount 10.5 mg with corresponding optimum activity 6.4 EU, and immobilization yield of only 71%.

But in the case of PF optimum activity and optimum immobilization yield (IY) was obtained at the same concentration. At initial protein amount of 10.1mg, IY of about 44% was obtained with maximum immobilized enzyme activity 7.7 EU.

For PI the optimum activity of 7.6 EU was observed when the protein load was 4.7 mg with initial protein amount of 15.6 mg.

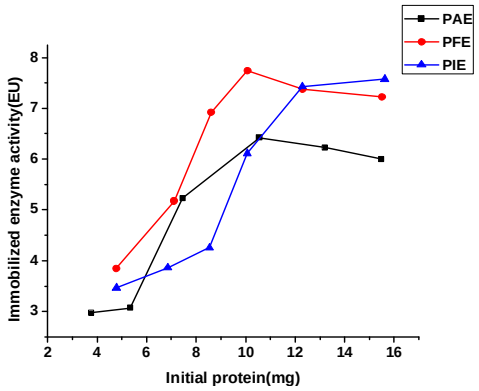

Figure: 3.10 The trend of immobilized enzyme activity when initial protein amount was varied.

The trend of immobilized enzyme activity when initial protein amount was varied for all adsorbents is shown in the figure: 3.10. The increase in immobilization yield of PA compared to other two is supported by the increase in surface area obtained

for it via BET analysis, than the other adsorbents. The SEM images also underline this fact as it is evident from the decrease in particle size of PA which results in increase in surface area.

The activity yield and immobilization efficiency are also evaluated. The results are tabulated in the table 3.3.

Table: 3.3: Immobilization efficiency of α-amylase on PPY prepared in presence of different oxidizing agents and different methods

Polymer	Initial protein (mg)	Immobilized protein mg/g support	Immobilization yield (%) IY	Initial activity (EU)	Immobilized enzyme activity (EU)	Activity yield (%) AY	Immobilization efficiency (%) IE=AY/IY
PA	10.5	7.5	71	34.5	6.4	19	26
PF	10.1	4.4	44	22.9	7.7	34	77
PI	15.6	4.7	43	21.3	7.6	36	82

Various binding capacities and preserved activities are given in the literature for α-amylase immobilized systems. When adsorption was achieved chemically onto polystyrene and polyaniline supports, coupling capacities and preserved activities are reported as 3 and 2.2 mg/g support and 7 and 18%, respectively [75,24].

3.5.5.2 Effect of pH on enzyme activity

The procedure of immobilization usually has a variety of effects on the conformation as well as on the state of ionization and dissociation of an enzyme and its environment; it results in changes in the relationship between pH, stability and activity of immobilized enzyme. These changes in pH would alter or totally inhibit the enzyme from catalyzing a reaction.

The pH effect on the activity of the free and immobilized forms of α-amylase has been studied in buffer solution at different pH in the range 4-8 and the results are presented in the figure: 3.11 and table: 3.4.

Table 3.4: Optimum pH found out for PAE, PFE and PIE

	Free enzyme	PAE	PFE	PIE
pH	5 & 5.5	5.5	5	6

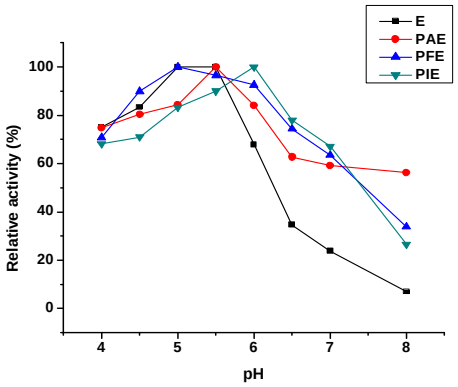

Figure: 3.11: Effect of pH on percentage relative activity of free and immobilized α-amylase

The optimum activity is represented as 100% and other activities are expressed relative to this optimum activity. Free enzyme exhibits maximum activity in the pH range (5-6) with optimum activity at 5 and 5.5. At pH 4 and 8 a decrease of the enzymatic activity is observed for both the immobilized and the free enzyme; however, at pH 8 the residual activity of the immobilized enzyme in most samples is significantly higher than that of free enzyme.

The native enzyme could not survive with increase in pH towards alkalinity. The immobilization process provides structural stability, preventing an irreversible unfolding of the enzymatic protein.

The immobilized enzyme has the same optimum pH in the range 5-6 but with a much broader profile, which was also beneficial for their applications. The inhibition of activity in the lower pH ranges may be due to two reasons: a lower

loading and a possible change of the enzyme conformation due to an unfavourable charge distribution on the amino acid residues [57]. A change in pH will affect the intra-molecular hydrogen bonding thus leading to a distorted conformation that will reduce the activity of the enzyme.

For amylase immobilization, shifts in the optimum pH towards both the acidic and alkaline directions have been observed [16, 58]. For PAE the optimum pH was at 5.5, for PFE it was at 5 and for PIE it was at 6. The slight differences in pH might be due to morphological differences in the PPY adsorbents that occurred as a result of difference in synthesis procedures adopted. Thus the charge on the carrier surface also changes the microenvironment of the enzyme bound to it thereby resulting in shift of the pH of the reaction medium after immobilization [224,225].

At very high pH, enzyme inactivation occurs via oxidation of sulphur containing aminoacids and/or deamidation of glutamine residues [59].

3.5.5.3 Effect of temperature on the activity

The effect of temperature on the activity of free and immobilized α-amylase was studied by carrying out the reaction in such a way that the incubation temperature during the reaction was varied in the range 30-60°C. The results are shown in the figure: 3.12.

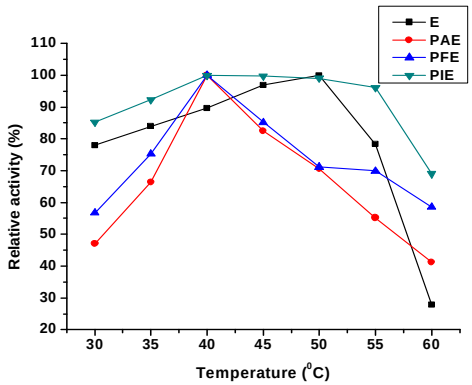

Figure: 3.12: Effect of temperature on the activity of free and immobilized α-amylase

The optimum temperature of native enzyme was 50°C which, as a result of immobilization, get shifted to 40°C for PAE and PFE but to 50°C for PIE. This change in temperature might arise from alterations that arise in the conformation of enzyme structure by immobilization which thus favoured amylase activity in a broad range.

The changes in optimum temperature among adsorbents occurred as a result of morphological differences among them which might affect the mode of adsorption that could cause significant alterations in the structural conformation of enzyme at the active site. Handa et al. have reported a 5°C decrease in optimum temperature when α-amylase was immobilized on to polyacrylonitrile [65]. Ashly et al. also reported a similar decrease in optimum temperature when α-amylase was immobilized on polyaniline and poly (o-toluidine) [24,23].

The decrease in the optimum temperature might be due to change in conformational integrity of the enzyme structure by immobilization which favoured amylase activity below 50°C [16, 66, 67].

On elevated temperature the denaturation of an enzyme corresponds to the unfolding of the enzyme by disruption of non-covalent intra-molecular interactions which affected the conformation of protein and resulted in an alteration of enzyme-substrate affinity [68].

3.5.5.4 Thermal stability of the free and immobilized enzymes

Besides affecting the biocatalyst, temperature, like pH, has an impact on substrate stability. Like all other proteins, enzymes are susceptible to thermal denaturation, whether they are immobilized or in the free state. In many cases, however, the rate of inactivation and denaturation of an immobilized enzyme is less than that of the free enzyme.

Since the mobility of enzyme is restricted upon immobilization, it retards the unfolding of protein thereby maintaining activity. But, as the time passes this reduction in mobility is eliminated due to weak nature of enzyme-support

interactions like electrostatic, Van der Waals, ionic and hydrophobic interactions and therefore results in protein unfolding and corresponding reduction in activity.

Thermal stability of both free and immobilized enzymes was investigated by incubating them in buffer solution of optimum reaction pH obtained, for 1hour at various temperatures in the range 30-60°C in a water bath. The results are shown in the figure: 3.13.

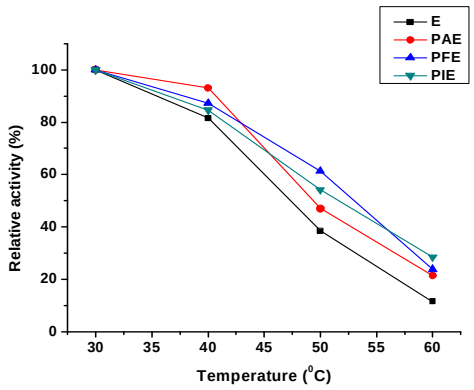

Figure: 3.13: Effect of temperature on the stability of both free and immobilized α-amylase

Both free and immobilized enzyme showed maximum activity when incubated at 30°C for 1hour. As the temperature increased, the stability dropped significantly for both free and immobilized amylase. At 40°C, both free and immobilized enzyme retained up to 80-90% of their activity. At 50°C for 1hour the immobilized enzyme was inactivated at a much lower rate than the free enzyme. Similar increase in thermal stability was observed when Pessela et al. performed immobilization of β-galactosidase from *Thermus sp. T2* via ionic adsorption onto two different supports: a new anionic exchanger resin, based on the coating of Sepabeads internal surfaces with polyethylenimine (PEI) polymers (Mw-25,000), and traditional DEAE-agarose [69]. The free enzyme lost almost 90% of its activity at 60°C after 1hour treatment whereas, immobilized amylase lost 80% of its activity. Figure: 3.14 shows effect of pre -incubation time on the activity of each immobilized enzyme.

About 50-60% of immobilized enzymes maintained their activity when subjected to 120 minutes of pre-incubation time at their respective optimum temperature whereas; free enzyme could retain only 10% of their initial activity when subjected to same period of time. These results suggest that the thermal stability of α-amylase increased considerably as a result of immobilization on to PPY adsorbents and is suitable for long term applications. Improved thermal stability of α-amylase was reported by Sanjay et al. while immobilizing α-amylase on clay supports; Reshmi et al. while immobilization of α-amylase on to zirconia, Ashly et al. during the immobilization of α-amylase on polyaniline and poly (o-toluidine) polymers and Bryjak when using acrylic carriers as the support for α-amylase immobilization [23,24,70,71].

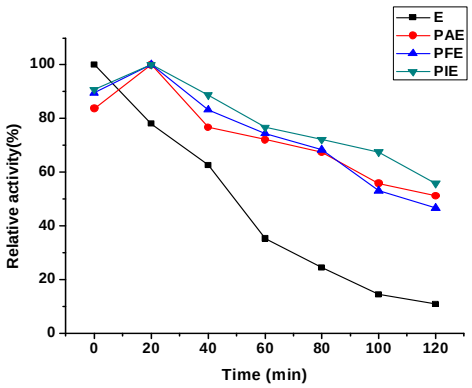

Figure: 3.14: Effect of pre-incubation time on the activity of free and immobilized α-amylase

In the case of adsorption increase in thermal stability was ascribed to enhanced enzyme rigidity due to strong direct electrostatic interaction of support with the enzyme thus preserving its tertiary structure from conformational transition that might occur at elevated temperatures. Similar enhancement in the thermal stability after immobilization was observed by Zhao et al. [72]. The authors immobilized glucoamylase from *Aspergillus niger* onto functionalized magnetic SBA-15 (FeSBA-15) as a regenerated support through metal-ion affinity interactions. After particular temperature the denaturation of an enzyme encounters

which corresponds to the unfolding of the enzyme by disruption of noncovalent intra-molecular interactions. This can be induced by any change in the enzyme environment because of increase in temperature.

3.5.5.5 Determination of kinetic parameters

The velocity of enzyme reaction is decisively influenced by the concentration of its substrate. In cases this relationship obeys Michaelis-Menten kinetics, K_m the Michaelis constant and V_{max}, the maximum rate at which the reaction proceeds at infinite substrate levels are the two most important parameters used to characterize the kinetic properties of the enzyme. These are determined by varying the concentration of starch in the reaction medium. The Michaelis constant provides a measure of affinity of enzyme active site for its substrate and apparent K_m values obtained were higher than those for native enzyme. This difference in K_m value occurred as a result of obstruction in the access of substrate to active site of the enzyme by diffusion barriers. This hindrance might be due to micro-environmental effects of the carrier as a result of immobilization method which thus alters the proper orientation and conformation of protein structure preventing it from being more accessible to substrate [73].

On the other hand, the V_{max} which measures the maximum catalytic potential of the enzyme follows an opposite trend. It usually shows a decrease in trend during immobilization of enzymes as is widely observed and reported in most studies [23,70]. This loss in activity may be attributed to either a loss in native conformation on account of immobilization or steric hindrance in immediate vicinity of the enzyme molecule caused by diffusional limitation of carrier or shielding effect of carrier.

The kinetic parameters of free and immobilized enzyme are shown in table 3.5. Lineweaver-Burk plots and Hanes-Woolf plots of free and immobilized α-amylase are shown in figure: 3.15

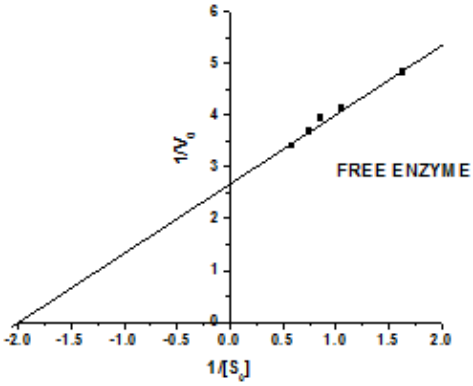

(i)

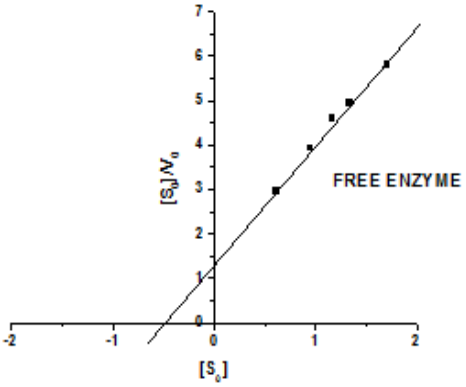

(v)

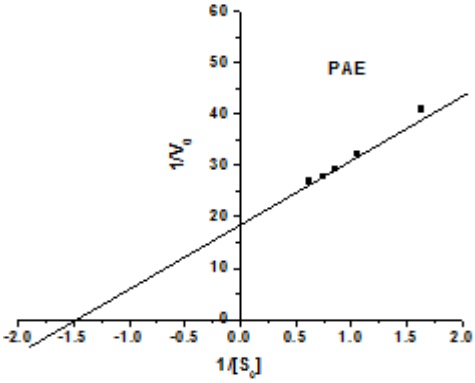

(ii)

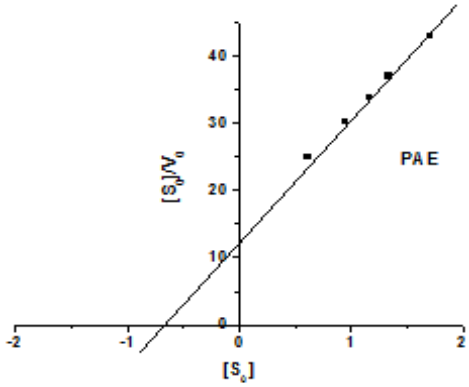

(vi)

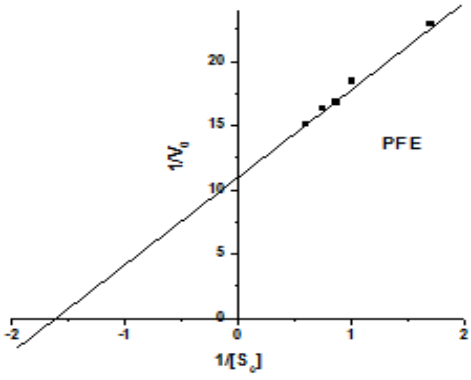

(iii)

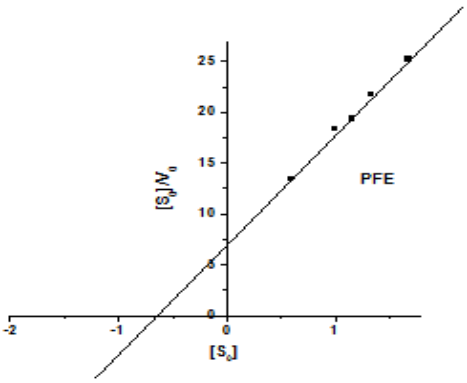

(vii)

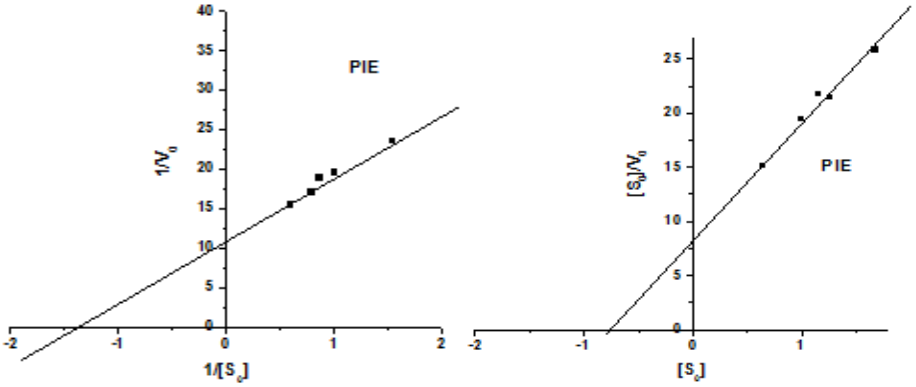

(iv) (viii)

Figure: 3.15: Lineweaver-Burk plots for evaluation of K_m and V_{max} for free and immobilized α-amylase (i) free enzyme (ii) PAE (iii) PFE (iv) PIE. Hanes-Woolf plots for (v) free enzyme (vi) PAE (vii) PFE (viii) PIE**.**

Table 3.5: Kinetic parameters for free and immobilized α-amylase

Lineweaver - burk plot	Free enzyme	PAE	PFE	PIE
K_m ($mgml^{-1}$)	0.50 ± 0.04	0.67 ± 0.01	0.63 ± 0.03	0.73 ± 0.01
V_{max} (mg/ml/min)	7.40 ± 0.05	2.45 ± 0.04	3.13 ± 0.04	3.20 ± 0.06

3.5.5.6 Storage stability of Immobilized α-amylase

It was observed that storage stability of an immobilized enzyme in the wet state is often better than that of free enzyme in a similar solution due to high local concentration of protein in the medium. If the enzyme is used soon after preparation, maximum activity was found to be obtained when it was suspended in buffer and stored at 4°C. While storing enzyme for long periods sometimes removal of water may be necessary for which freeze drying was found to be more effective than simple drying in retaining maximum activity. Simple drying is inadvisable since this can cause loss of the three dimensional structure of both enzyme and matrix.

In most cases results obtained showed that storage stability of the immobilized enzyme was significantly better than free enzyme. In order to

compare the efficiency in storage, free enzyme and immobilized enzymes were stored in buffer solution under same conditions. The free enzyme lost all of its activity within 2 days whereas; under storage less reduction in activity was observed for immobilized enzymes. The decrease in stability of immobilized enzyme during 6 months of storage is shown in the figure: 3.16.

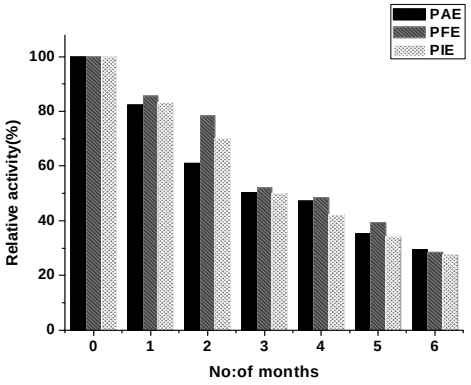

Figure: 3.16: Storage stability of immobilized enzymes at 4°C

From the bar diagram it is evident that all immobilized enzymes retained more than 50% of initial activity after 3 months of storage with PFE and PIE retaining more activity compared to PAE. This might be due to morphological differences among them which were favourable for immobilization of enzyme on PI and PF than PA. The results also suggest that immobilized enzyme exhibits improved storage stability over the free enzyme.

In the context of protein stability, there is evidence that adsorption onto solid surfaces may alter the conformation, i.e., lead to interfacial denaturing of some protein [60,61], while others appear to resist significant conformational change [62-64].

Lim et al. reported a 10% loss of activity in every 12 days of storage for amylase on silanized silica particles [74]. Ashly et al. reported 50% of original activity for α-amylase after checking the activity over a period of four months [24]. The stability achieved in the case of all immobilized enzymes can be attributed to

improved life of biocatayst due to efficiency gained against thermal inactivation and other denaturing agents by decreased flexibility which enhanced proper orientation of enzyme on the support.

3.5.5.7 Reusability

In our study activity for 12 cycles of use for the immobilized enzymes was monitored and the results are shown in the figure: 3.17.

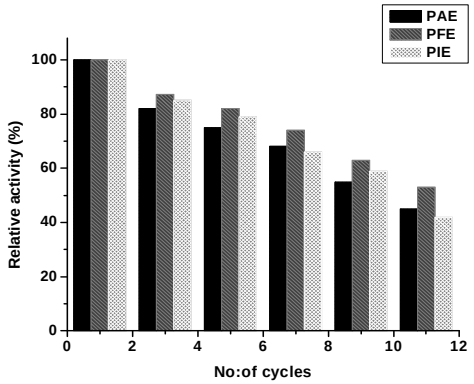

Figure: 3.17: Reusability studies of immobilized enzymes

Each time after the reaction, washing of immobilized biocatalyst was carried out using buffer solution to free the immobilized enzyme from any traces of initial substrate added. PAE retained about 69% of its initial activity; PFE retained about 44.4% of its initial activity while PIE retained 14% of its initial activity. Similar improvement of reusability after immobilization of α-amylase was observed by Cakmakci et al. while immobilizing the enzyme on to epoxy containing thiol-ene photocurable materials [76].

3.6 Significance of polypyrrole prepared in presence of surfactants as templates and its role as a support for enzyme immobilization

Obtaining PPY with excellent chemical and physical characteristics becomes more and more attractive because of its excellent characteristics that have

led to wide potential applications in various fields such as sensors, actuators etc. [77,78]. For this purpose, the polymerization of pyrrole in different surfactant systems has been developed. In tailoring the nanostructures of polypyrrole during polymerization, concentration of pyrrole monomer and surfactant have been proved to play a major role which thereby reflects in their morphology. This is because surfactants can induce pyrrole to grow in a certain manner and result in PPY with an ordered morphology, which will show properties superior to those from a conventional aqueous solution [79, 80].

The advantage of using these soft template materials is that they are easy to remove after the synthesis, and in the meantime, the micro-/nanostructures of the resulting polymers are formed. This template directed synthesized polypyrrole nanostructures have their potential applications in chemical and electrochemical sensors [81].

Micro-emulsion polymerization has been developed to prepare polymer nanostructures. This technique allows particles to transfer into spherical aggregates through the surfactant template. Surfactant creates a micro-reactor vessel via micelle formation, where monomer is restricted in a localized environment originated from encapsulation by the surfactant [82]. Compared with the aqueous solution and conventional emulsion polymerization, the micro-emulsion polymerization of PPY increased the extent of the pi-conjugation along the polymer backbone, and the ordered arrangement of the macromolecular chains.

Zhang et al. reported the controllable synthesis of PPY nanostructures with different kinds of surfactants, including Octyltrimethylammonium Bromide, Cetyl Trimethyl Ammonium Bromide (CTAB), Dodecyl Trimethyl Ammonium Bromide (DTAB), poly (ethylene glycol) mono-p-nonylphenyl ether (Opi-10), and sodium dodecyl sulfate (SDS) [81]. Grady et al. reported the formation of nanostructured PPY with controlled morphologies on atomically flat surfaces with adsorbed surfactant molecules as templates [83]. Omastova´ et al. conducted the synthesis of PPY in the

presence of anionic, cationic, and non-ionic types of surfactants [84]. Kwon et al. reported that PPY prepared without surfactant showed an arbitrary shape whereas, the PPY samples with surfactant showed a spherical shape [85]. From all these studies, it can be concluded that the surfactant provides a space to control morphology as template does.

3.6.1 Preparation of polypyrrole in the presence of surfactants

The 0.1 mol of anhydrous $FeCl_3$ (16.2g) was dissolved in 100 ml distilled water in a reactor vessel containing magnetic stirring bar. To this solution each surfactant with concentration above their cmc (SDS, CTAB, and Tween 80) dissolved in 100 ml distilled water was added and mixed. The whole mixture is then stirred for 30 minutes until surfactant is completely dissolved. The 0.15 mol freshly distilled pyrrole (10.4ml) was first dispersed in 50 ml of distilled water and then inserted drop wise into the stirred mixture of an oxidant and surfactant. Immediate formation of black PPY was clearly observed right after addition of the monomer. The polymerization was carried out for 24 hours at room temperature with moderate stirring. Finally the PPY is washed with acetone and dried in oven at 60°C for 2 hours.

The PPY prepared in presence of anionic surfactant was treated with an excess of 1M NaOH for 12 hours, then filtered and washed with distilled water and dried at 60°C in oven. This will help to remove the anionic surfactant leaving behind pure polypyrrole with controlled morphology. The cationic and non-ionic surfactants were removed by washing with methanol [84].

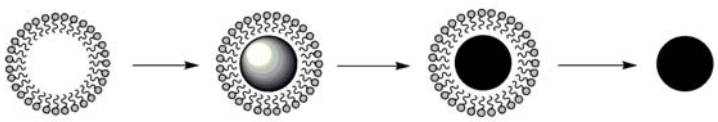

Scheme 3.3 Preparation of polypyrrole through surfactant template

3.6.2 Physico-chemical characterization

3.6.2.1 FT-IR Spectra of polypyrrole prepared in presence of surfactants

The FTIR spectra of PPY prepared in presence of different types of surfactants are shown in figure: 3.18, and the main peak positions are listed in the table: 3.6. The characteristic peaks of PPY can be clearly observed. For instance, the peak at about 3436 cm^{-1}, 3434 cm^{-1} and 3430 cm^{-1} correspond to N-H stretching vibrations in the pyrrole ring, of PS, PC and PT respectively. The peak near 2928 cm^{-1} and 2852 cm^{-1} corresponds to the C-H stretching vibration of the methylene group. The intensity of these peaks are so weak which indicates that surfactants have been completely removed from these polymers. These demonstrated that the resulting polypyrrole nanostructures were pure [81].

The most pronounced change after the deprotonation is the reduction of absorption above 1800 cm^{-1}. An additional peak at about 1748 cm^{-1} and 1710 cm^{-1} can be observed for all samples, indicating that PPY is slightly over oxidized during the growth process. The oxygen may enter the PPY structure during the polymerization process itself as the consequence of the water presence in polymerization solution, as well as by reaction of the prepared polymer with atmospheric oxygen.

The peak around 1028 cm^{-1} indicates N-H ring out of plane bending which is shifted to 1024cm^{-1} for PC and 1020 cm^{-1} for PT. The C-H ring out of plane bending around 592 cm^{-1} was seen in all samples.

For all samples there was a shift to lower wave number after enzyme has been immobilized. For all three samples characteristics peaks with respect to enzymes were also obtained. As per the literature review the main peaks around 1656 cm^{-1}, 1646 cm^{-1}, 1617 cm^{-1}, 1596cm^{-1}, 1542cm^{-1} and 1397 cm^{-1} are the characteristic peaks confirming the presence of α-amylase.

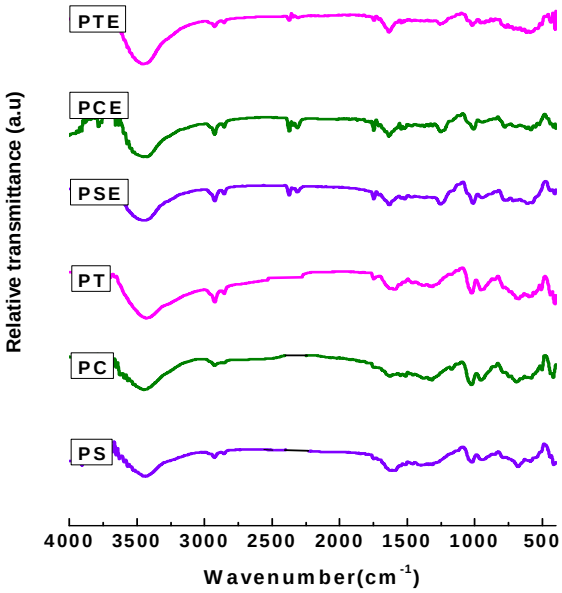

Figure: 3.18: FT -IR Spectrum of PPY prepared in presence of surfactants

Table: 3.6 Characteristic peaks corresponding to PPY prepared in presence of surfactants. (w - weak, vw-very weak, s-strong)

Peak assignments(cm^{-1})	PS	PSE	PC	PCE	PT	PTE
N-H stretch	3436	3449	3434	3454, 3460	3430	3457
C-H stretch	2928, 2852	2923 2852	2923, 2859	2928, 2852	2926, 2852	2931, 2854
C=N	1748, 1712	1752, 1710w	1745	1748, 1712w	1755	1747, 1710w
C-N-C ring -in plane deformation	1636	1656 1646, 1617w	1627w	1656. 1646	1628.8	1646 1656, 1617
C-C-N ,N-H ring in plane bending(s)	1518	1548, 1542, 1596	1550, 1518w	1548, 1596	1596m,	1542w 1524w,1596
C-N stretch(w)	1460	1467.2	1454w	1467vw 1408vvw	1459w	1462w
C=C-N in plane deformation	851	881	857	851vw	857	892,867vw

3.6.2.2 Thermogram of polypyrrole prepared in presence of surfactants

Thermogravimetric analysis showed that the PPY prepared in presence of SDS was relatively thermally stable in N_2 up to approximately 272°C. The subsequent weight loss curve (180°C - 350°C) is significantly steeper than that observed for either the PC or PT. The major weight loss was at temperature 272°C and minor weight loss starts at 430°C which continues upto 800°C.

When α-amylase get adsorbed on to this polymer the major weight loss starts at 196°C which is assigned to protein degradation and the other major weight loss corresponding to PPY structure starts at 332°C.

In the case of PC the major weight loss was observed at 211°C which is due to the decomposition of polymer backbone along with minor amounts of dopants if present. The other minor weight losses occur at 303°C and 490°C.

After immobilization the decomposition starts at 198°C which corresponds to degradation of amylase molecular structure. At 309°C the polymer decomposition starts which then continuously decompose up to 800°C.

For PT the decomposition of PPY initiates at 226°C with subsequent weight loss at 353°C. α-amylase immobilized on PT started decomposing at temperature above polymer decomposition as enzymes have delicate backbone that could not withstand elevated temperature. Thus at 176°C the amylase decomposition might have occurred subsequently followed by decomposition of the polymer organic structure at temperature of 363°C. The TG curves obtained are shown in the figure: 3.19

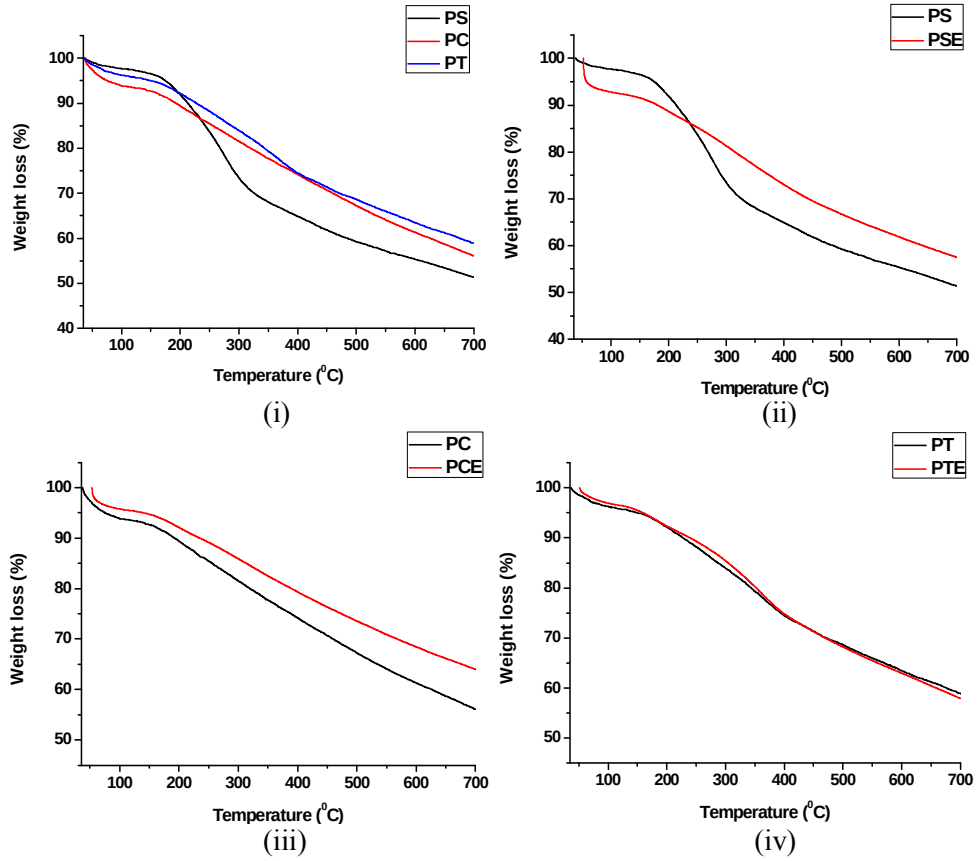

Figure: 3.19: TG curves of (i) PS, PC and PT (ii) PS and PSE (iii) PC and PCE (iv) PT and PTE

3.6.2.3 Surface area analysis

The BET surface area of polymers prepared are given in table: 3.7.

Table: 3.7 Surface area of PPY prepared in presence of surfactants and their enzyme immobilized forms

Polymers	Surface area (m^2/g)
PS	9.4
PC	11.9
PT	26
PSE	5.96
PCE	9.07
PTE	23.3

3.6.2.4 Scanning electron microscopy

The SEM images show that good spherical nanoparticles were obtained using surfactants as template during PPY synthesis. The surfactants played a major role on the surface morphology of products because upon the removal of the surfactant template the total surface area increases. There occurs agglomeration of particles in all the samples prepared. This is due to the close interactions between the polymer chains.

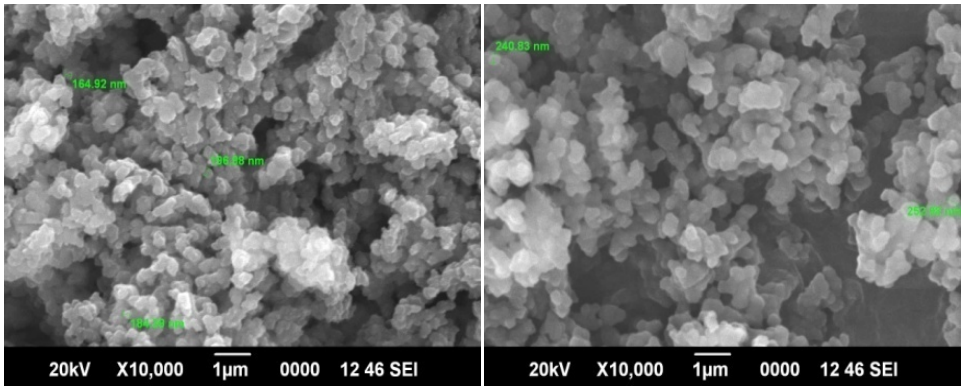

(i) (ii)

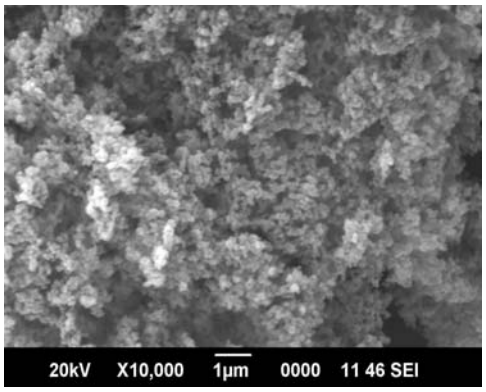

(iii)

Figure: 3.20 SEM images of (i) PS (ii) PC (iii) PT

3.6.3 Immobilization of α-amylase on polypyrrole prepared in presence of different surfactants.

3.6.3.1 Influence of pH during immobilization of α-amylase on polymer supports

To find the optimum binding condition necessary for the enzyme, we measured immobilized α-amylase activity under the conditions of different pH values. The effect of pH of the medium on the relative activity of the immobilized enzyme is shown in the figure: 3.21.

From the figure it is evident that the immobilized enzyme activity was highest in the pH range 5-6. The decrease in activity above and below this pH may be due to lower loadings which occurred as a result of change in conformation of tertiary structure due to unfavourable charge distribution of amino acid residues as a result of change in pH. Since the free enzyme used in this experiment was stable in the narrow pH range 4.5-5.5, the possible denaturation of enzyme in alkaline region was also expected.

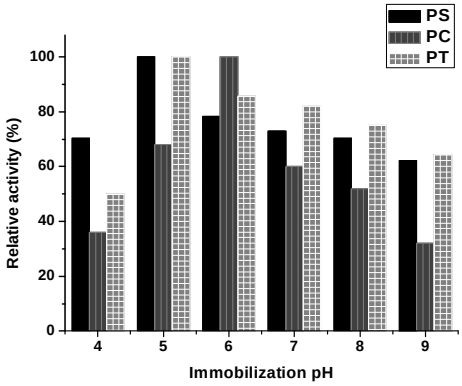

Figure: 3.21 Effect of pH of immobilization medium on the relative activity of immobilized α-amylase

Here we observed that pH 5 was best for the immobilization of α-amylaseon PS and PT whereas, for PC the best retention of enzyme activity was observed at

pH6. At pH 5 and 6, since polypyrrole is positively charged and amylase negatively charged, strong adsorption occurred in the case of all supports. This is due to significant electrostatic interaction between supports and the enzyme.

Furthermore, all of the polymers have conjugated rings for hydrophobic interactions. At pH 4, PPY adsorbents have overall net positive charge and lysine and arginine amino acid residues on the protein surface of amylase have slight positive charge as it is close to its isoelectric point. Hence PPY adsorbent should repel amylase enzyme. However, adsorption of proteins was still observed at pH 4 because hydrophobic interactions appeared to dominate over electrostatic interaction at pH 4. The small adsorption difference due to pH might originate from ionic effects, due to secondary amino groups of the pyrrole rings.

At pH 7 PPY has no charge whereas amylase is negatively charged. Hence the observed adsorption might have occurred as a result of hydrophobic interaction. When the immobilization is carried out at higher pH, the same amount of enzyme is immobilized, however the activity observed is lower than that attained at pH 5 and 6. This is because at higher pH PPY adsorbents have overall negative charge and amylase is also having net negative charge which results in electrostatic repulsion. Thus overall activity of the enzyme is very much dependent on the strength of the electrostatic interaction between enzyme and the support.

3.6.3.1.1 Effect of contact time on the activity of α-amylase

The contact time needed for enzyme to get adsorbed on PPY adsorbents is shown in the figure: 3.22.

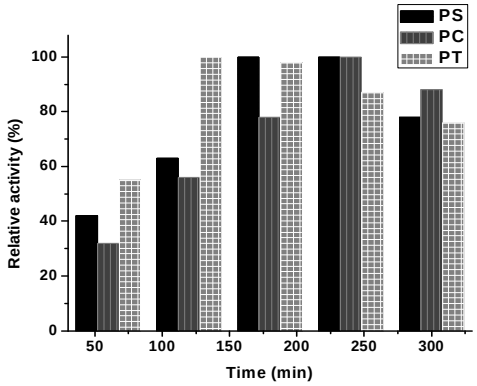

Figure: 3.22 Effect of contact time on immobilized enzyme activity

For PS the adsorption capacity was maximum within 180-240 minutes contact time. Whereas in the case of PC and PT contact time was 240 minutes and 120 minutes respectively in order to have maximum protein adsorption. The decrease in activity after this optimum time might be due to the fact that, as the first adsorption occurred the surface of the support get saturated with the enzyme and remaining enzymes in solution had to bind with the support surface via second adsorption site which needed more energy. This could have weakened the adsorption efficiency.

3.6.3.1.2 Effect of initial protein concentration on protein loading on to polymeric supports

The amount of protein bound to PPY adsorbents were analyzed based on the optimized conditions obtained; it is shown in figure: 3.23.

The effect of initial protein amount on protein loading is depicted in the graph shown. Adsorbed amount of enzyme increases with increase in enzyme concentration taken but after a particular concentration no further increase in adsorption occurs instead a saturation point is reached and enzyme starts desorbed from the surface if loaded heavily [86].

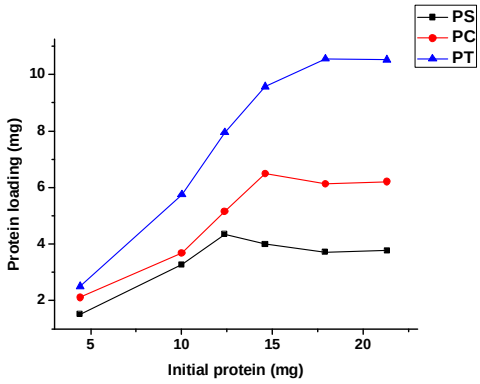

Figure: 3.23 Effect of initial protein amount on protein loading

3.6.3.1.3 Effect of initial protein concentration on immobilization yield and activity of loaded protein

Immobilization yield obtained for all adsorbents at various concentrations taken are shown in the figure: 3.24.

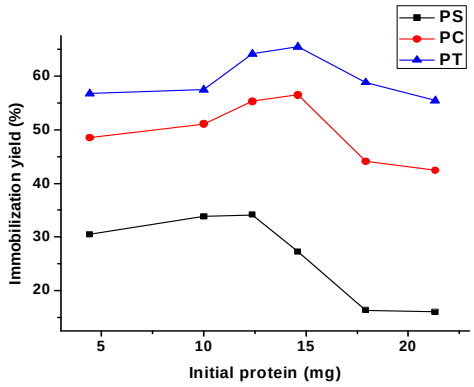

Figure: 3.24 Effect of initial protein concentration on immobilization yield of enzyme

From the graph, it is clear that enzyme loading increases as concentration increases which then reaches a saturation point and then starts decreasing or remains constant which might be due to desorption at high loading with increase in enzyme amount as a result of multilayer adsorption which causes weak binding of enzymes on to supports.

For PS optimum immobilization yield was 34% when 12.8 mg of initial protein was added. Protein load was also the maximum at this concentration with immobilized enzyme activity 26.5 EU.

For PT even if maximum loading of 65.5% was obtained when initial protein was 14.6 mg and protein load of 9.6 mg, the optimum immobilized activity 12.2 EU was obtained at the initial protein concentration of 17.9 mg with protein load of 10.6 mg. Similar is the case with PC.

Thus there are several unpredictable interactions that can cause change in protein conformation and thus cause deviation from theoretical trends. The trend of immobilized enzyme activity when initial protein amount was varied for all adsorbents is shown in the figure: 3.25.

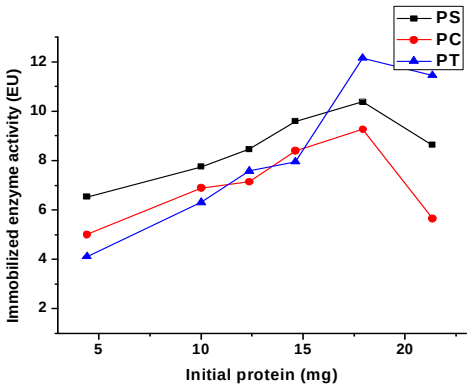

Figure: 3.25: Effect of initial protein concentration on immobilized enzyme activity

The immobilization yield, activity yield and immobilization efficiency were also evaluated. The results are tabulated in the table 3.8.

Table 3.8: Immobilization efficiency of PPY prepared in presence of surfactants

Polymer	Initial protein Mg	Immobilized protein mg/g	Immobili-zation yield (IY)	Initial Activity EU	Immobilized enzyme activity EU	Activity yield (%) AY	Immobilization efficiency (%) IE=AY/IY
PS	12.8	4.4	34	26.5	8.5	32	92
PC	17.9	6.1	44	27	9.3	34	78
PT	17.9	10.6	59	27	12.2	45	76

Because of comparatively small particle size and hence high surface area, protein loading was the maximum for PT compared to PS and PC. Correspondingly activity yield was also found to be higher for PT. But the immobilization efficiency was the highest for PS compared to PC and PT. This might be due to lower affinity of amylase towards PC and PT when compared to PS. Thus results indicate that loading efficiency was affected by increasing loading amount [87].

3.6.3.2 Effect of pH on enzyme activity

An enzyme's apparent response to pH may change when it is in a heterogeneous environment associated with polymer matrices. Figure: 3.26 show the effect of different pH on enzyme activity.

Free and immobilized α-amylase exhibits similar activity in the range from pH 4.5 to 5.5. Above pH 6.0 immobilized α-amylase showed better performance than free α-amylase. In the case of PSE optimum activity was observed at pH 5 whereas, optimum activity in the case of PCE and PTE was at pH 6.

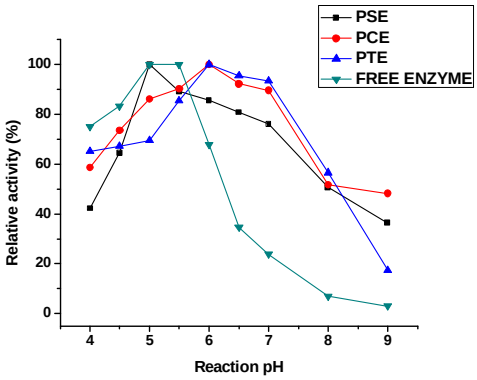

Figure: 3.26: Effect of pH on the activity of free and immobilized α-amylase

Table: 3.9 Optimum pH for free and immobilized α-amylase

	Free enzyme	PSE	PCE	PTE
pH	5 & 5.5	5	6	6

At pH 4 and 8 a decrease of the enzymatic activity is observed for both the immobilized and the free enzyme; however, at pH 8 the residual activity of the

immobilized enzyme in most samples is significantly higher than that of the unmodified form.

A greater bulk pH is required in providing an optimum pH in the microenvironment of the enzyme and hence a shift to higher value is encountered. Thus, the immobilization process provides structural stability, preventing an irreversible unfolding of the enzyme protein.

The enzyme is inactivated at lower pH values (pH < 5) [88]. The curve profile for all immobilized enzymes became much broader when compared to that of free enzyme.

3.6.3.3 Effect of temperature on the activity

The inactivation rate of an enzyme increases with temperature. Every enzyme therefore shows optimum activity at a particular temperature at which it assumes its more stable conformation. This can be directly related to the efficiency of immobilization process and hence will have a profound impact not only on enzyme activity but also on enzyme stability. Influence of temperature on activity of free and immobilized α-amylase is depicted in the figure: 3.27.

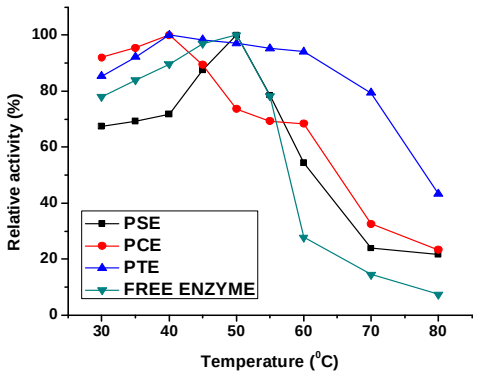

Figure: 3.27: Effect of temperature on the activity of free and immobilized α-amylase

The 10°C decrease in the optimum temperature combined with thermal stability exhibited by PCE and PTE was an interesting finding of this work. Similar

decrease in optimum temperature was reported by Su et al. when they immobilized β-glucosidase on alginate by combining cross-linking with entrapment and again, cross-linking. The energy reduction and lower time to cool the reaction mixture represents advantages acquired with the immobilization process.

In the case of PSE there was an increase in optimum temperature by 10°C compared to free enzyme. Since in the bound state enzymes are less mobile they resist denaturation of protein [89]. The decrease in optimum temperatures of PCE and PTE may be due to less activation energy required for starch hydrolysis because of the conformational change that occurred at the enzyme active site after immobilization. But increase in temperature for PSE might be due to increase in activation energy required for starch hydrolysis as a result of structure changes encountered at the active site after immobilization.

This can be either due to excess energy required to orient the enzyme into its native conformation or due to improper transport of substrate molecules from the bulk to the enzyme active site on account of diffusional resistances to mass transfer [90].

3.6.3.4 Thermal stability of the free and immobilized enzymes

Thermal stability obtained after immobilization conferred to PPY adsorbents a very good performance as can be seen in figure: 3.28. After pre-incubation at various temperatures in the range 30-60°C for 1hour with the support in respective buffer solution, PCE and PTE showed 80% of their initial activity whereas PSE showed 60% of its initial activity. This improvement in denaturation resistance of the immobilized α-amylase was probably a consequence of the multipoint attachment acquired in the immobilization process.

All the results obtained were very much better, as free enzyme cannot withstand such a prolonged period of thermal treatment [91]. For industrial application the enzyme should be stable towards temperature fluctuations. The

immobilized enzyme shows moderate decrease in activity, which emphasizes that the rate of inactivation is lowered upon immobilization.

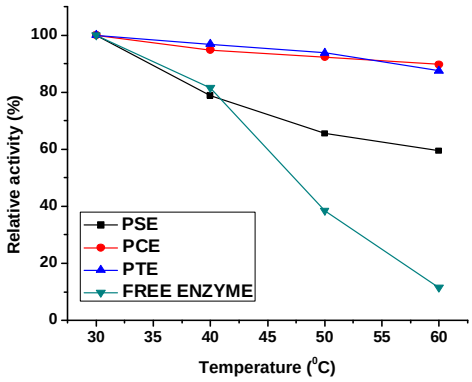

Figure: 3.28: Thermal stability of free and immobilized α-amylase

As the temperature increases, the stability drops significantly for both free and immobilized amylase. At 40°C, both free and immobilized enzyme retain up to 70-80% of their activity. At 50°C the immobilized enzyme was inactivated at a much lower rate than the free enzyme. The free enzymes lost almost 90% of their activity at 60°C after 1 hour treatment whereas immobilized amylase lost only 20-40% of its initial activity. Figure: 3.29 show the effect of pre - incubation time on the activity of each immobilized enzyme.

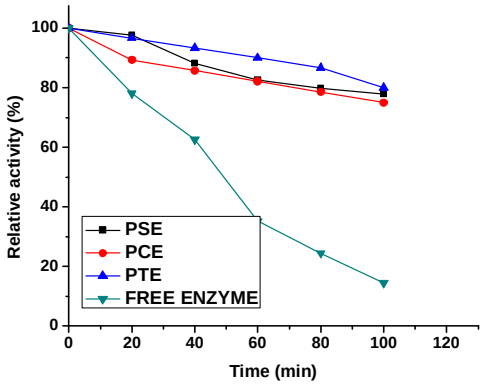

Figure: 3.29: Effect of pre-incubation time on the activity of free and immobilized α-amylase

About 70-80% of immobilized enzymes maintained their activity when subjected to 120 minutes of pre-incubation at their respective optimum temperature whereas, free enzyme could retain only 10% of their initial activity when subjected to same treatment.

These results suggest that the thermal stability of α-amylase increases considerably as a result of immobilization on to PPY adsorbents and is suitable for long term applications. Such an improvement in thermal stability was observed by Talekar and Chavare when they carried out immobilization of α-amylase on to calcium alginate via entrapment method [92]. It is reported that immobilization can help to distribute the thermal energy imposed to the protein at higher temperatures and hence it is less susceptible to temperature induced conformational changes.

3.6.3.5 Determination of kinetic parameters

K_m and V_{max} were calculated from the Lineweaver-Burk plots and Hanes-Woolf plots. Both plots are presented in the figure: 3.30.

Table 3.10: Kinetic parameters determined for free and immobilized α-amylase

	Free Enzyme	PSE	PCE	PTE
K_m (mgml^{-1})	0.50 ± 0.04	0.916 ± 0.01	1.07 ± 0.04	1.49 ± 0.05
V_{max} (mg/ml/min)	7.40± 0.05	2.34 ± 0.03	4.41 ± 0.02	3.44 ± 0.02

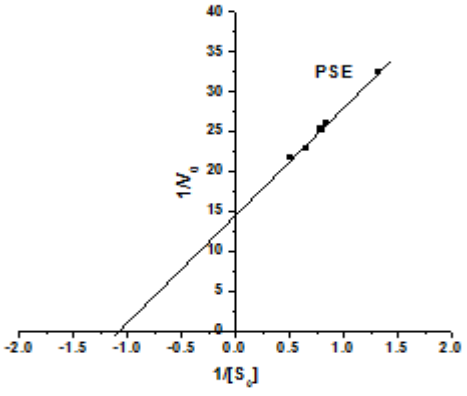

(i)

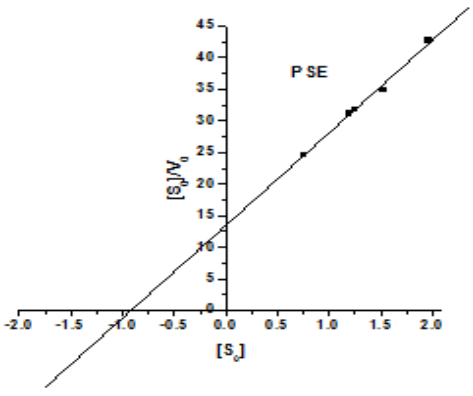

(iv)

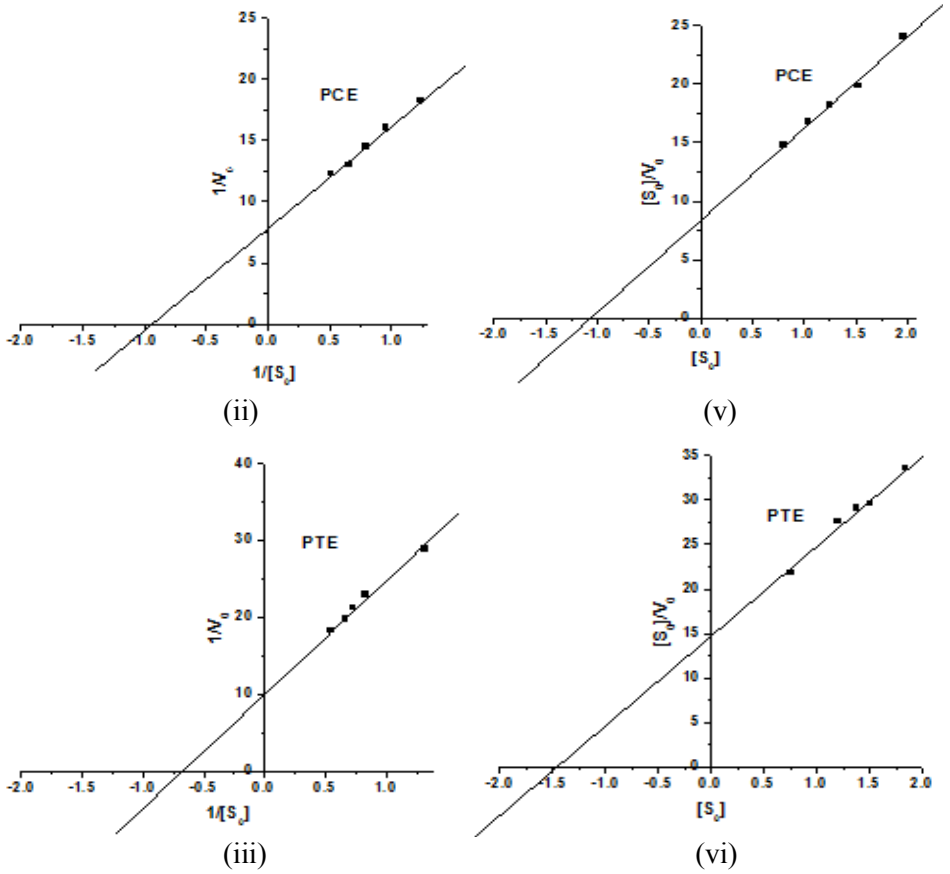

Figure: 3.30 Lineweaver-Burk plots for (i) PSE (ii) PCE (iii) PTE and Hanes-Woolf plots (iv) PSE (v) PCE (vi) PTE.

The K_m values were found to be increasing and V_{max} values decreasing in the case of PSE, PCE and PTE [93,94].

This demonstrates that there is a significant role played by mass transfer restrictions due to diffusional limitations. The change in affinity of the enzyme to its substrate is probably caused by structural changes in the enzyme as a result of immobilization on to a solid support and by lower accessibility of the substrate due to improper diffusion of the substrate to the active sites of enzyme [91]. Since

immobilization process does not control proper orientation of the enzyme on the supports, this may cause variation in the usual native conformation and thus changes the property of the active site thereby hindering the active site from binding the substrates [95].

3.6.3.6 Storage stability of Immobilized α-amylase

In the free form, enzyme has very short life time and hence gets easily inactivated with minor fluctuations in its local environment. Hence its reuse is impossible which impose a heavy wastage of enzymes and thus economically not beneficial. Immobilization of enzymes enables long-term storage of the enzyme and thus becomes available for various applications. In the dry form, the immobilized enzymes cannot maintain their stability and activity for long term storage. But, when stored in buffer solution under low temperature of 4°C immobilized enzymes exhibit better activity and could retain its stability.

On the other hand free enzyme even when stored in buffer solution under low temperature conditions lose complete activity within 7 days. Whereas PCE could retain 53% of its initial activity, PTE retained 60% of its initial activity and PSE 40% of its initial activity, all of which are far better than free enzyme as can be seen in the figure: 3.31. This decrease in activity among the immobilized enzymes can be explained as the time-dependent natural loss in enzyme activity which occurs due to conformational change in the active site of enzyme on long term storage that is caused by changes in its micro environment. Similar enhancement in storage stability after immobilization has been reported by other authors [76,96].

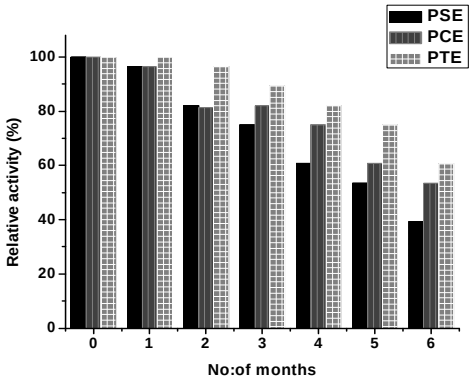

Figure: 3.31 Storage stabilities of immobilized enzymes

3.6.3.7 Reusability

In our systems reusability was checked for 20 continuous cycles and results obtained were given in the figure: 3.32. After 15 cycles PSE and PCE retained 50% of their initial activity whereas, PTE retained almost 60% of its initial activity. It was observed that the immobilized enzyme activity decreased when recycling number was increased. Similar results were obtained by other authors.

Jaiswal et al. reported that immobilized α-amylase on gelatin was reusable upto seven cycles. Almost 90% activity was retained upto three cycles, but with subsequent runs, there was a decline in the activity of the immobilized enzyme. The activity loss could be due to weakening in the strength of binding between the matrix and enzyme on repeated use and hence the enzyme might leach out from the matrix [97]. Besides, the frequent encountering of the substrate into the same active site might distort it which would dwindle the catalytic efficiency either partially or fully [98]. Om Prakash et al. reported that α-amylase immobilized on agarose and agar matrices could retain its activity upto 5 cycles after which there was a subsequent decrease in activity which may be due to enzyme denaturation and due to physical loss of enzyme from the carrier [226].

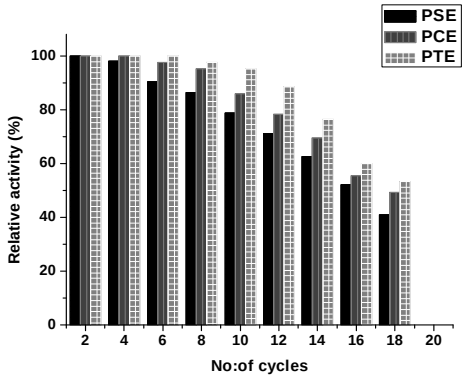

Figure: 3.32 Reusability of the immobilized enzymes

3.7 Significance of functionalized polypyrrole as support for enzyme immobilization

PPY is also associated with some limitations such as its roughness, rigidity, lack of processablity and absence of any functional group for surface immobilization of bioactive molecules. In order to perform as bioactive platform for the immobilization of biomolecules, it is necessary to carry out chemical modification of PPY [31]. The polymers were functionalized by introducing reactive groups that are able to react with -COOH and -NH_2 groups of the enzyme molecule. All these modifications opened up an easiest route for covalent attachment of drugs and biomolecules.

Recently, T. Sandu et al. reported a work based on functionalization of polypyrrole after polymerization is completed. The functionalization agent was glutaraldehyde, and the functionalization purpose was to create binding sites at certain distances from the polymer surface. This is necessary in view of covalently immobilize enzymes on polypyrrole [99,100].

Polypyrrole is an inherent biocompatible polymer. Here in our study the functionalization was not realized during polymerization process, but after polymerization. The functionalizing agents were glutaraldehyde and

aminopropyltriethoxysilane. The functionalization was done with the view that functional groups introduced will serve as binding sites that can react with functional groups of the enzyme. The α-amylase was immobilized on to glutaradehyde activated PPY via covalent binding and to APTES activated PPY via adsorption method.

Amylases contain a number of reactive lysine groups on their surfaces which are capable of reacting with the aldehyde groups from glutaraldehyde for enzyme rigidification. Glutaraldehyde is a bi-functional agent which could also serve as a spacer arm in enzyme immobilization [101,102]. A Schiff base was formed through the reaction between CHO groups from glutaraldehyde and -NH groups from polypyrrole. The unreacted CHO groups that remain free on the other side of bonded aldehyde are available for subsequent bonding with the enzyme [99,100].

Amino propyl triethoxy silane has an organic functional group (NH_2-) and three alkoxy groups. The chemical reaction began with the hydrolysis of the alkoxide groups into silanols that may condense to form siloxane bonds. Silane molecules can absorb, condense, or interact with the substrate, influencing coupling effectiveness. After silanization active sites were introduced on the surface or at the end of silanized polymer, which can be bonded with bio-molecules to attain sensitive elements for biosensor application by direct coagulation or through the format of amino bridge bio-molecules [103].

It was reported by Bernard et al. that silanization of crushed magnetite, synthetic magnetite or bio-magnetite with APTES further derivatized with glutaraldehyde does not yield a highly stable silane coating [104]. Hence we didn't activate APTES but direct linkage of APTES with amylase was adopted as the method.

3.7.1 Functionalization of polypyrrole with Glutaraldehyde

PPY was synthesized from pyrrole through the chemical oxidation-polymerization method, with Fe^{3+} as oxidant and water as solvent. In brief, 1.75 ml of pyrrole (0.025mol) was added drop wise into 150 ml of aqueous $FeCl_3.6H_2O$

(13.5g, 0.05mol) solution with stirring. The mixture was stirred for 3 hours to allow the oxidation-polymerization reaction to be fully completed. Then, the resultant black precipitate was separated by filtration, thoroughly washed with deionized water and methanol to remove any possible iron residues, and then dried in a vacuum desiccator for 24 hours. The powder so obtained were PPYCl that is PPY doped with chloride. This PPYCl is then functionalized using the procedure reported by T. Sandu et al. [99].

A liquid phase was first prepared by mixing water (80ml), glutaraldehyde (20ml) and sulphuric acid (1.36ml) respectively and was poured into polypyrrole solid phase. Polypyrrole (1g) thus mixed with liquid phase was then heated at 70°C for 2 hours. The final mixture was then filtered and washed with distilled water to remove the impurities. The precipitated polypyrrole powder is then dried at 40°C.

In this reaction hydroxyl groups were said to be formed through functionalization reaction between NH groups from polypyrrole and glutaraldehyde according to the scheme: 3.4.

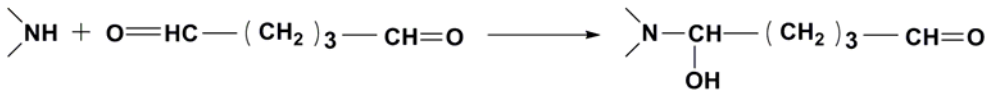

Scheme: 3.4 Functionalization reactions between polypyrrole and glutaraldehyde

Goldstein and Menecke suggested that the glutaraldehyde reaction most probably involves conjugated addition of protein amino groups to ethylene double bonds of α-β unsaturated glutaraldehyde oligomers, since the linkages formed between the protein and glutaraldehyde are irreversible and survive extremes of pH and temperature [105]. The possible reaction is as depicted in scheme: 3.5. Therefore, the possibility of Schiff base (aldiimine) formation has been kept to a minimum due to the reaction's reversibility in aqueous media, particularly at low pH values.

Scheme 3.5: Enzyme immobilization reaction between free CHO groups from glutaraldehyde and H_2N groups from the enzyme [106]

3.7.2 Functionalization of polypyrrole with Aminopropyltriethoxy silane.

PPYCl powder was dispersed in an APTES solution (2 wt%) with pH being adjusted to 4 by the addition of acetic acid. After 2 hours, the resultant precipitate was filtered, washed by soaking in a 0.01M NaCl solution at pH 4 and then separated and dried in a vacuum desiccator for 24 hours [107]. The reaction is depicted in the scheme: 3.6 [108].

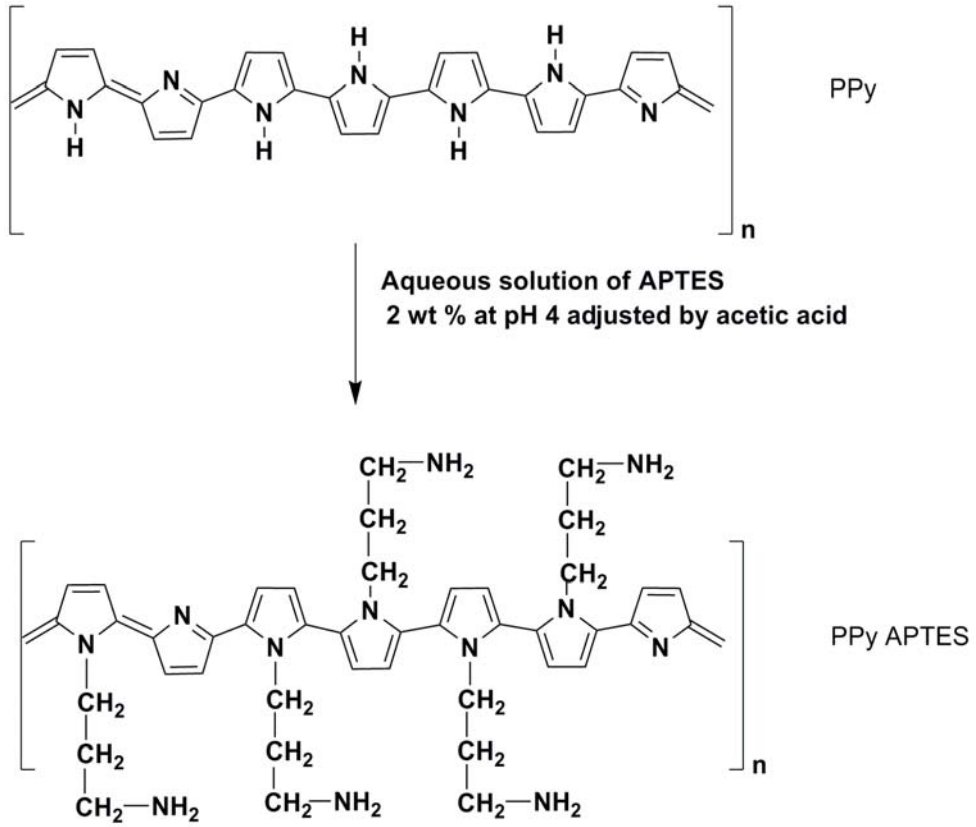

Scheme 3.6: Functionalization of polypyrrole with Aminopropyltriethoxy silane

3.7.3. Physico-chemical characterization

3.7.3.1. FT-IR Spectra of functionalized polypyrrole

FTIR spectra were obtained for the PN as shown in figure: 3.34. There were three peaks at the wave numbers at about 1550 cm^{-1}, 1470 cm^{-1} and 1309 cm^{-1} for PN, which stand for the C=C stretching, C-N stretching and C-C in ring stretching respectively. The peak at 3107 cm^{-1} stands for the C-H stretching on the ring of PN and the peak at 2924 cm^{-1} and 2854 cm^{-1} were assigned to a (C-H) stretching band of a (N-C-H) unit slightly shifted from the normal (C-H) position. A new peak at 2972 cm^{-1} (indicating the -C-NH_2 stretch vibration) was also observed in the spectrum. The FT-IR results prove that mixing APTES into the polymer powder is an efficient way to functionalize the polymeric nanostructure [109].

There was a C-N stretching peak for secondary nitrogen on PPY at 1179 cm^{-1} and the peaks at 1041cm^{-1} and 1427 cm^{-1} were assigned to the C-N stretching for primary amine and the N-CH_2 stretching for tertiary amine on PN respectively.

The major change in the transmittances can be observed at the wave number 3448 cm^{-1} (N-H stretching in secondary amine) for the PPY, which was replaced by two split peak at 3394 $cm^{-1}$and 3460 cm^{-1} for N-H stretching in primary amine and the other peak at 788 cm^{-1} (N-H deformation). Moreover, an additional peak appeared at around 1624 cm^{-1}, which was assigned to the NH_2 in-plane deformation for PN. All these changes indicate that the surface amination process added some primary amine groups on the surface and changed some secondary aromatic amine groups in PPY into tertiary amine groups.

It is observed that spectra has featureless shape above 1600 cm^{-1}, which may be caused by the conjugate molecular structure of PPY and the free charge carriers present in the polymers. At the wave numbers below 1600 cm^{-1}, the spectra show a characteristic series of seven absorption peaks which are intensified and sharp peaks [110]. This may be attributed to the assumption that the aminated chains bonded to the nitrogen atoms in the PPY backbone may disturb the conjugate structure of PPY and

thus limited the extent of charge delocalization along the polymer chain, leading to the increase of spectral features.

In particular, the intensities of the two peaks at 1550 cm^{-1} and 1309 cm^{-1} increased but the peak at 1470 cm^{-1} decreased significantly for the PN adsorbent, in comparison with those of un-aminated PPY-based adsorbent [107].

After immobilization of α-amylase for PN the peaks in the region of 400-1600 cm^{-1}were enhanced when compared to the spectra of PN before enzyme adsorption. As reported by Tian and Zerbi the relative intensities of the infrared bands at 1550 cm^{-1} and 1470 cm^{-1} were particularly sensitive to the extent of delocalization along the PPY polymer chain [111].

An intense sharp peak at 1680 cm^{-1} corresponds to C-N stretching whereas very weak peak at 1638 cm^{-1} corresponds to C=C stretching. Liang et al. proposed that the conjugation length of the doped PPY were inversely proportional to the ratio of the intensities of bands at 1550 $cm^{-1}$and 1470cm^{-1}. Hence it was concluded by X. Zhang et al. that the ratio changes in the intensities of bands at 1550 cm^{-1} and 1470 cm^{-1} are an indication of the decrease of conjugation length and extent of delocalization along PPY chain after the enzyme adsorption [107].

From the differences in the two spectra it is clear that the chemical interactions of enzyme have occurred directly with the PPY backbone. Thus X. Zhang et al. concluded that as a result of electrostatic interaction between some of the carboxyl groups of the protein with the positively charged nitrogen atoms in the PPY, some complexes might have formed which thus limit the extent of delocalization and the conjugation length and cause changes of the FT-IR bands in the region of 400-1600 cm^{-1} [107].

For PG a peak at 3428 cm^{-1} corresponds to NH stretching of pyrrole. Two strong bands in the region 2932 cm^{-1} and 2865 cm^{-1} was assigned to CH_2 groups which confirm the polypyrrole functionalization using glutaraldehyde [106]. A peak at 1718 cm^{-1} corresponds to carbonyl group. This peak which was common in PPY as a

result of over-oxidation is otherwise very weak. But after functionalization with glutaraldehyde this peak becomes so intense which confirms the presence of aldehyde groups from glutaraldehyde.

In the case of PG the additional peaks that are the characteristic of α-amylase was observed in the spectrum. Thus a new peak at 1643 cm^{-1} results which is the representative of peptide bonds from enzyme. This peak was absent in the spectra of PG before immobilization. Again another peak at 1283 cm^{-1} was present in spectra of PG which was absent in spectra of PGE. This is due to the presence of C=O groups in the parent compound which was utilized during immobilization and hence is absent in the spectra of immobilized enzyme. This confirms the fact that immobilization has occurred via glutaraldehyde functional groups through covalent bonding. The intensity of other peaks got increased after immobilization. Similar results were reported by T. Sandu et al. while immobilizing polyphenol oxidase on functionalized polypyrrole [106].

Peak assignments characteristic to that of PN, PNE and PG, PGE were presented in table 3.11.

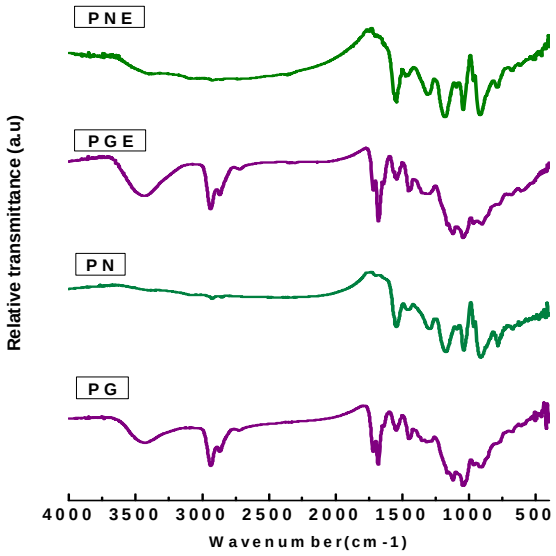

Figure: 3.34: FT-IR Spectra of PPY prepared in presence of surfactants and its immobilized forms.

Table 3.11 Peak assignments for immobilized enzymes and supports

Peak assignments (cm^{-1})	PG	PGE	PN	PNE
N-H stretch	3436	3443m	3432,3107vw,	3394
C-H stretch	2936,2862vs	2937,2866	2924,2854vvw	2923,2849vvw
C=O	1718,1683vs	1722w,1686s	-	-
C-N-C ring -in plane deformation	1638vw	1656	1548,1544s	1542
C-C-N , N-H ring in plane bending(s)	1550	1542	1550	1544m
C-N stretch(w)	1454	1448m	1456	1464
C-C in ring stretch(s)	1349mb, 1315	1334bm 1322	1295	1309w
C-C inter ring stretch(w)	1165 1279bm	1164vw	1175	1189
C-H,N-H ring out of plane bending (vs)	1043m,	1051	1042	1055
C-H, N-H ring out of plane bending(s)	788	785 vvw	775	788 w

3.7.3.2 Thermogram of functionalized polypyrrole

In the case of PG, the major degradation starts around 207°C which accounts for removal of moisture and other small chain fragments of polymer chain along with solvent molecules. The maximum degradation occurred around 425°C. This might include the degradation of polymer chain along with the methylene ammonium salt formed as a result of reaction between glutaraldehyde and PPY, which was reported to be a stable compound.

Thus it can be concluded that the functionalized PPY is more stable than pure PPY. Also similar to the reported literature by T. Sandu et al. maximum degradation was found to be higher for the functionalized sample when compared to pure polypyrrole [100].

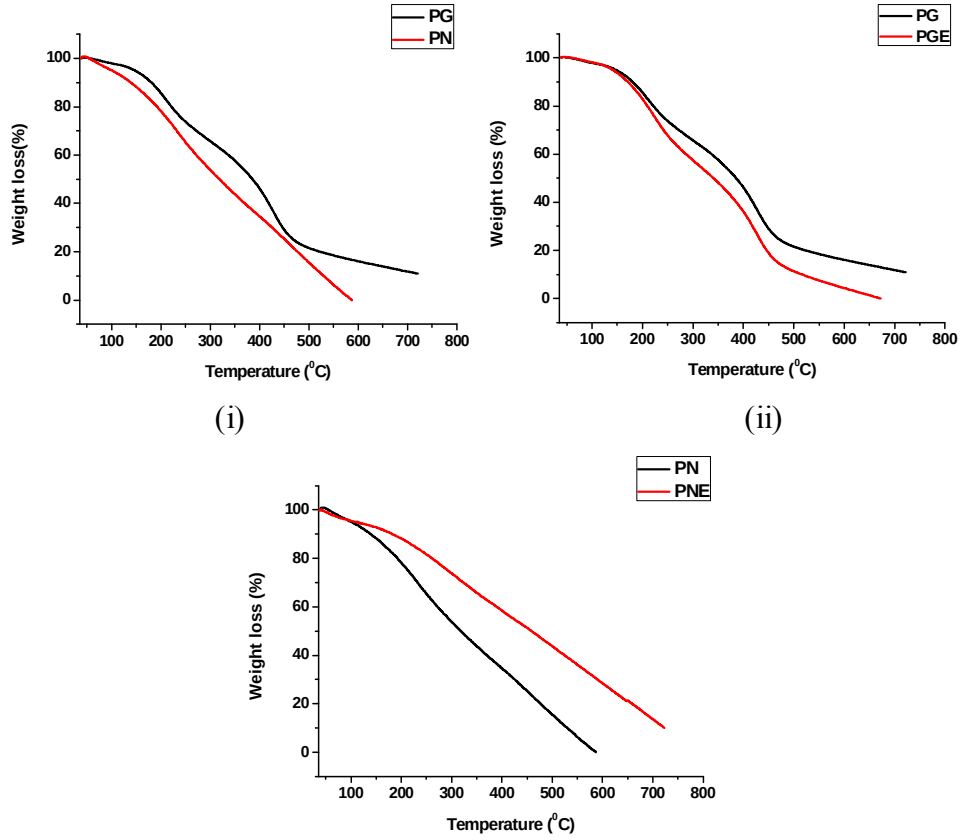

Figure: 3.35 TG curves of (i) PG and PN (ii) PG and PGE (iii) PN and PNE

In the case of PN the major decomposition peak was at 232°C. The minor decomposition peaks at 348°C, corresponds to removal of 1-(2-amino propyl pyrrole) - silica that remains unreacted along with small chain organic fragments of polymer chain. The minor peak that continues from 546°C corresponds to degradation of polymer chain backbone.

3.7.3.3 Scanning electron microscopy

The SEM images obtained for the functionalized supports are depicted in figure: 3.36. PN granules agglomeration was observed, thus giving the morphology being similar to PPY.

In the case of PG these particles are agglomerated exhibiting cluster morphology. After PPY functionalization with glutaraldehyde a cluster compactation also takes place which could be explained by aldehyde groups attachment on PPY chains or by PPY chains crosslinking [106].

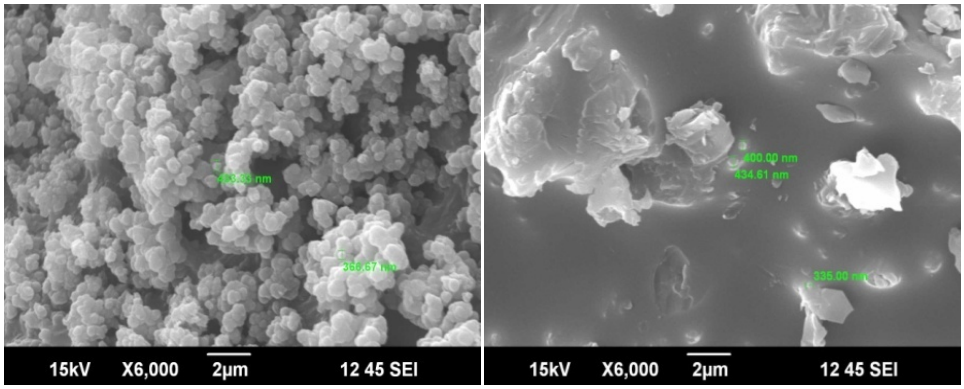

PN PG

Figure: 3.36: SEM images of PN and PG

3.7.3.4 Energy Dispersive X-ray spectroscopy

Elemental data obtained from Energy Dispersive X-ray analysis confirmed the functionalization of APTES on PPY. The higher C and N content and decreased Cl content in the modified sample compared to unmodified sample is a direct evidence for organo silane modification on the polypyrrole.

Table 3.12: Elemental data obtained from Energy Dispersive X-ray analysis

Element	(keV)	Mass%	Atom%
C K	0.277	50.57	72.64
N K	0.392	2.24	2.75
O K	0.525	2.77	2.99
Cl K	2.621	44.42	21.61

Element	(keV)	Mass%	Atom%
C K	0.277	77.56	87.22
N K	0.392	3.63	3.5
O K	0.525	4.56	3.85
Cl K	2.621	14.25	5.43

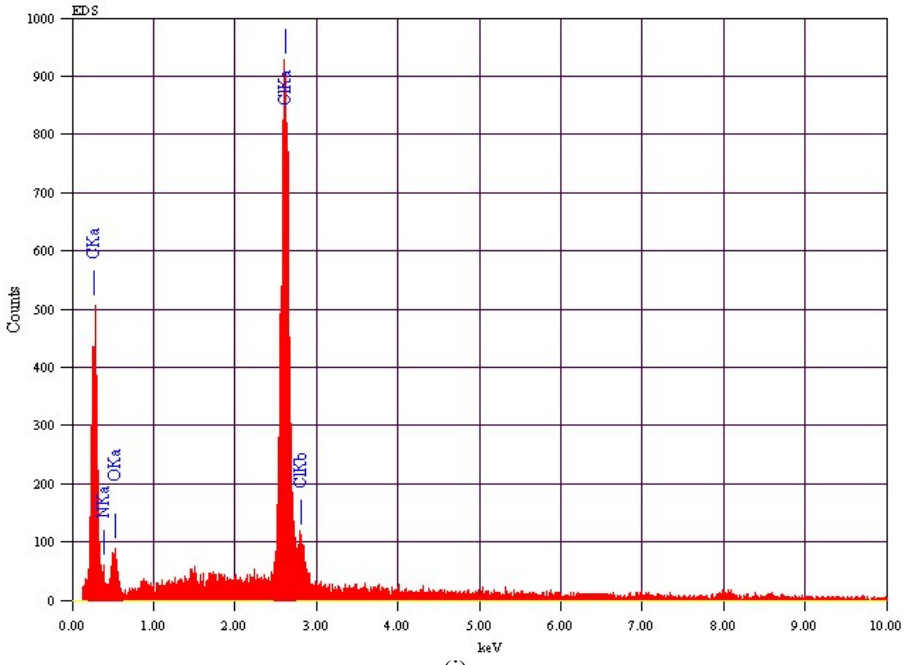

(i)

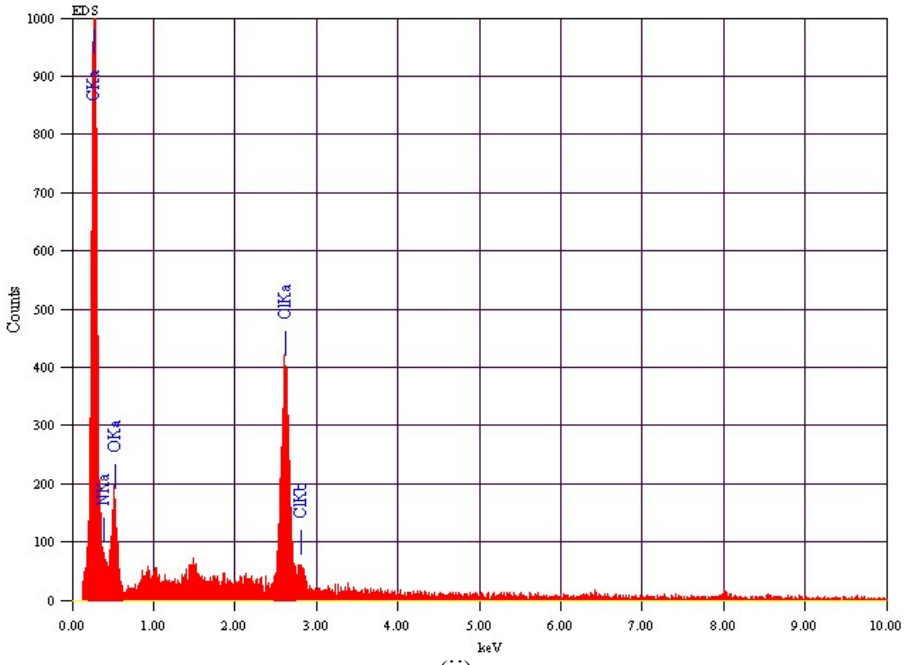

(ii)

Figure: 3.37 (i) EDS Spectrum of PPY (ii) EDS Spectrum of PN.

3.7.4 Immobilization of α-amylase on polypyrrole functionalized using glutaraldehyde and APTES as coupling agent

3.7.4.1 Optimization of immobilization parameters

The effect of pH of medium in which the enzyme is dissolved at the time of immobilization on to polymeric supports is shown in the figure: 3.38.

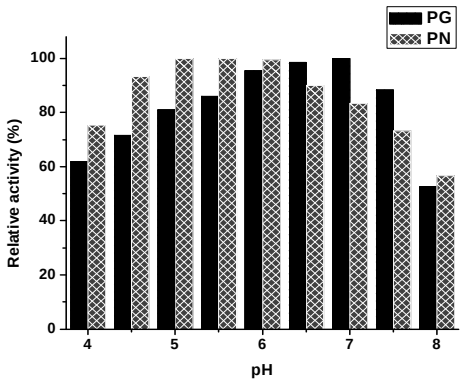

Figure: 3.38: Effect of pH of immobilization medium on the relative activity of immobilized α-amylase

Glutaraldehyde was reported to be most reactive in neutral or basic conditions. Immobilization can bring about a shift in pH towards acidic or alkaline side. From the graph it is clear that PGE was found to have highest activity when immobilization was carried out in the pH range 6-7 with optimum activity at pH 7. Similar shift in pH was reported for RSDA immobilized on agarose using spontaneous cross-linking method with glutaraldehyde as a cross linker [112].

Strong interactions between amylase and support via free aldehyde groups that remain on glutaraldehyde bonded to the support, affected intra-molecular forces responsible for maintaining the enzyme conformation, leading to a resultant change in enzyme activity. The stability of immobilized enzyme at neutral pH is an added advantage as this will promote storage of amylase for longer periods [113].

At lower pH activity was found to be decreasing which might be due to unfavourable environment that could not hold the enzyme on support efficiently. As the pH increases beyond 7 also there was a decline in activity which might be due to change in active conformation that caused denaturation of enzyme protein to a considerable extent.

In the case of PN, however, the amino-terminated chains were flexible and could extend far into the solution. The amino groups on the surfaces of PN can thus easily interact with enzyme molecules in the solution for adsorption, regardless of the feature of the net surface electrostatic interaction.

Although amylase was adsorbed on PN in whole pH range examined, the highest activity was obtained in the range 5-6 with the optimum activity at pH 5. This is due to the fact that at this pH range amino groups on PN gets protonated and surface charge of PN adsorbent turns positive. Amylase has negative charge at this pH due to its isoelectric point of 4.6. This results in specific interaction between the positively charged amino groups of PN and negatively charged carboxyl groups at the enzyme surface to form $R\text{-}NH_3^+ \ldots {}^-OOC\text{-}R$ complexes, which enhanced the amylase adsorption on PN.

At pH lower than 5 both amylase and PN are positively charged and hence electrostatic repulsion will prevent adsorption. Also, at pH greater than 7 both amylase and PN are negatively charged which again results in electrostatic repulsion thereby causing hindrance to amylase molecules from getting strongly attached to PN.

But from the graph it is clear that significant amounts of adsorption occurs at these lower and higher pH's which may be explained from the macromolecular feature of the proteins and the location of the amino groups on PN being at the exterior ends of the chain, which allowed some parts of the protein molecules to penetrate through the electrostatic barrier and form complexes with amino groups

on PN to undergo effective adsorption. The results obtained led to the conclusion that surface complexation may be another important adsorption mechanism for enzymes attached to polymeric support [107].

3.7.4.1.1 Effect of contact time on the activity of immobilized enzyme

The period of contact needed for enzyme and support so as to achieve maximum loading are shown in the figure 3.39.

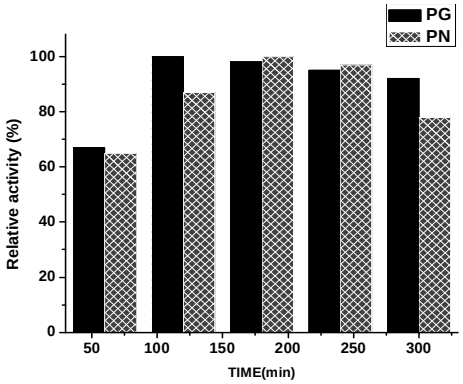

Figure: 3.39: Influence of contact time on immobilized enzyme activity

PGE showed an optimum activity after a contact period of 1hour. Further increase in time will lead to multilayer adsorption of enzyme and active sites on the surfaces get blocked with the enzyme that gets added in excess. This will cause corresponding reduction in activity.

For PNE the contact time of 180 minutes was sufficient to attain optimum activity. Since the same type of enzymes carried the same type of electric charges, after 180 minutes repulsive electrostatic interaction between already adsorbed enzymes on PN and the enzymes to be adsorbed from the solution would always occur, which can hinder further adsorption of enzymes from the solution on to the adsorbents. So, activity did not further get enhanced even if time of contact between support and the enzyme was increased.

3.7.4.1.2 Effect of initial protein concentration on protein loading and activity of immobilized enzyme

The trend of protein load that follows when initial concentration of enzyme was varied is shown in the figure: 3.40.

In the case of PG when concentration of initial protein was increased protein load also increased and then after an optimum of 19.5 mg it reached a plateau and further increase did not show any increase in loading. The optimum concentration indicates the maximum amount of enzyme that support can hold with retention of its activity. But this may not be the same for all supports because as multilayer adsorption comes into play, masking of number of active sites available may occur at optimum concentration and that will result in decrease in activity for some supports.

PN also showed an increase in loading of enzyme as concentration of initial protein was increased. This is because an increase in concentration will result in an increase of transport rate from the bulk solution to the solid-liquid interface and lead to the formation of clusters by aggregation of protein molecules [114,115].

For PN at initial concentration of 19.5 mg maximum protein load of 8.38 mg was obtained. This can be also explained based on the increase in surface area for PN when compared to PG, which allowed maximum amount of protein to be adsorbed on PN than on PG. After this range loading get decreased and this might be due to desorption of enzymes as result of weakening of the bonds that hold enzyme to the support.

It has been concluded that maximum adsorption occurs at near the isoelectric point [116,117]. Thus PN had its highest adsorption of amylase at pH 5. So this pH was selected as pH of immobilization medium to find out further optimization parameters.

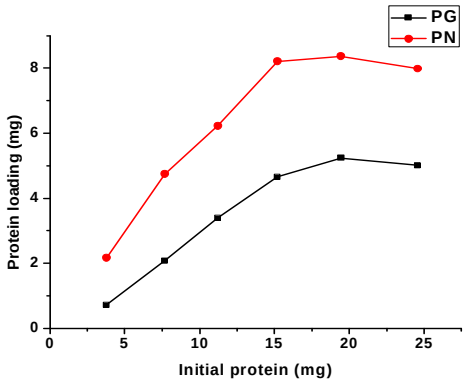

Figure: 3.40: Influence of initial protein concentration on protein loading

The trend of immobilized enzyme activity for PGE and PNE when initial protein concentration was varied is shown in the figure: 3.41.

The higher the concentration of anchor groups, the higher will be the amount of bound protein and the probability of the multipoint attachment of proteins to the carrier increases. As a consequence of such relation, three kinds of responses in the immobilized enzyme activity could be noticed. "Firstly, the overloading of carrier's surface may cause steric hindrance of large starch molecule and enzyme active site, lowering the enzyme activity. Secondly, decrease of activity as a result of changes in the enzyme structure by multipoint covalent modification. Thirdly, greater number of linkages between protein and support should result in more stable immobilized preparation" [71,118].

In the case of PNE activity enhanced when compared to PGE. This is because of the increase in surface positive charge for PN which arises as a result of protonation of amino groups at their surfaces. The increase in positive charge will result in strong electrostatic interaction between PN and amylase particularly near their isoelectric point. Hence change in structural conformation of enzyme at its active site will be negligible and hence the resultant loss in activity is not as much as that occurs via covalent bonding.

For PG the optimum activity was 8.5 EU at initial protein concentration of 19.5 mg and for PN it was 12.24 EU at the same initial protein concentration.

As the amount of bound enzyme increased the total activity of immobilized enzyme increased also but the rate of increase slackened as more enzymes was bound [119]. The results are shown in the figure: 3.41.

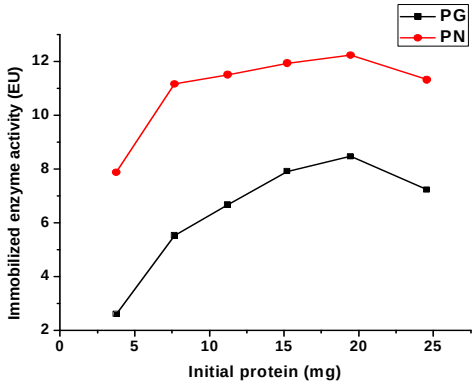

Figure: 3.41 Influence of initial protein concentration on immobilized enzyme activity

3.7.4.1.3 Effect of initial protein concentration on the immobilization yield and activity of loaded enzyme.

Immobilization yield obtained for all adsorbents at various concentration taken are shown in the figure: 3.42.

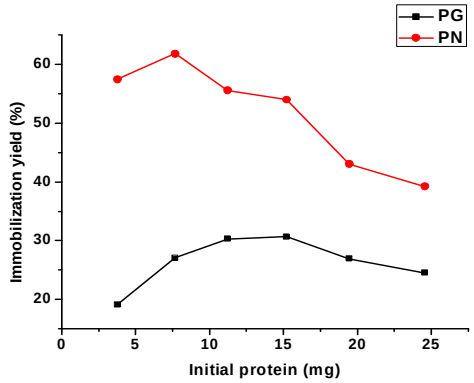

Figure: 3.42: Variation of immobilization yield with initial protein concentration

Immobilization using glutaraldehyde activated support was done via rapid "intra-molecular" reaction between nucleophiles of the enzyme and very near glutaraldehyde groups in the support. Immobilization yield was not as much as expected which might be due to cross-linking that occurred between glutaraldehyde reactive end groups as a result of which few number of activated ends was available for enzyme binding.

For PG when 19.4 mg of initial protein was added the immobilized enzyme showed maximum activity even if immobilization yield was low. This might be due to availability of more active sites at this concentration for the enzyme to carry out starch hydrolysis with maximum retention of its activity. The change in conformation of enzyme structure is the final parameter upon which the optimum activity depends and not on the immobilization yield which increases with increase in protein concentration.

Thus immobilization yield for PN was found to be 43% which was higher than PG. This is because of presence of amino groups at the surface of PN which enhanced the enzyme adsorption capacity as a result of strong positive charge near its isoelectric point.

Immobilization efficiency and activity yield can thus be summarized as follows in the table: 3.13. As shown in the table PG has the immobilization efficiency of 95% whereas, PN has 86%. But activity yield was higher for PN than for PG which was 37% and 26% respectively.

Table 3.13 Immobilization efficiency of PG and PN

Polymer	Initial protein (mg)	Immobilized protein mg/g support	Immobilization yield (%)IY	Initial activity (EU)	Immobilized enzyme activity EU	Activity Yield (%)AY	Immobilization efficiency (%) IE=AY/IY
PG	19.5	5.24	27	33	8.5	26	95
PN	19.5	8.38	43	33	12.2	37	86

3.7.4.2 Effect of pH on enzyme activity.

The variation in enzyme activity with change in pH of the reaction medium is shown in the figure: 3.43. The reaction pH was varied in the range 4-8 for all supports and it was found that both covalently bound amylase and adsorbed amylase followed a different trend.

Table 3.14: Optimum pH obtained for free enzyme, immobilized PG and PN

	Free enzyme	PGE	PNE
pH	5 & 5.5	5	6

For PNE the pH range in which maximum activity observed was within the range 6-7 with optimum pH at 6. This shifts results due to change in structural configuration of the immobilized enzyme. According to Singh et al. the strength of the electrostatic interaction between the enzyme and the support is very important in deciding the overall activity of the enzyme. As pH was increased the activity of both free and immobilized enzyme declined. The activity of immobilized enzyme is higher as compared to free enzyme in the studied pH range [167].

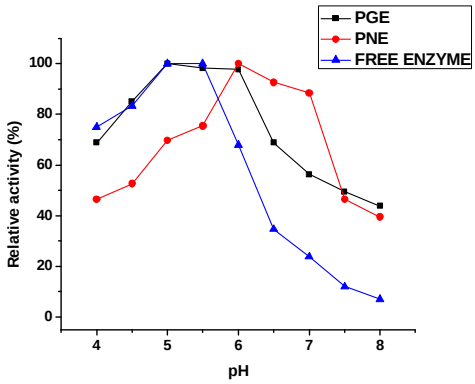

Figure: 3.43: Effect of pH on the activity of free and immobilized α-amylase

For PGE, immobilized enzyme was active in the range pH 5-6 with optimum at pH 5. This enhanced activity over a wider pH range could result from the change in acidic and basic amino acid side chain ionization in the microenvironment around the active site, which was caused by the newly formed

interactions between basic residues of enzyme and glutaraldehyde activated support [120,121].

The decline in amylase activity in the presence of glutaraldehyde may be the result of steric hindrance caused by the presence of the cross linking agent, which may have affected the accessibility of the substrate to amylase [122]. This can be explained by the fact that covalent bonding between enzyme and support restrict chain mobility within protein molecules and therefore conformational changes that are essential during catalysis are disabled. However, despite this rather low relative activity, immobilized enzymes with an activity approximately the same as the free enzyme have the potential to be used in industry. The costs saved by recovery and reuse of the enzymes can compensate for the loss of activity [123].

3.7.4.3 Effect of temperature on the activity

The temperature of the free and immobilized enzymes was determined by incubation at temperatures ranging from 30 to 70°C.

From the figure: 3.44 it is clear that the maximum activity of PGE was observed at 55°C. The soluble enzyme exhibited 27% activity at 60°C, whereas, PGE had around 69% activity at 60°C. At 70°C PGE showed 54% of activity whereas, free enzyme could give only 14% of its initial activity at same temperature. The increase in optimum temperature was caused by the change in physical and chemical properties of the enzyme as a result of immobilization. The covalent bond formation via amino groups of the immobilized enzyme might have also reduced the conformational flexibility, thereby resulting in higher activation energy for the molecule to reorganize and attain the proper conformation for binding to substrate [124].

For PNE the optimum temperature shifted to 60°C with the retention of 95% of its activity. Similar shift by 10°C to higher temperature was observed by Singh et al. in their work where they have immobilized Pullulanase from *Bacillus*

acidopullulyticus on to the hydrophobic synthetic macroporous resin Duolite XAD761 via covalent method, through the formation of a Schiff base [125]. Even at 70°C 68% of activity was retained by PNE.

Both the immobilization systems could provide better heat resistance compared to free enzyme allowing activity at elevated temperatures. In short, the free preparations showed a remarkable decrease of the activity surpassed their optimal temperature, whereas, the immobilized preparations exhibited an activity that was never less than 60% in the entire interval of temperatures considered. This might be due to the presence of coupling agents which prevents intense rigidification and unfavourable conformational changes in the enzyme structure [126].

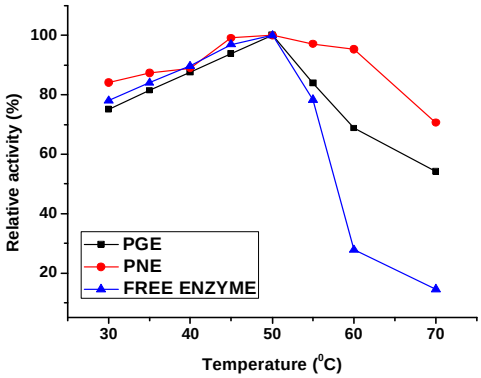

Figure: 3.44 Effect of temperature on the percentage relative activity of free and immobilized enzymes

3.7.4.4 Thermal stability of the free and immobilized enzymes

The thermal stability of the enzyme preparations was determined by incubation in appropriate buffer at temperatures ranging from 30° to 60°C for 1 hour. The results of thermal stability experiments showed that both covalent and adsorbed enzymes have improved thermal stability than free enzyme.

The activity is less for covalently immobilized enzyme compared to adsorbed one. Stability at higher temperature when analyzed was more for covalently

immobilized enzyme. This is due to the fact that covalently immobilized enzyme PGE was protected from the conformational changes caused by the environment.

The increase of thermal stability after immobilization can be explained by the fact that immobilization of the enzyme in their respective supports were able to preserve the tertiary structure of the enzyme from conformational changes caused by the environment [127]. The results are summarized in the figure: 3.45 shown below.

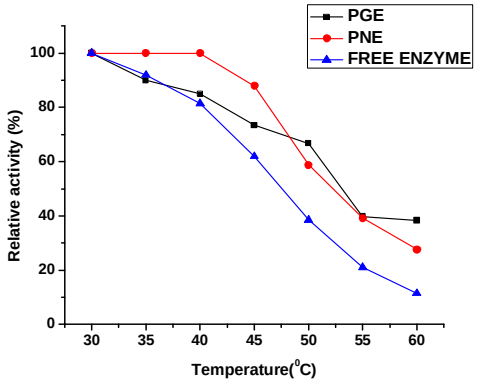

Figure: 3.45 Thermal stability of free and immobilized enzyme

When the immobilized enzymes were subjected to pre-incubation at regular time intervals in their respective buffer solutions similar trend was again repeated and results obtained are shown in the figure: 3.46 below.

Both the immobilized forms retained 80-90% of their initial activity after 40 minutes of pre-incubation time. With increase of pre-incubation time PGE retained 76% of its initial activity whereas, PNE retained 72% after 60 minutes at 40°C. After 80 minutes of pre-incubation time PGE retained 65% of its initial activity and PNE retained 61%. Finally an activity of 55% was retained by PGE and 45% by PNE after 100 minutes of pre-incubation time. This indicates greater rigidity of the immobilized α-amylase leading to enzyme molecules that are more resistant to unfolding at higher temperatures than the free form.

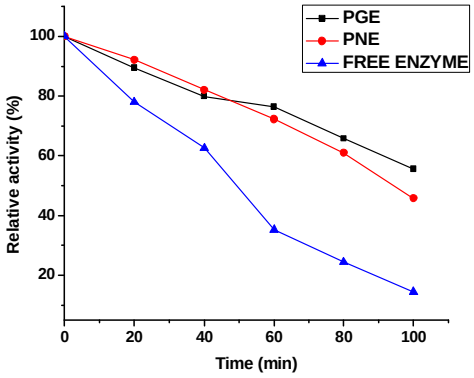

Figure: 3.46: Effect of pre-incubation time on relative enzyme activity of free and immobilized enzymes.

The surface on which the enzyme gets immobilized is responsible for retaining the tertiary structure in the enzyme through hydrogen bonding or the formation of electron transition complexes. These links will prevent vibration of the enzyme and thus increase thermal stability [128,129]. The stability of immobilized enzymes at low pH and its increased activity at high temperatures implies that the enzyme can be applied in starch hydrolysis at low pH and moderately in high temperatures of 60°C and above to minimize contamination during processing [130,112].

3.7.4.5 Determination of kinetic parameters

When a biocatalyst is immobilized, kinetic parameters K_m and V_{max} undergo variations with respect to the corresponding parameters of the free form, revealing an affinity change for the substrate [131].

The effect of immobilization on kinetic parameters was studied by measuring the rates of starch hydrolysis by free and immobilized amylase at various concentrations of starch. The Lineweaver-Burk plot and Hanes-Woolf plots for the free and immobilized α-amylase is given in figure: 3.47. The K_m and V_{max} values were calculated from the slope and intercept of the straight lines, respectively and results are tabulated in the table 3.15.

An increase of the K_m suggests the requirement of higher substrate concentration to achieve the same reaction rate observed for the free enzyme [132].

Table 3.15: Kinetic parameters for immobilized α-amylase on PG and PN

	Free enzyme	PGE	PNE
K_m (mgml^{-1})	0.50 ± 0.04	1.88 ± 0.03	3.57 ± 0.04
V_{max} (mg/ml/min)	7.40 ± 0.05	1.80 ± 0.02	3.56 ± 0.03

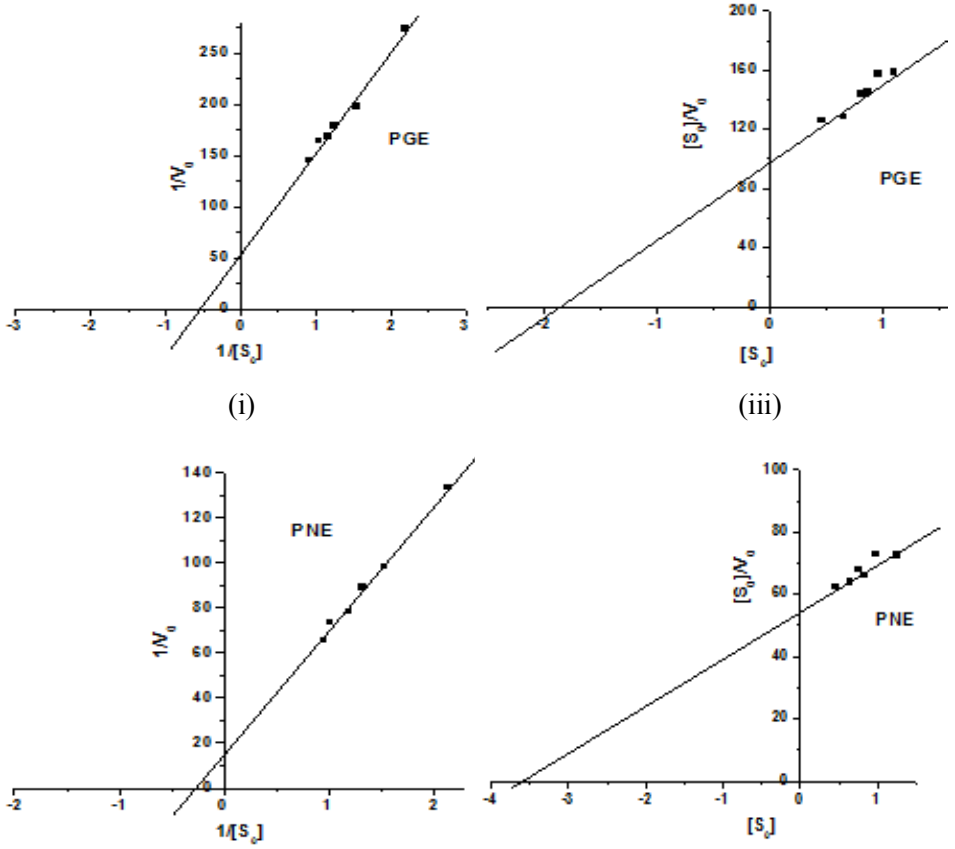

Figure: 3.47: Lineweaver-Burk plots for α-amylase immobilized on (i) PG (ii) PN and Hanes-Woolf plots of (iii) PG and (iv) PN

Since the enzymatic reactions take place through a carrier medium the affinity of the enzyme towards the substrate is not the same in every carrier media.

Thus higher K_m value can be attributed to the diffusional resistance of the carrier against substrate and or product and less porous structure. This occur either due to structural changes in the enzyme induced by the applied immobilization procedure or due to the lower accessibility of the substrate to the active site of the immobilized enzymes [133,134]. In other words, the increase in K_m values after immobilization may be partially due to mass transfer resistance of the substrate into the immobilization medium.

The decrease in V_{max} value as a result of immobilization should be related with the increase in K_m value. Since immobilization brings about conformational changes of the enzyme, which usually decreases the affinity to the substrate. As a result of this partial inactivation of all or the complete inactivation of the part of the enzyme molecules may occur and hence decrease of V_{max}.

Hanefeld et al. reported that the difference in kinetics between lipases immobilized on different supports was ascribable to conformational changes induced upon enzyme-polymer interaction [135]. A similar observation had been reported for immobilized invertase on white and black lahar (volcanic mudflow) by the silane-glutaraldehyde method [136]. Immobilization brought about an increase in the K_m but a decrease in the V_{max} and these changes were correlated to immobilization induced conformational changes in the enzyme [137].

3.7.4.6 Storage stability of Immobilized α-amylase

When stored in buffer solution the starch hydrolyzing activity of the α-amylase immobilized via covalent coupling decreased at a slower rate than that of the adsorbed enzyme. Upon 4 months of storage, the adsorbed enzyme preserved 40% of its initial activity whereas; covalently bound enzyme retained 55% of its initial activity. This is because conformational changes due to immobilization help the enzyme to suitably orient its active site towards the substrate [138].

The immobilization of enzyme to a support often limits its freedom to undergo drastic conformational changes and hence results in increased stability. Storage stabilities of free and immobilized enzymes studied at 4°C is depicted in the figure: 3.48. The decrease in activity was explained as time-dependent natural loss in enzyme activity.

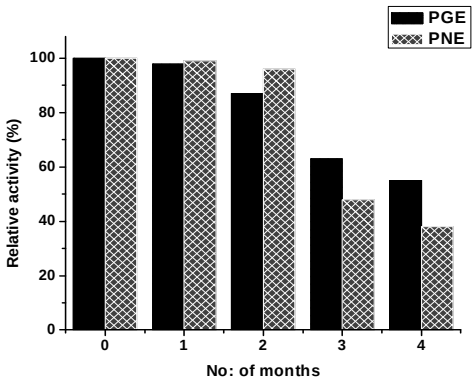

Figure: 3.48: Storage stability studies of α-amylase immobilized on PG and PN

3.7.4.7 Reusability

The operational stability of the α-amylase was evaluated in a repeated batch process. The results in figure: 3.49 indicated that the catalytic activity of the immobilized enzyme was durable under repeated use.

In the case of PNE up to 7 cycles 70% activity was retained which decreased drastically for further cycles. PGE the immobilized enzyme was able to maintain good activity up to 60% even after five runs. There was no drastic decrease in percent hydrolysis even after five uses, which could be due to glutaraldehyde treatment of polypyrrole which prevented the leakage of enzyme. Similar results were reported by S. Talekar et al. [139]. As per their study α-amylase CLEAs retained 65% activity after 4 reuses with 30 min of reaction time.

Ates and Mehmetoglu found that after treatment with glutaraldehyde the Cu-alginate immobilized enzyme could be used 8 times with high activity. This

improved stability of immobilized α-amylase can be attributed to the improved resistance to denaturation and conformational changes of the enzyme in buffer solution, as a result of the covalent bonding procedure of the amylase molecules on PG [140].

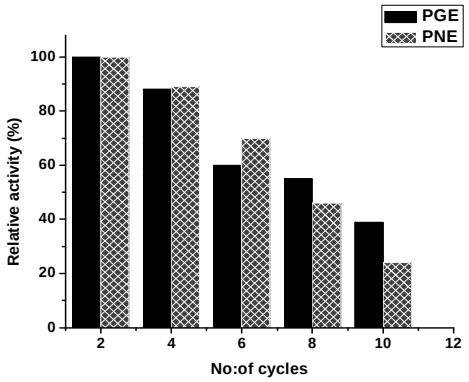

Figure: 3.49: Reusability studies and for α-amylase immobilized on PG and PN

3.8 Significance of polypyrrole copolymers as support for enzyme immobilization

In order to further enlarge the application of PPY in sensors, much effort has been carried out in recent years to fabricate functionalized PPY derivatives through either modification of the pyrrole monomer's structure or the preparation of block and graft copolymers [141,142]. The former method, namely, the synthesis of pyrrole monomer substituents, is very appealing because of the ease of polymerization and the wide variety of functional groups that can be linked to pyrrole, which enables post functionalization of the resulting polymer. Surface modification of these materials with biological moieties is desired to enhance the biomaterial-tissue interface and to promote desired tissue responses.

Copolymerization of a pair of monomers will lead to an increase in the number of conductive polymers that can be made from the same set of monomers

[143]. Moreover, it is also likely that the copolymer will incorporate the unique properties of homo-polymers. A growing interest in copolymers as immobilization supports can be observed, since by changing the ratio between the monomers, the properties of the copolymer (hydrophilicity / hydrophobicity, amount of functional groups, mechanical properties, porosity, etc.) can be desirably changed. Therefore custom-made supports for enzyme immobilization of all kinds for different purposes can be produced [144].

Among the various conductive polymers studied, polyaniline (PANI) and polypyrrole (PPY) have been of particular interest due to their high electric conductivity, environmental stability and low cost of production and favourable physico-chemical properties associated with the chain heteroatoms. Another reason for the great deal of attention given to PANI-PPY copolymers is probably attributed to the great difficulty to synthesize new conducting polymers with electric properties and stability that are better than polyaniline and polypyrrole. Fusalba et al. have reported that the main motivation for preparing copolymer composites lies in the possibility that these materials overcome the limitation of the rareness of new conjugated pi bond containing monomers [145]. Both polyaniline and polypyrrole have secondary amino groups in their polymer backbone. In polyaniline, steric effects of benzene rings might block access by the amino groups in the polymer backbone. Amino groups in polypyrrole are accessible to face protein molecules without steric hindrance. So for polyaniline adsorbent very low loading was observed during enzyme immobilization [146]. Copolymerization will enhance the enzyme loading capacity as it has the added advantage of polypyrrole along with polyaniline in the polymer backbone.

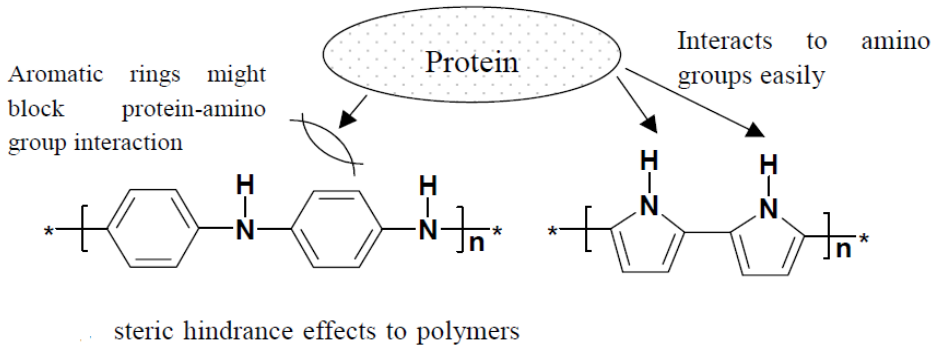

Scheme 3.7: Steric hindrance effects on polypyrrole and polyaniline

Another way of increasing enzyme adsorption efficiency is by copolymerizing with a modified monomer having any substituted functional group. 3-substituted and N-substituted pyrroles are the most used derivatives of pyrrole. When compared to 3-substituted pyrrole which are asymmetric molecules, N substituted pyrrole are fundamentally symmetric. Thus polymerization of N-substituted pyrrole will result in an increased order and a planarity of polymer backbone. Consequently N-substituted pyrrole derivatives are more desirable forms than their 3-substituted counterparts. Thus amylase immobilization was carried out on two copolymers namely pyrrole-aniline copolymer and pyrrole - 1-(2- amino phenyl) pyrrole. Songul et al. have reported the use of N-substituted polypyrrole derivatives towards glucose sensing electrodes [147].

3.8.1 Preparation of polypyrrole co-polymers

3.8.1.1 Preparation of poly (Pyrrole -co-1-(2-aminophenyl pyrrole)

1-(2- aminophenyl pyrrole) (4.0×10^{-3}mol, 0.632 g) was dissolved in 200ml $CHCl_3$. This solution was treated with an ultrasonic bath for 15 minutes to obtain the best dispersion of NoaPy. Pyrrole (4.0×10^{-3} mol, 0.278ml) was added to this solution. The solution was maintained in an inert N_2 atmosphere and under

magnetic stirring, whereas $FeCl_3$ (0.01 mol, 0.812g) in 200 ml of $CHCl_3$ were slowly dropped to the monomer solution during 30 minutes. n_{ox}/n_{mon} ratio was taken as 2.5 for the synthesis. After polymerization time 24 hours, precipitated polymer was filtered and washed with firstly $CHCl_3$ then with ethanol until the filtrate was colorless. Finally, the polymer was dried at 50°C for 24 hours under vacuum environment [147].

The reaction is depicted as follows:

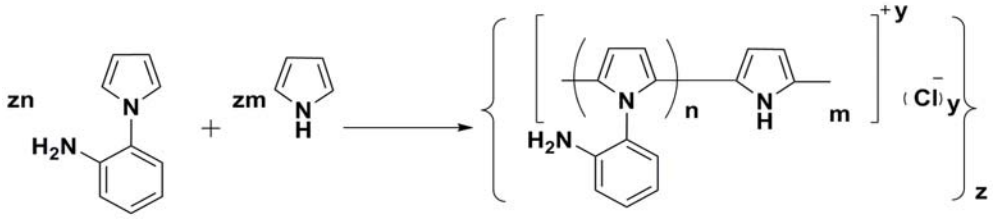

Scheme 3.8 Copolymerization of pyrrole with 1-(2- aminophenyl pyrrole)

3.8.1.2 Preparation of poly (aniline-co-pyrrole)

Copolymerization of pyrrole and aniline was carried out similar to the polymerization of pyrrole. Typical experimental procedure (aniline: pyrrole = 1:1) was as follows. Aniline (0.9313g, 0.01mol) was added to 100ml 0.1M HCl solution, which was soon followed by addition of pyrrole (0.67g, 0.01mol) dissolved in 100ml 0.1M HCl with stirring. Final mixture was stirred vigorously for 30 minutes in an ice bath. To this pre-cooled solution of 10 ml 2M APS was added drop wise with constant stirring and the temperature is maintained at 0-5°C. Further agitation was applied for 24 hours after the dropping process was completed. The product was then washed and filtered three times with de-ionized water to eliminate unreacted oxidants and the oligomers. Finally black powder obtained was washed with methanol [148,149].

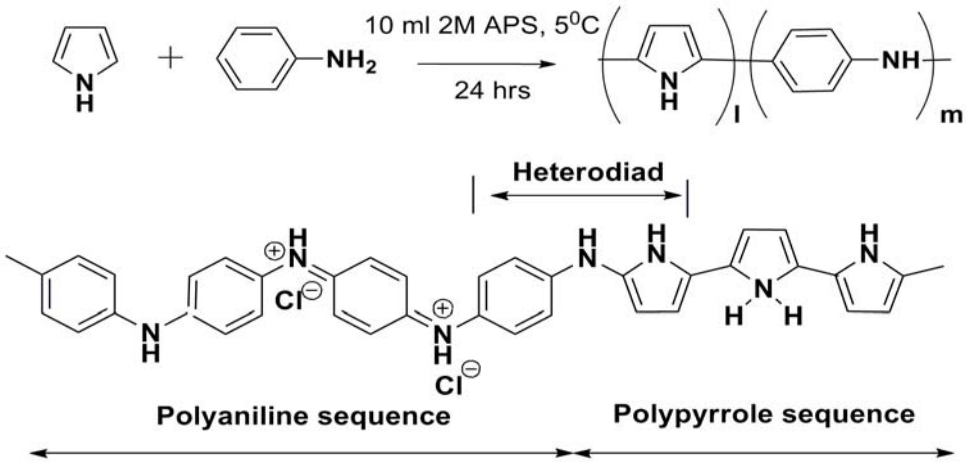

Scheme 3.9: Copolymerization of pyrrole with aniline

3.8.2 Physico-chemical characterization

3.8.2.1 FT-IR Spectra of polypyrrole copolymers.

Pyrrole -aniline copolymer:

For the PYPA copolymer, the spectra recorded show most of the characteristic bands of PPY and PANI. The peaks at 1385 cm^{-1}, 1288 $cm^{-1}$and 1196 cm^{-1} is due to various C-N stretching vibrations. It is observed that the peaks shifted to a lower wave number for the copolymer (poly (aniline-co-pyrrole)) demonstrating the presence of neighbouring aniline and pyrrole constitutional units [150].

Another interesting point of the spectra is that the quinonoid phenyl ring C-C stretch band of PANI at 1600 cm^{-1} and the C=C / C-C stretching mode of PPY at 1560 cm^{-1} have combined to form a broader band at around 1588 cm^{-1}. A new band at 1112 cm^{-1} can be observed which can be attributed to the C-H in plane bending on the 1,2,4-substituted benzene of PANI. From this new band, it may be deduced that the pyrrole units in the copolymer are likely to be attached to the 1,2 or 4 positions on the benzene ring [151].

Secondly, the para-substituted aromatic C-H out of plane bending band of PANI at 840 cm^{-1} has greatly diminished in copolymer spectra and is shifted to a lower wavelength which is only a very weak band at 832 cm^{-1}.This observation is likely to be caused by the replacement of aniline units by pyrrole units along the chains.

The C-H out of plane bending mode of copolymers show more complicated absorption bands than that of polyaniline or polypyrrole.

After immobilization of α-amylase wavenumber gets shifted for both copolymers. Thus for poly (pyrrole- co- aniline) the wave number at 3454 cm^{-1} corresponds to N-H stretching vibration. The bands at 2928 $cm^{-1}$and 2854 cm^{-1} are attributed to C-H stretching vibration. The bands at 1648 cm^{-1}, 1542 cm^{-1},1504 $cm^{-1}$and 1397 cm^{-1} were of increase in intensity and is attributed to that of α-amylase. The other bands were lowered in intensity and wave number compared to parent polymer.

Pyrrole-1-(2 aminophenyl pyrrole) copolymer

FTIR spectra of PYPH copolymer were shown in figure: 3.50. The sharp peak at 1512 cm^{-1} is one of the characteristic C=C aromatic stretching vibration. Whereas the peaks around 1000 cm^{-1} are out of plane C-H vibrations, absorption band at 1462 cm^{-1} is attributed to in plane C-H stretching vibrations of pyrrole and phenyl rings [152].

The peaks appeared in the range of 1265 cm^{-1} and 1045 cm^{-1} are the characteristic peaks for pyrrole rings [153]. The bands, which belongs to either pyrrole or phenyl ring were observed from the FTIR spectra. The peak at 1162 cm^{-1} and 1090 cm^{-1} confirm the presence of benzene ring in the structure.

The peaks at around 793 cm^{-1},742 $cm^{-1}$and 621cm^{-1} in the spectra were assigned to the out-of-plane vibration of three adjacent carbon-hydrogen bonds which reflected the substituted benzene ring [147,154].

The peak at 609 cm^{-1} is attributed to C-H aromatic in plane vibration. Several bands occurring in the regions, 1609-1581 $cm^{-1}$and the 1574-1490 cm^{-1} can be attributed to the phenyl υC=C stretching vibrations.

The bands located in the 1498-1424 cm^{-1} region are due to the C=C pyrrolic ring stretching vibrations. The intensities of the absorption band characteristic for the collective vibration mode located around 1550 cm^{-1} decrease due to the presence of substituted pyrrole monomer. This fact also indicates a reduction of the effective conjugation length of the polymeric chains due to the conformational modifications induced by the substituted pyrrole [155].

For immobilized poly (pyrrole-co-1-(2-aminophenylpyrrole)) decrease in intensity of characteristic bands occur. Along with that some additional bands assigned to α-amylase was also observed at 1656 cm^{-1}, 1542 cm^{-1}, 1398 cm^{-1}, 1317 cm^{-1} which was absent in the spectra of parent polymer.

Peak assignments for copolymers and their immobilized forms are given in the table 3.16.

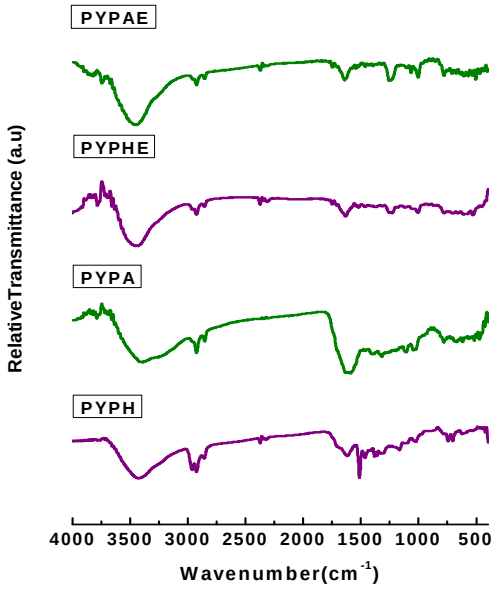

Figure: 3.50 FT-IR spectra of copolymers

Table 3.16 Peak assignments for copolymers before and after enzyme immobilization

Peak assignments (cm^{-1})	PYPH	PYPH E	PYPA	PYPAE
N-H stretch	3433	3440	3396	3452.
C-H stretch	2965,2929,2857	2961,2924, 2854	2961, 2926, 2852	2924,2855
C=O	1688 vvw	1708,1747	1710	1748,1704
C-N-C ring -in plane deformation		1646, 1656b	1590	1650bm,
NH_2 in plane deformattion	1615bm	1621	1624	1617
N-H ring in plane bending(s)	1550	1542	1582, 1492, 1457	1542
C-C in ring stretch(s)	1337	1336,1317	1336, 1316	1363,1317
Aromatic C-H in plane bend	1158,benz	1176	1171	1170
C-H ring in plane bending(w)	1112,	1115	1112,1123 sub,benz.	1100
C=C-N ring in plane deformation	1094	1070	1072	1061
Aromatic C-H out of plane bend	783,742,621 Sub.benz ring	782	784	780

3.8.2.2 Thermogram of copolymers

Thermogram of copolymers PYPA and PYPH are shown in the figure: 3.51. In the case of PYPA a minor weight loss occur at 76°C due to water desorption. The major weight loss was observed in the range 264-564°C. This slow weight loss below 564°C may be due to degradation of low molecular weight and small chain segments. The next weight loss above 564°C is assigned to the structural decomposition of the polymer backbone.

In the case of immobilized PYPA, the minor peak at 198°C and 270°C is attributed to protein degradation. The major weight loss at 339°C and 568°C is assigned to degradation of copolymer structure. The minor weight loss which continues to occur after this temperature is the result of structural decomposition of polymer backbone.

Thermogram of PYPH showed more thermal stability than the PYPA which might be due to the presence of phenyl ring in the former. Two major decomposition and two minor decompositions were observed in the PYPH. The minor weight loss was observed in DTG (not shown) at 156°C which might be due to elimination of water molecules and unreacted monomers. The major weight loss at 305°C and 338°C might be due to the decomposition of copolymer of pyrrole-1-(2-amino phenyl pyrrole). The peak at 595°C corresponds to degradation of polymer backbone.

After immobilization the major weight loss was in the range 170°C -513°C, which correspondingly showed peaks in DTG at 305°C, 372°C and 428°C. These are assigned to protein organic structure decomposition, water desorption and polymer degradation.

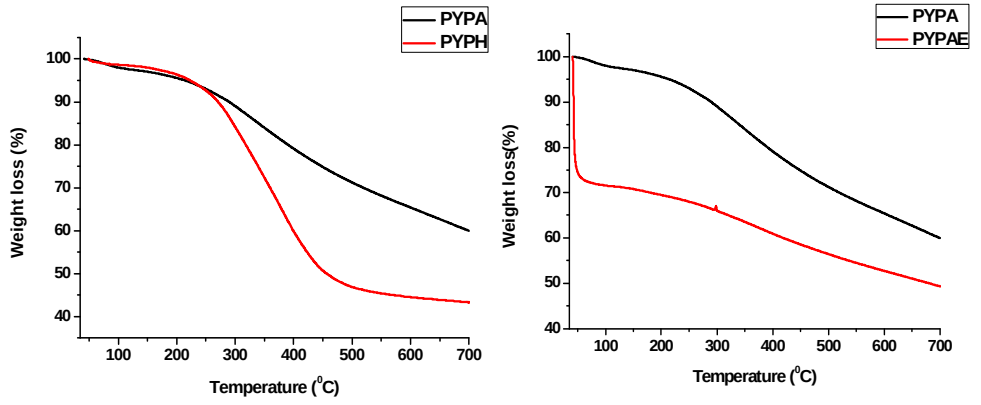

(i) (ii)

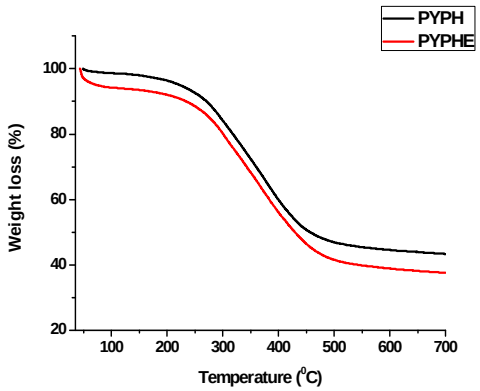

(iii)

Figure: 3.51: TG curves for (i) PYPA and PYPH (ii) PYPA and PYPAE (iii) PYPH and PYPHE

3.8.2.3 Surface area analysis

For PYPA appreciable surface area was there and it comes in the range 37mg/g but for PYPH surface area was too low. This might be due to the presence of aminophenyl groups on the surface of copolymer that resulted in reduction of surface area when compared to bare polypyrrole.

The enzyme immobilized samples of all polymers showed corresponding decrease in surface area. Protein loading was found to be proportional to surface area of polymers. Thus as surface area increases loading capacity of the supports also increased.

3.8.2.4 Scanning electron microscopy

The copolymer formed between pyrrole and aniline PYPA showed spherical structures that are agglomerated. The size of the particles varied in the range 90-100 nm. It can be seen that pyrrole and aniline monomer affected the morphology of the obtained copolymer.

The copolymer of pyrrole and 1-(2-amino phenyl pyrrole) (PYPH) was found to have rough surface with flaky structures. The particles seems to aggregate into irregular shape and hence distributed non-uniformly.

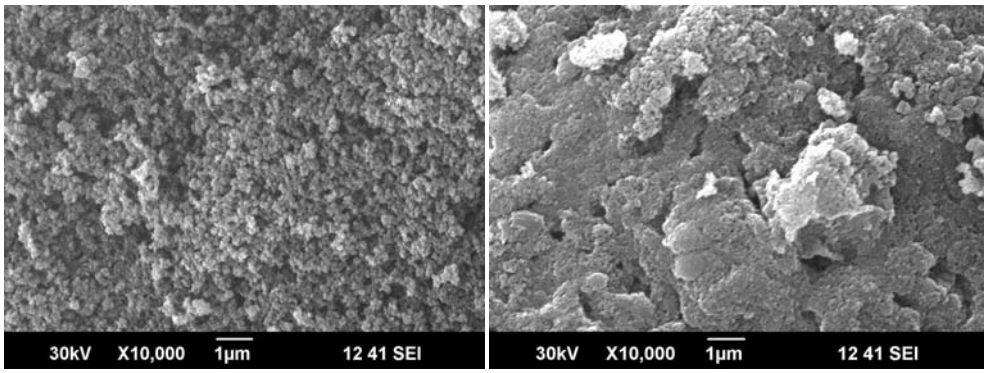

(i) (ii)

Figure: 3.52: SEM images for (i) PYPA (ii) PYPH

3.8.3. Immobilization of α-Amylase on Polypyrrole Copolymers

3.8.3.1 Optimization of immobilization conditions

PYPH, co-polymer has (2-amino phenyl) functional group at N-position. So the conjugated backbone will be available for hydrophobic interaction and amino end will be favouring electrostatic interactions. Thus it is well documented that no particular property dominates the adsorption process; rather it is a combination of some, if not all, of the processes that determine the adsorption characteristics of proteins.

For PYPA copolymer both monomers are having conjugated rings which leads to hydrophobic interaction with proteins. But electrostatic interaction also has a secondary role here.

Even though isoelectric point of copolymers is not available it can be assumed from isoelectric point of homopolymers. As isoelectric point of polypyrrole is 7 and that of polyaniline is around 7.6, isoelectric point of copolymer must be close to this [146]. Also, in the case of PYPH isoelectric point will be close to that for polypyrrole. The variations in the adsorption capacity of copolymers are attributed to the influence of groups in the copolymers and also their surface area.

The pH dependence of the immobilized enzyme activity was compared with that of the free enzyme in the pH range of 3-8 at 30°C, and the results are presented in figure: 3.53.

The best pH for immobilization was found to be at pH 4 for PYPH and at pH 5 for PYPA. At pH 4 - 4.5 both amylase and amine groups on the support surfaces are positively charged and hence they repel each other. But results are contradictory showing adsorption in this region. This is because hydrophobic interaction might have dominated here which thus minimised the pH effect and electrostatic interaction is only having a secondary role.

Immobilization affects the three dimensional structure and the distribution of the functional groups of enzyme and as a result, a change in the microenvironment of the enzyme is expected. Therefore the stable substrate-enzyme transition complex may form at different pH values compared to that of free enzyme [156].

Below pH 4 and above pH 5 the relative activity of immobilized PYPH decreased sharply. Similarly below pH 5 and above pH 6 for PYPA the relative activity of the immobilized enzyme suffers a decline in activity.

These two observations might be due to the fact that difference in charge separation on surface of both supports have affected the free enzyme differently and that may owe to desorption of enzyme from the carrier or instability of pure enzyme in the regions below and above the optimum immobilization pH's of both immobilized enzymes. This happens because the changes in pH bring about apparent changes in enzyme structure, which influence its activity.

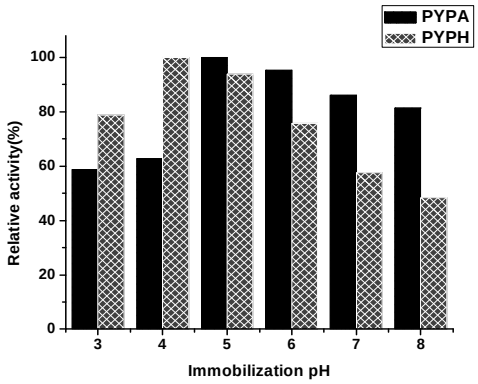

Figure: 3.53 Effect of pH on the immobilization of α-amylase on to copolymers

3.8.3.1.1 Effect of contact time on the activity of immobilized enzymes

The contact time needed for enzyme to get adsorbed on PPY adsorbents is shown in the figure: 3.54.

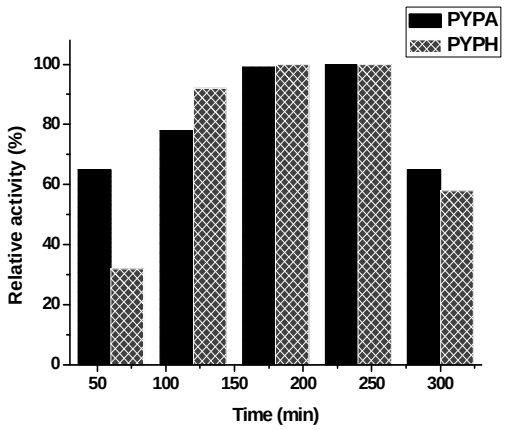

Figure: 3.54: Effect of contact time on immobilized enzyme relative activity

It was optimized by allowing free enzyme in buffer solution to be in contact with the supports for different known time intervals. The support gets saturated with the enzyme after a particular interval of time. The maximum activity was represented as 100% and other activities are represented as relative to this optimum activity. After this particular contact time enzyme starts to get desorbed from the

support due to multilayer adsorption and hence will show corresponding loss in activity when compared with optimum.

Thus PYPA shows maximum adsorption rate when kept in contact with enzyme for 240 minutes, and PYPH shows maximum adsorption rate within 180-240 minutes of contact time. Above this time interval there was decrease in enzyme loading on the support which thereby reflected in its activity.

3.8.3.1.2 Effect of initial protein concentration on the protein loading

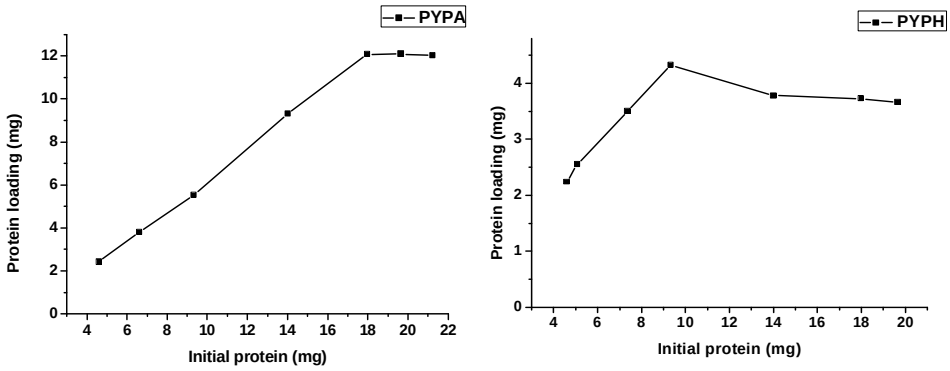

(i) (ii)

Figure: 3.55: Effect of initial protein concentration on the loading capacity of copolymers (i) PYPA (ii) PYPH.

The amount of protein loaded to PPY copolymers, is given in figure: 3.55.

On the addition of protein to support, immobilization occurs immediately and loaded amount increases and reaches a saturation point. Further addition of enzyme did not make any remarkable increase in loading. The saturation point depends upon the properties of the support and the methods of immobilization.

Effects of immobilization depends on several parameters like surface area of supports, accessibility of support surface for enzymes, number of activated functional groups on the support, distance between bound enzyme and the surface of the support and conformation at the active site. Mono- or multipoint binding of

an enzyme to the support, chemical affinity of the protein to the material of the support are further factors influencing immobilization [157,158].

Here, in the case of PYPA surface area obtained was higher than PYPH and that correspondingly reflected in loading of protein on to the supports. Consequently protein load of PYPA is found to be maximum compared to PYPH. For PYPH enzyme loading of 4.3 mg/g support was the maximum whereas, for PYPA 12 mg/g support was the optimum loading.

After the saturation point for both supports immobilization rate starts decreasing because multilayer adsorption will result in lowering of available active sites of enzyme thus favouring only weaker interaction of proteins with the support. This will result in easy desorption of protein molecules anchored strongly on to the support.

3.8.3.1.3 Effect of initial protein on immobilization yield and activity of loaded enzyme

Immobilization yield obtained for all adsorbents at various concentrations taken are shown in the figure: 3.56.

For PYPA as concentration of enzyme increases immobilization yield which gives the percentage of protein loaded, increases, up to 17 mg which then starts decreasing. The optimum percentage yield thus obtained for PYPA is 67%.

Even though optimum yield obtained for PYPH was 74% the higher protein load was at lower concentration of 9.3 mg where immobilization yield was only 46%. This lower loading is due to the multilayer adsorption which results in poor interaction between enzyme and support. As a consequence chances of enzyme desorption from the surface increases or it may cause lesser exposure of all active sites of the enzyme present on the support.

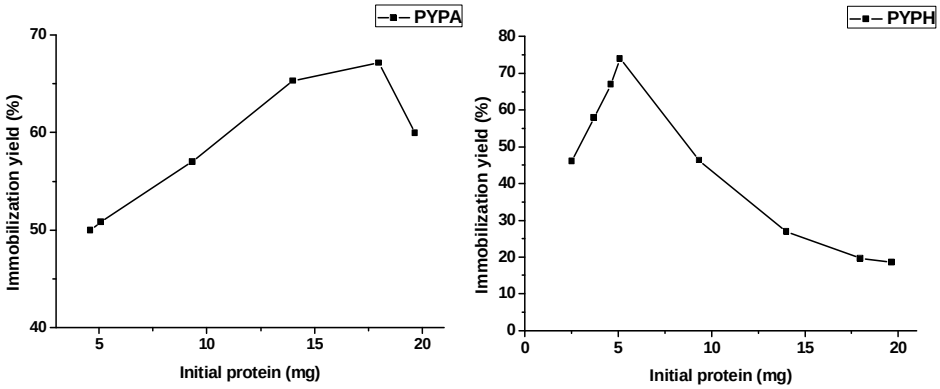

(i) (ii)

Figure: 3.56: Effect of initial protein concentration on the immobilization yield of protein bound on copolymers (i) PYPA (ii) PYPH

Corresponding variation in immobilized enzyme activity is shown in the figure: 3.57. In both cases optimum immobilized enzyme activity was shown at the concentration in which optimum loading occurred. This might be due to the presence of greater number of available active sites with proper orientation, which was favourable for the substrate to undergo chemical reaction easily and hence resulted in enhanced activity of immobilized enzyme.

For PYPA optimum immobilized enzyme activity of 14 EU was at protein load of 12 mg and for PYPH the optimum activity of 7 EU was at optimum protein load of 9 mg. To get overall results of enzyme support interaction evaluation of activity yield and immobilization efficiency is inevitable. Hence they were calculated using standard equations using results obtained above and is tabulated as shown below.

Table 3.17: Immobilization efficiency of α-amylase on copolymers

Polymer	Initial protein (mg)	Immobilized protein mg/g support	Immobilizationyield (%)IY	Initial activity(EU)	Immobilized enzyme activity EU	Activity Yield (%)AY	Immobilization efficiency (%) IE=AY/IY
PYPA	18	12.1	67	40	14.4	36	54
PYPH	9.3	4.3	46	26	4.7	18	39

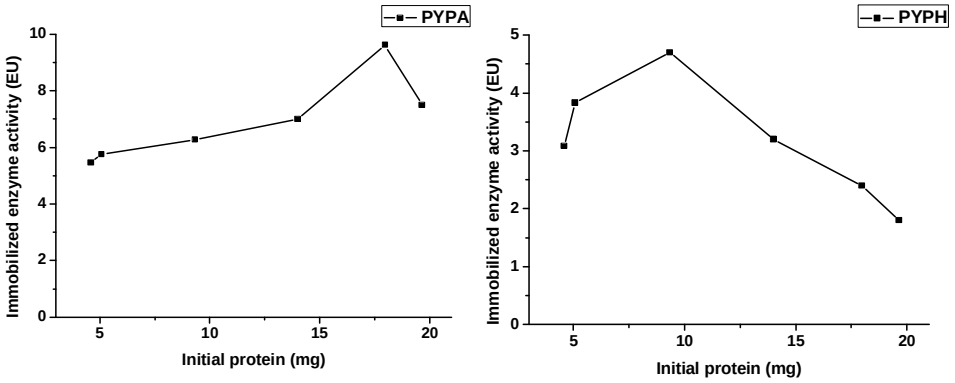

(i) (ii)

Figure: 3.57: Effect of initial protein concentration on immobilized enzyme activity in the case of copolymeric supports (i) PYPA (ii) PYPH

The maximum activity yield obtained for PYPA was 36% which has the highest value for immobilization efficiency of 53.7% .indicating that immobilized enzymes retained their original activity.

PYPH loading was lower due to its low surface area and hence activity yield was only 18% with immobilization efficiency of about 39% .This is the consequence of lower loading and improper conformational orientation of enzyme that get anchored to the support. The enzyme-substrate affinity correspondingly gets lowered which is reflected in the poor activity yield and subsequent decline in the immobilization efficiency. Hasirci et al. studied poly (dimer acid-co-alkyl polyamine) particles that were activated by CDI, EDA, and HMDA, respectively [159]. The amount of bound enzyme was found as 7.6, 6.5 and 39.3 mg/g of each particle respectively. Several studies reported shows that binding capacity of the support materials is labile due to characteristic properties of prepared materials [160].

3.8.3.2 Effect of pH on enzyme activity

The pH dependent activity profiles of both free and immobilized amylase are shown in figure: 3.58.

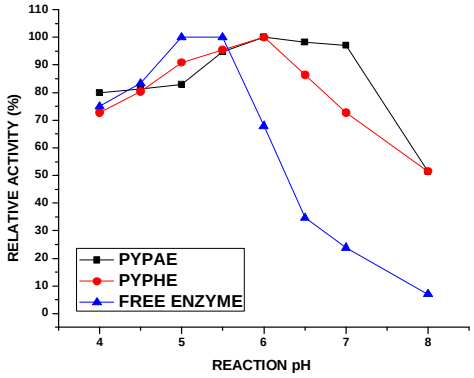

Figure: 3.58: Effect of pH on the relative activity of free and immobilized enzymes on copolymers

Table 3.18: Optimum pH for immobilized enzymes

	Free enzyme	PYPAE	PYPHE
pH	5 & 5.5	6	6

In the pH range 5-7 all the copolymers are having positive charges on their surfaces which thus favours strong electrostatic interaction with amylase which is negatively charged at this pH [162]. For both copolymers optimum reaction pH was 6. This shift is due to the increase in positive charge on amine groups on both copolymers. As a result, the concentration of H^+ions in the microenvironment of the immobilized enzyme decreases which means that the pH of the immobilized region is more alkaline than that of external solution. Immobilization often times lead to a shift in pH either towards the acidic side or towards the alkaline side [163,164].

Factors which influence the pH of immobilized enzyme include surface and residual charges on solid matrix and the enzyme bound pH in the micro-environment as compared to the bulk environment [165]. According to Dhingra et al. optimum pH of an enzyme shifts upon immobilization, particularly when the support material is charged. Strong interactions between enzyme and support affect intra-molecular

forces responsible for maintaining the enzyme conformation leading to a resultant change in enzyme activity [161]. Increased stability of immobilized α-amylase over a wide range of pH (4 to 8) is an indication of greater insensitivity of the enzyme to changes in environmental pH, brought about by conformational changes following immobilization [166].

3.8.3.3 Effect of temperature on the activity

The effect of reaction temperature on the activity of both free and immobilized enzymes are shown in the figure: 3.59. In fact the free preparation showed a remarkable decrease of the activity, surpassed their optimal temperature, whereas, the immobilized preparations exhibited an activity that was never less than 60% in the entire interval of temperatures considered.

For PYPH the optimum temperature was at 50°C which is same as that of free enzyme. Similar result showing no change in optimum temperature was also observed by Tanriseven and Olcer [168].

For PYPA, optimum temperature shifted to 60°C. Similar shift to higher temperature after immobilization has been observed by other authors [169,170]. Thus the results again confirmed that the immobilized α-amylase holds greater heat resistance than that of free enzyme.

The decrease of relative activity of the free enzyme is probably due to its thermal denaturation [167], while the relative activity of the immobilized enzyme decreased only slowly because of some protections of the carrier for the immobilized enzyme. The increase of optimum temperature for the immobilized enzyme may arise from the change of the conformational integrity of the enzyme structure upon adsorption to the carrier materials [165,171].

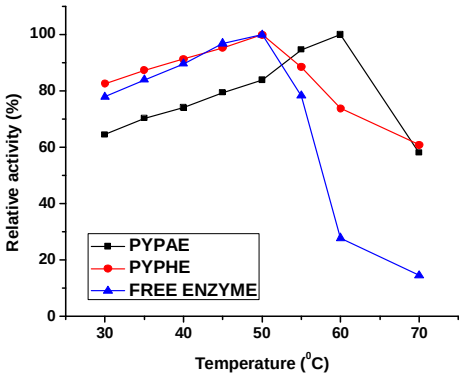

Figure: 3.59: Effect of temperature on relative activity of free and immobilized α-amylase

Compared to the free enzyme, the higher activity of immobilized enzymes at elevated temperatures and ability to hydrolyze starch would help overcoming problems related to gelatinization of starch during hydrolysis [172].

3.8.3.4 Thermal stability of the free and immobilized enzymes

Thermal stability of both free and immobilized enzymes were investigated and the results are shown in the figure: 3.60.

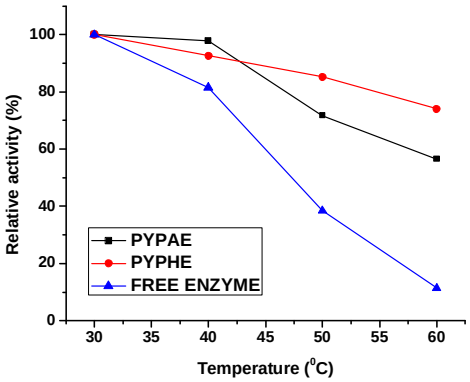

Figure: 3.60: Effect of thermal stability on free and immobilized α-amylase

Both free and immobilized enzyme showed maximum activity when incubated at 30°C for 1hour. As the temperature increases, the stability dropped significantly for both free and immobilized amylase. At 40°C, both free and

immobilized enzyme retained 80-90% of their activity. At 50°C for 1hour the immobilized enzyme was inactivated at a much lower rate than the free enzyme. The free enzyme lost almost 75 % of their activity at 60°C after 1hour treatment whereas, immobilized amylase lost only 20-30% of their activity [174]. Figure: 3.61 shows effect of pre-incubation time on the activity of each immobilized enzyme.

About 50-60% of immobilized enzymes maintained their activity when subjected to 120 minutes of pre-incubation time at their respective optimum temperature whereas free enzyme could retain only 10% of their initial activity when subjected to same period of time. These results suggest that the thermal stability of α-amylase increased considerably as a result of immobilization on to PPY adsorbents and is suitable for industrial applications. Thermal stability upon immobilization is the result of molecular rigidity and the creation of a protected microenvironment [173].

Similar increase in thermal stability was also reported by N. Tuzmen et al. [175]. The authors have carried out adsorption of α-amylase on to Magnetic poly (2-hydroxyethylmethacrylate)/Cibacron blue [mPHEMA]/CB beads. Immobilization brings about more stable conformation by restricting the mobility of the enzyme due to which thermal denaturation of enzyme native conformation via unfolding is hindered and hence enzyme can withstand distortion or damage by heat exchange.

Similar observation was also observed by P. Singh et al. when α-amylase was immobilized on cation exchange resin [176]. The stability of α-amylase at low pH and its increased activity at high temperatures implies that the enzyme can be applied in starch hydrolysis at low pH and moderately in high temperatures of 60°C to minimize contamination during processing [112,177].

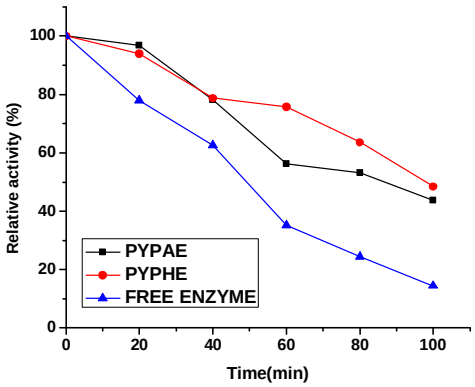

Figure: 3.61: Effect of pre-incubation time on the relative activity of free and immobilized enzymes

3.8.3.5 Determination of kinetic parameters

Enzyme immobilization may produce both conformational and micro-environmental effects that will affect the kinetics of enzyme catalyzed reactions [178].

Conformational effects refer to the structural changes produced in the enzyme molecule as a consequence of the immobilization procedure. Alteration of the native three-dimensional structure of the enzyme protein and the steric effects due to its close proximity to the surface of the support are the conformational changes that may produce differences in kinetic behavior of immobilized enzyme with respect to the free enzyme.

Micro environmental effects refer to partition and mass transfer limitations. Partition of substrates and products to the biocatalyst and products, transport from it back into the bulk reaction medium affect the kinetics of the enzyme catalyzed reaction [179]. The kinetic parameters of free and immobilized enzyme are shown in table 3.19. Lineweaver-Burk Plots and Hanes-Woolf plots of free and immobilized α-amylase is shown in figure: 3.62

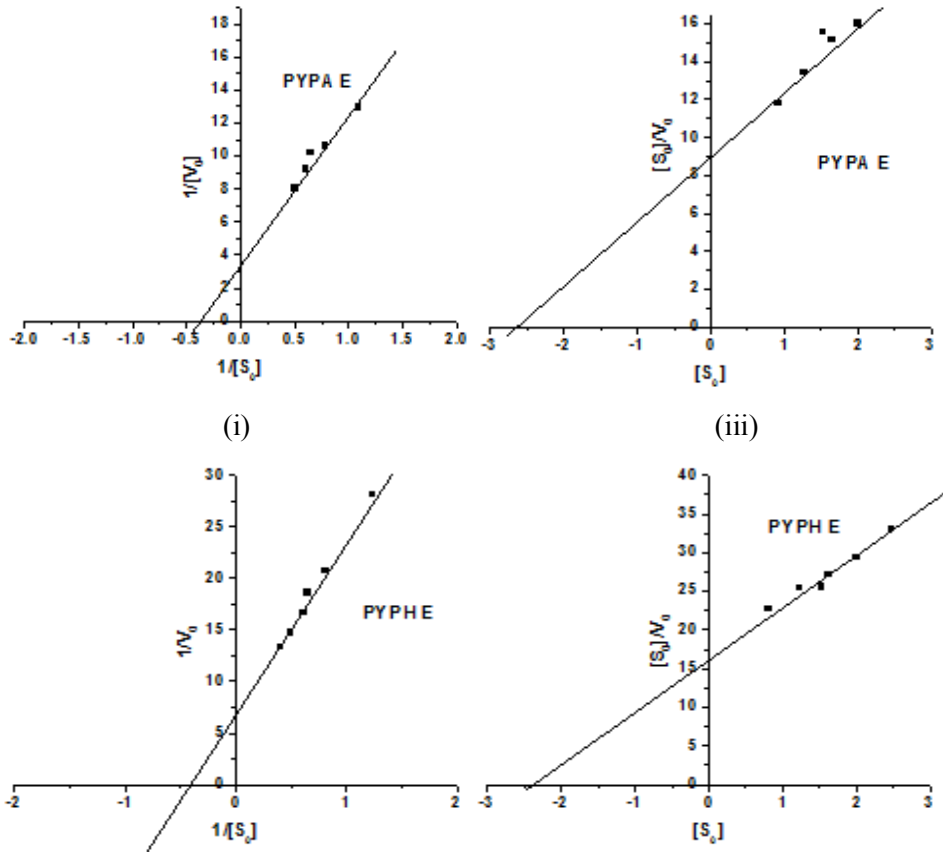

Figure: 3.62: Lineweaver-Burk plots for α-amylase immobilized on copolymers (i) PYPA (ii) PYPH. Hanes-Woolf plots (i) PYPA (ii) PYPH

Table 3.19 Kinetic parameters for free and immobilized enzymes on copolymers

	Free enzyme	PYPA	PYPH
K_m (mgml^{-1})	0.50 ± 0.04	2.73 ± 0.06	2.47± 0.04
V_{max} (mg/ml/min)	7.40 ± 0.05	4.21 ± 0.04	2.95 ± 0.03

3.8.3.6 Storage stability of Immobilized α-Amylase

The stability of immobilized α-amylase stored at 4°C in buffer solution was determined by periodically analyzing samples over 6 months for its activity retention. The trend in stability during 6 months of storage is shown in the figure: 3.63.

PYPA retained 50% of its initial activity and PYPH retained 25% of its initial activity after 6 months. Similar improvement in storage stability for a longer period was reported by S. Dhingra et al. [180]. This difference in activity between two immobilized enzymes is dictated by many factors such as number of bonds formed between enzyme and support, the nature of the bonds, the degree of confinement of enzyme molecules in the matrix, and immobilization conditions [172,181,182].

On the basis of results obtained it was concluded that these supports provide better stabilization effect, minimizing possible distortion effects, which might be imposed from aqueous medium on the active site of the immobilized enzyme. PYPA shows outstanding performance compared to PYPH. The generated multipoint ionic interactions between enzyme and matrixes also conveyed a higher conformational stability to the immobilized enzyme.

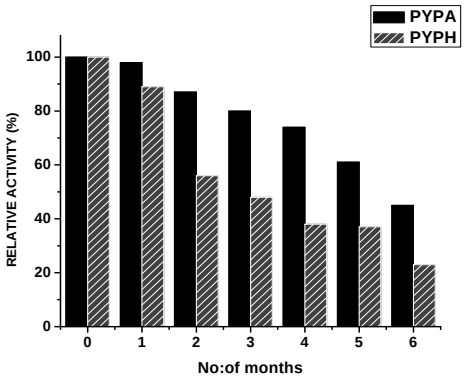

Figure: 3.63 Storage stability studies of α-amylase immobilized on copolymers

3.8.3.7 Reusability

In the case of immobilized enzymes reusability is a vital parameter as it is necessary to make enzyme cost effective. The number of successive cycles for which a biocatalyst can be efficiently reused depends on several parameters like biocatalyst stability upon immobilization, its biochemical parameters like pH in which it is undergoing reaction, temperature, nature of linkage to the support etc.

Here we have carried out reaction for 14 cycles in order to check the feasibility of reusing the catalyst. Also, after each reaction immobilized enzymes were thoroughly washed with buffer so as to remove the products completely from the medium.

PYPAE could be used without much loss in its activity up to 14 cycles after which there was reduction in activity due to the natural inactivation of enzyme as a result of its continuous usage.

PYPH but retained its activity significantly only for 6 cycles after which it showed decline in activity that might have occurred due to poor adsorption capacity of support to hold enzyme in a proper orientation for long time. Similar results are reported by other authors for example Tanyolac et al. have reported complete reusability for α-amylase immobilized onto nitrocellulose membrane up to 10 successive cycles followed by a 35% reduction in activity [183]. The results are shown in the figure: 3.64.

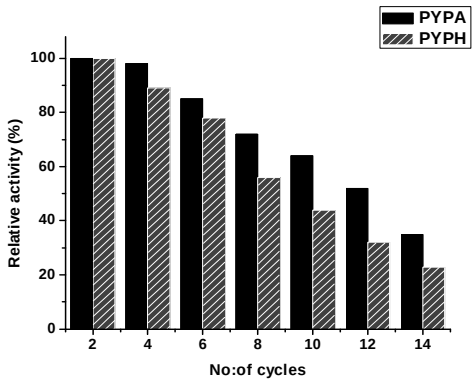

Figure: 3.64 Reusability studies of immobilized enzymes on copolymers

3.9 Significance of polypyrrole composites as support for enzyme immobilization

Polymeric nanocomposites are special class of hybrid materials formed by the intimate combinations of one or more organic or inorganic nanoparticles with a

polymer so that unique properties of former can be taken together with the existing qualities of the latter. From the point of versatility of synthesis techniques, properties, and broadness of the scope of application, these materials have raised a great deal of scientific and technological interest and have led the research in materials science in a new direction [184].

It was found that unfunctionalized PPY-silica particles are much more effective than the corresponding PPY bulk powders in adsorbing human serum albumin (HSA) [185]. Saoudi et al. have reported DNA adsorption onto PPY powder, a colloidal silica sol, and three PPY-silica nanocomposite particles (untreated and amine- and carboxylic acid-functionalized) [186].

From the reports available it is clear that because of the attractive properties together with ease of synthesis in aqueous media, conductivity, intrinsic deep black colour suitable for visual diagnostic tests [187], redox chemistry and long term stability, PPY composites are suitable candidate in the fabrication of biosensors [188], and as adsorbents of enzymes and proteins [189,190].

Literature reviews also shows that enzyme adsorption rather than covalent grafting can be sufficient for the development of a new assay using polypyrrole based material as a carrier [187].

3.9.1 Preparation of polypyrrole composites

3.9.1.1 Preparation of polypyrrole by template directed synthesis method

Polypyrrole was prepared using commercial colloidal silica sol as template via chemical polymerization method. Surface of colloidal silica was first modified prior to reaction. In order to achieve this 2 ml of chlorodimethylvinylsilane (CDVS) was added into a solution containing 4 ml of Ludox SM-30 colloidal silica sol solution and 26 ml of distilled water, and the mixture solution was stirred overnight for the surface modification of colloidal silica particles by CDVS.

Distilled 1.34 ml of pyrrole was added to the prepared solution, and stirred for 3hours. Then 7.46 g of ferric chloride was added and stirred for 3 hours at room temperature to polymerize the pyrrole containing the surface modified silica particles .The product was washed with distilled water to remove free silica particles. To fabricate PPY from the PPY/Silica nanocomposites, silica templates were etched by 1M NaOH solution in water/ethanol mixture [191].

3.9.1.2 Preparation of Polypyrrole -silica composites

The synthesis of PPY-silica composites were done using the method described by Goller et al. As per the method reported by them aminated polypyrrole silica particles were produced via two synthetic routes. The main advantage of Route 1 is that the precursor homopolypyrrole-silica particles can be readily obtained with uniform particle size in a narrow range. Since such particles are known to have silica-rich surfaces the protocol described by Goodwin et al. for the amination of silica was applied [192]. In the Route 2 the aminated particles are synthesized in a single step. However, the amine-functionalized pyrrole comonomer required for Route 2 is not commercially available and therefore was synthesized prior to the reaction.

3.9.1.2.1 Materials

Pyrrole, 1-(2-cyanoethyl)pyrrole, ammonium persulfate,iron(III) chloride, lithium aluminium hydride (1.0M solution in diethyl ether), anhydrous diethyl ether, sodium chloride, potassium hydroxide and acetic acid were obtained from Aldrich. Pyrrole was distilled and stored at $4^{o}C$ prior to use. Water was de-ionized and doubly distilled.

3.9.1.2.2 Synthesis of nanocomposites

In order to prepare homopolypyrrole-silica nanocomposites pyrrole (1.0 ml) was added to a vigorously stirred dispersion of colloidal silica (3.47 w/v%) in

deionized water containing $(NH4)_2S_2O_8$ (3.84 w/v%) as oxidant. Subsequently, the mixture was stirred for a further 24 hours to allow the pyrrole polymerization to proceed to completion. The resulting colloidal nanocomposite particles were isolated from the soluble inorganic byproducts and excess silica sol via four centrifugation/re-dispersion cycles (6000 rpm for 30 min), with successive supernatants being replaced with water. [193,194].

3.9.1.2.3 Silylation of nanocomposites

To functionalize the nano-composite particles 1 wt% of APTES at pH 4 (adjusted by the addition of acetic acid) was added to 3.1 wt% of the particles weighed and stirred the mixture for 2 hours at 25°C. The resulting silylated sols were purified by four centrifugation/redispersion cycles at 6000 rpm for 40 minutes and were re-dispersed in 0.01M aqueous NaCl solution, adjusted to pH 4 with 0.1M HCl [195].

3.9.1.3 Nanocomposite preparation via copolymerization

The comonomer 1-(3-aminopropyl) pyrrole comonomer was synthesized by the reduction of 1-(2-cyanoethyl) pyrrole in anhydrous diethyl ether [196]. 1-(2-cyanoethyl) pyrrole (5g) was added drop wise to a two molar excess of $LiAlH_4$ in anhydrous diethyl ether. The reaction was stirred under nitrogen atmosphere for 2 hours and then quenched by successive additions of water and sodium hydroxide (20 wt %). The ethereal layer was decanted and the product was collected as yellow oil after evaporation of the ether phase. The comonomer was characterized by 1H NMR spectroscopy using a 250 MHz instrument ($CDCl_3$ solvent and TMS reference).

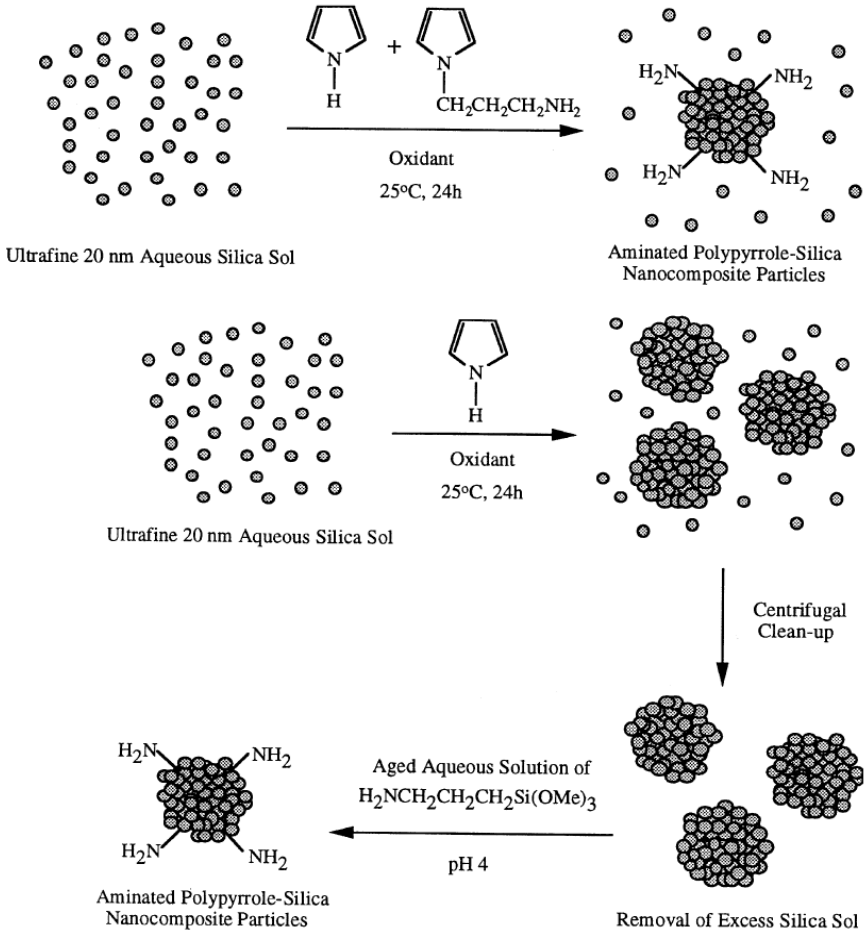

Scheme 3.10 Synthesis of polypyrrole -silica composites

3.9.2 Physico-chemical characterization

3.9.2.1 FT-IR spectra of polypyrrole composites

FT-IR spectra recorded for polypyrrole-silica (PSi) nanocomposites and its APTES functionalized derivative (PSiA) prepared in presence of $FeCl_3$ as oxidant is shown in the figure: 3.65.

Bands attributed to both the doped polypyrrole and silica components are observed. The very weak bands at 2928 cm^{-1} and 2856 cm^{-1} are attributed to C-H

stretch of pyrrole ring. The intensities of these bands increased after immobilization due to CH_2 groups of amylase.

The major peak at about 1110 cm^{-1} (varying with different samples in the range of 1000-1200 cm^{-1}) that is attributed to the asymmetric stretching vibrations of Si-O-Si bonds of silica can be found in the hybrids. The bands present around 802 cm^{-1} and 788 cm^{-1} is assigned to scissor deformation of commercial silica particles [197]. Also bands at 700 cm^{-1} are attributed to Si-O-Si asymmetric stretching and that at 462 cm^{-1} is assigned to Si-O-Si asymmetric bending vibrations.

For PSiA broad peak in the range 3591-3213 cm^{-1} is assigned to NH_2 stretching vibration. Peaks around 3300 cm^{-1} indicate the NH_2 stretch vibration and 2972 cm^{-1} indicates the -C-NH_2 stretch vibration [198]. On the other hand, the peak at 2954 cm^{-1} indicating the C-H stretch that was observed in the PSi disappeared in the PSiA.

Bands in the range of 2965-2853 cm^{-1} are attributed to aliphatic CH_2 stretching vibration. Broad band at 1605 cm^{-1} is assigned to NH bending vibration. A weak band at 1522 cm^{-1} is due to NH_2 deformation. In addition to all these bands, the characteristic bands due to polypyrrole also appear in the spectra of PSiA, which imply that PPY chains have been formed. However, these peaks shift to higher wave number compared to pure PPY suggesting that PPY chain in nanocomposite is shorter than in pure PPY.

For PAM broad peak in the range 3425-3392 cm^{-1} is assigned to NH_2 stretching vibration. Bands in the range 2928 and 2852 cm^{-1} are attributed to aliphatic CH_2 stretching vibration. The weak band at 2969 cm^{-1} is assigned to C-NH_2 stretching vibration. A broad band at 1606 cm^{-1} with strong intensity is due to NH bending vibration. The other characteristic peaks which are assigned to pyrrole ring confirmed the formation of poly-1-(2-aminopropyl) pyrrole silica nanocomposites.

For PM characteristic pyrrole ring stretch absorption bands were observed in the region 1600-1100 cm^{-1}. But majority of the bands were shifted to lower wave number than in the pure polpyrrole [199]. No peaks corresponding to silica was obtained as it was used as template during the synthesis and has been removed [191].

For immobilized samples PSiE, PSiAE, PAME and PME the characteristic peaks due to presence of enzymes were observed in the spectra of all samples.

For PSiE the characteristic peak of N-H stretching vibration was shifted to lower wave number 3432 cm^{-1}. The peak of aliphatic CH_2 stretching vibration was also shifted to 2926 cm^{-1} and 2854 cm^{-1}. Peaks corresponding to silane groups have either completely disappeared or decreased in intensity confirming the fact that enzymes have been anchored on to support via those functional groups. The characteristic peaks of PPY were also present with shifts to lower wave number. The characteristic peaks due to enzyme at 1646 cm^{-1} be ascribed to the amide I band that represents the stretching vibrations of C=O bonds in the backbone of the protein . In turn, obtained results could indicate adsorption of proteins on the surface of the polymers. FT-IR spectra shows bands centered at 1548 cm^{-1} that can be attributed to amide II band, spectrum clearly indicates the presence of carboxylate ion groups at 1646 cm^{-1} and 1377cm^{-1} respectively [22]. All bands get broadened after immobilization of α-amylase.

For PSiAE and PAME the characteristic bands at 3449 cm^{-1} and 3454 cm^{-1} was observed for NH_2 stretching vibration of pyrrole ring. The bands at 2926 and 2854 cm^{-1} were assigned to CH_2 stretching vibration for PSiAE whereas for PAME these bands were at 2924 and 2856 cm^{-1} respectively. The rest of characteristic bands were also present in both polymers with shift in wave number with respect to different functional groups present. Bands at 1656, 1547, 1515, 1317 and 1377cm^{-1} were attributed to that of α-amylase.

For PME the characteristic bands due to enzyme were present at 1656 cm^{-1}, 1646 cm^{-1}, 1544 cm^{-1}, 1510 $cm^{-1}$and 1315 cm^{-1} [200].

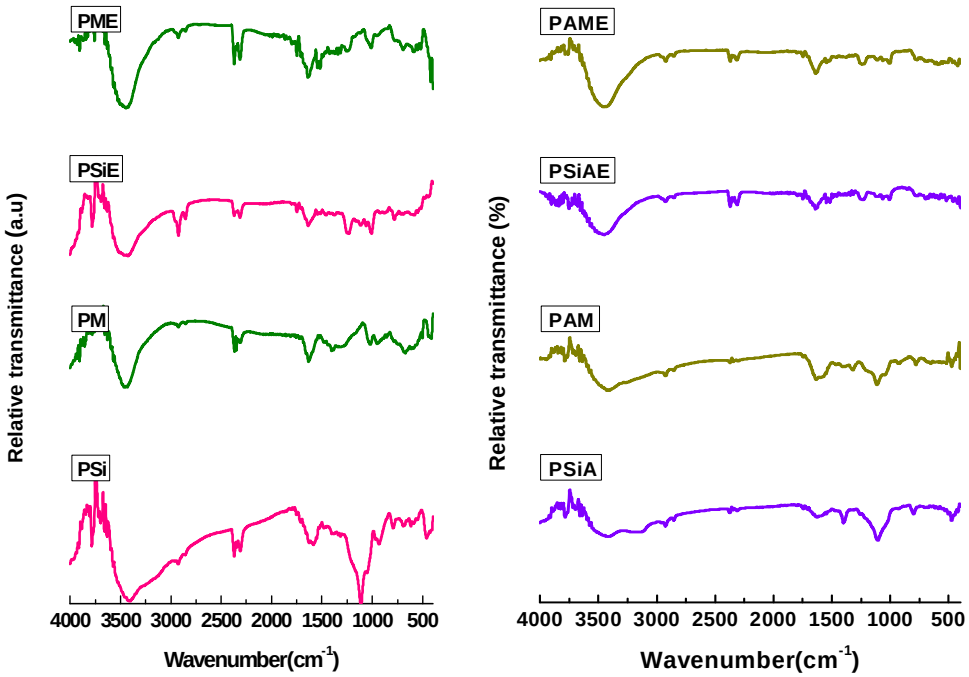

(i) (ii)

Figure: 3.65: FT -IR Spectra of PPYSi composites before and after α-amylase immobilization (i) Spectra of PM and PSi (ii) Spectra of PAM and PSiA

Table 3.20: (i) Peak assignments for PM and PSi before and after enzyme immobilization (ii) Peak assignments for PAM and PSiA before and after enzyme immobilization.

Peak assignments (cm^{-1})	P Si	PSi E	PM	PME
N-H stretch	3438	3443	3438s	3436
C-H stretch	2923vw, 2854 vvw	2926m2854m	2928,2851vw	2928 2854vw
C=O	1710w 1748 vvw	1745,1710w	1718vw	1745,1707bw
C-N-C ring -in plane deformation	1657vvw	1656bm	1654,1631.6s	1656,1638
N-H ring in plane bending	1523	1545	1526	1542,m1521m
C-N stretch	1476vw	1456w	1476	1488,1459w
C-C in ring stretch	1339vw	1379,1342vvw1316	1394,1317	1340,1316,1396w
C-C inter ring stretch		1243	1288vw	1256
C=C-N ring in plane deformation	1113bs	1160w1113w		1121vw
C-H,N-H ring out of plane bending	1051	1008	1024	1012
C=C-C, ring in plane deformation		881w	880	852
C-H,N-H ring out of plane bending(s)	792	779m	787	779w

(i)

Peak assignments (cm^{-1})	PSi A	PSi AE	PAM	PAM E
N-H stretch	3420	3447	3419	3436
C-H stretch	2924w 2857w	2924, 2853w	2924,2856w	2924w2952vw
C=O	1746, 1710vvw	1746,1710w	1745	1745,1708vw
C-N-C ring -in plane deformation	1622bm	1656bm,1642s,1622m	1606,1632mb,	1640mb
N-H ring in plane bending(s)	1596w1546w	1544,1526,1515	1596w	1544w1521.6w
C-N stretch(w)	1454	1462,1490	1467w	1462.2 1425
C-C in ring stretch(s)	1334,1310	1338,1317w,	1318w,1387	1376vw, 1340.8vw, 1316.8
C-C inter ring stretch(w)	1259.6	1230m	1204	1233, 1244mb
C-N stretch,N-H ring in plane bending(w)	1116.8mb 1107 mb	1155vw 1110, 1100vw	1113mb 1110vw 1116.8w	1115.4w
C=C-N ring in plane deformation,		1062w,1008	1046	1065.4 1006w
C=C-C, ring in plane deformation	873vw	886,854w	859	894vvw
C-H,N-H ring out of plane bending(s)	803w	769w	780	774vw
C-H ring out of planebending(w)	731 vw	734	723	744vw

(ii)

3.9.2.2 Thermogram of polypyrrole composites

Figure: 3.66 show the thermograms of PSi, PSiA and PAM.

The thermograms have roughly similar shapes at high temperature showing a plateau value of weight loss *vs.* temperature. The thermogram of PSi shows a higher mass loss compared to bare PPY. The weight loss of PSiA is also significantly higher than PSi which is mainly due to removal of the APTES moiety.

After immobilization weight loss enhances again which is the result of adsorption of enzyme on to these polymers. The increase in weight loss was found to be more in PSiAE and PAME than on PSiE which is due to presence of $-NH_2$ groups on the other two. Moreover APTES is an adhesion promoter which favoured the specific interactions of lewis acid-base type between the basic amino group and the acidic N-H bonds and the positively charged polypyrrole backbone.

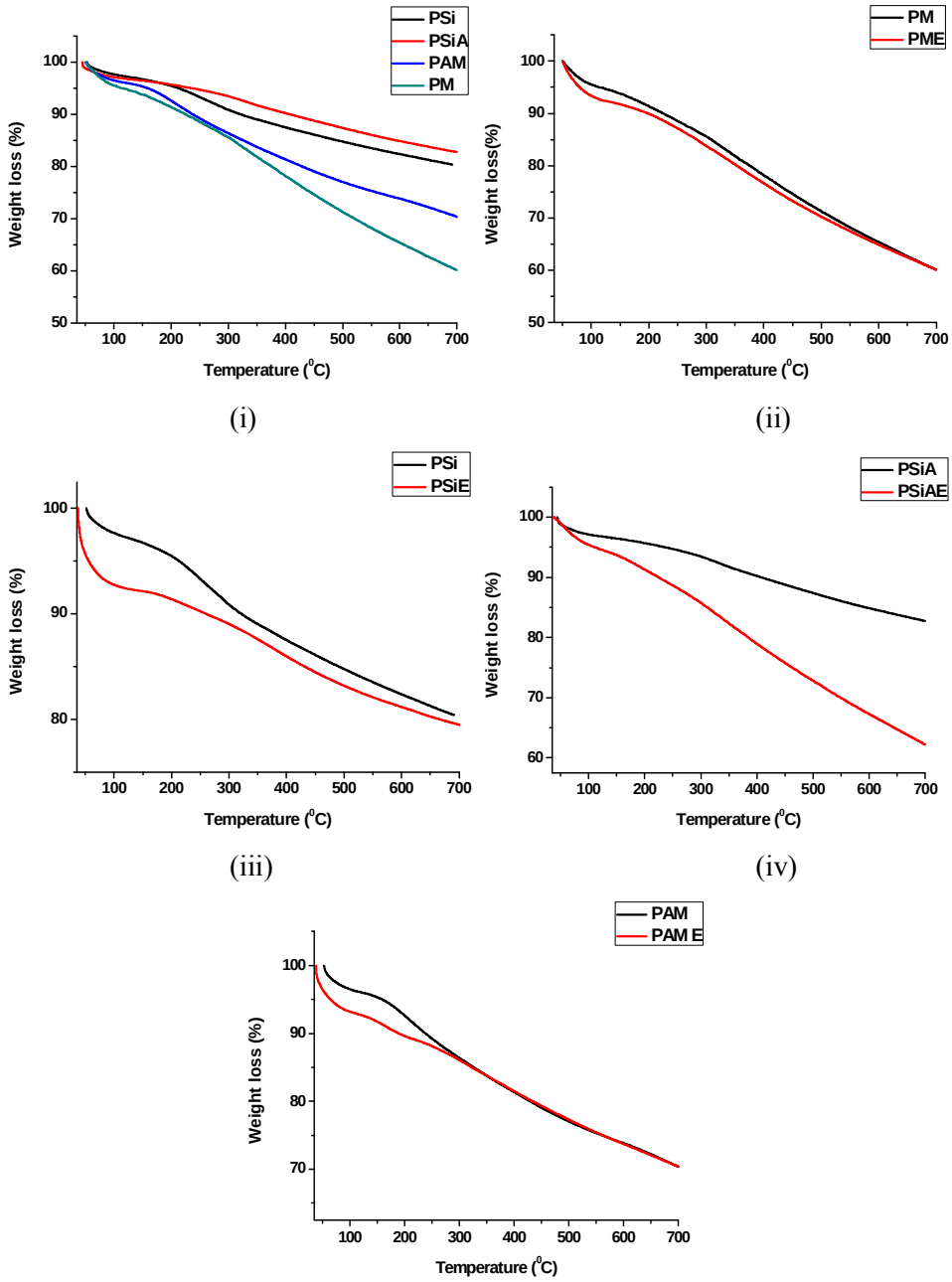

Figure: 3.66: TG curves for composites before and after immobilization. (i) TG curves of PSi, PSiA, PAM, PM (ii) TG curves of PM and PME (iii) PSi and PSiE (iv) PSiA and PSiAE (v) PAM and PAME.

In all cases the initial loss is mainly attributed to the elimination of residual water, dopant molecules and unreacted monomer.

In the case of PSi the major sharp peak at 266°C would be the beginning of degradation of polypyrrole chains. At 383°C minor weight loss starts which along with the decomposition of polypyrrole also includes silica particles. The continuous weight loss starts at 465°C and continues up to 800°C. After immobilization of α-amylase the decomposition due to enzyme protein structure occurs at 209°C. The next major loss occurs in the range 241-392°C which is a broad peak. The other minor loss at 635°C might be the polymer decomposition.

In the case of PSiA minor weight loss at 218°C might be the beginning of polypyrrole backbone. The major weight loss occurred in the range 283-332°C which accounts for polymer degradation, APTES removal, and silica decomposition. The continuous degradation of polymer structure then occurs at 541°C which gradually occurs till 800°C.

When thermogram of PAM was analyzed the initial decomposition due to residual water occurs before 100°C and the polymer decomposition occurs at 209°C. The other decomposition which includes the removal of unreacted (1-(3-aminopropyl pyrrole)) silica comonomer occurs at 339°C. When α-amylase was immobilized the corresponding weight loss was observed in the thermogram. It was at 164°C the protein structure degradation observed in PAME. The other major weight loss occurs at 257°C which corresponds to initial decomposition of polymer backbone. The subsequent decomposition occurs at 307°C which correspondingly reflects the decomposition of 1-(3-aminopropyl group)) silica and the polymer structure.

3.9.2.3 Surface area analysis

BET surface area of PPYSi composites before and after immobilization of α-amylase is given in the table 3.21.

Table: 3.21 Surface areas of PSi composites and PM

Polymers	PSi	PSiA	PAM	PM
Surface area (m^2/g)	125.5	82	85.8	103.5

Highest surface area is shown by PPY-silica composite (PSi) and polypyrrole prepared using silica as template (PM).

For PSiA the surface area is found to reduce. This might be due to the fact that pores of silica on polypyrrole might get prefilled or have blocked with APTES. In other words APTES might have grafted on the outermost layers of silica or sorbed in the pores but near the outermost surface of silica. Similar reduction in surface area was reported by several authors.

Luo et al. have clearly shown that the silica pretreatment entails a significant decrease of both porosity and pore radii in addition to specific surface area compared to the untreated silica gel particles [222]. C. Perruchot et al. have reported that specific surface area of PPY-silica particles matched that of untreated silica gel, whereas the APTES treatment of silica yields a sharp decrease in the surface area of the latter [201].

In the case of PAM also surface area was reduced than PSi. This might be due to the fact that addition of pyrrole and 1-(3-aminopropyl pyrrole) mixture on to silica gel followed by polymerization step have promoted the growth of copolymer on the surface of silica thereby reducing its surface area. Whereas, etching of silica after the polymerization process have resulted in the formation of pores on polypyrrole produced and thereby increase in surface area in the case of PM.

3.9.2.4 Scanning electron microscopy

The SEM images of PPYSi composites prepared were shown in the figure: 3.67 below

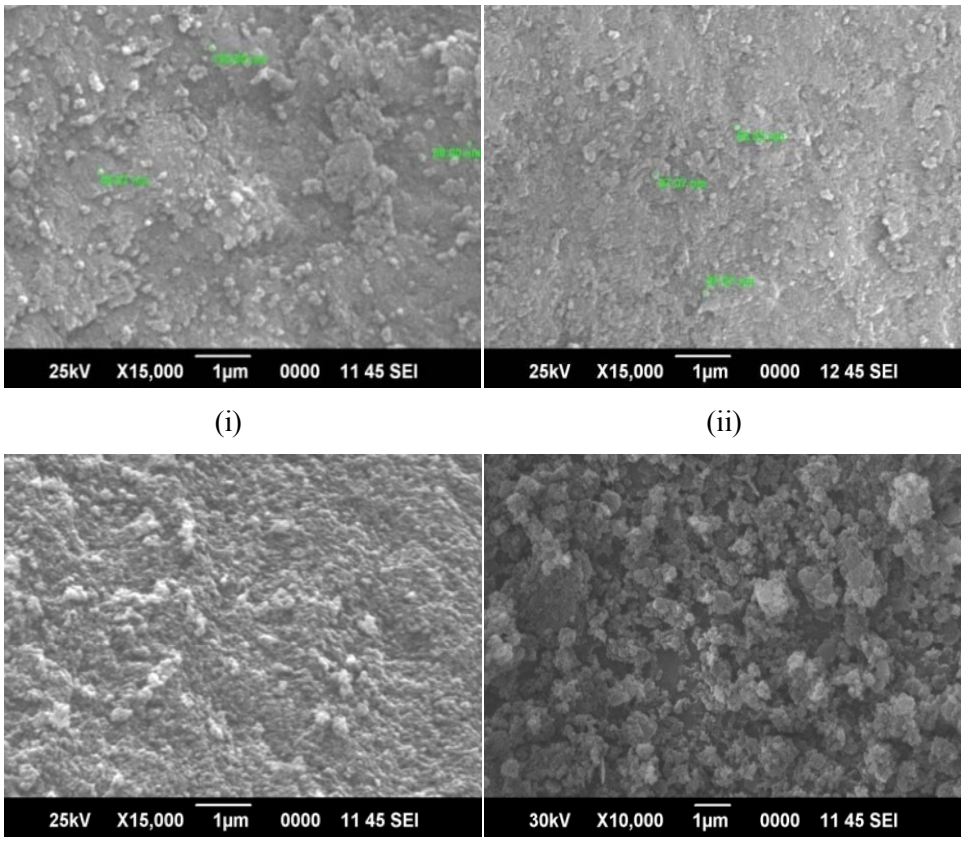

Figure: 3.67 SEM images of (i) PSi (ii) PSiA (iii) PAM (iv) PM

The samples prepared with colloidal silica as templates (PM) were found to have flaky structures. It is known that the interaction between the pyrrole main chains is very strong. Therefore it has a tendency to aggregate into irregular morphology, which is commonly observed in the polypyrrole obtained by the chemical oxidative polymerization. The SEM image showed a rough surface morphology with non irregular particle size.

Polypyrrole silica composites (PSi, PSiA and PAM) exhibit uniform texture with a granular morphology, with non-regular shape particles. PSi particles obtained

were found to have rough surface morphology with particles of granular shape ranging from 67-120 nm. This might be due to high silica rich surface which on further amination with APTES (PAM) becomes weakly flocculated. The particle size is in the range 53-97 nm for PAM. PAM is much more spherical compared to other two.

3.9.3 Immobilization of α-Amylase on Polypyrrole Composites

3.9.3.1 Optimization of immobilization conditions

In this section we have reported a study of interaction of Diastase α-amylase with PPY powder (PM), and three nanocomposite systems-unfunctionalized PPY-silica (PSi), aminated PPY-silica (PSiA) and copolymerized poly (pyrrole-co-1-(3-aminopropyl)-pyrrole-silica (PAM) nanocomposites. The amylase adsorption capacities of various PPY adsorbents at various immobilization pH are shown in the figure: 3.68.

α-amylase was adsorbed on to all adsorbents via both electrostatic and hydrophobic interactions [186]. Thus depending on the relative surface hydrophobicity and presence or absence of surface functional groups, either hydrogen bonding and/or hydrophobic interaction may enhance the extent of amylase adsorption. All these phenomena can be clearly explained based on isoelectric points of PPY adsorbents.

PM has a high surface area when compared to bare PPY and expected isoelectric point approximately 7 as that of PPY. When solution pH is below 7, PM will be positively charged and above 7 negatively charged [201]. α-amylase having isoelectric point around 4.6 will be positively charged at pH 3 and 4. So at pH 3 and 4 less adsorption occurs on PM as both amylase and PM having similar charge faces electrostatic repulsion.

When pH > 5, amylase is negatively charged whereas, PM is positively charged up to pH 6. So, strong electrostatic attraction encounters at pH 5 and 6. At pH 7 no charge exists for PM and amylase is negatively charged. Hence considerable adsorption was not expected but results were contradictory showing appreciable adsorption at this pH which might be due to hydrophobic interaction between PM and negatively charged amylase which dominated over electrostatic attraction. This is because polypyrrole is hydrophobic as it has large aromatic rings in the polymer backbone [202]. Therefore, for these adsorbents, hydrophobic interactions dominate and the effect of pH is minimized.

At pH 8 and 9 again electrostatic repulsion occurs as both enzyme and support are negatively charged, but it might be due to dominant hydrophobic interaction that resulted in adsorption capacity at this pH too even if it is not significant as at other pH. That is activity obtained at this pH is less compared to other pH [146]. The optimum pH for PM was found to be at pH 6.

In the case of PSi optimum adsorption occurred at immobilization pH 4. This is because for PSi isoelectric point is at pH 2. As reported by C. Perrchot et al., the X-ray photoelectron spectroscopy studies of these nanocomposites exhibit silica rich surfaces an observation that was subsequently confirmed by zeta potential measurements [201].

But at pH above 4 since both amylase and PSi are negatively charged poor adsorption occurs due to prominent electrostatic repulsion. Still very low adsorption occurs which is driven by hydrophobic interaction between support and enzyme.

PSiA nanocomposites show a different trend. As reported by M.I Goller et al. from zeta potential measurements PSiN has isoelectric point around 7.5 an approximate charge balance between the anionic silanol groups and cationic $-NH_3^+$groups [203]. At pH 7.5 surface amine sites on the PSiA particles

are extensively protonated as $-NH_3^+$ groups. Thus a net positive surface charge is not a prerequisite; the attractive electrostatic interactions between amylase and isolated $-NH_3^+$ groups are apparently sufficient for amylase adsorption.

The optimum immobilization pH obtained for PSiA was at pH 5. Thus immobilized enzyme has the same pH optimum as the free enzyme (pH 5), and so immobilization did not change the optimal pH of α-amylase. Similar observation was reported by T. Kalburcu et al. when α-amylase was immobilized on metal ion affinity nanospheres [204]. This is because PSiA was positively charged below 7.5 and negatively charged above 7.5. Therefore most prominent and effective electrostatic interaction occurs in the pH range 5-7 as amylase will be negatively charged in this range and PSiA will be positively charged. Above and below this range adsorption occurs mainly due to hydrophobic interactions between enzyme and the support. This might be the reason for lower loadings at higher and lower pH.

PAM on the other hand has an isoelectric point of about 8.5 as reported by Goller et al. [203]. Hence most proper orientation of enzyme with the support occurs in the pH range 5-7 where more favourable electrostatic interaction comes to play. The optimum pH for amylase adsorption occurred at pH 6 for PAM. The lower loadings at pH above 7 and below 5 are the result of hydrophobic interaction which dominates over electrostatic repulsion. The variation of activity with respect to change in pH of the environment, within the range 2-3 units each side of the pI is normally a reversible process [205].

In addition to these, both PSiA and PAM have higher adsorption than PSi at higher pH values. This happens because of the presences of amino groups which accounts for greater zeta potential and thus have stronger electrostatic interaction with amylase than PSi. When pH is below 5, PSi has more adsorption capacity and activity compared to other two aminated PSi nano composites.

Similar results were obtained by Y. Nakashimada when lysozyme and BSA was adsorbed on polypyrrole synthesized on to model silica gel through APTES [146].

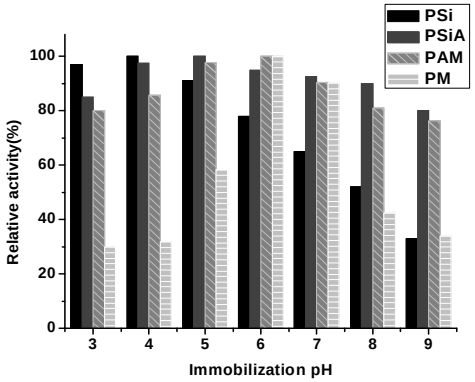

Figure: 3.68 Effect of pH at the time of immobilization on the relative activity of α-amylase

3.9.3.1.1 Effect of contact time on immobilized enzyme activity

The contact time needed for enzyme to get adsorbed on PPY composites is shown in the figure: 3.69. As soon as the addition of enzyme to these adsorbents, immediate interaction occurs and this varies with the nature of the support.

In the present case for PM immediate saturation of the support with the enzyme occurs as contact time reaches 120 minutes. For PSi the optimum level was attained when the contact time of 240 minutes was allowed. This might be due to poor adsorption capacity of PSi compared to others which is the consequence of its surface charges. PSiA and PAM reached maximum adsorption limit when kept for 180 minutes of contact time. The easily accomplished adsorption rate might be due to the presence of surface functional groups on these polymers which favoured electrostatic interactions effectively and hence resulted in subsequent loading of enzymes on support while retaining maximum activity.

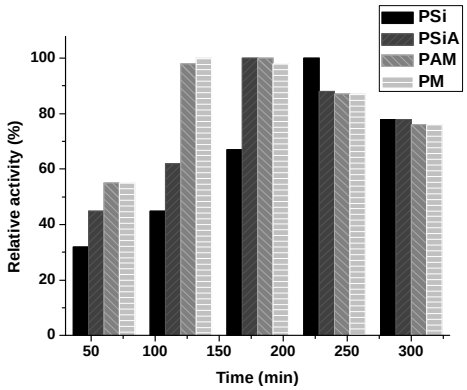

Figure: 3.69 Influence of contact time on the relative activity of enzyme.

3.9.3.1.2 Effect of initial protein on protein loading of immobilized enzyme

The amount of protein bound to PPY adsorbents was analyzed based on the optimized conditions obtained; it is shown in figure: 3.70.

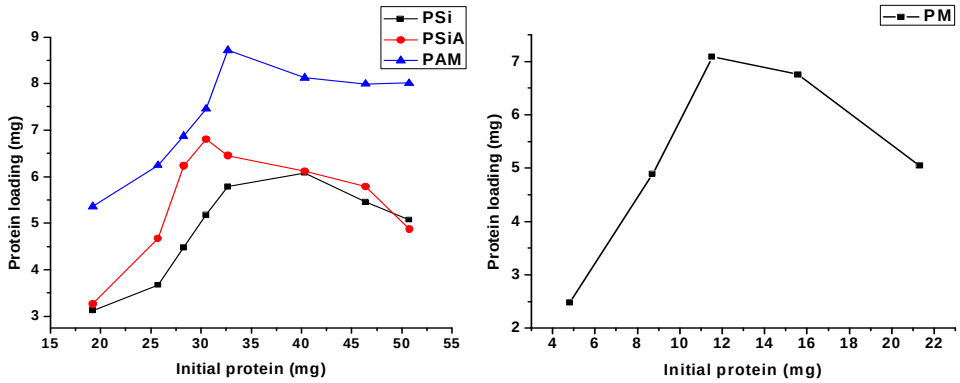

(i) (ii)

Figure: 3.70 Influence of initial protein concentration on protein loading on to supports (i) PSi, PSiA, PAM (ii) PM

As far as nanocomposites are concerned surface functionalization with amine groups produced much higher amylase adsorption in the order PAM > PSiA > PSi.

For PM, since the surface area is high, loading was also high and was about 6.8 mg. PAM has amino group at the surface and was found to hold more proteins

strongly than PSiA particles. This might be due to difference in distribution of amino groups at the surface of both composites which ultimately favoured the copolymerized one. But both have better binding capacity compared to unfunctionalized PSi, which has a poor binding capacity due to its isoelectric point which is unfavourable for its strong electrostatic interaction with amylase. In case of other three, electrostatic interactions play a key role that facilitates proper orientation of enzyme with the support so that less conformational changes were encountered during the immobilization process that would have caused alterations in their activity.

In all three cases as the initial protein concentration increases protein load also get increased gradually which then reaches a saturation point after which loading gets decreased [204]. This might be either due to insufficient binding sites at higher loadings or due to desorption of enzyme from the surface of the supports as a result of multilayer adsorption of enzymes [206]. The corresponding activity when evaluated showed similar trend for PSi and PAM, but a different trend for PSiA.

For PSiA optimum immobilized enzyme activity was obtained not at maximum protein load but on the concentration below it. This might be due to masking of many active sites on higher loading which caused mass transfer diffusional limitation of substrate molecules towards the active site. From the graph it is clear that protein load of PSi, PSiA, PAM and PM was 6.1, 6.8, 9.2 and 7.1 mg respectively.

3.9.3.1.3 Effect of initial protein concentration on immobilization yield and activity of loaded enzyme.

Immobilization yield obtained for all adsorbents at various concentrations taken are shown in the figure: 3.71.

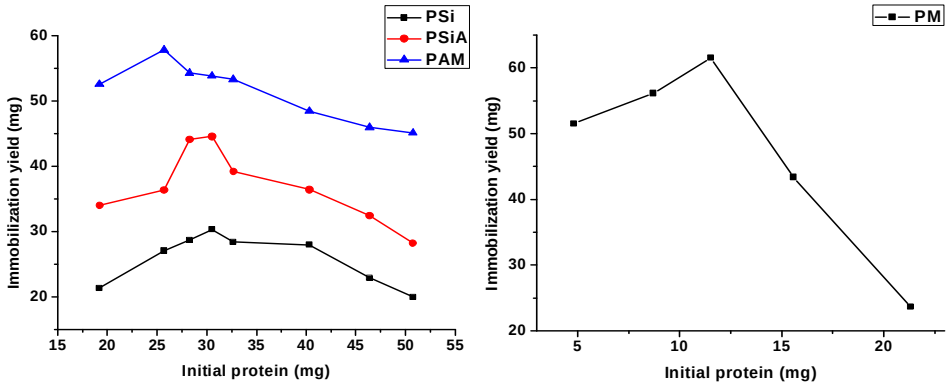

(i) (ii)

Figure: 3.71: Influence of initial protein concentration taken on the immobilization yield of enzyme (i) PSi, PSiA, PAM (ii) PM

From the graph it is evident that for PM immobilization yield was about 43% at initial protein concentration of 40.3 mg. PSi showed maximum immobilization yield of 28% at initial concentration of 30.5 mg whereas, PSiA showed maximum yield of 44% at initial protein concentration of 30.5 mg and PAM showed maximum immobilization yield of 53% at initial protein concentration of 19.2 mg.

For PSi maximum activity of 6.5 EU was obtained at maximum loading but with less immobilization yield. PSiA showed maximum activity of 9.8 EU at enzyme loading of 6.2 mg with immobilization yield 44%, both were not the optimum. For PAM maximum activity of 9.2 EU was obtained at initial enzyme concentration of 32.7 mg with 8.7 mg protein load having immobilization yield of 53%. Finally for PM immobilized enzyme activity was a maximum of 7.1 EU at initial enzyme concentration of 15.6 mg which attained the protein loading of 6.8mg with an immobilization yield of 43%. All results are depicted in the graphs below in figure: 3.72.

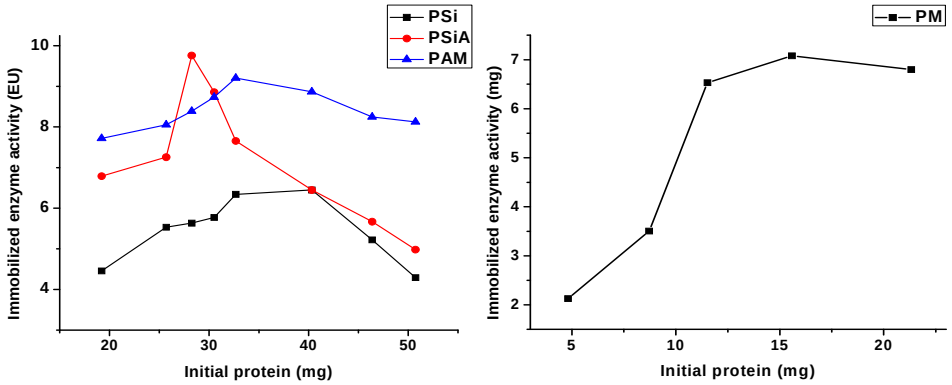

(i) (ii)

Figure: 3.72: Effect of initial protein concentration on the immobilized enzyme activity

Immobilized enzyme activity yield and immobilization efficiency are also evaluated. The results are tabulated in the table 3.22.

Table 3.22: Immobilization efficiency of α-amylase on polypyrrole composites

Polymer	Initial protein (mg)	Immobilized protein mg/g support	Immobilizationyield (%) IY	Initial activity (EU)	Immobilized enzyme activity EU	Activity Yield (%)AY	Immobilizationefficiency (%) IE=AY/IY
PSi	40.3	6.1	28	36.2	6.5	18	64
PSiA	28.3	6.2	44	30.8	9.8	32	72
PAM	32.7	8.7	53	26.3	9.2	35	66
PM	15.6	6.8	43	25.9	7.1	27	63

3.9.3.2 Effect of pH on enzyme activity

The optimum pH of an immobilized enzyme may be different from that of free one because of non-uniform distribution of charges between the microenvironment of enzyme and the bulk solution. This effect becomes more predominant when support contains ionizable groups at its surface [207].

The immobilized enzyme demonstrates greater stability than the free form and hence shows a much broader pH profile. This is because during immobilization enzymes movement is restricted as it is bonded to support in a favourable orientation retaining its activity at the optimum. Hence immobilized enzyme can withstand

sudden conformational changes thereby lowering the rate of inactivation [208,209,210]. Diffusional limitations or secondary interactions between the enzyme and the carrier may also influence this change [211,212]. Similar observations have been reported for immobilization of α-amylase and other enzymes [213].

The pH effect on the activity of the free and immobilized forms of α-amylase has been studied in buffer solution at different pH in the range 4-8 and the results are presented in the figure: 3.73.

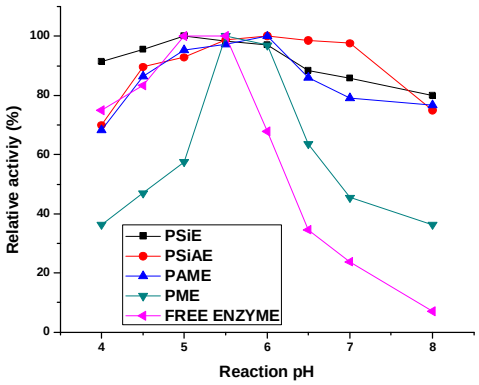

Figure: 3.73: Effect of pH on the relative activity of immobilized α- amylase

The optimum activity is assigned as 100% and other activities are expressed as relative to this optimum activity. A change in pH will affect the intra-molecular hydrogen bonding leading to a distorted conformation that will reduce the activity of the enzyme [214].

For amylase immobilization, shifts in the optimum pH towards both the acidic and alkaline directions have been observed [58, 165, 226]. This is because, when an enzyme is linked to a support, some strain is enforced on the enzyme, which causes slight unfolding of its native conformation and at this juncture contact with buffer solution causes additional strain that may be beneficial or destructive. The nature of linkage between enzyme and support also decides the shift of pH which becomes more prominent when surface functional groups are present on the support.

Free enzyme exhibits maximum activity in the pH range (5-6) with optimum activity at 5 and 5.5. At pH 4 and 8 a decrease of the enzymatic activity is observed for both the immobilized and the free enzyme; however, at pH 8 the residual activity of the immobilized enzyme in most samples is significantly higher than that of free enzyme. Thus, the immobilization process provides a structural stability, preventing an irreversible unfolding of the enzymatic protein. The native enzyme could not survive such a shift towards basic side.

In the case of PSi optimum activity was obtained at pH 5. For PSiA optimum activity was obtained at reaction pH 6 and the shift towards the basic side is required to maintain the enzyme conformation after immobilization. In the case of PAM also optimum pH was obtained at 6.

Table 3.23: Optimum pH obtained for immobilized α-amylase on Polypyrrole composites

	Free enzyme	PSi	PSiA	PAM	PM
pH	5&5.5	5	6	6	5.5

3.9.3.3 Effect of temperature on the enzyme activity

The effect of temperature on the activity of α-amylase on PPY composites and PPY powder was analyzed and the results are shown in the figure: 3.74.

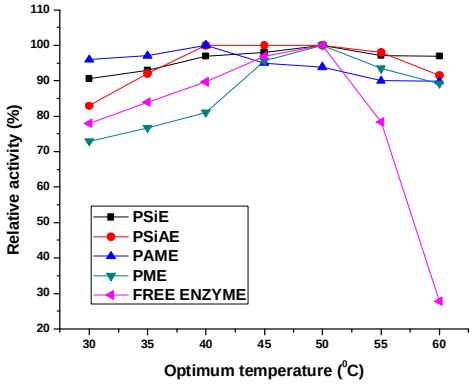

Figure: 3.74: Effect of temperature on the relative activity of free and immobilized enzyme

From the graph it is evident that optimum temperature for all composites and PPY powder was 50°C. But the added advantage is that activity of about 89-96% was retained even at 60°C whereas, free enzyme could retain only 25% of its initial activity. For PSiAE maximum activity was shown in the range 40-50°C. Enzyme thermal inactivation is the consequence of the weakening of the intermolecular forces responsible of the preservation of its three-dimensional structure leading to a reduction in its catalytic activity.

3.9.3.4 Thermal stability of the free and immobilized enzymes

Thermal stability of both free and immobilized enzymes was investigated and the results are shown in the figure: 3.75.

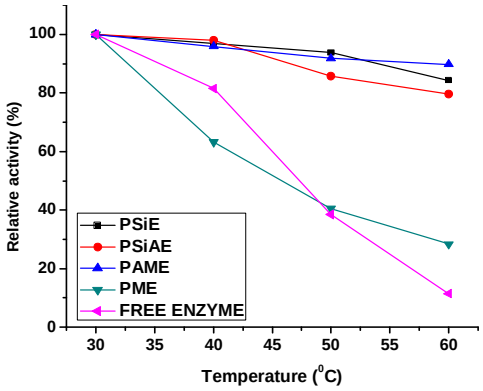

Figure: 3.75: Thermal stability studies of free and immobilized enzyme

From the figure: 3.75 it is evident that the immobilized enzymes show moderate decrease in activity, which emphasizes that the rate of inactivation is lowered upon immobilization. This is because immobilization brings about a restriction in the free movement of the enzyme by fixing it on a solid support. As a result, thermal denaturation that might result due to unfolding of protein structure is hindered and hence the enzyme can withstand higher temperature compared to free state.

The added advantage of using composites is very much clear from the graph. Enzymes immobilized on composites are found to have more thermal stability than PPY powder. At 60°C, 80-90% of activity was retained by immobilized enzymes as it is less susceptible to conformational changes. Further increase of temperature will lead to loss of activity, as for adsorbed enzymes, enzyme-support interaction is weaker resulting in unfolding of protein structure.

After incubation at 30°C for 1hour the activity showed by free and immobilized enzyme was taken as optimum and activity at other temperatures are expressed as relative to this activity. As the temperature increased, the stability dropped significantly for both free and immobilized amylase. At 40°C, enzyme immobilized on composites retained up to 95-97% of their activity whereas, only 63% activity was retained by PM. At 50°C for 1hour the immobilized enzyme was inactivated at a much lower rate than the free enzyme. 80-90% activity was retained by enzymes on composites and 40% by enzymes on PM. The free enzyme lost almost 90% of its activity at 60°C after 1hour treatment whereas, immobilized amylase lost 20-30% of its activity.

Figure: 3.76 show the effect of pre-incubation time on the activity of each immobilized enzyme.

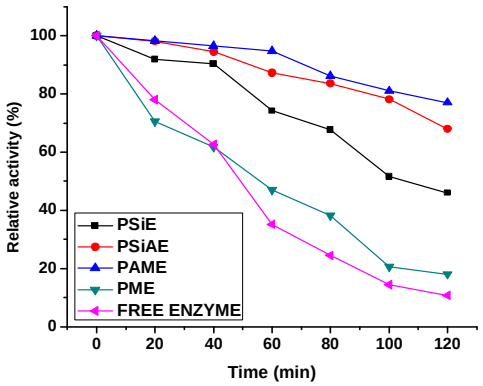

Figure: 3.76: Effect of pre-incubation time on the activity of immobilized enzymes

PSiAE and PAME maintained 60-77% of their initial activity when subjected to 120 minutes of pre-incubation time at their respective optimum temperature whereas, 46% of initial activity was maintained by PSiE; PME could retain 20% and free enzyme could retain only 10% of their initial activity when subjected to thermal treatment for same period of time.

This thermal stability results suggest lower flexibility due to multi point attachment on to supports enhances the stability of enzyme which makes the potential utilization of such enzymes extensive [215].

3.9.3.5 Determination of kinetic parameters

The K_m and V_{max} was calculated using Lineweaver-Burk plot [216].

K_m increase and V_{max} decrease after immobilization. There are several reasons that can explain the difference in behaviour of free and immobilized amylase. First, the immobilized amylase resides in an environment that is quite different from that of free enzyme in bulk solution. In addition, attachment of amylase to composite particles will cause some change in conformation or steric hindrance. This conformational change might have resulted in decreased activity and decreased affinity of enzyme for its substrate. The ionic, hydrophobic or other interaction between the enzyme and the matrix which produce micro-environmental effects may also result in changed K_m and V_{max} values. These essentially reversible effects are caused by the variations in the dissociation equilibria of charged groups at the active centre. Again non uniform distribution of substrate and/or product between the enzyme matrix and the surrounding solution affects the measured (apparent) kinetic constants. Similar increase in K_m and decrease in V_{max} was observed by other authors [217,218].

Table 3.24: Kinetic parameters for α-amylase immobilized on composites

	Free enzyme	PSiE	PSiAE	PAME	PME
K_m (mg/ml)	0.50 ± 0.04	1.6 ± 0.03	0.84 ± 0.02	0.669 ± 0.05	0.59 ± 0.06
V_{max} (mg/ml/min)	7.40 ± 0.05	1.94 ± 0.06	2.86 ± 0.09	2.21 ± 0.09	3.91 ± 0.07

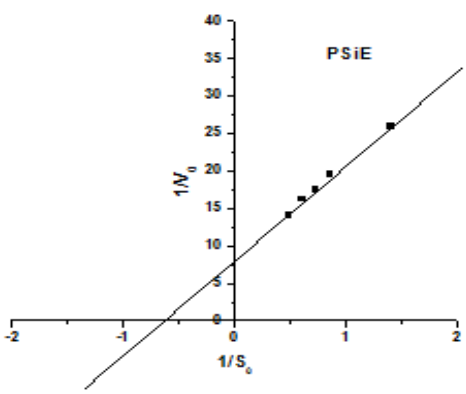

(i)

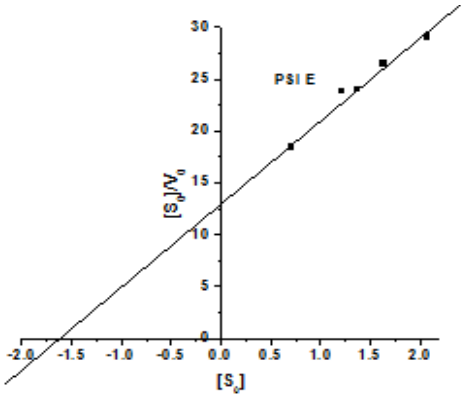

(v)

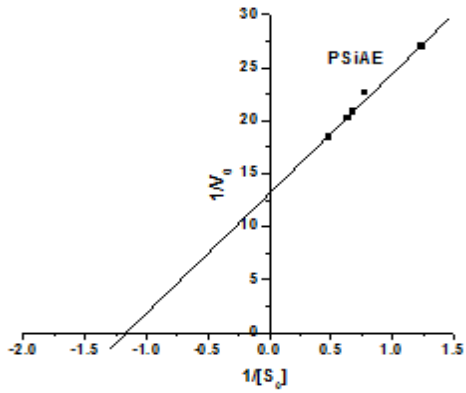

(ii)

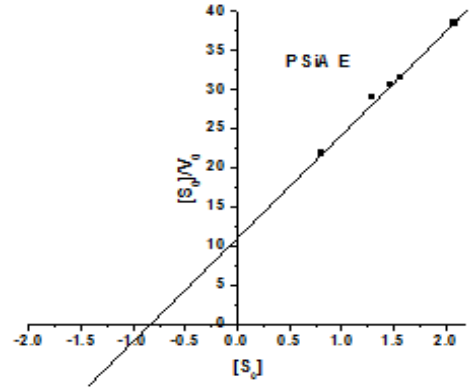

(vi)

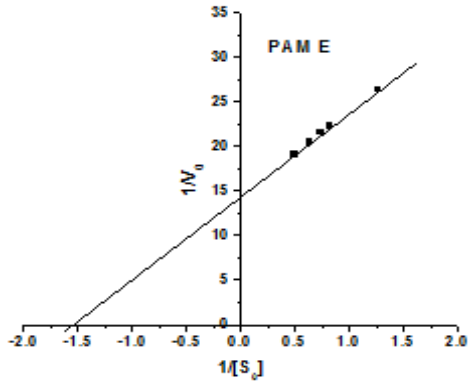

(iii)

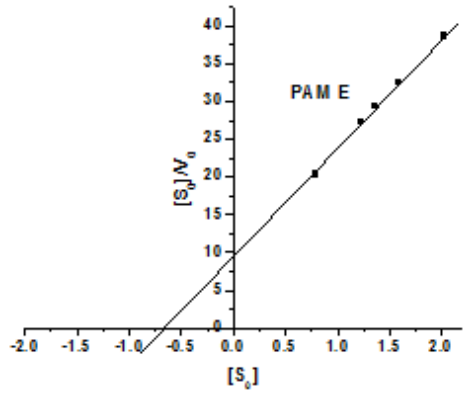

(vii)

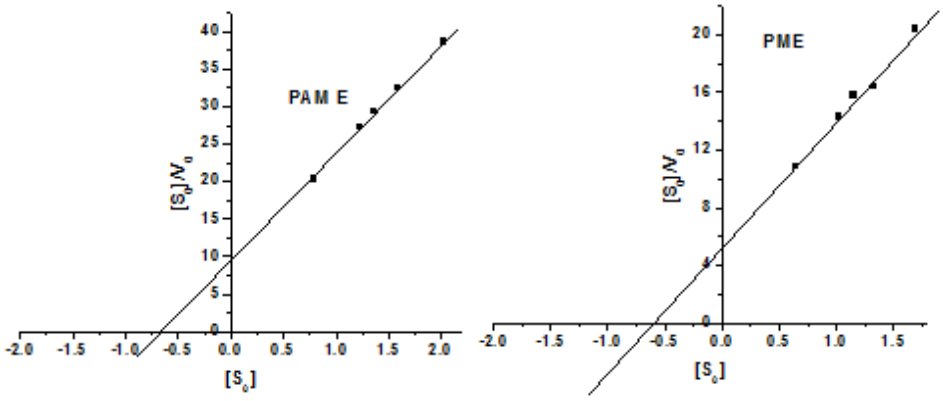

(iv) (viii)

Figure: 3.76: Lineweaver- Burk plots for (i) PSiE (ii) PSiAE (iii) PAME (iv) PME. Hanes-Woolf plots for (v) PSiE (vi) PSiAE (vii) PAME (viii) PME

3.9.3.6 Storage stability of Immobilized α- amylase

The storage stability during 4 months is shown in the figure: 3.77.

The results showed that in dry form immobilized enzyme could not retain its stability and activity for long term usage. But in wet form about 90% of activity was found to be retained by all PPY adsorbents. After 1 month of storage the loss in activity occurs due to natural inactivation of enzyme as a result of time dependent denaturation of enzyme protein. The rate of denaturation varies with type of support as it is based on how strongly and perfectly the enzyme is anchored to the support.

PM is found to retain stability up to 50% after four months. PAM could retain 30%, PSiA retained 38% and finally PSi retained only 10% of its initial activity after 4 months of storage in buffer solution.

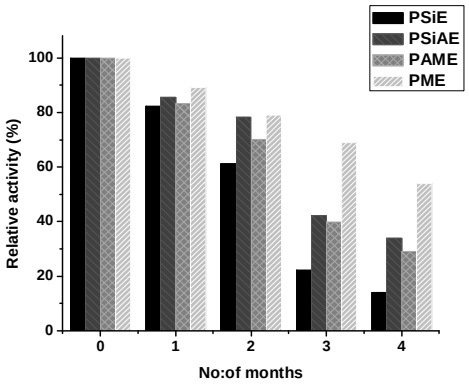

Figure: 3.77 Storage stabilities of immobilized enzymes.

3.9.3.7 Reusability

In order to check reusability of immobilized enzymes a continuous assay of amylase immobilized on PPY adsorbents was performed. The results obtained are shown in the figure: 3.78. The activity loss of immobilized enzymes upon reuse could be due to the weakening of binding strength between the enzyme and the support. Moreover there also exists the possibility of distortion of the enzyme structure as a result of frequent encountering between the active site and substrate which consequently retards its catalytic efficiency [219].

PM retained about 80% of its initial activity; PAM retained about 25% of its initial activity while PSiA and PSi retained 45% and 30% of their initial activity respectively, which are all far better than using free enzyme without immobilization. The loss of activity may be caused by the restriction of the support which resulted in limited mobility and accessibility of the active sites [220].

Similar loss of activity after repeated use of immobilized α-amylase was observed by Mobasher [217] while immobilizing α-amylase from *Aspergillus niger* on to natural polymers consisting of chitosan and alginate and synthetic polymer consisting N- isopropyl acrylamide and alginate via entrapment method. Similar results were reported in other immobilization studies [215,221].

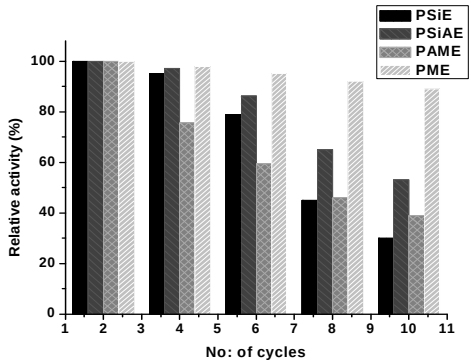

Figure: 3.78: Reusability studies of immobilized enzyme on PPY composites

3.10 Conclusions

Immobilization of Diastase α-amylase on to polypyrrole and its derivatives were successfully carried out via adsorption method. Functionalization of polypyrrole with glutaraldehyde was also performed as per the reported procedure by T. Sandu et al. and α-amylase has been immobilized on to the functionalized PPY via covalent binding method. The optimal immobilization conditions for the α-amylase were found out by the process of trial and error so as to ensure the highest possible retention of activity of the enzyme, its operational stability and reusability. The major outcomes of the work can be summarized as follows:

- ✓ The optimum pH for free enzyme was found to be in the range 5 -5.5 and temperature 50°C. The enzyme lost almost 90% of its activity at 60°C after 1hour treatment. The kinetic parameters for starch hydrolysis when evaluated gave 0.50 mg/ml as K_m and 7.40 mg/ml/min as V_{max}. When stored under 4°C free enzyme lost all its activity within 2 days.
- ✓ All the PPY supports and its derivatives were prepared as per the reported procedures. The physico-chemical characterization of supports before and after enzyme immobilization were carried out using the FT-IR, TG, SEM, BET and EDS analytical techniques.

- ✓ Diastase α-amylase when immobilized on to PPY prepared in the presence of different oxidizing agents and different methods showed enhanced activity and stability when compared to free enzyme. Evaluation of optimal binding parameters was carried out. It was found that all the immobilized enzymes showed a broader pH profile compared to free enzyme. The optimum pH for PA, PF and PI were 5.5, 5 and 6 respectively. PA having surface area higher than other two possess highest immobilization yield. But activity yield was higher for PI. The optimum temperature for PA and PF get shifted to 40°C, whereas for PI the optimum temperature was about 50°C. The kinetic parameters K_m and V_{max} were also determined via Lineweaver-Burk plot. In most cases results obtained showed that storage stability of the immobilized enzyme was significantly better than free enzyme. In our study activity for 12 cycles of use for the immobilized enzymes was monitored and PF exhibit better reusability than other two.

- ✓ PPY prepared in presence of surfactant templates were found be suitable supports for enzyme immobilization as PPY particles formed are having controlled well tailored morphology when compared to those prepared in absence of surfactants. Biochemical characterization conducted revealed that optimum pH for PS is pH 5 which is same as that of free enzyme, whereas for PC and PT it gets shifted to pH6. The 10°C decrease in the optimum temperature combined with thermal stability exhibited by α-amylase immobilized on PC and PT was an interesting finding of this work. α-amylase immobilized on PS showed an increase in the optimum temperature. The K_m values were found to be increasing for PS, PC and PT. The V_{max} values of immobilized enzymes were decreasing for PS, PC and PT. Enzyme immobilized on PS retained 40% of its initial activity even after 6 months of storage in buffer solution at 4°C whereas, enzyme immobilized on PC and PT retained 53 and 60% respectively under similar

conditions. The reusability was checked for 20 continuous cycles. After 15 cycles PS and PC retained 50% of their initial activity whereas, PT retained almost 60% of its initial activity.

- ✓ α-amylase was successfully immobilized on PPY functionalized with glutaraldehyde (PG) via covalent binding. Whereas in the case of PPY modified with APTES (PN), immobilization of amylase occurs via adsorption. The optimum pH for PGE was found to be at pH 5 which is same as that of free enzyme but for PNE it was shifted to pH 6. The optimum temperature for PGE was obtained at 55°C whereas for PNE the optimum temperature gets shifted to 60°C. Immobilization efficiency for PGE was found to be 95% and for PNE it was about 86%. But the activity yield was higher for PNE than for PGE. The kinetic parameters evaluated showed an increase in K_m and decrease of V_{max} for both immobilized enzymes. Upon 4 months of storage, the adsorbed enzyme preserved 40% of its initial activity whereas; covalently bound enzyme retained 55% of its initial activity. The reusability studies showed that in the case of PNE up to 7 cycle 70% activity was retained which decreased drastically for further cycles. Whereas PGE was able to maintain good activity up to 60% even after five runs.
- ✓ The copolymers prepared were found to exhibit enhanced enzyme loading capacity than the bare PPY. For both PYPAE and PYPHE the optimum pH get shifted to pH 6. The optimum temperature for PYPH was same as that of free enzyme that is 50°C but that of PYPA get shifted to 60°C. About 50-60% of immobilized enzymes maintained their activity when subjected to 120 minutes of pre-incubation time at their respective optimum temperature whereas free enzyme could retain only 10% of their initial activity when subjected to same period of time. K_m value for PYPA was found to be 2.73 mg/ml and that for PYPH was about 2.47 mg/ml which

was comparable. But the V_{max} values of both immobilized enzymes varied significantly as 4.21 mg/ml/min for PYPA and 2.95mg/ml for PYPH. On examining the storage stability it was found that PYPA retained 70% of its initial activity and PYPH retained 25% of its initial activity after 6 months. The reusability studies indicated that PYPA adsorbed enzyme could be used without much loss in its activity up to 14 cycles. PYPH but retained its activity significantly only for 6 cycles after which it showed decline in activity.

- ✓ Both functionalized and unfunctionalized PPY silica composites possess higher surface area compared to other PPY supports previously discussed and hence the enzyme loading capacity of these PPY composites also get enhanced. As far as nanocomposites are concerned surface functionalization with amine groups produced much higher contents of amylase adsorption in the order PAM > PSiA > PSi. Immobilization efficiency was maximum for aminated PSi composite. The optimum pH for PSi was same as that of free enzyme. For aminated PSi composites optimum pH shifted towards pH6. The optimum temperature for PPY composites was same as that of free enzyme. But the added advantage is that activity of about 89-96% was retained even at 60°C whereas, free enzyme could retain only 25% of its initial activity. For PSiA almost 100% activity was shown in the range 40-50°C. The free enzyme lost almost 90% of its activity at 60°C after 1hour treatment whereas, immobilized amylase lost 20-30% of its activity. The kinetic parameters when evaluated showed an increase in K_m value and decrease of V_{max} value for all PPYSi composites. The maximum in activity was obtained in the case of aminated polypyrrole composites compared to other three. The stability during 4 months of storage at 4°C when analyzed it was found that PAM could retain 30%, PSiA -38% and finally PSi retained only 10% of its initial activity. The reusability when

checked it was observed that PM retained about 80% of its initial activity; PAM retained about 25% of its initial activity while PSiA and PPYSi retained 45 and 30 % of initial activity respectively, which are all far better than using free enzyme without immobilization.

3.11 References

[1] A. Ramanaviciene, A. Ramanavicius, Application of polypyrrole for the creation of immunosensors, Crit. Rev. Anal. Chem. 32 (2002) 245-252.

[2] A. Ramanaviciene, A. Ramanavicius, Towards the hybrid biosensors based on biocompatible conducting polymers, in M.S. Shur, A. Zukauskas (Eds), UV Solid - State Light Emitters and Detectors, Kluwer Academic Publishers, The Netherlands, (2004) 287-296.

[3] S. Sakkopoulos, E. Vitoratos, E. Dalas, Conductivity degradation due to thermal aging in conducting polyaniline and polypyrrole, Synth. Met. 92 (1998) 63-67.

[4] Z. Zang, R. Roy, F.J. Dugre, D. Tessier, L.H. Dao, In vitro bio- compatibility study of electrically conductive polypyrrole -coated polyester fabrics, J. Biomed. Mater. Res. 57 (2001) 63-71.

[5] B. Jakubiec, Y. Marios, Z. Zang, R. Roy, M. F. Sigot - luizard, F.J. Dugre, M.W. King, L.Dao, G. Larche, R. Guidoin, In vitro cellular response to polypyrrole - coated woven polyester fabrics: potential benefits of electrical conductivity, J. Biomed. Mater. Res. 41 (1998) 519 -526.

[6] Z. Wang, C. Roberge, Y. Wan, L.H. Dao, R. Guidoi, Z. Zhang, A biodegradable electrical bioconductor made of polypyrrole nanoparticle / poly (d, l- lactide) composite: a preliminary in vitro biostability study, Biomed. Mater. Res. (2003) 38-746.

[7] D.T. Seshadri, N.V. Bhat, Synthesis and properties of cotton fabrics modified with polypyrrole, Sen - i -Gakkaishi 61 (2005) 103-108.

[8] A. Azioune, A.B. Slimane, L.A. Hamou, A. Pleuvy, M.M. Chehimi, C. Perruchot, S.P. Armes, Synthesis and characterization of active ester-functionalized polypyrrole-silica nanoparticles: application to the covalent attachment of proteins, Langmuir 20 (2004) 3350-6.

[9] A. Ramanavicius, K. Habermuller, J. Razumiene, R. Meskys, L. Marcinkeviciene, I. Bachmatova, E. Csoregi, V. Laurinavicius, W. Schuhmann, An oxygen - independent ethanol biosensor based on quinohemoprotein alcohol dehydrogenase covalently bound to a functionalized polypyrrole film, Prog. Colloid Polym. Sci. 116 (2000) 143 - 148.

[10] A. Ramanavicius, A. Kausaite, A. Ramanaviciene, Polypyrrole-coated glucose oxidase nanoparticles for biosensor design, Sens. Actuators, B. 111-112 (2005) 532-539.

[11] M. Trojanowicz, W. Matuszewski, M. Podsiadla, Enzyme entrapped polypyrrole modified electrode for flow - injection determination of glucose, Biosens. Bioelectron. 5 (1990) 149 -156.

[12] S. Cete, A. Yasar, F. Arslan, Immobilization of Uricase Upon Polypyrrole-Ferrocenium Film, Artif. Cell Blood Sub. 6 (2007) 607 - 620.

[13] F.W. Schenck, R.E. Hebeda, "Starch Hydrolysis Products: An Introduction and History'' in Starch Hydrolysis Products, Worldwide Technology, Production, and Applications, F.W. Schenck, R.E. Hebeda, eds., VCH Publishers, Inc., New York, (1992) 1-21.

[14] S. Talekar, S. Chavare, Optimization of immobilization of α-amylase in alginate gel and its comparative biochemical studies with free α-amylase, Recent Research in Science and Technology, 4 (2012) 01-05.

[15] V. Singh, S. Ahmed, Silver nanoparticle (AgNPs) doped gum acacia-gelatin-silica nanohybrid: An effective support for diastase immobilization, Int. J. Biol. Macromol. 50 (2012) 353-361.

[16] M.Y. Arica, V. Hasirici, N.G. Alaeddinoglu, Covalent immobilization of α-amylase on to pHEMA microspheres: preparation and application to fixed bed reactor, Biomat. 16(1995) 761-768.

[17] B.A. Saville, M. Khavkine, S. Gayathri, B. Marandi, Z. Yong-Li, Characterization and performance of immobilized amylase and cellulose, Appl. Biochem. Biotechnol. 113 (2004) 251-259.

[18] S. Aksoy, H. Tumturk, N. Hasirci, Stability of α-amylase immobilized on poly (methyl methacrylate-acrylic acid) microspheres, J Biotechnol. 60 (1998) 37-46.

[19] O.I. Kubrak, V.I. Lushchak, Optimization of conditions for immobilization of α-amylase from Bacillus sp. BKL_{20} in Ca^{2+}-alginate beads, Ukr. Biokhim Zh. 80 (2008) 32-41.

[20] M.I.G. Siso, M. Graber, J.S. Condoret, D. Combes, Effect of diffusional resistances on the action pattern of immobilized α-amylase, J. Chem. Technol. Biotechnol. 48 (1990) 185-200.

[21] F. Ertan, H. Yagar, B. Balkan, Some properties of free and immobilized α-amylase from Penicillium griseofulvum by solid state fermentation, Prep Biochem Biotechnol. 36 (2006) 81-91.

[22] A.K. Bajpai, S. Bhanu, Immobilization of *a*-amylase in vinyl polymer - based interpenetrating polymer networks, Colloid Polym Sci. 282 (2003) 76-83.

[23] P.C. Ashly, P.V. Mohanan, Preparation and characterization of Rhizopus amyloglucosidase immobilized on poly(o-toluidine), Process Biochem. 45 (2010) 1422-1426.

[24] P.C. Ashly, M.J. Joseph, P.V. Mohanan, Activity of diastase α-amylase immobilized on polyanilines (PANIs), Food Chem. 127 (2011) 1808-1813.

[25] Y. Ohtsuka, H. Kawaguchi*, T. Yamamoto Immobilization of α-amylase on polymeric carriers having different structures, J. Appl. Polym. Sci. 29 (1984) 3295-3306.

[26] J. Stejskal, R.G. Gilbert, Polyaniline. Preparation of a conducting polymer, Pure Appl. Chem. 74 (2002) 857-867.

[27] S.M. Kuhn, Synthesis of electrically conductive polypyrrole thin films via ammonium persulfate chemistry Thesis (B.S.)--Massachusetts Institute of Technology, Dept. of Materials Science and Engineering, 1990.

[28] V. Shaktawat, K. Sharma, N.S. Saxena, Structural and electrical Characterization of protonic acid doped polypyrrole, J.Ovonic Res. 6 (2010) 239 - 245.

[29] M. Omastova´, M. Trchovab, J. Kovarova, J. Stejskal, Synthesis and structural study of polypyrroles prepared in the presence of surfactants, Synth. Met. 138 (2003) 447-455.

[30] G.D. Nestorovic, K.B. Jeremic, S.M. Jovanovic, Kinetics of aniline polymerization initiated with iron(III) chloride, J. Serb. Chem. Soc. 71(2006) 895—904.

[31] K. Anuar, S. Murali, A. Fariz, H.N.M.M. Ekramul, Conducting Polymer / Clay Composites: Preparation and Characterization, Mater. Sci. 10 (2004) 255-258.

[32] D.-V. Brezoi, Polypyrrole films prepared by chemical oxidation of Pyrrole in aqueous $FeCl_3$ solution, J. Sci. Arts 12 (2010) 53-58.

[33] S. Goel, A. Gupta, K.P. Singh, R. Mehrotra, H.C. Kandpal, Structural and Optical Studies of Polypyrrole Nanostructures, Int. J. Appl. Chem. 2 (2006) 157-168.

[34] V.Q. Trung, D.N. Tung, D.N. Huyen, Polypyrrole/Al_2O_3 nanocomposites: preparation, characterisation and electromagnetic shielding properties, J. Exp. Nanosci. 4 (2009) 213-219.

[35] J. Lei, C.R. Martin, "Infrared Investigations of Pristine Polypyrrole - Is the Polymer called Polypyrrole Really Poly (Pyrrole-Co-Hydroxypyrrole)?", Synth. Met. 48 (1992) 331-336

[36] G. Maia, E.A. Ticianelli, F.C. Nart, FTIR Investigation of the Polypyrrole Oxidation in Na_2SO_4 and $NaNO_3$ Aqueous Solutions, Zeitschrift Phys. Chem. 186 (1994) 245-257.

[37] W. Prissanaroon, L. Ruangchuay, A. Sirivat, J. Schwank, Electrical conductivity response of dodecyl benzene sulphonic acid - doped polypyrrole films to SO_2 - N_2 mixtures, Synth. Met. 114 (2000) 65 - 72.

[38] B. Tian, G. Zerbi, "Lattice Dynamics and Vibrational Spectra of Pristine and Doped Polypyrrole: Effective Conjugation Coordinate." J. Chem. Phys., 92 (1990) 3886.

[39] T. Sandu, A. Sarbu, F. Constantin, E. Ocnaru, S. Vulpe, A. Dumitru, H. Iovu, Polyphenol oxidase immobilization of functionalized polypyrrole, Rev. Roum. Chim. 56 (2011) 875-882.

[40] A. Adhikari, Ph.D. Thesis "Conducting polyaniline and Polypyrrole: studies of their catalytic Properties. PhD thesis, National Chemical Laboratory, Pune, 2004.

[41] M. Reghu, S.V. Subramanyam, The contribution of polarons, bipolarons and intersite tunneling to low temperature conductivity in doped polypyrrole, Synth. Met. 41-43 (1991) 455-458.

[42] Y. Jiang, Q. Gu, L. Li, D.-Y. Shen, X.-G. Jin, C.-M. Chan, Conformational changes induced in the induction period of crystallization as measured by FT - IR, Polymer 44 (2003) 3509-3513.

[43] S. Krimm, J. Bandekar, Vibrational spectroscopy and conformation of peptides, polypeptides, and proteins, Adv. Prot. Chem. 38 (1986) 181-367.

[44] J. Xie, C. Riley, M. Kumar, K. Chittur, FTIR / ATR study of protein adsorption and brushite transformation to hydroxyapatite, Biomater. 23 (2002) 3609-16.

[45] A. Barth, C. Zscherp, What vibrations tell us about proteins, Q. Rev. Biophys. 35 (2002) 369-430.

[46] D.V. Dhar, S. Tanuj, P. Amit, M. S. Kumar, Insights to sequence information of α-amylase enzyme from different source organisms, IJABB 1 (2012) 87-91.

[47] S. Aleti, H. Karaturi, C.V.S. Subrahmanyam, M. Lakshmi Narasu, Complexation and Characterization of α-amylase with Hydroxypropyl ß- Cyclodextrin, Int. J. Pharm. Phytopharmacol. Res. 1(2012) 375-378. (Research Article).

[48] M. Omastova´, M. Trchova, J. Kovarova´, J. Stejskal, Synthesis and structural study of polypyrroles prepared in the presence of surfactants, Synth. Met. 138 (2003) 447-455.

[49] A. Rosevear, J.F. Kennedy, J.M.S Cabral, Immobilised enzymes and cells Ist edn Taylor & Francis (1987) 264.

[50] J. March, Advanced Organic Chemistry: Reactions, Mechanisms and Structure. 3rd ed. Wiley Eastern, New Delhi.1986.

[51] C. Perruchot, M.M. Chehimi, M. Delamar, F. Fievet, Use of Aminosilane Coupling Agent in the synthesis of conducting, hybrid polypyrrole - silica gel particles, Surf. Interface Anal. 26 (1998) 689-698.

[52] G. Bayramoglu, M. Yilmaz, M.Y. Arica, Immobilization of thermostable α-amylaseonto reactive membrane, Kinetics characterization and application to continuos starch hydrolysis, Food Chem. 84 (2004) 591-599.

[53] J.L. Brash, T.A. Horbett, Proteins at Interface Physico-chemical and Biochemical Studies, ACS Symposium Series. American Chemical Society, Washington, DC 343 (1987).

[54] V. Ball, J.J. Ramsden, Absence of surface exclusion in the first stage of lysozyme: Adsorption is driven through electrostatic self assembly, J. Phys. Chem. B 101 (1997) 5465-5469.

[55] J. Klein, "Probing the interactions of proteins and nanoparticles", Proc. Natl. Acad. Sci. U. S. A. 104 (2007) 2029-2030.

[56] Y. Fang, X.-J. Huang, P.-C. Chen, Z.-K. Xu, Polymer materials for enzyme immobilization and their application in bioreactors, BMB reports, 44 (2011) 87-95.

[57] A. Salis, , D. Meloni, S. Ligas, M.F. Casula, M. Monduzzi, V. Solinas, E. Dumitriu, Physical and Chemical Adsorption of Mucor javanicus Lipase on SBA-15 Mesoporous Silica. Synthesis, Structural Characterization, and Activity Performance, Langmuir 21 (2005) 5511-5516.

[58] Z. Bayramoglu, U. Akbulut, S. Sungur, Immobilization of α-amylase into photographic gelatin by chemical cross - linking, Biometrials 13 (1992) 704-709.

[59] J.M. Hess., R.M. Kelly, Influence of polymolecular events on inactivation behavior of xylose isomerase from *Thermotoga neapolitana* 5068, Biotechnol. Bioeng. 62 (1999) 509-517.

[60] J. Buijs, W. Norde, J.W.T. Lichtenbelt, Changes in the Secondary Structure of Adsorbed IgG and F(ab') 2 Studied by FTIR Spectroscopy, Langmuir 12 (1996) 1605-1613.

[61] C.F. Wertz, M.M. Santore, Adsorption and relaxation kinetics of albumin and fibrinogen on hydrophobic surfaces: single-species and competitive behavior, Langmuir 15 (1999) 8884-8894.

[62] H. Elwing, B. Nilsson, K.-E. Svensson, A. Askendahl, U. R. Nilsson, I. Lundstrom, Conformational changes of a model protein (complement factor 3) adsorbed on hydrophilic and hydrophobic solid surfaces, J. Colloid Interface Sci. 125 (1988) 139-145.

[63] E. Blomberg, P.M. Claesson, R.D Tilton,. Short-range interaction between adsorbed layers of human serum albumin, J. Colloid Interface Sci. 166 (1994) 427-436.

[64] J.C. Fröberg, T. Arnebrant, J. McGuire, P.M. Claesson, Effect of Structural Stability on the Characteristics of Adsorbed Layers of T4 Lysozyme, Langmuir14 (1998) 456-462.

[65] T. Handa, A. Hirose, T. Akino, K. Watanabe, H. Tsuchiya, Preparation of immobilized α-amylase covalently attached to granular polyacrylonitrile, Biotechnol. Bioeng. 25 (1983) 2957-2967.

[66] E. Su, T. Xia, L. Gao, Q. Dai, Z. Zhang, Immobilization of β-glucosidase and its aroma-increasing effect on tea beverage, Food Bioprod. Process. 88 (2010) 83-89.

[67] G. Delcheva, G. Dobrev, I. Pishtiyski, Performance of Aspergillus niger B 03 β-xylosidase immobilized on polyamide membrane support, J. Mol. Catal.B: Enzymatic 54 (2008) 109-115.

[68] G. Dey, V. Nagpal, R. Banerjee, Immobilization of α-amylase from Bacillus circulans GRS 313 on coconut fibre, Appl. Biochem. Biotechnol. 102-103 (2002) 303-314.

[69] B.C.C. Pessela, R.-L. Fernandez, M. Fuentes, A. Vian, J. L. Garca, A.V. Carrascosa, C. Mateo, J.M. Guisan, Reversible immobilization of a thermophilic beta-galactosidase via ionic adsorption on PEI-coated Sepabeads, Enzyme Microb. Technol. 32 (2003) 369-374.

[70] R. Reshmi, G. Sanjay, S. Sugunan, Immobilization of α-amylase on zirconia: A heterogeneous biocatalyst for starch hydrolysis, Catal. Commun. 8 (2007) 393-399.

[71] J. Bryjak, Glucoamylase, α-amylase and β-amylase immobilisation on acrylic carriers, Biochem. Eng. J. 16 (2003) 347-355.

[72] G. Zhao, J. Wang., Y. Li, H. Huang, X. Chen, Reversible immobilization of glucoamylase onto metal-ligand functionalized magnetic FeSBA-15, Biochem. Eng. J. 68 (2012) 159-166.

[73] T. Palmer, P.L. Bonner, Enzymes: Biochemistry, Biotechnology, Clinical chemistry, 2nd edn, Horwood Publishing Ltd, USA, 2007.

[74] L.H. Lim, D.G. MacDonald, G.A. Hill, Hydrolysis of starch particles using immobilized barley α-amylase, Biochem. Eng. J. 13 (2003) 53-62.

[75] R.J. Wykes, P.M. Dunnill, D. Lilly, Immobilization of α-amylase by attachment to soluble support materials, Biochim. Biophys. Acta 250 (1971) 52.

[76] E. Cakmakci, O. Danis, S. Demir, Y. Mulazim , M.V. Kahraman, α-amylase immobilization on epoxy containing thiol-ene photocurable materials, J. Microbiol. Biotechnol. 23 (2013) 205-10.

[77] T.F. Otero, I Boyano, M.T. Cortés, G. Vázquez, Nucleation, non-stoiquiometry and sensing muscles from conducting polymers, Electrochim. Acta 49 (2004) 3719-3726.

[78] V. Saxena, B.D. Malhotra, 'Prospects of conducting polymers in molecular electronics,'Curr. Appl. Phys.3 (2003) 293-305.

[79] Y. Berdichevsky, Y.-H. Lo, "Polypyrrole Nanowire Actuators," Adv. Mater. 18 (2006) 122-125.

[80] J. Huang, S. Virji, B.H. Weiller, R.B. Kaner, Nanostructured Polyaniline Sensors, Chem. Eur. J. 10 (2004) 1314-1319.

[81] X. Zhang, J. Zhang, W. Song, Z. Liu, Controllable synthesis of conducting polypyrrole nanostructures, J. Phys. Chem. B. 110 (2006) 1158-65.

[82] J. Stejskal, M. Omastova, S. Fedorova, J. Prokes, M. Trchova, Polyaniline and polypyrrole prepared in the presence of surfactants: a comparative conductivity study, Polymer. 44 (2003) 1353-1358.

[83] A.D.W. Carswell, E.A. O'Rear, B.P. Grady, Adsorbed surfactants as templates for the synthesis of morphologically controlled polyaniline and polypyrrole nanostructures on flat surfaces: from spheres to wires to flat films, J. Am. Chem. Soc. 125 (2003) 14793-14800.

[84] M. Omastova, M. Trchova, J. Kovarova, J. Stejskal, Synthesis and structural study of polypyrroles prepared in the presence of surfactants, Synth. Met. 138 (2003) 447-455.

[85] W.J. Kwon, D.H. Suh, B.D. Chin, J.-W. Yu, Preparation of polypyrrole nanoparticles in mixed surfactants system, J. Appl. Polym. Sci. (2008) 1324-1329.

[86] M.A. Usman, V.I. Ekwueme, T.O. Alaje, M.T. Afolabi, S.O. Bolakale Immobilization of α-amylase on Mesoporous Silica KIT-6 and Palm Wood Chips for Starch Hydrolysis, Chemical and Process Engineering Research, 9 (2013) 7-13.

[87] E. Demirkan, S. Dincbas, N. Sevinc, F. Ertan, Immobilization of B. amyloliquefaciens α-amylase and comparison of some of its enzymatic properties with the free form, Rom. Biotech. Lett. 16 (2011) 6690-6701.

[88] A. Vinu, V. Murugesan, M. Hartmann, Adsorption of Lysozyme over Mesoporous Molecular Sieves MCM-41 and SBA-15: Influence of pH and Aluminum Incorporation, J. Phys. Chem. B 108 (2004) 7273-7330.

[89] A. Tanriseven, S. Doan, Immobilization of invertase within calcium alginate gel capsules, Process Biochem. 36 (2001) 1081-3.

[90] T. Bahar, S.S. Celebi, "Immobilization of glucoamylase on magnetic poly (styrene) particles", J. Appl. Polym. Sci. 72 (1999) 69-73.

[91] B.A. Kikani, S. Pandey, S.P. Singh, Immobilization of the α-amylase of Bacillus amyloliquifaciens TSWK1-1 for the improved biocatalytic properties and solvent tolerance, Bioprocess Biosyst. Eng. 36 (2013) 567.

[92] S. Talekar, S. Chavare, Optimization of immobilization of α-amylase in alginate gel and its comparative biochemical studies with free α-amylase, Rec. Res. Sci. Technol. 4 (2012) 1-5.

[93] P.N. Nehete, M.V. Hedge, G. Reddy, V. Shankar, Immobilization of amyloglucosidase on polystyrene anion exchange resin II. Kinetics and stabilities, Biotechnol. Lett. 9 (1987) 651-654.

[94] D.D. Lee, G.K. Lee, P.J. Reilly, Effect of Pore Diffusion Limitation on Dextrin Hydrolysis by Immobilized Glucoamylase, Biotechnol. Bioeng. XXII (1980) 1-17.

[95] G. Bayramoglu, H. Erdogan, M.Y. Arica, Studies of adsorption of alkaline trypsin by poly (methacrylic acid) brushes on chitosan membranes, J. Appl. Polym. Sci. 108 (2008) 456-465.

[96] K. Kharkrang, P.K. Ambasht, Immobilization of α-amylase from Pennisetum typhoides inside gelatin beads and its characterization, Research Article, 2013.

[97] N. Jaiswal, O. Prakash, Immobilization of Soyabean α-amylase on Gelatin and its Application as a Detergent additive, Asian J.Biochem. 6 (2011) 337-346

[98] V. Swarnalatha, R.A. Esther, R. Dhamodharan, Immobilization of α-amylase on gum acacia stabilized magnetite nanoparticles, an easily recoverable and reusable support, J. Mol. Catal. B Enzym. 96 **(**2013**)** 6-13.

[99] T. Sandu, A. Sârbu, S.A. Gârea, H. Iovu, Study of Polypyrrole Functionalization Parameters, UPB Sci. Bull; Series B 73 (2011) 123-132.

[100] T. Sandu, A. Sarbu, F. Constantin, C.I. Spataru, R.A. Gabor, R. Somoghi, H. Iovu, Characterization of functionalized polypyrrole, Rev. Roum. Chim. 57 (2012) 177-185.

[101] C. Mateo, J.M. Palomo, G.-L Fernández, R.-F Fernandez, J.M Guisán Improvement of enzyme activity, stability and selectivity via immobilization techniques, Enzyme Microbial. Technol. 40 (2007) 1451-1463.

[102] C.J.M. Silva, F. Sousa, G. Gübitz, A.-P. Cavaco, Crosslinking of proteins with glutaraldehyde, Food Technol. Biotechnol. 42 (2004) 51-56.

[103] Y. Wang, X. Pang, Y. Zhang, H. Wang, Characterization of covalent immobilization on the surface of optical fibers by scanning electron microscopy and energy dispersive X-ray spectrometry, Surf. Interface Anal. 41 (2009) 775-778.

[104] B.R. Pieters, G. Bardeletti, Enzyme immobilization on a low cost magnetic support: Kinetic studies on immobilized and coimmobilized glucose oxidase and gluco amylase Enzyme Micro.Technol. 14 (1992) 361 - 70.

[105] L.E. Goldstein, G. Manecke, Immobilized enzyme principles. In: Applied Biochemistry and Bioengineering, L.B. Wingard, E.-K Katchalskei, L. Goldstein., eds., Academic Press, New York, (1976) 23-110.

[106] T. Sandu, A. Sarbu, F. Constantin, E. Ocnaru, S. Vulpe, A. Dumitru, H. Iovu, Polyphenol oxidase immobilization of functionalized polypyrrole, Rev. Roum. Chim. 56 (2011) 875-882.

[107] X. Zhang, R. Bai, Y.W. Tong, Selective adsorption behaviors of proteins on polypyrrole-based adsorbents, Sep. Purif. Technol. 52 (2006) 161-169.

[108] W. Lei, Study of aminated polypyrrole-coated granules for humic acid and bovine serum albumin adsorption, A thesis submitted for the degree of master of engineering department of chemical and biomolecular engineering, National University of Singapore, 2004.

[109] V.K.S. Hsiao, J.R. Waldeisen, Y. Zheng, P.F. Lloyd, T.J. Bunning, T.J. Huang, Aminopropyltriethoxysilane (APTES) - functionalized nanoporous polymeric gratings: fabrication and application in biosensing, J. Mater. Chem. 17 (2007) 4896-4901.

[110] J. Lei, W. Liang, C.R. Martin, Infrared investigations of pristine, doped and partially doped polypyrrole, Synth. Met. 48 (1992) 301.

[111] B. Tian, G. Zerbi, Lattice Dynamics and Vibrational Spectra of Pristine and Doped Polypyrrole; Effective Conjugation Coordinate, J. Chem. Phys. 92 (1990) 3892.

[112] T.N. Nwagu, B.N. Okolo, H. Aoyagi, Immobilization of raw starch digesting amylase on silica gel: A comparative study, Afr. J. Biotechnol. 10 (2011) 15989-15997.

[113] T.N. Nwagu, B.N. Okolo, H. Aoyagi, Stabilization of a raw starch digesting amylase from Aspergillus carbonarius via immobilization on activated and non-activated agarose gel, World J. Microbiol. Biotechnol. 28 (2012) 335-45.

[114] W. Norde, C.E. Giacomelli, BSA structural changes during homomolecular exchange between the adsorbed and the dissolved states, J Biotechnol. 79 (2000) 259-68.

[115] A.N. Asanov, L.J. Delucas, P.B. Oldham, W.W. Wilson, Interfacial Aggregation of Bovine Serum Albumin Related to Crystallization Conditions Studied by Total Internal Reflection Fluorescence, J Colloid Interface Sci. 196 (1997) 62-73.

[116] W.J. Dillman, Jr. I. Miller, On the adsorption of serum proteins on polymer membrane surfaces, J.Colloid. Interface Sci. 44 (1973) 221-241.

[117] H. Urano, S. Fukuzaki, "Conformation of adsorbed bovine serum albumin governing its desorption behavior at alumina-water interfaces", J. Biosci. Bioeng. 90 (2000) 105-111.

[118] H. Kamal, G. M. Sabry, S. Lotfy, N. M. Abdallah, J. Rosiak, E. A. Hegazy, Immobilization of Glucoamylase on Polypropylene Fibers Modified by Radiation Induced Graft Copolymerization, J. Macromol. Sci., Pure Appl. Chem. 45 (2008) 65-75.

[119] J.-T. Oha, J.-H. Kimb, Preparation and properties of immobilized amyloglucosidase on nonporous PS/PNaSS microspheres, Enzyme Microb. Technol. 27 (2000) 356-361.

[120] D.A. Butterfield, D. Bhattacharyya, S. Daunerta, L. Bachas, Catalytic biofunctional membranes containing site-specifically immobilized enzyme arrays: a review, J. Membr. Sci. 181 (2001) 29-37.

[121] B.S. Aytar, U. Bakir, Preparation of cross-linked tyrosinase aggregates. Process Biochem. 43 (2008) 125-131.

[122] I. Alkorta, C. Garbisu, M.J. Llama, J.L. Serra, Immobilization of pectin lyase from Penicillium italicum by covalent binding to nylon. Enzyme Microb. Technol. 18 (1996) 141-146.

[123] N. Miletic, A. Nastasovic, K. Loos, Immobilization of biocatalysts for enzymatic polymerizations: Possibilities, advantages, applications, Bioresour. Technol. 115 (2012) 126-135.

[124] G. Bayramoglu, B. Karagoz, M. Yilmaz, N. Bicak, M.Y. Arica, Immobilization of catalase via adsorption on poly(styrene-d-glycidylmethacrylate) grafted and tetraethyldiethylenetriamine ligand attached microbeads, Bioresour. Technol. 102 (2011) 3653-3661.

[125] R.S. Singh, G.K. Saini, J.F. Kennedy, Covalent immobilization and thermodynamic characterization of pullulanase for the hydrolysis of pullulan in batch system, Carbohydr. Polym. 81 (2010) 252-259.

[126] K.S. Siddiqui, A.H. Shemsi, M.A. Anwar, M.H. Rashid, M.I. Rajoka, Partial and complete alteration surface charges of carboxymethylcellulase by chemical modification: thermostabilization in water-miscible organic solvents, Enzyme Microb. Technol. 24 (1999) 599-608.

[127] M.V. Kahraman, G. Bayramoglu, N.K. -Apohan, A. Gtingor, α-amylase immobilization on functionalized glass beads by covalent attachment, Food Chem. 104 (2007) 1385-1392.

[128] M.K. Goel, Immobilized enzymes 1994.www.rpi.edu/dept/chem-eng/ Biotech-Environ/IMMOB/goel2nd.htm.

[129] S.S. Kundu, Immobilization of enzymes and their applications, (2011) 12.

[130] T. Kaneko, T. Ohno, N. Ohisa, Purification and characterization of a thermostable raw starch digesting amylase from a Streptomyces sp. isolated in a milling factory, Biosci. Biotechnol. Biochem. 69 (2005) 1073-1081.

[131] H.V. Adikane, D.M. Thakar, Studies of penicillin g acylase immobilization using highly porous cellulose-based polymeric membrane, Appl. Biochem Biotechnol. 160 (2010) 1130-45.

[132] M. S. Mohy Eldin, M. Portaccio, N. Diano, S. Rossi, U. Bencivenga, A. D'Uva, P. Canciglia, F. S. Gaeta, D. G. Mita, Influence of the microenvironment on the activity of enzymes immobilized on Teflon membranes grafted by α-radiation, J. Mol. Catal. B: Enzym. 7 (1999) 251-261.

[133] M.R. Karim, F. Hashinaga, Preparation and properties of immobilized pummelo limonoid glycosyl transferase, Proc. Biochem. 38 (2002) 809-814.

[134] S. Rauf, A. Ihsan, K. Akhtar, M.A. Ghauri, M. Rahman, M.A. Anwar, A.M. Khalid, Glucose oxidase immobilization on a novel cellulose acetate polymethylmethacrylate membrane, J. Biotechnol. 121 (2006) 351-360.

[135] U. Hanefeld, L. Gardossi, E. Magner, Understanding enzyme immobilisation. Chem. Soc. Rev. 38 (2009) 453-468.

[136] V.C. Sabularse, M.T Tud, M.S. Lacsamana, J.L. Solivas, Black and white lahar as inorganic support for the immobilization of yeast invertase, ASEAN J. Sci. Technol. Dev. 22 (2005) 331-344.

[137] S.M. Kotwal, V. Shankar, Immobilized invertase, Biotechnol. Adv. 27 (2009) 311-322.

[138] K. Sangeetha, T.E. Abraham, Preparation and characterization of cross-linked enzyme aggregates (CLEA) of subtilisin for controlled release applications, Int. J. Biol. Macromol. 43 (2008) 314-319.

[139] S. Talekar, S. Waingade, V. Gaikwad, S. Patil, N. Nagavekar, Preparation and characterization of cross linked enzyme aggregates (CLEAs) of Bacillus amyloliquefaciens α-amylase, J. Biochem. Tech. 3 (2012) 349-353.

[140] S. Ates, E. Cortenlioglu, E. Bayraktar, U. Mehmetoglu, Production of I-DOPA using Cu - alginate gel immobilized tyrosinase in a batch and packed bed reactor, Enzyme Microb. Technol. 40 (2007) 683-687.

[141] G. Zotti, S. Zecchin, G. Schiavon, B. Vercelli, A. Berlin, S. Grimoldi, Poly (N- hexyl - cyclopenta [c] pyrrole) - a novel 1,3,4 - alkyl -substituted polypyrrole soluble in organic solvents and redox conducting", Macromol. Chem. Phys. 205 (2004) 2026-2031.

[142] J.W. Lee, F. Serna, J. Nickels, C.E. Schmidt, Carboxylic acid-functionalized conductive polypyrrole as a bioactive platform for cell adhesion, Biomacromolecules, 7 (2006) 1692-5.

[143] B. Sari, M. Talu, Electrochemical copolymerization of pyrrole and aniline, Synth.Met. 94 (1998) 221.

[144] N. Miletić, A. Nastasović, K. Loos, Immobilization of biocatalysts for enzymatic polymerizations: Possibilities, advantages, applications, Bioresour. Technol. 115 (2012) 126 - 135.

[145] F. Fusalba, D. Bélanger "Electropolymerization of polypyrrole and polyaniline-polypyrrole from organic acidic medium", J. Phys. Chem. B 103 (1999) 9044-9054.

[146] Y. Nakashimada, Synthesis and Characterization of Conducting Polymers for usein Protein Chromatography on a MEMS Fabricated Micro Open Parallel Plate Separators (μOPPS) A thesis submitted to the Division of Graduate Studies and Research of the University of Cincinnati 2005.

[147] S.S. Gursoy, A. Uygun (GOK), T. Tilki, Synthesis and Characterization of Some N-substituted Polypyrrole Derivatives: Towards Glucose Sensing Electrodes, J. Macromol. Sci. Part A Pure Appl. Chem. 47 (2010) 681-688.

[148] C.H. Cho, H.J. Choi, J.W. Kim, M.S. Jhon, Synthesis and electrorheology of aniline/pyrrole copolymer, J. Mater.Sci. 39 (2004) 1883 - 1885.

[149] J. Stejskal, M. Trchova, I. A. Ananieva, J. Janca, J. Prokes, S. Fedorova, I. Sapurina, Poly(aniline-co-pyrrole): powders, films, and colloids. Thermophoretic mobility of colloidal particles, Synth. Met. 146 (2004) 29-36.

[150] V.W.L. Lim, E.T. Kang, K.G. Neoh, Z.H. Ma, K.L. Tan, Determination of pyrrole-aniline copolymer compositions by X-ray photoelectron spectroscopy, Appl. Surf. Sci. 181 (2001) 317-326.

[151] J.S. Tang, X.B. Jing, B.C. Wang, F.S. Wang, Infrared-spectra of soluble polyaniline, Synth. Met. 24 (1988) 231-238.

[152] V.L. Colvin, M.C. Schlamp, A.P. Alivisatos,"Light-emitting diodes made from cadmium selenide nanocrystals and a semiconducting polymer." Nature 370 (1994) 354-357.

[153] M.V. Kulkami, A.K. Viswanath, U.P. Mulik, Studies on chemically synthesized organic acid doped poly(o-toluidine), Mater. Chem. Phys. 89 (2005) 1-5.

[154] B. Lu, J. Xu, C. Fan, F. Jiang, H. Miao, Facile electrosynthesis of nitro-group-substituted oligopyrene with bicolored emission, Electrochim. Acta 54 (2008) 334-340.

[155] A. Nan, I. Craciunescu, R. Turcu, D. Reichert, J. Liebscher, Synthesis and characterization of new functionalized pyrrole copolymers, J. Optoelectron. Adv. Mater. 10 (2008) 2265-2270.

[156] R. Bergamasco, F.J. Bassetti, F.F. de Moraes, G.M. Zanin, Characterization of free and immobilized invertase regarding activity and energy of activation, Braz. J. Chem. Eng. 17 (2000) 4-7.

[157] A.M. Klibanov Approaches to enzyme stabilization, Biochem. Soc. Trans. 11 (1983) 19-20.

[158] M.N. Gupta, Thermostabilization of proteins, Biotechnol. Appl. Biochem. 14 (1991) 1-11.

[159] N. Hasirci, S Aksoy, H. Tümtürk, Activation of poly (dimer acid-co-alkyl polyamine) particles for covalent immobilization of α-amylase, React. Funct. Polym. 66 (2006) 1546-1551.

[160] A.-C. Beyler, E. Çakmakçı, Ö. Danış, S. Demir, M.V. Kahraman, α-amylase Immobilization on Modified Polyimide Material, Chem. Eng. Trans. 32 (2013) 1687-1692.

[161] V. Mozhaev, Mechanism- based strategies for protein thermo-stabilization, Trends Biotechnol. 11 (1993) 88-95.

[162] J. Csapo, Cs. Albert, K. Loki, Zs. Csapo-Kiss, Separation and determination of the amino acids by ion exchange column chromatography applying post column derivatization, Acta Univ. Sapientiae, Alimentaria, 1 (2008) 5-29.

[163] M.V. Kahraman, G. Bayramoğlu, N. -A. Kayaman, A. Güngör , UV-Curable methacrylated/fumaric acid modified epoxy as a potential support for enzyme immobilization, React. Funct. Polym. 67 (2007) 1385-1392.

[164] T.P. Li, N. Wang, Q.C. Zhao, M. Guo, C.Y. Zhang, Optimization of covalent immobilization of pectinases on sodium alginate support, Biotechnol. Lett. 29 (2007) 1413-1416.

[165] M.Y. Arica, V. Hasirci, N.G. Alaeddinoglu, Covalent immobilisation of α-amylase onto pHEMA microspheres: preparation and application to fixed bed reactor, Biomat.16 (1995) 761-768.

[166] A.I. El-Batal, K.S. Atia, M. Eid, Stabilization of α-amylase by using anionic surfactant during the immobilization process, Rad. Phys. Chem. 74 (2005). 96-101.

[167] V. Singh, D. Singh, Diastase α-amylase immobilization on sol-gel derived guar gum - gelatin- silica nanohybrid, Adv. Mat. Lett. 5 (2014) 17-23.

[168] A. Tanriseven, Z. Olcer, A novel method for the immobilization of glucoamylase onto polyglutaraldehyde - activated gelatin, Biochem. Eng. J. 39 (2008) 430-434.

[169] P.H. Pandya, R.V. Jarsa, B.L. Newalkar, P.N. Bhalt, Studies on the activity and stability of immobilized α-amylase in ordered mesoporous silicas, Microporous Mesoporous Mater. 77 (2005) 67-77.

[170] Z. Konsoula, M.L. Kyriakides, Starch hydrolsis by the action of an entrapped in alginate capsules α-amylase from Bacillus subtilis, Process Biochem. 41 (2006) 343-349.

[171] U. Demircioglu, H. Beyenal, A. Tanyolac, N. Hasirci, Immobilization of urease and estimation of effective diffusion coefficients of urea in HEMA and VP copolymer matrices, Polym. Int. 35 (1994) 321-7.

[172] D. Gangadharan, K.M. Nampoothiri, S. Sivaramakrishnan, A. Pandey, Immobilized bacterial α-amylase for effective hydrolysis of raw and soluble starch, Food Res. Int. 42 (2009) 436-442.

[173] E. Edet, M. Ntekpe, S. Omereji, Current Trend in Enzyme Immobilization: A Review, Int. J. Mod. Biochem. 2 (2013) 31-49.

[174] M. Trevan, Effect of immobilization on enzyme activity. In: Immobilized Enzymes: An Introduction and Applications in Biotechnology, Trevan, M. (ed.). Wiley, Chichester, New York, (1980) 11-56.

[175] N. Tüzmen, T. Kalburcu, A Denizli. α-amylase immobilization onto dye attached magnetic beads: Optimization and characterization, J. Mol. Catal. B Enzym.78 (2012) 16-23.

[176] P. Singh, P. Gupta, R. Singh, R. Sharma, Activity and stability of immobilized α-amylase produced by Bacillus acidocaldarius, Int. J. of Pharm. & Life Sci. (IJPLS) 3 (2012) 2247-2253.

[177] T. Kaneko, T. Ohno, N. Ohisa, Purification and characterization of a thermostable raw starch digesting amylase from a Streptomyces sp. isolated in a milling factory, Biosci. Biotechnol. Biochem. 69 (2005) 1073-1081.

[178] T. Kobayashi, K.J. Laidler, Kinetic analysis for solid - supported enzymes, Biochim. Biophys. Acta 1 (1973) 302.

[179] W. Hartmeier, Immobilized Biocatalysts - an Introduction, (Trans. J. Wieser), Springer - Verlag, Berlin (1988).

[180] S. Dhingra, M. Khanna, C.S. Pundit, Immobilization of α-amylase onto alkyamine glass beads affixed inside a plastic beaker: Kinetic properties and application, Indian J. Chem.Technol. 13 (2006) 119-121.

[181] L. Cao, Immobilized enzymes: science or art?, Curr. Opin. Chem. Biol. 9 (2005) 217-226.

[182] C. Mateo, J.M. Palomo, G.-L. Fernández, R.-L. Fernandez, J.M. Guisán, Improvement of enzyme activity, stability and selectivity via immobilization techniques, Enzyme Microbial. Technol. 40 (2007) 1451-1463.

[183] D. Tanyolac, B. I. Yuruksoy, A. R. Ozdural, Immobilization of a thermostable α-amylase,Termamyl®, onto nitrocellulose membrane by cibacron blue F3GA dye binding, Biochem. Engg. J. 2 (1998) 179-186.

[184] R. Gangopadhyay, A. De, Conducting Polymer Nanocomposites: A Brief Overview, Chem. Mater.12 (2000) 608.

[185] A. Azioune, A.B. Slimane, L.A. Hamou, A. Pleuvy, M.M. Chehimi, C. Perruchot, S.P. Armes, Synthesis and Characterization of Active Ester-

Functionalized Polypyrrole-Silica Nanoparticles: Application to the Covalent Attachment of Proteins, Langmuir 20 (2004) 3350-3356.

[186] B. Saoudi, N. Jammul, M.M. Chehimi, G.P. McCarthy, S.P. Armes, Adsorption of DNA onto Polypyrrole-Silica Nanocomposites, J. Colloid Interface Sci. 192 (1997) 269-273.

[187] M.R. Pope, S.P. Armes, P.J. Tarcha, Specific activity of polypyrrole nanoparticulate immunoreagents: comparison of surface chemistry and immobilization options, Bioconjug Chem. 7 (1996) 436-44.

[188] Z. Sun, H. Tachikawa, Polypyrrole Film Electrode Incorporating Glucose oxidase, ACS Symposium Series, 487 (1992) 134-149.

[189] A.B. Smith, C.J. Knowles, Potential Role of a Conducting Polymer in Biochemistry - Protein Binding Properties, Biotechnol. Appl. Biochem. 12 (1990) 661-669.

[190] D.S. Minehan, K.A. Marx, S.K. Tripathy, Kinetics of DNA binding to electrically conducting polypyrrole films, Macromolecules. 27 (1994) 777-783.

[191] S. Kim, J. Jang, Heavy Metal Ion Removal of Mesoporous Polypyrrole, Appl. Chem. 9 (2005) 269-272.

[192] J.W. Goodwin, R.S. Harbron, P.A. Reynolds, Functionalization of colloidal silica and silica surfaces via silylation reactions, Colloid Polym. Sci. 268 (1990) 766-777.

[193] S. Maeda, S.P. Armes, Preparation of Novel Polypyrrole - Silica Colloidal Nanocomposites, J. Colloid Interface Sci. 159 (1993) 257-259.

[194] S. Maeda, S.P. Armes, Preparation and characterisation of novel polypyrrole-silica colloidal nanocomposites, J. Mater. Chem. 4 (1994) 935 - 942.

[195] M.I. Goller, C. Barthet, G.P. McCarthy, R. Corradi, B.P. Newby, S.A. Wilson, S.P. Armes, S.Y. Luk, Synthesis and characterization of surface-

aminated polypyrrole - silica nanocomposites, Colloid Polym. Sci. 276 (1998) 1010-1018.

[196] N.C. Foulds, C.R. Lowe, Immobilization of glucose oxidase in ferrocene-modified pyrrole polymers, Anal. Chem. 60 (1988) 2473-8.

[197] S. Maeda, R. Corradi, S.P. Armes, Synthesis and Characterization of Carboxylic Acid - Functionalized Polypyrrole-Silica Microparticles, Macromolecules 28 (1995) 2905-2911.

[198] V.K.S. Hsiao, J.R. Waldeisen, Y. Zheng, P.F. Lloyd, T.J. Bunning, T.J. Huang Aminopropyltriethoxysilane (APTES)-functionalized nanoporous polymeric gratings: fabrication and application in biosensing, J. Mater. Chem. 17 (2007) 4896-4901.

[199] R. Kostic´, D. Rakovic´, S.A. Stepanyan, I.E. Davidova, L.A. Gribov, Vibrational spectroscopy of polypyrrole, theoretical study, J. Chem. Phys. 102 (1995) 3104-3109.

[200] S. Aleti, H. Karaturi, C.V.S. Subrahmanyam, M. Lakshmi Narasu, Complexation and Characterization of α-amylase with Hydroxypropyl ß- Cyclodextrin, Int. J. Pharm. Phytopharmacol. Res. 1 (2012) 375-378. (Research Article).

[201] C. Perruchot, M.M. Chehimi, M. Delamar**,** F. Fievet**,** Use of Aminosilane Coupling Agent in the Synthesis of Conducting, Hybrid Polypyrrole-Silica Gel Particles. Surf. Interface Anal. 26 (1998) 689 - 698.

[202] T.V. Vernitskaya, O.N Efimov, Polypyrrole: a conducting polymer; its synthesis, properties and applications, Russ. Chem. Rev. 66 (1997) 443.

[203] M.I. Goller, C. Barthet, G.P. McCarthy, R. Corradi, B.P. Newby, S.A. Wilson, S.P. Armes, S.Y. Luk, Synthesis and characterization of surface-aminated polypyrrole **-** silica nanocomposites, Colloid Polym. Sci. 276 (1998) 1010 - 1018.

[204] T. Kalburcu, M.N. Tuzmen, S. Akgol, A. Denizli, Immobilized metal ion affinity nanospheres for α-amylase immobilization, Turk. J. Chem. 38 (2014) 28 - 40.

[205] G. Bayramoglu, M. Yilmaz, M.Y. Arica, Immobilization of thermostable α-amylase onto reactive membrane: Kinetics, Characaterization and application to continuous starch hydrolysis, Food Chem. 84 (2004) 591-599.

[206] M. Johnsson, M.J. Levine, G.H. Nancollas, Hydroxyapatite Binding Domains in Salivary Proteins, CROBM 4 (1993) 371.

[207] J.M. Gonzalez-Saiz, C. Pizarro, Polyacrylamide gels as support for enzyme immobilization by entrapment. Effect of polyelectrolyte carrier, pH and temperature on enzyme action and kinetics parameters, Eur. Polym. J. 37 (2001) 435 - 444.

[208] C. Mateo, J.M. Palomo, G.-L. Fernandez, J.M. Guisan, R.-L. Fernandez, Improvement of enzyme activity, stability and selectivity via immobilization techniques, Enzyme Microb. Technol. 40 (2007) 1451-1463.

[209] P.V. Iyer, L. Ananthanarayan, Enzyme stability and stabilization-Aqueous and non-aqueous environment, Process Biochem. 43 (2008) 1019-1032.

[210] D. Brady, J. Jordaan, Advances in enzyme immobilisation, Biotechnol. Lett. 31 (2009) 1639-1650.

[211] J. Ida, T. Matsuyama, H. Yamamoto, Immobilization of glucoamylase on ceramic membrane surfaces modified with a new method of treatment utilizing SPCP-CVD, Biochem Eng J. 5 (2000) 179-184.

[212] D. He, Y. Cai, W. Wei, L. Nie, S. Yao, α-amylase immobilized on bulk acoustic-wave sensor by UV-curing coating, Biochem. Eng. J. 6 (2000) 7-11.

[213] D. Tanyolac, B.I. Yuruksoy, A.R. Ozdural, Immobilization of a thermostable α-amylase, termamyl, onto nitrocellulose membrane by Cibacron Blue F3GA dye binding, Biochem. Eng. J. 2 **(**1998) 179-186.

[214] R. Reshmi, G. Sanjay, S. Sugunan, Enhanced activity and stability of α-amylase immobilized on alumina, Catalysis Commun. 7 (2006) 460-465.

[215] H. O'neill, C.V. Angley, I. Hemery, B.R. Evans, S. Dai, J. Woodward, Properties of carbohydrate-metabolizing enzymes immobilized in sol-gel beads:

Stabilization of invertase and β-glucosidase by Blue Dextran, Biotechnol. Lett. 24 (2002) 783-790.

[216] H. Lineweaver, D. Burk, The determination of enzyme dissociation constants, J. Am. Chem. Soc. 56 (1934) 658-666.

[217] E.E.F. Mobasher, Production and immobilization of α-amylase using biotechnology techniques for use in biological and medical applications, Thesis (M.Sc), 44 (2009) 127.

[218] B.A. Saville, M. Khavkine, S. Gayathri, B. Marandi, Z. Yong-Li, Characterization and performance of immobilized amylase and cellulose, Appl. Biochem. Biotechnol. 113 (2004) 251-259.

[219] A. Dwevedi, A.M. Kayastha, Optimal immobilization of *β*-galactosidase from Pea (*Ps*BGAL) onto Sephadex and chitosan beads using response surface methodology and its applications, Bioresour.Technol. 100 (2009) 2667-2675.

[220] Q.H. Fan, Y.M. Li, A.S.C. Chan, Recoverable catalysts for asymmetric organic synthesis, Chem. Rev.102 (2002) 3385-3466.

[221] R.K. Singh, Y.W. Zhang, N.P.T. Nguyen, M. Jeya, J.K. Lee, Covalent immobilization of β-1,4-glucosidase from Agaricus arvensisonto functionalized silicon oxide nanoparticles, Appl. Microbiol. Biotechnol. 89 (2011) 337-344.

[222] L.B. Luo, J.S. Jie, W.F. Zhang, Z.B. He, J.X. Wang, G.D. Yuan, W.J. Zhang, L. C.M. Wu, S.T. Lee, Silicon nanowire sensors for Hg^{2+} and Cd^{2+} ions. Appl. Phys. Lett. 94 (2009) 3.

[223] A.A. Yakovleva, Electrochemistry of Polypyrrole Films in Aqueous Solutions: The Character of the Bond between the Anion and the Polymer Matrix, Russ. J. Electrochem. 36 (2000) 1275-1282.

[224] H.N. Chang, G.H. Seong, I.K. Yoo, J.K. Park, J.H. Seo, Microencapsulation of recombinant Saccharomyces cerevisiae cells with invertase activity in liquid core alginate capsules. Biotechnol. Bioeng. 51 (1996) 157-162.

[225] R.S.S. Kumar, K.S. Vishwanath, S.A. Singh, A.G.A. Rao, Entrapment of α-amylase in alginate beads: Single step protocol for purification and thermal stabilization, Process Biochem. 41 (2006) 2282-2288.

[226] O. Prakash, N. Jaiswal, Immobilization of a thermostable α-amylase on Agarose and Agar Matrices and its Application in Starch Stain Removal, World Appl. Sci. J. 13 (2011) 572-577.

****

Chapter 4

Immobilization of Diastase α-amylase on to Natural Polymers

Contents

4.1 Relevance of Natural Polymers as support for Enzyme Immobilization.

During the past decade, increasing environmental awareness, new global agreements and international government policies and regulations have generated a renewed interest in the natural fibers. Natural fibers are now emerging as viable alternatives to synthetic fibers either alone or combined in composite materials for various applications.

In addition to their low density, availability and low cost, natural fibers are recyclable and biodegradable [1]. Besides, natural fibers being ecofriendly are expected to give less health problems for the people producing the composites. Natural fibers do not cause skin irritations. The abundance of natural fibers combined with the ease of their processability is an attractive feature, which makes it a covetable substitute for synthetic fibers that are potentially toxic [2].

In this respect, sugarcane bagasse and coconut fiber have already been used with promising results as supports in different bioprocesses [3,4]. Enzymes can be

immobilized on natural fibers in a variety of ways. These include adsorption, binding via complex formation on the surface of cellulose activated by coupling agents, via covalent binding through available functional groups on the surface etc.

In the case of natural fibers, presence of hydroxyl groups on the surface promotes anchoring of enzymes whose interactions can be still further enhanced by proper introduction of appropriate organic monomers or coupling reagents. Thus surface treatment of natural fibers is beneficial in order to promote interfacial adhesion and improve the water resistance.

In our study we have used diastase α-amylase enzyme as model enzyme and have selected adsorption method to immobilize the enzyme on sugarcane bagasse and coconut fibers. Both the fiber surfaces were modified with APTES and they have also been used as support of amylase immobilization.

4.2 Immobilization of Diastase α-amylase on coconut fibers

Coir is a natural fiber extracted from the husk surrounding the seed of a coconut. It thus comes under the classification of fruit fibers. Coir is a cellulosic waste product of coconut fruit and its cost is negligible. The seed is separated from the husk for the extraction of the oil-rich kernel for various food products such as fresh kernel, copra and desiccated coconut. The husk is thus a byproduct of copra or desiccated coconut.

Figure: 4.1 Coconut fibers

Some advantages of coir are that it is non-abrasive, stiff, resilient, hydroscopic, biodegradable, compostable, and a natural product amenable to chemical changes. It is thus an ecofriendly, durable, renewable and sustainable product [5].

4.2.1 Preparation of chemically modified coconut fibers

Fibers of coconut and sugarcane bagasse were selected for our study. They were obtained in the dried form and were purified before using as supports via the method followed by S. Varavinit et al. [6].

Pretreatments are usually carried out aiming to increase the affinity of the biocatalyst to the ligno-cellulosic materials [7]. The fibers were first washed with water till the supernatant were colourless. After that the coconut fibers were purified three times by boiling in 1.25% sulphuric acid and 1.25% sodium hydroxide followed by washing with distilled water for 1hour. Then these fibers were dried and cut into small pieces

Figure: 4.2 Photograph of coconut fiber cut into small pieces for using as support for enzyme immobilization

4.2.2 Coupling of natural fibers with APTES

Silane treatment was carried out as per the method reported by J. G. Gwon et al. [8]. For APTES functionalization, 5% APTES was hydrolyzed for 1hour in the ethanol solution

at a pH of 4.5 - 5, and then the fibers were immersed for 2 hours at room temperature for silane coupling. Then the fibers were filtered and dried at 80°C in the convection oven for 24 hours.

The coupling with APTES increases the hydrophobicity at the surface of coconut fibers. The low amount of APTES selected was an advantage because, it should also be noted that a highly hydrophobic surface may also have an adverse effect on the enzymatic performance of an immobilized enzyme as the active sites of the enzyme are believed to line up with hydrophobic residues, leading to blockage of the active sites by the support. In addition, the hydrophobic forces may also cause conformation changes of the enzyme. Nevertheless, when only a low amount of aminopropyl groups was on the surface of coconut fiber, such adverse effects can be ignored [39].

The reaction is represented as shown in the scheme 4.1.

Different cellulosic fibers of coconut have been established as enzyme carriers for amylase [9] and lipase [10]. Rintu Banerjee et al. immobilized α-amylase from *Bacillus circulans GRS 313* on coconut fiber via adsorption [11]. As reported by Brigida et al. green coconut fiber can be used as cheap immobilization support, and is compatible with *C. antarctica lipase,* rendering a biocatalyst with interesting properties that can be used in aqueous or organic media [10].

Coconut fiber without any pretreatment will be designated as BCF. Chemically treated coconut fiber will be designated as CCF, APTES functionalized coconut fiber will be designated as CFF, Enzyme immobilized coconut fibers will be designated as CCFE and CFFE.

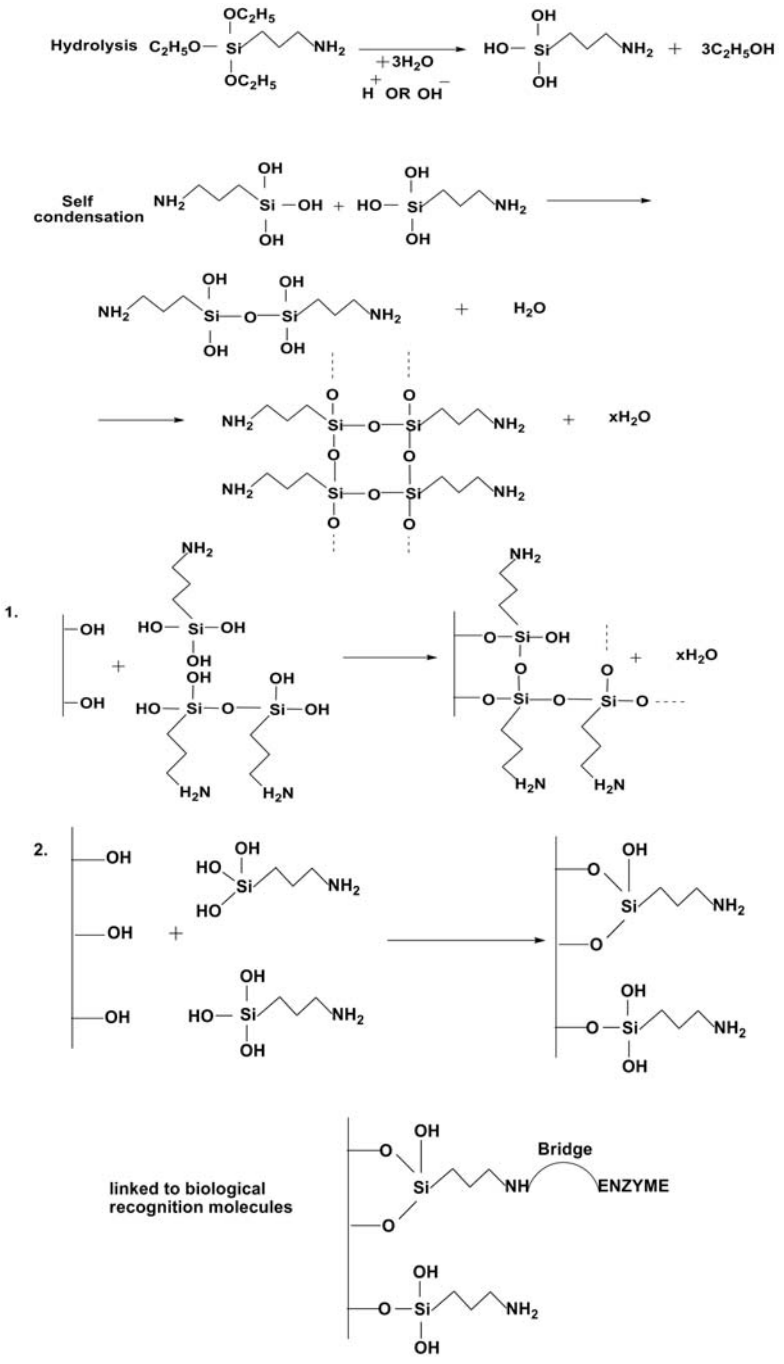

Scheme 4.1 Coupling of coconut fiber with APTES

4.2.3 Physico- chemical characterization

4.2.3.1 FT - IR Spectra of coconut fiber

Infra red spectroscopy is an inevitable tool for investigating the structure of constituents and the chemical changes in lignocellulosic materials after chemical treatment and subsequent functionalization [12]. Natural cellulosic fibers contain 60-95% cellulose. Hemicelluloses, lignin, pectin, waxes, and proteins are the remaining constituents, and their proportion depending on the conditions of growth, fiber source, and method of fiber extraction.

The absorption bands in the spectra are typical of lignocellulose materials, which are composed of cellulose, hemicelluloses and lignin [13]. Although the fibers possess the same constituents, these are present in different contents in each fiber and hence the shape of absorption bands also differs depending on the source of the fiber.

For the pure cellulose, peaks at 3390 cm^{-1} and shouldering around 3400 cm^{-1} to 3500 cm^{-1} indicates O-H stretching, 2800 cm^{-1} to 2925 cm^{-1} indicates C-H stretching, 1160 cm^{-1} indicates C-O-C stretching and 1035 cm^{-1} to 1060 cm^{-1} indicates C-O stretching. Other fingerprint regions for cellulose are peaks around 1300 cm^{-1} indicating C-H bending and around 1400 cm^{-1} indicating CH_2 bending [14]. As per Neo et al. peaks at 3423, 2921, 1625, 1379, 1054 and 896 cm^{-1} are all associated with cellulose.

The FTIR spectra of untreated and treated coconut fibers are shown in figure: 4.3. All these spectra reveal a broad and intense peak around 3392 cm^{-1} suggesting hydrogen-bonded (O-H) stretching vibration from the cellulose and lignin structure of the fiber.

FTIR analysis also reveals a reduction in hemicelluloses content in the fiber treated with NaOH (figure: 4.3). The broad and strong band ranging from

3000-3700 cm^{-1} indicates presence of -OH and -NH groups, which is consistent with the peaks at 1051cm^{-1} and 1164 cm^{-1} assigned to alcoholic C-O and C-N stretching vibration. The peaks at 2925 cm^{-1} can be assigned to asymmetric CH_2 groups.

The characteristic bands of hemicellulose, observed in the untreated coconut fiber around 1737 cm^{-1} [15] are not present in NaOH treated fibers [8]. This phenomenon has been verified by Rout et al. where NaOH is used in the treatment of fiber surfaces [16].

Between 1373 and 1421cm^{-1}, the absorption peak refers to a symmetrical and an asymmetrical deformation of C-H in cellulose and hemicelluloses groups. In spectra of fibers treated with NaOH, these bands are more accentuated, which can be an indicative of a larger exposition of cellulose and hemicelluloses on the fiber surface.

The band at 1267 cm^{-1} is related to the vibration (C-O) of esters, ethers and phenols groups attributed mainly to a presence of waxes in the epidermal tissue [17], and the disappearance of this band in the treated fibers results from the removal of those waxes.

The absorption intensity of CH angular deformation at 1260 cm^{-1} diminished significantly in the mercerized coconut fiber spectrum. These changes indicate the partial removal of lignin and hemicelluloses from the fiber surfaces.

A shoulder band at 1105 cm^{-1} was assigned to glucose ring structure of cellulose and aromatic C-H in plane deformation of lignin. Other characteristic bands include a band at 898 cm^{-1} due to glucose ring structure and C-H deformation of hemicelluloses and cellulose, C-H out of plane deformations of lignin at 852 cm^{-1} and 771 cm^{-1} [18].

Figure: 4.3 shows the gradual increase in peak height for the wave number at 3392 cm^{-1} assigned as NH_2 stretching vibration, at 2921 cm^{-1} assigned as

CH_2 stretching vibration [19] at 1224 cm^{-1} assigned as Si-O-C band, and 1118 cm^{-1} assigned as NH bending vibration with the APTES coupling reaction. Treatments of coconut fibers with APTES also showed peak changes, at 763 cm^{-1} assigned as Si-C symmetric stretching bond, at 700 cm^{-1} assigned as Si-O-Si symmetric stretching [20], and at 466 cm^{-1} assigned as Si-O-C asymmetric bending [21].

After immobilization all the bands get broadened. The peaks characteristic to that of α-amylase was present in the spectra of enzyme immobilized samples. The major peaks are at 1596 cm^{-1} (N-H bending), at 1656 cm^{-1} C=O stretching, at 1646 cm^{-1} a strong band characteristic to that of [asymmetrical $(C-O)_2$ stretch], 1398 cm^{-1} [symmetrical $(C-O)_2$ stretch], and at 1319 cm^{-1} characteristic of the asymmetrical $(-NH_3)^+$ N-H band.

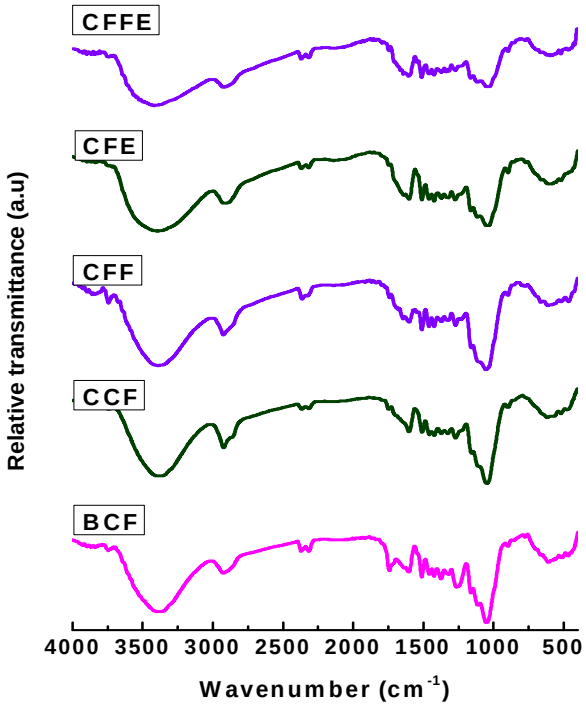

Figure: 4.3 FT-IR spectrum of coconut fiber before and after chemical modifications and immobilization

Table 4.1 Peak assignments for coconut fiber and its modified forms before and after immobilization (HC-Hemicellulose, L-Lignin, C-Cellulose)

Peak assignments (cm^{-1})	BCF	CCF	CFF	CFE	CFFE
C=O str of HC and L	1742s	-	-	-	-
C=C arom. skeletal vibr. of L	1510vs	1510vvw	1510w	1510w	1509
C=C arom. skeletal vibr. of L; C-H def.(HC,L)	1457m	1457vvw	1457vvw	1457	1456
C-H def .of HC,C and L	1368m	1366vvw	1366vvw	1366vvw	1366vvw
C-O str.of HC and L	1262bs	1267m	1267w	1267	1266
C-O-C asymmetric str.of HC,C and L	1161vw	1155vvw	1161	1161	1160
Glucose ring str (C), arom.C-H in plane def.(L)	1114	1108	1103	1119	1118
C-O str.(HC,L)	1050s	1050m	1050m	1050	1044
Glucose ring str., C-H def(HC,C)	897w	897s	897s	897s	897s
C-H out of plane def.(L)	849s	849w	849w	849w	849w

4.2.3.2 Thermogram of coconut fibers

The thermogravimetric analysis of coconut fibers before and after chemical treatment and functionalization and also after immobilization has been carried out.

From the results obtained it can be seen that decomposition profiles of the fibers are characterized by three peaks.

The first one is attributed to evaporation of water and occurs between room temperature and 180°C. The second step starts at about 190°C and corresponds to hemicelluloses degradation. The third step occurs between 300 and 375°C and indicates thermal degradation of cellulose.

Lignin degradation occurs over a broad range of 290-600°C. After the chemical pretreatment using acid and alkali, there was a significant effect on the thermal degradation behaviour of fibers. Thus there was an increase in the degradation temperature which might be due to removal of some easily hydrolyzed substances such as water soluble impurities, waxes and hemicelluloses that decompose earlier than the major components like lignin and cellulose and hence leading to a high thermal stability at second as well as third stage of treated coir [18].

Similar increase in thermal stability after pretreatments has been reported by other authors [18,22]. According to Varma et al. as a result of surface treatment partial removal of lignin and hemicelluloses helps to increase the amount of cellulose exposed and thus increases accessible surface area [23].

From the TG curves the removal of significant amount of hemicelluloses after the pretreatment with acid and alkali was confirmed by the disappearance of inflection that was present in the untreated fiber.

In the case of functionalized fiber strong peak at 355°C with additional weight loss and an additional small peak showing weight loss at 293°C was noticed which could be due to the decomposition of attached functional groups.

The coconut fibers both chemically treated and functionalized fibers after immobilization showed additional weight loss peaks which extend over a wide range of temperature. There was also a decrease in degradation temperature where the maximum decomposition occurs, which also gives an indication about the presence of immobilized enzymes on these fibers. The decrease in temperature might be due to degradation of enzyme's delicate organic structural backbone at lower temperature. The results are summarized in the table 4.2.

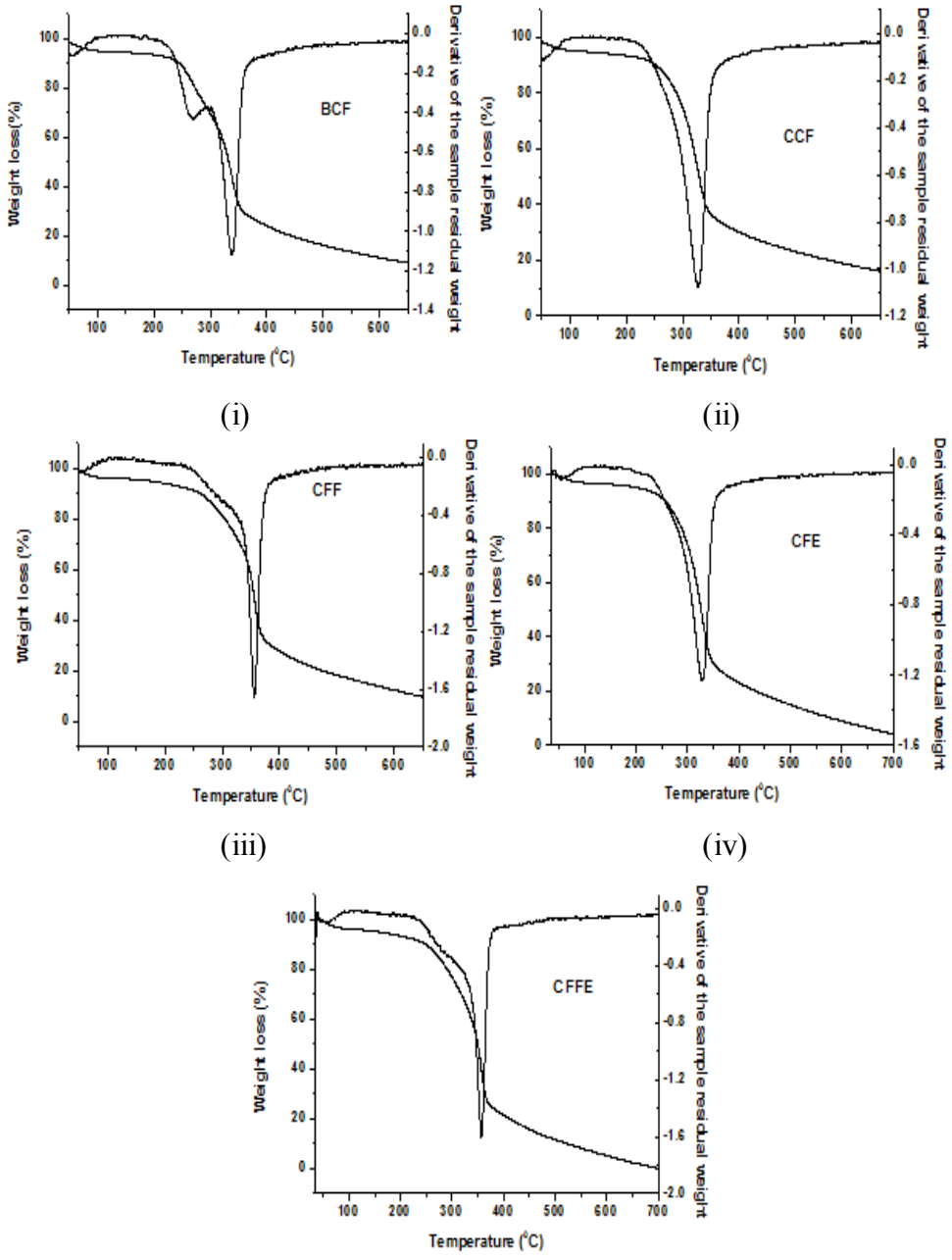

Figure: 4.4 TG -DTG curves for (i) BCF (ii) CCF (iii) CFF (iv) CFE (v) CFFE

Table 4.2 Thermogravimetric results of coconut fibers subjected to different treatment

Coconut fiber	Transition temperature range (°C)	Maximum degradation Temperature (°C)	Weight loss at a given temperature range
BCF	30-180	52	5
	180-300	268	28
	300-375	337	40
	375-600	398	16
CCF	30-180	51	5.5
	180-369	328	61
	369-500	406	4
CFF	30-180	54	5
	180-332	293	24.6
	332-400	355	42.4
	400-600	426	14.7
CFE	30-180	51	5
	180-367	326	68
	367-600	394	18
CFFE	30-180	52	5.5
	180-320	283	25
	320-392	354	45
	392-600	428	17

4.2.3.3 X-ray diffraction study for natural fibers

The sample crystallinity of fibers before and after pre-treatment and after immobilization of enzymes was determined by X-ray diffractometry measurements. The crystallinity index (CI) for all the samples was calculated

according to the procedure proposed by R. Ibbett and co-workers [24]. The apparent crystallinity (%) is calculated from the ratio of the area of all crystalline peaks to the total area including non-crystalline fraction following the equation:

$$C = 100 \bullet \frac{I_{cr\,peak1} + I_{cr\,peak\ 3} + I_{cr\,peak\ 4}}{I_{cr\,peak1} + I_{cr\,peak\ 3} + I_{cr\,peak\ 4} + I_{non\text{-}cr}} \quad [\%]$$

Scheme 4.2: Equation for calculating crystallinity

where: *C* is apparent crystallinity [%], *Icrpeak1* represents the area under the first crystalline peak in the diffraction pattern corresponding to the Miller index 110, *Icr peak 3* and *Icr peak 4* stand for the two areas under the second deconvoluted crystalline peak corresponding to the Miller index 110 and *I non-cr* is the area under the noncrystalline peak of the cellulose diffraction.

The spectrum corresponding to untreated coconut fiber showed maximum diffraction peak at the 2θ angle of 22.49 for untreated fiber (BCF). The same peak of chemically treated fibers was observed at 22.9 and for functionalized fibers at 22.7. After immobilization on to chemically treated fiber and functionalized fiber maximum diffraction peak were observed at 22.48 and 23.1 respectively. The results are tabulated in table 4.3 and are depicted in figure: 4.5.

The superposition of the X-ray diagrams shows that the signal characteristics of fibers with different treatments were almost similar. However chemically treated fiber and APTES functionalized fiber were more intense than untreated fibers' peaks, which means that both treatments were able to expose the cellulose which had the characteristic crystalline structure of native cellulose.

In the case of chemically treated fiber, first acid treatment hydrolyze part of hemicelluloses whereas further alkali treatment lead to the disruption of lignocellulosic cell wall by dissolving rest of hemicelluloses, lignin and silica by hydrolyzing uronic and acetic acid esters. The increase in crystallinity at lower concentration of NaOH is

explained by the fact that hydroxide ions was able to get fully hydrated and hence unable to penetrate and disrupt the cellulose lattice due to size restriction. Thus only the amorphous parts which include, lignin, pectin, waxes and hemicelluloses can react with alkali and can be removed. This makes inter fibrillar region less dense and less rigid and thereby make cellulose fibers capable of rearranging themselves resulting in increase in crystallinity index of the treated fiber [25,26].

Whereas the increase in crystallinity after APTES treatment was observed because cellulose support could maintain the crystalline structure of cellulose I as amino groups were introduced selectively to the crystal surface of cellulose fibers.

Table 4.3: (i) Diffraction peaks at various angles for modified and unmodified coconut fiber (ii) Crystallinity index of the coconut fibers before and after modifications and immobilization

	BCF	CCF	CFF	CFE	CFFE
2θ(degree)	22.49	22.9	22.7	22.48	23.1

(i)

	BCF	CCF	CFF	CFE	CFFE
CI	31.5	57.17	51	30.76	40.59

(ii)

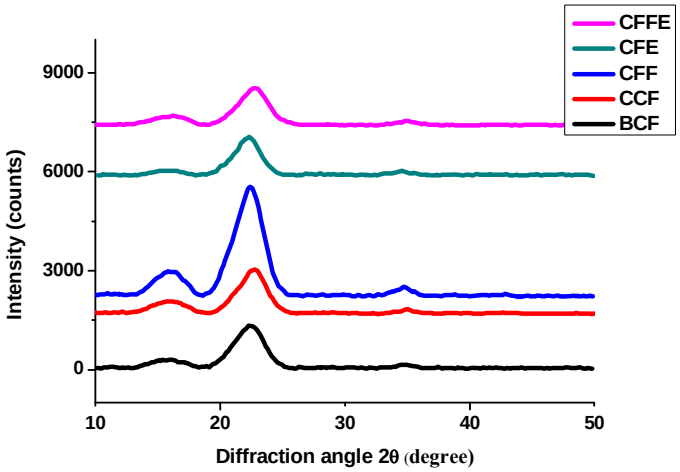

Figure: 4.5 XRD of untreated, treated and immobilized coconut fibers

4.2.3.4 Energy Dispersive X-ray spectroscopy

Elemental data obtained from Energy Dispersive X-ray analysis was carried out in order to confirm the functionalization of coconut fibers. The higher Carbon and Silicon content in the modified fibers compared to unmodified fibers is a direct evidence for organo silane modification on the fibers. The results are given in table 4.4.

Table: 4.4 (i) Elemental data for untreated coconut fiber (ii) Elemental data for coconut fiber after coupling with APTES

Element	(keV)	Mass%	Atom%
C K	0.277	83.17	86.81
O K	0.525	16.83	13.19
Si	-	-	-

(i)

Element	(keV)	Mass%	Atom%
C K	0.277	81.6	86.16
O K	0.525	16.21	12.85
Si	1.739	2.2	0.99

(ii)

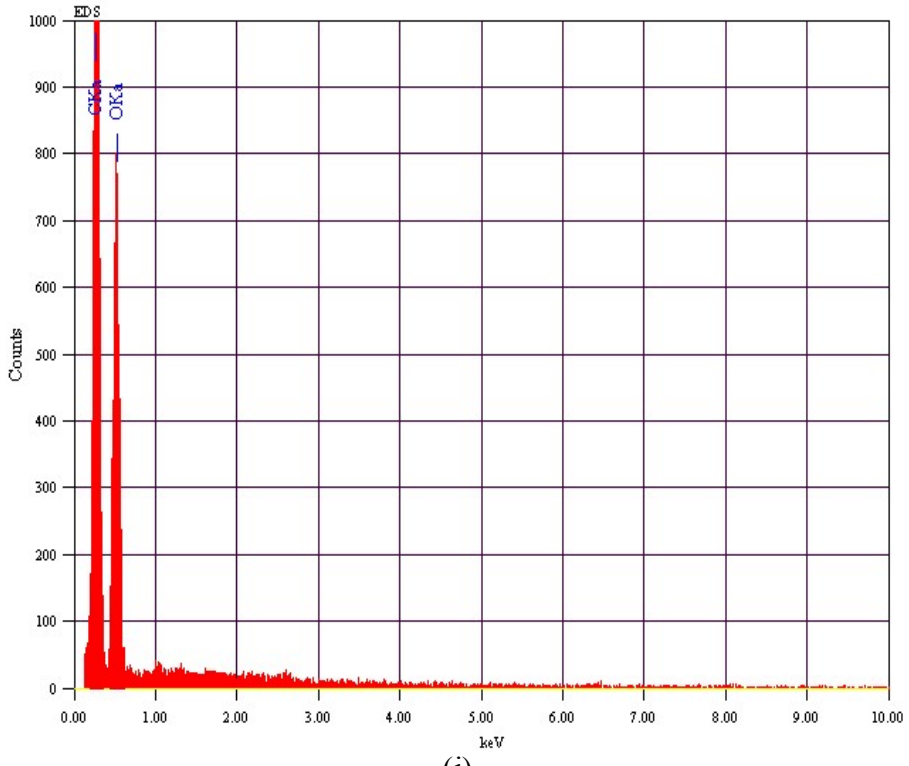

(i)

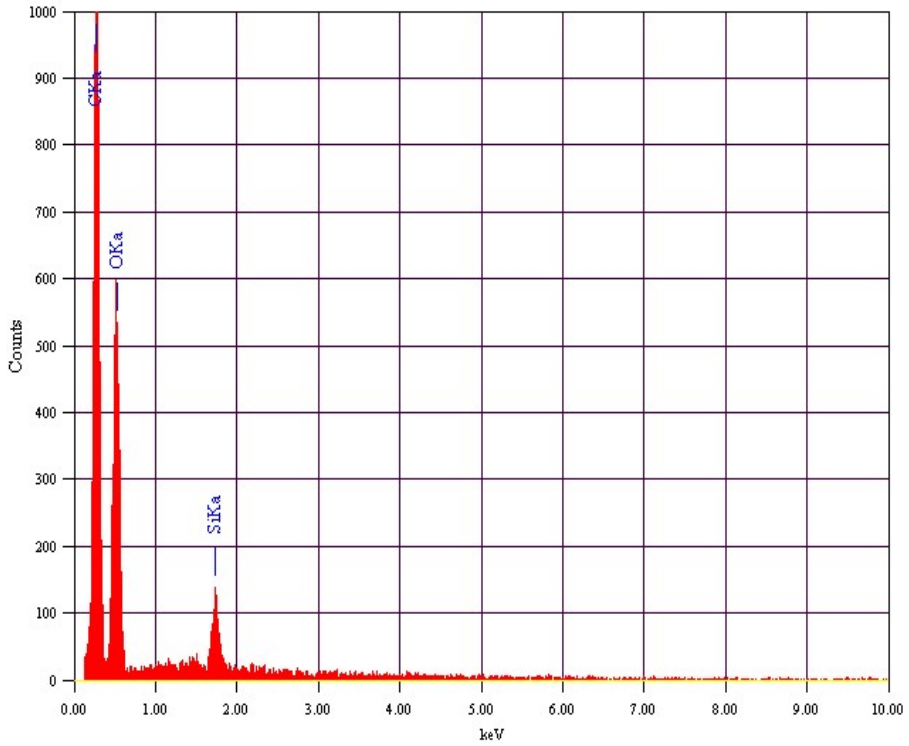

(ii)

Figure: 4.6 (i) EDS spectrum for untreated coconut fiber (ii) EDS spectrum for coconut fiber after coupling with APTES.

4.2.3.5 Scanning electron microscopy

The surface morphology of both fibers before and after chemical treatment and functionalization with APTES was investigated. SEM is a powerful and effortless technique to image the fibers in micrometer scale. The SEM micrographs of untreated fiber indicates that coconut fiber surface was covered with a layer of substances such as oils, waxes and extractives, part of the natural constitution of lignocellulosic fibers. Similar observation is reported by Huang Gu in the analysis of the tensile behavior of brown coir fiber [27].

In the untreated coconut fiber the globular protrusions seen are fatty deposits called tyloses [16]. These are arranged in regular intervals. Their presence was observed by other authors too [22,28,29].

Finally after chemical treatment most of these deposits were removed which revealed on the fiber surface empty cavities. Thus the effective surface area and roughness increases. Circular holes called pits were not revealed on the surfaces of untreated fibers [18] (Fig. 1a) and they were partly revealed on the surfaces of washed fibers.

After alkali treatment the SEM images obtained were shown in the figures. They all showed a rough surface, which is the consequence of the alkali treatment, as a result of which extractives, waxes and oil from fiber surface get removed.

Thus in effect cellulose parts of the fiber get exposed after chemical treatment. This favours the possibility of attaching functional groups to cellulose. Similar results were reported by other authors [16,22,30,31]. However surface topography of APTES treated fibers appeared to be smooth. This could be due to the fact that APTES aggregates are formed on the fiber surface which have a tendency to spread over the surface and thus increasing the support hydrophobicity and rigidity.

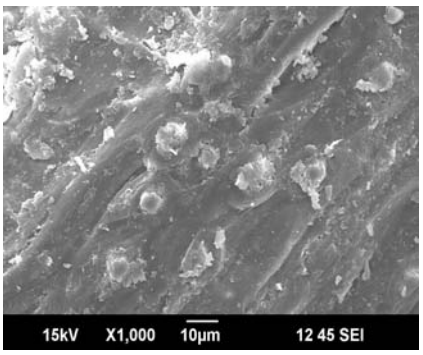

(ia)

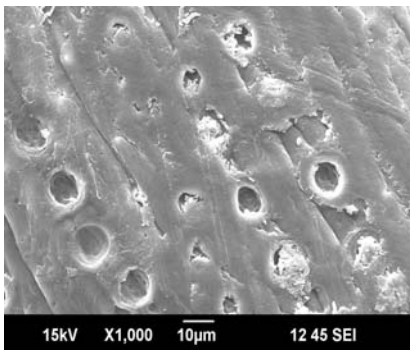

(iib)

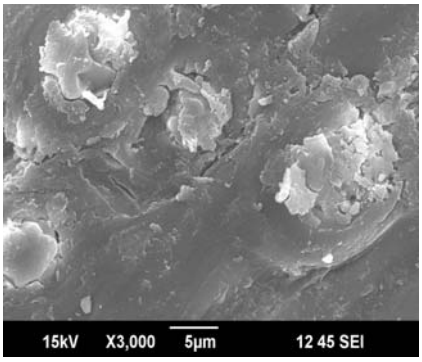

(ic)

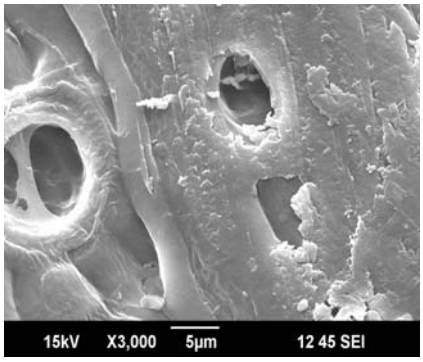

(iid)

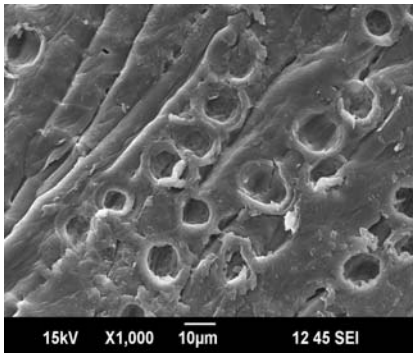

(iii)

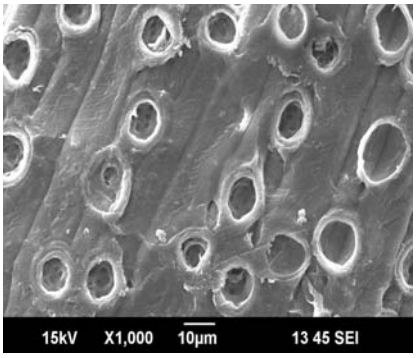

(iv)

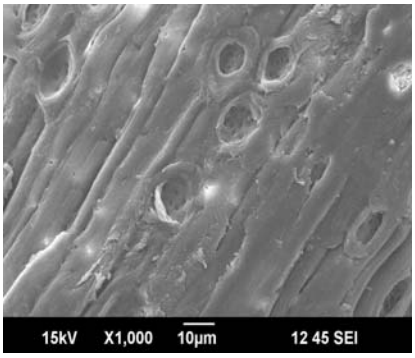

(v)

Figure: 4.7 SEM images of coconut fibers before and after modifications (ia), (ic): before pretreatment (iib), (iid) after pretreatment with H_2SO_4 and NaOH (iii) after functionalization with APTES (iv) after immobilization of enzyme on pretreated coconut fiber (v) after immobilization of enzyme on functionalized fiber.

4.2.4 Biochemical characterization

4.2.4.1 Influence of pH during immobilization of α-amylase on coconut fibers

Formation of chemical bridge between the amylase and the coconut fibers occurs via hydrogen bonding, hydrophobic interactions, electrostatic interactions all of which are decided by the charge present on the support and enzyme which is again affected by pH of the surrounding medium. Hence optimization of immobilization pH has to be carried out with utmost care so that enzyme support interaction is properly designed.

The pI of the enzyme can be an important parameter to determine its adsorption on the support materials [32,33]. Here, bare coconut fiber has the isoelectric point supposed to be 4.76 [34] whereas, diastase α-amylase has the isoelectric point around 4.6. Also, coconut fiber functionalized with APTES will have positive charge at acidic pH due to the presence of protonated $-NH_2$ groups and negative charge at alkaline pH due to more $-NH_2$ groups. Similar results are reported by Y. Zhao et al. and according to them after silane treatment, the aminosilane introduced amino groups which shift the isoelectric point (where zeta potential is 0) towards the alkaline range, at low pH the zeta potential was positive due to the protonation of the amino groups [40].

At pH 3 amylase, CCF and CFF are positively charged and hence electrostatic interaction is repulsive resulting in lesser rate of adsorption of enzyme and hence lesser activity.

At pH 4 amylase and coconut fibers have no appreciable charge as this is close to their isoelectric points. Hence even if no much electrostatic interaction occurs here, the major driving force that promotes adsorption at this pH is via

hydrophobic interaction which dominated over electrostatic interaction. Compared to CFF, amylase adsorption was faster on CCF at this pH which might be due to difference in amylase conformational changes with respect to both surfaces.

At pH 5 also no appreciable charge present on CCF and CFF and amylase and hence enzyme uptake would be based on hydrophobic interaction. The APTES functionalized sample showed a significant faster adsorption rate and a high adsorption capacity than bare coconut fiber. This is due to increase in hydrophobicity of APTES functionalized sample compared to bare sample and enzyme tends to have high affinity to a hydrophobic surface as indicated by the enzyme uptake in a very short amount of time.

For CCF optimum activity was observed at pH 5 whereas CFF showed more activity at pH 6 which can be explained in terms of the presence of more positively charged $-NH_2$ groups that cause electrostatic attraction between negatively charged amylase and positively charged CFF. The shift of pH towards alkaline region was also reported by Samanta et al. [4], while immobilizing bacterial α-amylase on coconut coir. Whereas no change in optimum pH was observed in the case of commercial α-amylase (*Bacillus sp*) immobilized onto pHEMA microspheres and to a composite temperature sensitive membrane, respectively [35,36].

At pH 7 electrostatic interactions gets lowered due to presence of like charges on the supports and the enzyme which correspondingly cause decline in activity due to low enzyme uptake by the supports. Among CCF and CFF, adsorption rate and hence activity was found to be again more for CFF which might be based on its hydrophobic surface.

At pH 8 a free enzyme is not at all stable but after immobilization the immobilized enzyme had a higher stability at alkaline pH. This is because the procedure of enzyme immobilization on these insoluble supports has a variety of effects on protein conformation as well as on the state of ionization and dissociation of the enzyme and its environment [37]. The stabilization depends on the position of the support attachment to the protein molecule. In general, unfolding of soluble proteins is initiated at their most labile site. The stabilization is most successful when this unfolding region is strengthened through immobilization [38]. The results are depicted in the figure: 4.8.

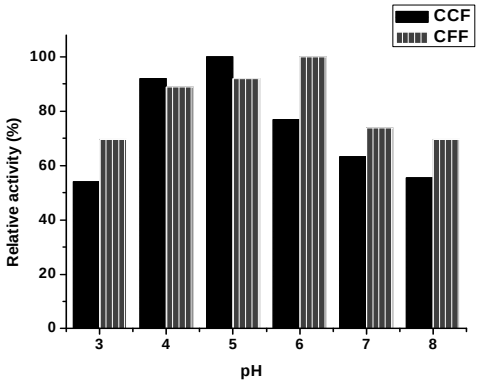

Figure: 4.8 Effect of immobilization pH on the relative activity of α-amylase

4.2.4.1.1 Effect of contact time on relative activity of immobilized enzyme

The contact time needed for maximum adsorption was evaluated at different time intervals (1, 2, 3, 4, 5 and 6 hours) for each supports. These results are shown in figure: 4.9. It can be observed that for CFF the maximum measured activity of the immobilized enzyme was achieved after 2 hours of contact time, whereas, for CCF optimum activity was seen after 4 hours of contact time. For higher contact times, no improvement on activity was observed; on the contrary, the activity decreases with the increase of contact time, probably due to the

increase of enzyme uptake which results in multilayer adsorption, and subsequent reduction in the available active site for the substrate molecules.

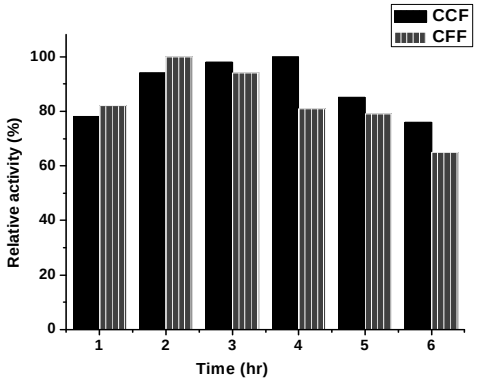

Figure: 4.9 Effect of contact time of enzyme with supports on the relative activity of α-amylase.

4.2.4.1.2 Effect of initial protein concentration on the protein loading

The amount of protein bound to coconut fibers were analyzed based on the optimized conditions obtained and is shown in the figure: 4.10. From the figure it is clear that both CCF and CFF follow a different trend in activity.

Higher loading and higher activity was shown by CFF compared to bare CCF. This can be due to following facts.

The coconut fibers are cellulosic materials rich in surface hydroxyl groups. The physical forces existing between the amylase and the bare coconut fiber are the result of interaction between amino and carboxyl groups on the enzyme with hydroxyl groups of cellulose via hydrogen bonding.

Surface modification of coconut fibers with organo silane provided more hydrophobicity to the support CFF which could thus enhance the interactions with enzymes more strongly than bare CCF. This is because in comparison with the

hydrophobic interactions and electrostatic interactions, hydrogen bonding is weaker, and this has resulted in a slower adsorption rate of α-amylase on CCF.

Thus when the initial enzyme concentration was 2.1 mg protein load on CCF was 0.43 mg and on CFF was 0.61 mg. When initial protein concentration was 5.2 mg enzyme loading on CCF raised to 0.79 mg and on CFF raised to 1.62 mg. At the initial protein concentration of 10.9 mg CCF attained protein loading of 1.95 mg and CFF attained its maximum protein loading of 2.6 mg. With further increase in initial enzyme concentration as 14.5, 17.2 and 22.24 mg, protein loadings on CCF were 2.26, 2.59 and 2.64 mg per gram of support respectively, whereas, for CFF it was 1.4, 0.94, 1.21 mg respectively.

Thus for CCF after a particular concentration enzyme uptake remained constant which might be due to the reason that support get saturated with enzyme within its available surface.

In the case of CFF further increase of concentration after the optimum caused decrease in protein loading which might be due to desorption of enzyme due to weak bonding as result of multilayer adsorption.

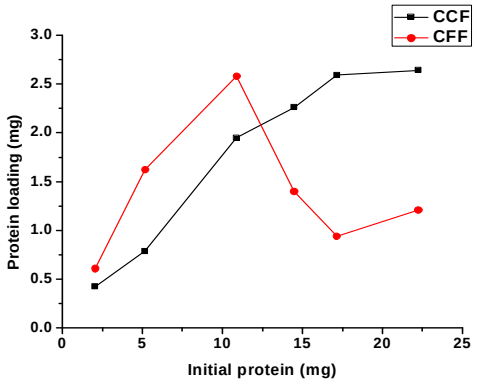

Figure: 4.10: Effect of initial protein concentration on the protein loading

4.2.4.1.3 Effect of initial protein concentration on immobilization yield and activity of immobilized α-amylase

Immobilization yield obtained for all adsorbents at various concentration taken are shown in the figure: 4.11.

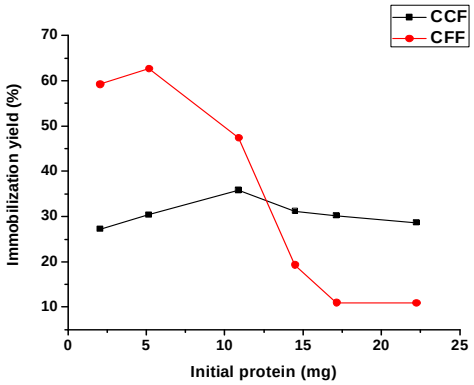

Figure: 4.11: Effect of initial protein concentration on immobilization yield of α-amylase

For CCF optimum immobilization yield was 36% and for CFF it was 47% when 10.9 mg of initial protein was added.

When immobilized enzyme activity of CCF was analyzed we found that optimum activity was not obtained at the concentration in which the optimum immobilization yield was obtained and the results were as follows:

At initial enzyme concentration of 2, 5, 11, 14, 17 and 22 mg immobilized enzyme activities obtained were 0.95, 1.28, 1.74, 2.83, 2.95 and 2.89 EU respectively. The optimum activity was at the initial concentration of 17 mg, whereas, the optimum immobilization yield was at the initial enzyme concentration of 10 mg. This might be due to the fact that in order for the enzyme to exert the optimum activity proper orientation of its native conformation after immobilization should be maintained so that maximum active sites are available for the substrate molecules to react. But, as the enzyme loading increases enzyme get adsorbed on

multi-layers, which thus hide many of the active sites of enzyme molecules underlying the superficial level. Hence, even if we obtained a maximum loading of enzyme, activity was not much increased; instead it remained constant or else decreased. So, for further analysis to be continued this concentration at which optimum activity was obtained was selected as the optimum concentration.

Similar criteria were followed by CFF also whose activities at different initial concentrations were 1.45, 2.65, 4.2, 4.64, 4.8 and 4.5 EU respectively. Here also even if optimum immobilization yield was at 5mg optimum activity was at 17mg. But the activities were almost constant in the range of 14-22 mg initial concentrations. The results of variation in immobilized enzyme activity with increase in concentration for CCF and CFF is given below in figure: 4.12.

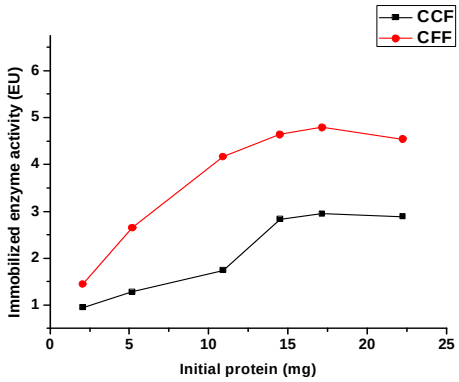

Figure: 4.12: Effect of initial protein concentration on immobilized α-amylase activity

The activity yield and immobilization efficiency were also evaluated. The results are tabulated in the table 4.5.

Table 4.5 Immobilization efficiency of α-amylase on untreated and treated coconut fibers

Polymer	Initial protein (mg)	Immobilized protein mg/g support	Immobilization yield (%)IY	Initial activity(EU)	Immobilized enzyme activity EU	Activity Yield (%)AY	Immobilization efficiency (%) IE=AY/IY
CCF	10.9	1.95	36	7.7	1.74	23	64
CFF	10.9	2.58	47	12.5	4.17	34	71

4.2.4.2 Effect of pH on enzyme activity

The activity profile for CCFE and CFFE obtained is shown below in figure: 4.13.

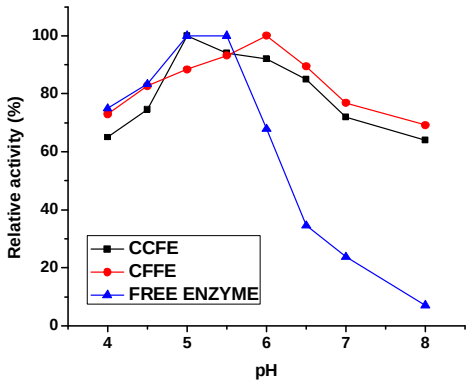

Figure: 4.13 Effect of pH on the relative activity of free and immobilized α-amylase

The graph clearly depicts the enhanced activity after surface modification by APTES compared with CCFE. The high activity for CFFE also indicates that the enzyme immobilized on this material maintained a stable conformation structure, a flexible mobility of the active sites, negligible blocking effect of the active sites, and a high accessibility of the active sites to the substrate. In addition to this, such an improved enzymatic performance can be explained as due to the enhanced surface hydrophobicity because of the presence of amino propyl groups, which induced a higher affinity of the substrate to the immobilized enzyme

For CFFE better activity was obtained over a broader pH ranging between pH 4.5 - 6.5. But optimum activity was obtained at pH 6. Usually, carriers with negative surface charges exhibit an apparent pH optimum higher than that observed with the free enzyme [41], suggesting that the coconut fiber may have negative surface charges at this pH.

In the case of CCFE better activity was in the range 5 - 6.5. The optimum activity was at pH 5.

4.2.4.3 Effect of temperature on the activity

The data for relative activity of enzyme versus temperature for CCFE and CFFE are shown in figure: 4.14. It was found that the optimum temperature for both the free and the immobilized enzyme was 50-55°C. But the activity retained by immobilized enzyme in the range of 55-70°C was about 85 - 44% for CCFE and 90 - 67% for CFFE, whereas, free enzyme retained only about 78 - 15%.

The slow rate of inactivation at elevated temperature can be explained by alterations of the physical and chemical properties of the enzyme upon immobilization. Immobilization on to these supports might also reduce the conformational flexibility of the enzyme and make it more stable against temperature changes.

Diffusion of substrate to the immobilized enzyme increases as the temperature increases, and formation of enzyme-substrate complex easily occurs. But further increase of temperature may cause inactivation of the enzyme and hence shows reduction in activity. After the temperature that the maximum activity was observed, there is a slight decrease in activity based on the denaturation of the molecular structure and the catalytic center of enzyme.

Similar results were obtained when thermostable α-amylase was immobilized on cellulose fibers from bagasse oxidized by periodic acid [42]. Dey et al. reported that after optimization, the adsorbed amylase from *B. circulans* GRS 313 had an optimum temperature same as that of free enzyme (48°C) [9]. C.J. Tien et al. reported optimum temperature of 40°C when amylase was adsorbed on zirconium dynamic membrane [35].

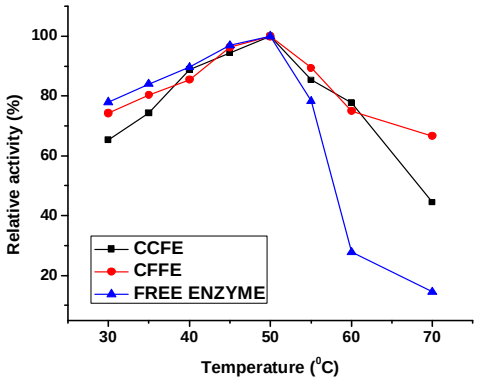

Figure: 4.14: Effect of temperature on relative activity of free and immobilized α-amylase.

4.2.4.4 Thermal stability of the free and immobilized enzymes

Thermal stabilities of soluble and immobilized α-amylase were studied at different temperatures. The activity retained by the soluble and immobilized enzyme at 30°C was considered as optimum and activity at other temperatures are represented relative to the activity at 30°C. It was observed that thermal stability of the immobilized enzymes was much better than that of soluble enzyme at 40-70°C.

Thermal stability after immobilization was higher for CFFE than CCFE. At 40°C, the soluble enzyme retained 81% of its activity after 60 minutes, whereas, the CCFE retained 85% of its activity and CFFE 92% of its initial activity under identical conditions.

At 50°C free enzyme retained 38% of its initial activity, whereas, CCFE retained 53% and CFFE retained 62% of their initial activity under identical conditions.

At 60°C both CCFE and CFFE retained 50% of their initial activity, whereas, free enzyme could retain only 11% of its original activity. The CCFE and CFFE retained 33% and 46% of its initial activity respectively at 70°C. But free enzyme lost almost all its activity at this temperature.

The results of thermal stability studies showed that adsorption of α-amylase on coconut fibers improved thermal stability of this enzyme. The increase of thermal stability after immobilization can be explained by the immobilization of the enzyme on coconut fibers which are supposed to preserve the tertiary structure of the enzyme from conformational changes caused by the environment, resulting in its enhanced activity and stability.

Arica et al. [43] speculated that hydrophobic interactions and other secondary interactions of the immobilized enzyme might impair conformational flexibility necessitating higher temperatures for the enzyme molecules to reorganize and attain a proper conformation for its functioning and binding of the substrate. The results obtained are shown below in figure: 4.15.

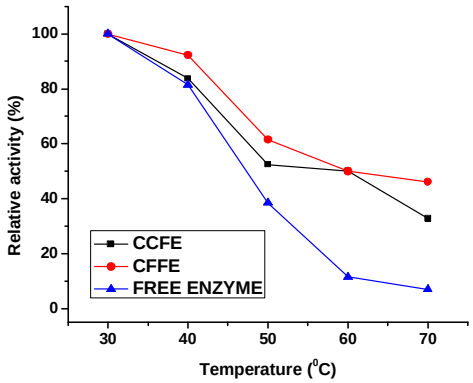

Figure: 4.15: Thermal stability of free and immobilized α-amylase

When kept for 20 minutes CCFE retained 92%, CFFE 99% of its initial activity, whereas, free enzyme could retain only 78% of its initial activity. Pre-incubating for 40 minutes yields 83% of initial activity for CCFE and 89% for CFFE, whereas, free enzyme could yield only 62% of its initial activity. After 60 minutes activity retained by CCFE was 75% and that by CFFE was 86%, whereas free amylase retained only 35% at same time period of incubation.

Finally, when thermal treatment of 80 minutes was applied 57% was the activity remained for CCFE while 82% of initial activity was still shown by CFFE underlining its ability in withstanding denaturation during long duration of thermal treatment. This might be acquired via surface modification that favoured proper anchoring of enzyme on its surface. Free enzyme showed a drastic decline in its activity of about 24% as it was difficult to withstand unfolding at higher thermal treatment.

About of 50% of CCFE and 79% of CFFE retained their activity when subjected to 120 minutes of pre-incubation at their respective optimum temperature, whereas, free enzyme could retain only 10% of their initial activity when subjected to same period of time.

The results obtained are depicted in the figure: 4.16.

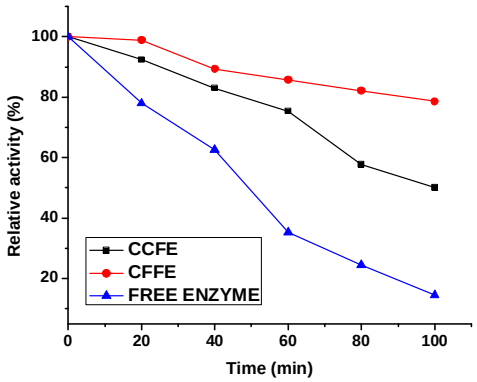

Figure: 4.16: Effect of pre-incubation time on the relative activity of free and immobilized α-amylase

4.2.4.5 Determination of kinetic parameters

The kinetic constants are related to the effect of substrate concentration on the activity of enzyme when the concentration of enzyme was kept constant. The Michaelis Menten constants, V_{max} is dependent on the amount of immobilized

enzyme while K_m is a reciprocal indicator of substrate-enzyme affinity. On comparison of the kinetic constants of immobilized enzymes and free amylase, it was observed that K_m and V_{max} were altered in the case of immobilized enzymes.

In the present case of adsorption of amylase on coconut fiber and its surface modified with APTES, the change in K_m suggests the presence of charge-charge interactions during the immobilization of the enzyme. Consequently, V_{max} of the immobilized enzyme declined compared with that of the free enzyme. The results are depicted in the figure: 4.17 and table 4.6.

The increase in K_m values for immobilized enzymes have been reported by various authors. Increase in K_m value is the result of steric effects and diffusional limitations of substrate upon immobilization of enzyme. Conformational changes of structure of the enzyme alter the interactions between substrate and matrix.

Table 4.6: Evaluation of kinetic parameters measured.

	Free enzyme	CCFE	CFFE
K_m (mgml^{-1})	0.50 ± 0.04	1.73 ± 0.02	2.76 ± 0.05
V_{max} (mg/ml/min)	7.52 ± 0.05	2.08 ± 0.04	4.10 ± 0.06

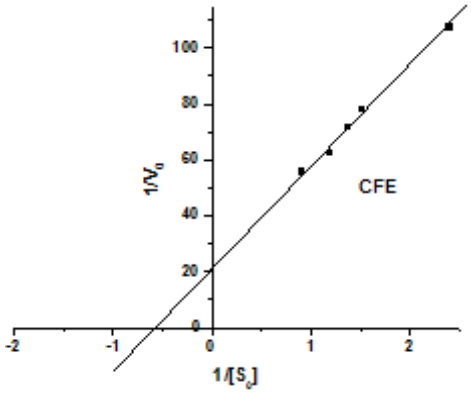

(i)

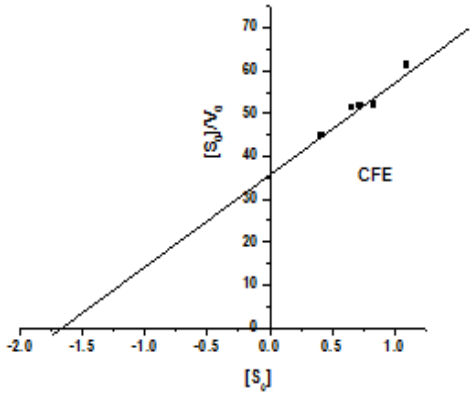

(iii)

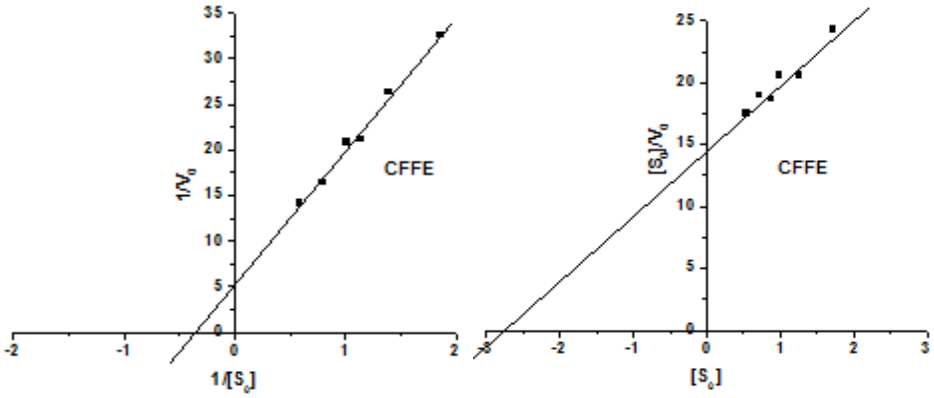

(ii) (iv)

Figure: 4.17: Lineweaver-Burk plots for (i) chemically pretreated coconut fiber and (ii) APTES functionalized coconut fiber. Hanes Woolf plots for (iii) chemically pretreated coconut fiber and (iv) APTES functionalized coconut fiber.

4.2.4.6 Storage stability of Immobilized α-amylase

Storage stabilities of immobilized enzymes at 4°C were investigated for a period of 30 days and the results are given in the figure: 4.18.

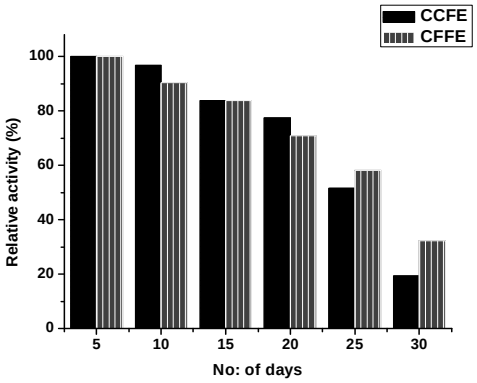

Figure: 4.18: Storage stability studies for immobilized enzymes on treated and functionalized coconut fibers

Free enzyme lost complete activity within 10 days of storage. Whereas CCFE and CFFE retained 52% and 58% of their original activity respectively even after 25 days. The increase in storage stability for CFFE might be due to the presence

of charged groups on its surface which put the enzyme into a more stable position in comparison to CCFE. But in comparison with free enzyme stabilities of both immobilized enzyme get enhanced after immobilization.

4.2.4.7 Reusability

CFFE retained 100% of its initial activity upto 4 cycles after which it gradually lost its activity in the range 20% and 30% during 5th and 6th cycle.

In the case of CCFE 92% of its activity was retained in the second run and during the 3rd and 4th run 20% and 30% of activity loss occurred. When reaction was carried out during 5th cycle 60% activity loss and during the 6th run 70% of activity loss was found. CCFE lost 75% its initial activity after 7cycles, whereas, CFFE lost only 30% of its initial activity after 7 cycles during the same period.

As can be seen, the immobilization definitely holds the enzyme in a stable position in comparison to the free counterpart. The activity declines after each subsequent use could be due to weakening in the strength of binding between the enzyme and support. Moreover repeated encountering of the substrate into the same active site of the enzyme might distort it which would have resulted in retarding its catalytic efficiency upon its subsequent use [44,45.46,47]. The results are given in the graph 4.19.

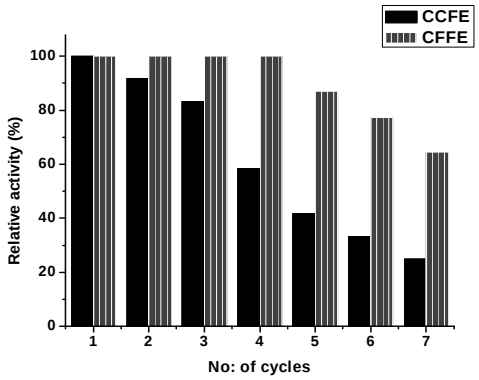

Figure: 4.19: Reusability studies of immobilized enzymes on coconut fibers

4.3 Immobilization of α-amylase on sugarcane bagasse fibers

Sugarcane is an abundant agricultural lignocellulosic byproduct which is a fibrous residue of cane stalks left over after crushing and extraction process of the juice from sugarcane [48]. It offers the advantage of being easily available, cheap, plentiful and low polluting. However, there is an excess of bagasse available and some alternatives for its use have been researched, including its use as support material for enzyme immobilization.

Many investigations have been carried out by various researchers in developing a technique to prepare long life immobilized enzyme using bagasse as a cheap immobilization support. S. Varavinit et al. have reported that cellulose in bagasse can be oxidized by periodic acid to form dialdehyde cellulose which can be reacted with the amino groups of glucoamylase to form covalent bound immobilized enzyme. This immobilized enzyme has possible uses in the production of glucose syrup, glucose powder and fructose [6].

Santos et al. have reported the use of sugarcane bagasse as immobilization support for xylitol production. Their study summarized the fact that treatment of the bagasse with hexamethylene diamine prior to fermentation resulted in the highest amount of immobilized cells [49].

Figure: 4.20 Sugarcane Bagasse

In our study immobilization of diastase α-amylase was carried out on bagasse and bagasse functionalized with coupling agent APTES via adsorption.

4.3.1 Preparation of chemically modified sugarcane bagasse

The procedure adopted for the pretreatment and chemical modification of sugarcane bagasse was same as that used for coconut fibers that have been described in section 4.2.1. Coupling of sugarcane bagasse with APTES was performed as per the method reported by J.G. Gwon et al. [8] and is given in section 4.2.2.

Figure:4.21: Photograph of sugarcane bagasse cut into small pieces for its use as support for enzyme immobilization

Sugarcane bagasse without any pretreatment will be designated as BBF. Chemically treated sugarcane bagasse fiber will be designated as CBF, APTES functionalized sugarcane bagasse fiber will be designated as BFF. In case of specifically mentioning immobilized enzyme on sugarcane bagasse fibers, CBFE and BFFE will be used.

4.3.2 Physico - chemical characterization

4.3.2.1 FT-IR Spectra of sugarcane bagasse

The FT-IR spectrum of sugarcane bagasse is given in the figure: 4.22. For the sugarcane bagasse the peak appeared at 3392 cm^{-1} is due to the O-H stretching. At 2921 cm^{-1} the observed absorption band is related to the axial deformation of C-H group. The peaks at 1746, 1721 cm^{-1} is characteristic of the carbonyl band (C=O) of the hemicelluloses in the sugarcane bagasse. This peak was very weak in the spectrum after treating with NaOH.

The C-O-C pyranose ring skeletal vibration gives a prominent band at 1044 cm^{-1}. A small sharp peak at 897 cm^{-1} corresponds to the glycosidic C-H deformation with ring vibration contribution, which is characteristic of β-glycosidic linkages between glucose in cellulose. The chemical groups of fiber were not changed during drying. Thus fiber can maintain its natural performance. The band at 1166 cm^{-1} is in connection with the asymmetric deformation of C-O-C of the cellulose and hemicelluloses [50].

For APTES coupled bagasse the gradual increase in peak height for the wave number at 3396 cm^{-1} assigned as NH_2 stretching vibration [51] at 2930 cm^{-1} assigned as CH_2 stretching vibration, at 1229 cm^{-1} assigned as Si-O-C band, and 1118 cm^{-1} assigned as NH bending vibration with the APTES coupling reaction. Treatments of bagasse fibers with amino- silanes also showed peak changes at 1200 cm^{-1} assigned as Si-O-C band, at 700 cm^{-1} assigned as Si-O-Si symmetric stretching, and at 467 cm^{-1} assigned as Si-O-C asymmetric bending [8].

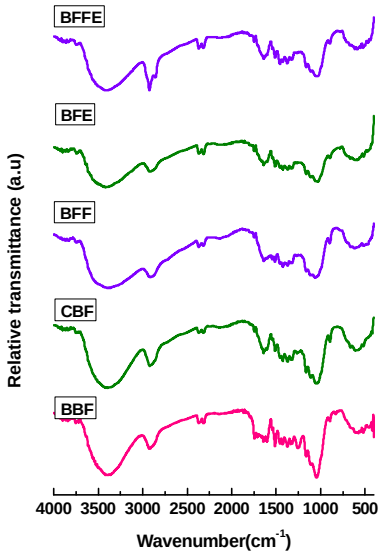

Figure: 4.22 FT-IR Spectra of sugarcane bagasse before and after modifications and immobilization

Table4.7: Peak assignments for bagasse fibers before and after modification.

Peak assignments (cm^{-1})	BBF	CBF	BFF	BFE	BFFE
OH stretching	3396	3401	3401	3401	3403
C-H (aliphatic + aromatic)	2921	2925	2926	2915	2929,2856
CO(ketone + carbonyl stretching)	1748	-	-	-	-
Water absorbed in cellulose	1637	1640	1637	1642,1656	1644
Aromatic skeletal modes	1605	-	-	-	-
CO + aromatic skeletal modes	1597	-	1546	-	1596
C-H bending	1462	1462	1457	1457	1461
C-H bending	1425	1425	1425	1425	1415
O-H,C-C,CO	1330	1319	1314	1314	1315
CO streching	1256	1261	1230	-	-
C-O-C,C-OH	1166	1166	1161	1166	1160
O-H ass.,CO def(lignin)	1113	1108	1113	1110	1115
C-O-C skeletal vibration	1044	1044	-	-	1041
CO stre.,CO def.	1060	-	1060	1060	-
C-H aromatic	897	897	897	897	897

4.3.2.2 Thermogram of sugarcane bagasse

In the TG curve of the sugarcane bagasse three mass loss steps were observed. The first decomposition occurs in the range 30 and 150°C and is attributed to the moisture elimination from the fibers.

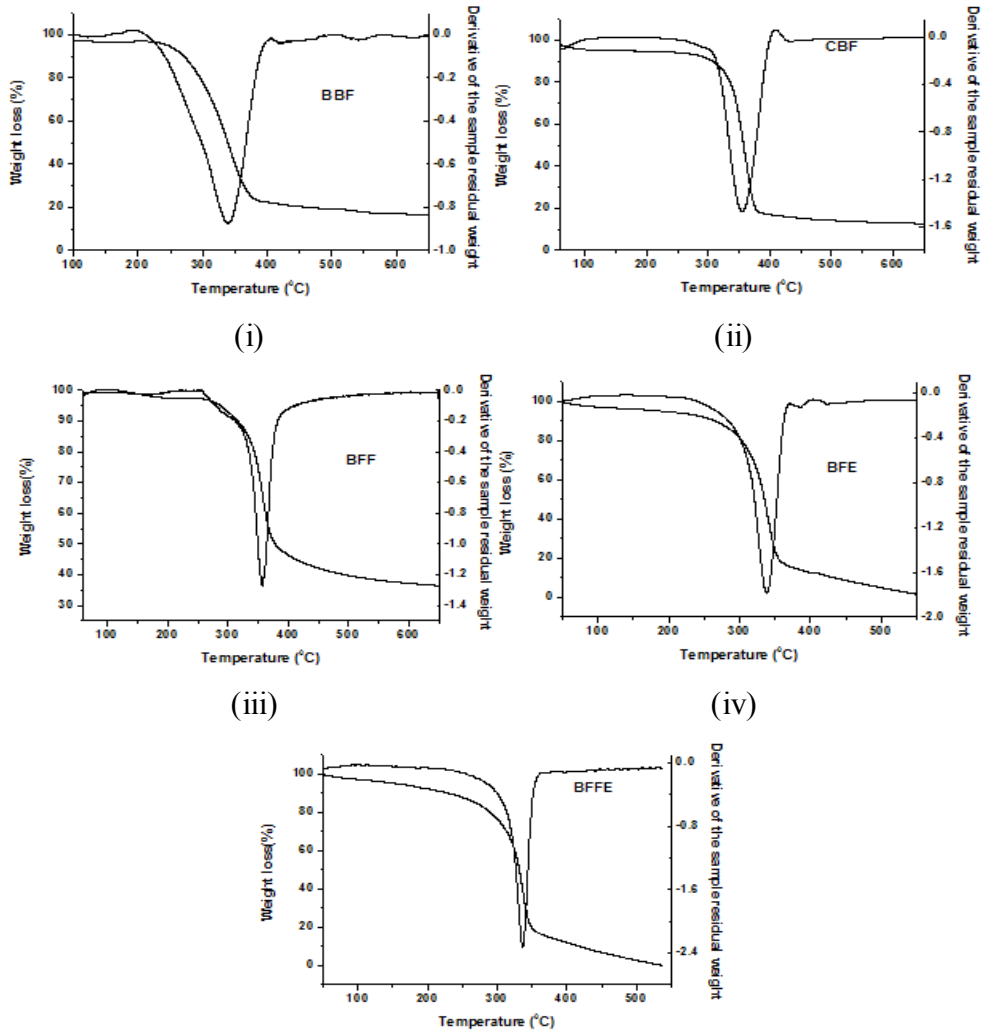

Figure: 4.23 TG -DTG curves for (i) BBF (ii) CBF (iii) BFF (iv) BFE (v) BFFE

The second weight loss occurs in the range 250-320°C, which might include the decomposition of waxes, impurities, fats, pectin and some amount of hemicelluloses.

The third weight loss was happened in the range 320-420°C. The major decomposition temperature for all kinds of treated fibers was in this range and is attributed to the loss of lignin, hemicelluloses and cellulose.

In the case of functionalized fiber additional small weight loss peaks appeared which might be the result of decomposition of organic functional groups present in the sample.

Table 4.8: Thermogravimetric results of sugarcane bagasse subjected to different treatment

Sugarcane bagasse	Transition temperature range (°C)	Maximum degradation Temperature (°C)	Weight loss at a given temperature range
BBF	30-180	63	3
	180-309	279	22.5
	309-412	339	52.7
	412-600	445	4.2
CBF	30-180	54	5.5
	180-333	288	14
	333-449	355	66.2
	420-600	409	3.2
BFF	30-190	52	3
	190-317	293	8
	317-424	357	45.3
	424-600	412	6.5
CBFE	30-180	56	6
	180-312	274	14
	312-394	339	68
	394-600	383	11.64
BFFE	30-180	61	7
	180-309	289	19.9
	309-376	337	58.3
	376-600	380	14.4

The decomposition peaks due to the enzyme organic structure backbone degradation occurred at lower temperatures compared to the temperature for bare fibers before enzyme immobilization.

4.3.2.3 X-ray diffraction study

The method adopted for the interpretation of the crystallinity index of the samples was same as discussed previously in the section 4.2.3.3. The X-ray diffractogram of untreated bagasse fiber and treated bagasse fiber showed that the major crystalline peak on each pattern occurred at around $2\theta=22.48°$ which represents the cellulose crystallographic plane (002).

It can be observed that intensity and crystallinity index of bagasse fibers increased with chemical treatment with acid followed by alkali. This was attributed to the better packing and stress relaxation of cellulose chains. This is caused by an increase in van der waals and hydrogen bonding between neighbouring molecules as a result of the increased interaction of hydroxyl groups found in cellulose.

As per the reported literature the increase in crystallinity also confirms the removal of amorphous part of the fiber as a result of chemical pre-treatment applied [53,54].

The decrease in CI after APTES treatment is due to increase of amorphous content upon chemical treatment. But the characteristic peak corresponding to cellulose I was seen in all samples which implies the fact that the treatment conditions - time temperature and concentration applied to fibers did not modify the crystal packing chains of native cellulose I to cellulose II. The results are tabulated in table 4.7 and are depicted in figure: 4.24.

Table 4.7: (i) Diffraction peaks at various angles for modified and unmodified Sugarcane bagasse (ii) Crystallinity index of the sugarcane bagasse before and after modifications and immobilization

	BBF	CBF	BFF
2θ(degree)	22.15	22.48	22.4

(i)

	BBF	CBF	BFF
CI	57.15	83.53	80.76

(ii)

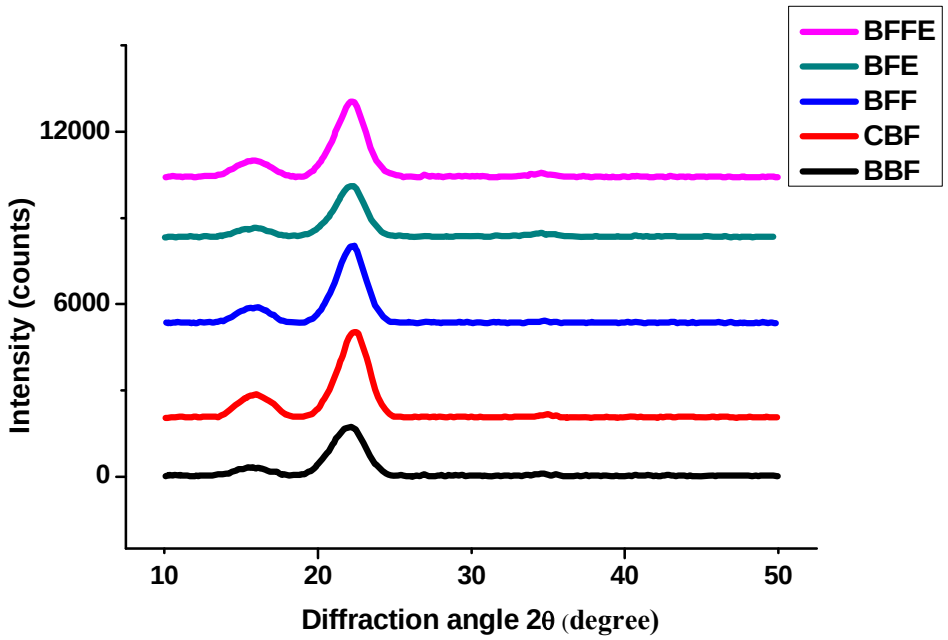

Figure: 4.24: XRD of untreated, treated and immobilized sugarcane bagasse

4.3.2.4 Energy Dispersive X-ray spectroscopy

Elemental data obtained from Energy Dispersive X-ray analysis was carried out in order to confirm the functionalization of sugarcane bagasse. The higher C and Si content in the modified fibers compared to unmodified fibers is a direct evidence for organosilane modification on the fibers.

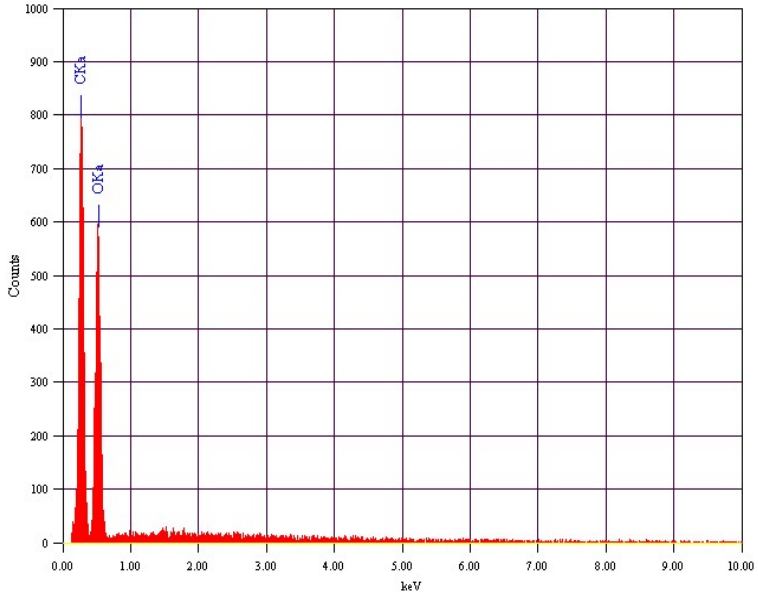

(i)

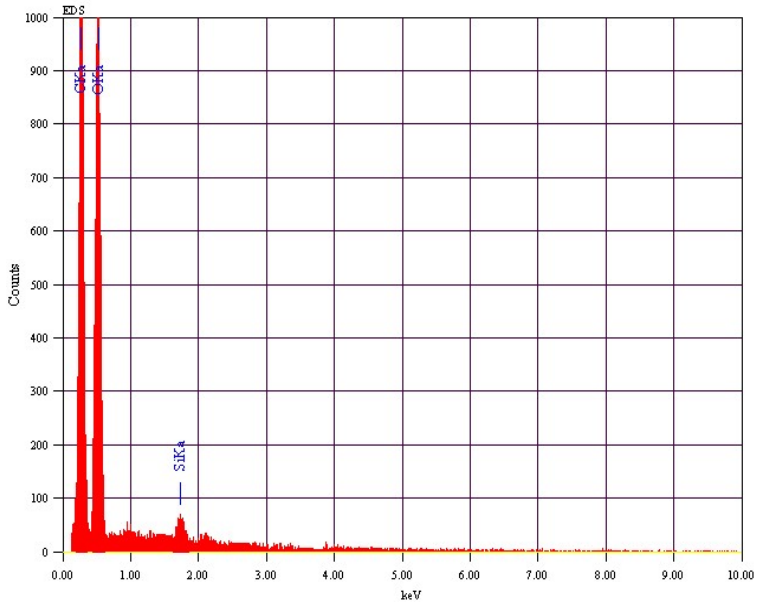

(ii)

Figure: 4.25: (i) EDS spectrum for untreated sugarcane bagasse (ii) EDS spectrum for sugarcane bagasse after coupling with APTES

Table 4.8: (i) Elemental data for untreated sugarcane bagasse (ii) Elemental data for sugarcane bagasse after coupling with APTES

Element	(keV)	Mass%	Atom%
C K	0.277	79.42	83.71
O K	0.525	20.58	16.29
Si K	-	-	-

Element	(keV)	Mass%	Atom%
C K	0.277	74.31	79.6
O K	0.525	24.94	20.06
Si K	1.739	0.75	0.34

4.3.2.5 Scanning electron microscopy

The surface morphology of fibers before and after chemical treatments and functionalization with APTES was investigated. The SEM micrograph of untreated bagasse fiber surface was formed by parallel strips and was covered with residual materials called piths. Similar observations are reported by Vilay et al. in the analysis of untreated sugarcane bagasse micrographs [55]. The SEM images obtained were shown in the figure: 4.26.

After alkali treatment, extractives, waxes and oil from fiber surface get removed which thus correspondingly increased surface roughness as is evident from SEM images.

In the bagasse fibers, surface residual pith was removed and parallel strips appeared more exposed. The Pits that were remained hidden under the piths containing superficial layer of waxes and extractives are clearly observed after alkali treatment [29]. These pits are seen as small pores which connects the neighboring cells on the surface of walls. Thus in effect cellulose part of the fiber gets exposed after chemical treatment. This favours the possibility of attaching functional groups to cellulose.

Similar results were observed by many authors [16, 22, 30, 31] and was reported that alkali treatment resulted in a higher amount of cellulose exposed on the fiber surface, thereby increasing the number of possible reaction sites.

However surface topography of APTES treated fibers appeared to be smooth. This could be due to the fact that APTES form an interpenetrating polymer network with the fiber surface thus increasing the support hydrophobicity and rigidity.

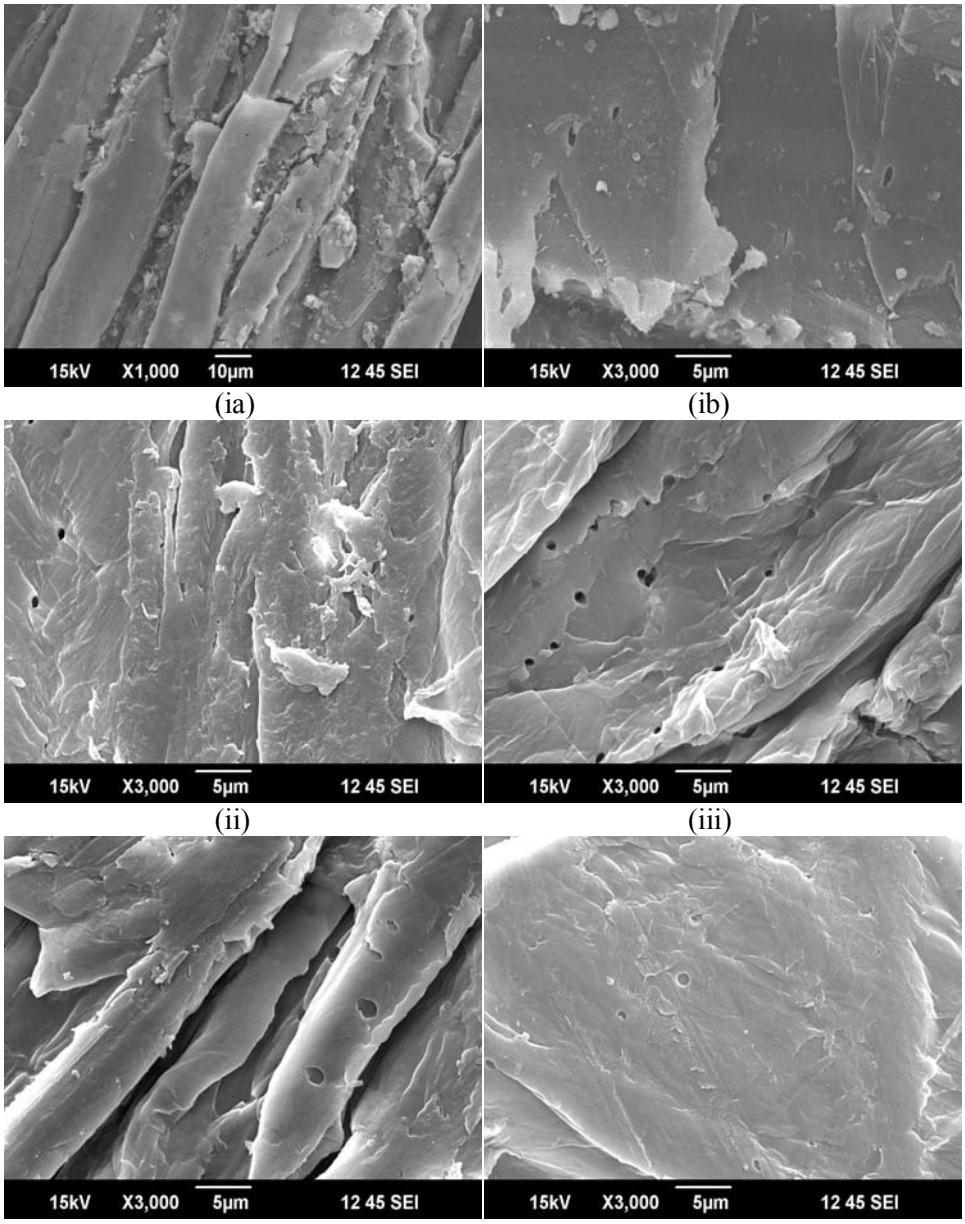

Figure: 4.26: SEM images of sugarcane bagasse before and after modifications: (ia), (ib): before pretreatment (ii) after pretreatment with H_2SO_4 and NaOH (iii) after functionalization with APTES (iv) after immobilization of enzyme on pretreated sugarcane bagasse (v) after immobilization of enzyme on functionalized fiber

4.3.3. Biochemical characterization

4.3.3.1 Influence of pH during immobilization of α-amylase on bagasse fibers

The forces binding proteins to bagasse fiber surfaces included hydrogen bonding, hydrophobic interactions and electrostatic interactions. It is on the basis of isoelectric point that overall surface charge of the enzyme can be predicted. When the adsorption is performed at a pH lower than the pI of the α-amylase which is about 4.6, the protein will be positively charged and when the pH of the reaction medium is above pI the protein will be negatively charged. The isoelectric point of the bagasse fibers is reported to be around 5 [56] and hence the adsorbent surface is negatively charged at pH above 5 and positively charged below 5.

The effect of pH on adsorption was studied at room temperature by varying the pH in the range 4-8. It could be seen that depending on the pH of the reaction medium the adsorption capacity changed significantly. The adsorbed amount of proteins measured in the pH range 4-6 showed a sharp initial rise, which suggested a high affinity between amylase and the adsorbent surface. At pH 8, adsorption was very low and it takes longer time to reach equilibrium.

The maximum adsorption at pH 5-6 could be explained as follows; near the isoelectric point the net charge of the protein would be low and the electrostatic repulsion between the molecules would be minimal. Consequently a closer packing of the protein molecules was possible and the amount of adsorption increased.

It was observed that there was a large reduction in the amount of α-amylase adsorbed on bagasse at pH below and above pI. At pH below the enzyme pI α-amylase assumed a positive charge and so the electrostatic repulsion between enzyme molecules increased. As a consequence, the enzyme molecule requires more space and the adsorption capacity decreased. At pH 8 the surface of the α-amylase became

negatively charged and that of bagasse surface also will be negative resulting in electrostatic repulsion between protein molecules and the support.

In the case of CBF the maximum adsorption occurred at pH 6. Even the electrostatic repulsion was expected to hinder the adsorption, still appreciable activity at this pH is due to partial charge at bagasse, as pH 6 being close to its isoelectric point or hydrogen bonding might have occurred with hydroxyl groups on bagasse surface which thus favoured the enzyme in its most stable conformation at pH 6.

In the case of BFF after immobilization a shift towards acidic side occurred due to the protonation of amino groups of APTES. This positively charged BFF can thus form chemical bridge via electrostatic interaction with negatively charged α-amylase. Even though less adsorption was expected at pH 5 the optimum activity was observed at this pH. This deviation from expected result may be explained by the fact that during surface functionalization with organo silane groups, hydrophobicity of bagasse fibers were increased and hence weak electrostatic interactions might get dominated by hydrophobic interaction at pH 5 [57,58].

The results obtained are shown in the figure: 4.27.

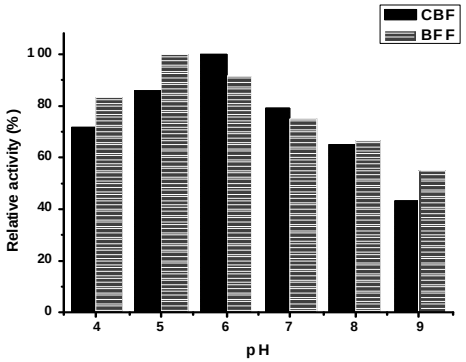

Figure: 4.27: Effect of immobilization pH on the relative activity of α-amylase

4.3.3.1.1 Effect of contact time on immobilized enzyme activity

The contact time needed to obtain maximum adsorption was evaluated at different time intervals for each supports. These results are shown in Figure: 4.28. It can be observed that for both CBF and BFF the maximum measured activity of the immobilized enzyme was achieved after 2 hours of contact time.

When contact time was increased, no improvement on activity was observed; on the contrary, the activity first remains constant and then decreases with the increase of contact time, probably due to the increase of enzyme uptake as a result of multilayer adsorption, which causes reduction in the available active site for the substrate molecules.

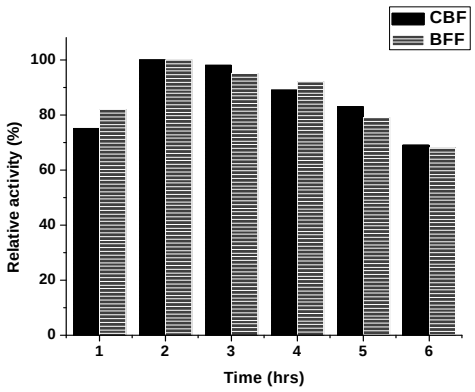

Figure: 4.28: Effect of contact time of enzyme with supports on the relative activity of α-amylase.

4.3.3.1.2 Effect of initial protein concentration on protein loading

In the case of CBF on varying the initial concentration as 2 mg, 4 mg, 6 mg and 9 mg the amount of protein that get immobilized was about 0.143mg, 0.53mg 0.98 mg and 1.24 mg after which further increase in concentration did not produce any remarkable increase in adsorption of proteins.

Enhanced enzyme adsorption occurs due to better surface accessibility for enzymes towards CBF as a result of increase in the population of pores after acid and

alkali pretreatment [59, 60]. Moreover, pretreatment also provides more hydroxyl groups projected at the cellulose surface which also allows easy interaction with the enzymes via hydrogen bonding. The results of variation of protein load with increase in concentration of enzyme are shown in the figure: 4.29.

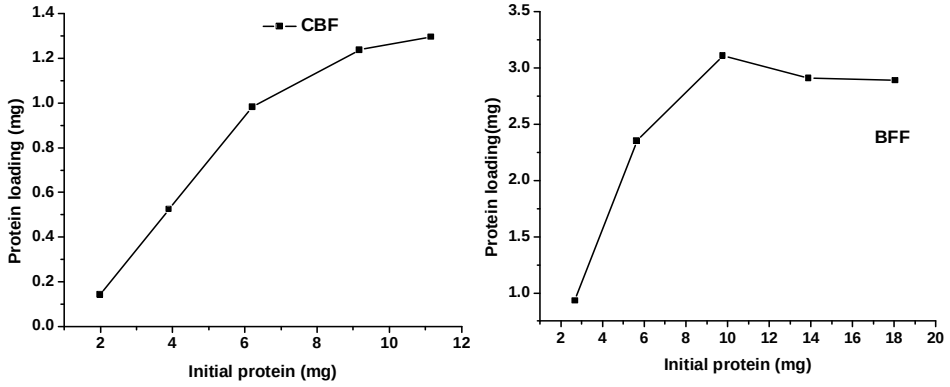

(i) (ii)

Figure: 4.29: Effect of initial protein concentration on the protein loading for (i) Pretreated sugarcane bagasse (ii) Sugarcane bagasse functionalized using APTES.

The coupling of APTES have considerably enabled in enhancing the protein adsorption for BFF when compared to CBF [61, 62].

The protein load at initial concentrations 2.7 mg, 5.6 mg, 10 mg, 14 mg and 18 mg were 0.93, 2.35, 3.11, 2.9 and 3 mg respectively. Thus it is clear that optimum loading occurred at initial concentration of about 10mg which was much higher than that in CBF. After this concentration there was no appreciable increase in loading instead adsorption was shown to reach a plateau indicating that supports get saturated with the enzyme.

This difference in adsorption amount on CBF and BFF might be due increased hydrophobicity of BFF compared to CBF which thus provided more favourable surface for protein adsorption.

4.3.3.1.3 Effect of initial protein concentration on immobilization yield and activity of loaded enzyme.

Evaluation of immobilization yield gave an entirely different observation as follows: For CBF even if the maximum protein load was found at the initial concentration of 9 mg, optimum yield was obtained at 6.2 mg. This might be due to decline in residual activity at maximum protein loaded concentration as a result of decreased number of active sites available than actually present.

The immobilization yield at different initial concentrations of 2 mg, 4 mg, 6mg, 9 mg and 11 mg were 14, 27, 32, 27 and 26% respectively. The values obtained are represented in the figure: 4.30.

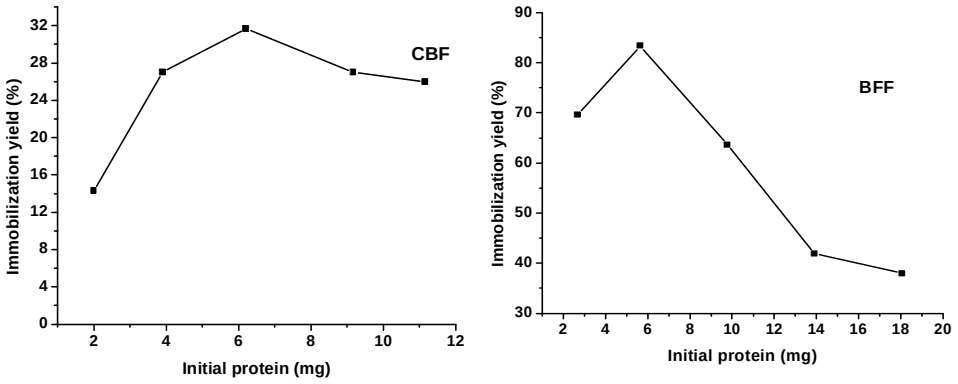

(i) (ii)

Figure: 4.30: Effect of initial protein concentration on immobilization yield of α-amylase on (i) chemically pretreated sugarcane bagasse (ii) Sugarcane bagasse functionalized using APTES.

In the case of BFF the yield was higher than for CBF which might be due to enhanced uptake of enzymes by BFF as a result of surface modification which enhanced its hydrophobicity. Thus at initial concentrations of 2.7 mg, 5.6 mg, 10mg, 14 mg and 18 mg the immobilization yield obtained were 70%, 83%, 67%, 42% and 40% respectively. Even if protein loaded maximum at 10mg, optimum immobilization yield was obtained at 5.6 mg.

Corresponding immobilized enzyme activities were also measured. In the case of CBF the maximum activity obtained was at initial concentration of 6.2 mg even if the protein loaded maximum at 10 mg. This again confirms that as the loading increases sometimes multilayer adsorption may result in decline in activity.

In the case of BFF the results tally with protein load measured. Since it was at optimum protein load the immobilized enzyme exhibited optimum activity and as the rate of adsorption remained constant the residual activity also remained constant. The results are shown in the figure: 4.31. For BFF the optimum immobilized enzyme activity was 5.3 EU whereas, for CBF it was only 2.2 EU.

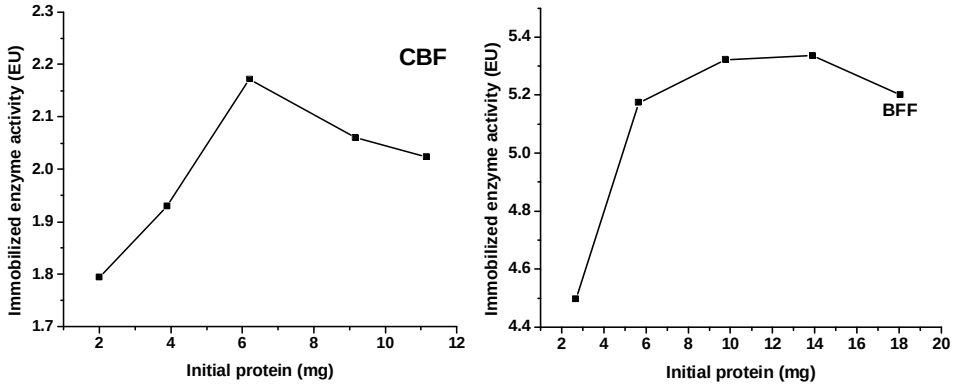

(i) (ii)

Figure: 4.31: Effect of initial protein concentration on immobilized α-amylase activity on (i) chemically pretreated sugarcane bagasse (ii) Sugarcane bagasse functionalized using APTES.

The activity yield and immobilization efficiency were also evaluated. The results are tabulated in the table 4.9.

From the table it is clear that the activity yield obtained for BFF was higher than CBF which might be due to proper orientation of enzyme conformational structure via immobilization over BFF than CBF.

Table 4.9: Immobilization efficiency of α-amylase on untreated and treated sugarcane bagasse

Polymer	Initial protein (mg)	Immobilized protein mg/g support	Immobilization yield (%)IY	Initial activity(EU)	Immobilized enzyme activity EU	Activity Yield (%)AY	Immobilization efficiency (%) IE=AY/IY
CBF	6.2	0.98	32	12.5	2.2	17	54
BFF	9.8	3.11	64	10.4	5.3	51	80

4.3.3.2 Effect of pH on enzyme activity

After immobilization the optimum pH shifted to pH 6 for both CBFE and BFFE. This might be due to the formation of more favourable conformation at this pH for both immobilized enzymes [71]. For CBF the activity gets enhanced in the range 5-6, whereas, for BFF this enhancement in activity was observed in the range 5.5-7.

Similar shift of pH was reported by other authors; Jaiswal et al. reported a shift of 1.5 units after the immobilization of α-amylase on gelatin [72]. A similar trend of shift of pH was observed when α-amylase was immobilized on both chitosan and amberlite [73]. A shift of pH optimum from 7.5 to 8.0 on immobilization of glutamate dehydrogenase on gelatin beads via cross linking with glutaraldehyde was observed by El-Shora et al. [64].

In the case CBFE and BFFE activity profile obtained is shown below in figure: 4.32.

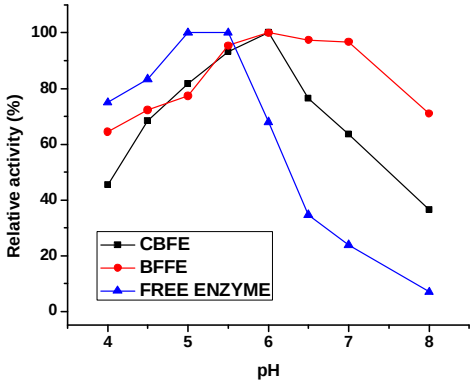

Figure: 4.32: Effect of pH on the relative activity of free and immobilized α-amylase

At pH 4 the residual activity for CBFE was 45%, whereas, for BFFE it was 65%. At pH 5.5, activity again gets enhanced for both as 93% for CBFE and 95% for BFFE. When the pH is 6.5, relative activity of CBFE was about 76%, whereas for BFFE relativity activity was about 97%. At pH 7, residual activity for CBFE was 64% and that for BFFE was 96.7%. Finally at pH 8 relative activity of CBFE decreased drastically, whereas, for BFFE it was 71%.

4.3.3.3 Effect of temperature on the activity

The temperature required for the CBFE and BFFE to exhibit maximum activity was analyzed by incubating them in buffered medium at different temperature range of 30-60°C. The results are shown in the figure: 4.33.

After incubating the immobilized enzyme together with the substrate at 30°C, 89% relative activity was shown by CBFE and 96% relativity activity by BFFE. As the temperature was raised to 35°C CBFE had 92% of relative activity, whereas, BFFE had 98%. This is because, as the temperature rises, reacting molecules gain more and more kinetic energy. This increases the chances of a successful collision and so the rate increases.

At 40°C the relative activity of CBFE was about 94% and that for BFFE was 100%. This decrease in optimum temperature for BFFE might result from change in conformational structure of enzyme after immobilization. But for CBFE optimum temperature was attained at 50°C. After the optimum temperature relative activity for BFFE was 96, 91, 89 and 86% at 45°C, 50°C, 55°C and 60°C respectively.

In the case of CBFE relative activity was 89% and 56% at 55°C and 60°C respectively. This decrease is because of the fact that above the optimum temperature the enzyme structure begins to break down. At higher temperatures rupturing of intra- and intermolecular bonds occur as the enzyme molecules gain

more kinetic energy. However, this performance was much better than that for the free enzyme which had only 27% of its residual activity at this temperature.

Immobilization can effect on the structure of enzyme and lead to an increase in the activation energy for reorganization of the enzyme to an appropriate conformation for binding to its substrate.

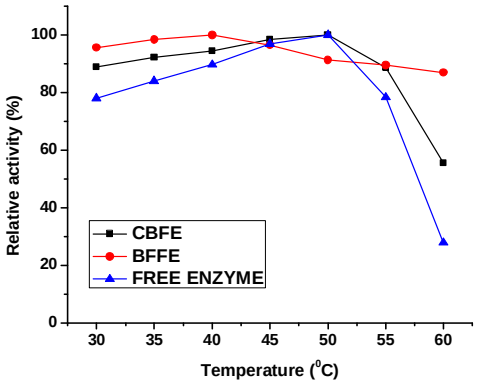

Figure: 4.33: Effect of temperature on relative activity of free and immobilized α-amylase

The increase in optimum temperature might be due to creation of conformational limitations on the enzyme movements as a result interactive forces between enzyme and the support. This also retards the unfolding of enzyme structure bringing about retention of the activity at elevated temperatures [65,66]

Tumturk et al. was of the opinion that the increase in optimum temperature was caused by the change in the physical and chemical properties of the enzyme [67].

4.3.3.4 Thermal stability of the free and immobilized enzymes

The thermal denaturation was studied by incubating immobilized enzyme alone in buffer at different temperatures for 1hour. After the thermal treatment at 30°C, the activity retained by immobilized enzyme was assigned as 100% and activity at other temperatures are expressed relative to this activity. As the

temperature was raised residual activity showed a drastic decrease with immobilized enzymes retaining more activity compared to free enzyme.

At 60°C there was a sudden decline in activity for CBFE to 35%, whereas, for BFFE it was about 55% at this temperature. Free enzyme could have only 11% of the residual activity at this elevated temperature. This might be due to easy unfolding of native enzyme because of its more flexible conformational structure in homogenous media whereas, after immobilization structural rigidity and hence stability of immobilized biocatalyst occurs which thus withstands unfolding of the protein structure at elevated temperatures [68]. The retention of activity at various temperature treatments are shown in the graph 4.34.

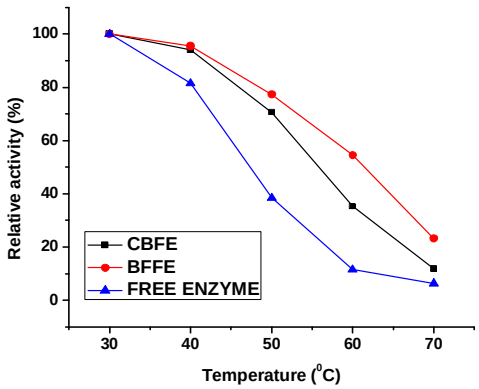

Figure: 4.34: Thermal stability of free and immobilized α-amylase

Even after 100 minutes of pre-incubation at 40°C, 61% of original activity was exhibited by CBFE and 87% by BFFE, whereas, free enzyme lost almost 86% of its original activity. This increased thermal stability may be due to both the rigidification of the three-dimensional structure of the immobilized molecules, as explained earlier and some additional ionic and hydrophobic intermolecular contacts.

The results are summarized in the figure: 4.35.

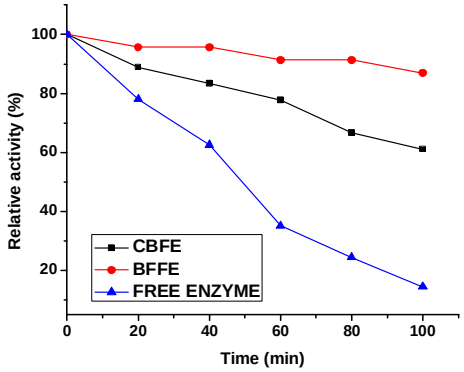

Figure: 4.35: Effect of pre- incubation time on the relative activity of α-amylase

4.3.3.5 Determination of kinetic parameters

The kinetic parameters obtained from Lineweaver-Burk plots (figure: 4.36) are summarized and in table 4.10.

The kinetic parameters V_{max} decreased and K_m increased with immobilization. The altered kinetic parameters might be due to blocking of active sites during immobilization which thus reduced the affinity of enzyme for the substrate and hence corresponding reduction in activity encountered. The quantity is thus a measure of the stability of the ES complex.

But decrease in K_m for BFFE when compared to CBFE indicates more affinity of enzyme for its substrate as a result of favourable positioned active sites on this surface modified bagasse. This was also reflected in the value of V_{max} for both immobilized enzymes, BFFE exhibiting more activity than CBFE [69].

Table 4.10: Evaluation of kinetic parameters K_m and V_{max}

	Free enzyme	CBFE	BFFE
K_m ($mgml^{-1}$)	0.50 ± 0.04	3.89 ± 0.05	2.32 ± 0.02
V_{max} (mg/ml/min)	7.52 ± 0.05	2.88 ± 0.06	4.57 ± 0.03

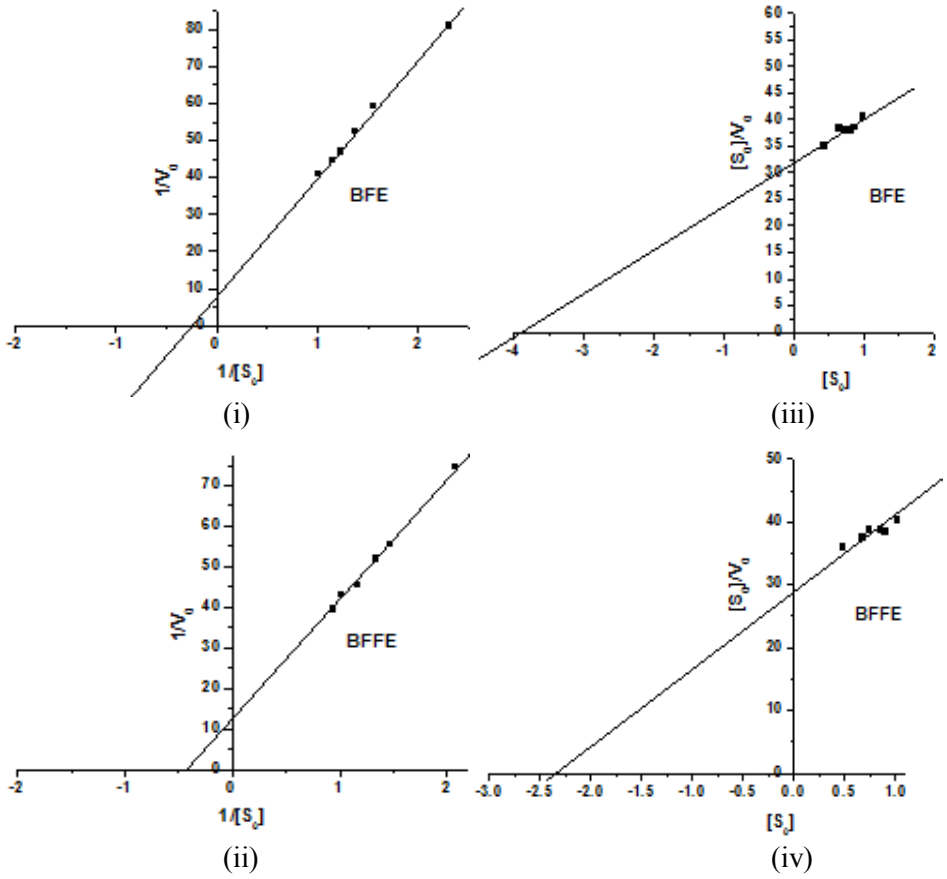

Figure: 4.36: Lineweaver-Burk plots for (i) chemically pretreated sugarcane bagasse and (ii) APTES functionalized sugarcane bagasse. Hanes Woolf plots for (iii) chemically pretreated sugarcane bagasse and (iv) APTES functionalized sugarcane bagasse.

4.3.3.6 Storage stability of Immobilized α-amylase

Storage stability measurements were conducted in semi-dry form at 4°C for a period of 30 days of storage. It is clear from the figure: 4.37 that all forms of immobilized enzymes shows appreciable amount of activity upto 20 days of storage. The activity was not decreased much for the first five days but decreased to 45% for CBFE and 57% for BFFE after 30 days of storage.

There are plenty of hydroxyl groups on the surface of bagasse fibers which account for enhanced stability of enzyme immobilized on bagasse fibers compared with free enzyme.

Storage stability for BFFE was much more enhanced compared with CBFE. This is due to higher hydrophobicity of these surfaces which hold the enzyme more strongly than via hydrogen bonding through hydroxyl groups on CBFE.

As a whole, the improvement in the stability upon immobilization is the result of modification occurred in enzyme conformational structure. The enzyme-polymer systems help in preventing denaturation resulting from conformational fluctuations [70]. The results are given in the figure: 4.37.

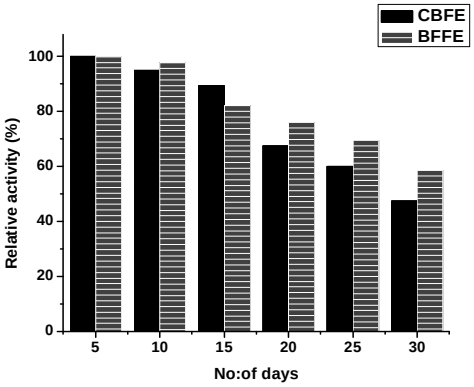

Figure: 4.37: Storage stability studies for immobilized enzymes on treated and functionalized sugarcane bagasse

4.3.3.7 Reusability

In order to check reusability of immobilized enzymes, the system was submitted to 7 consecutive reaction cycles. Up to 4 cycles not much denaturation occurred and hence the activity of immobilized enzymes was at its optimum. After the 5^{th} run denaturation starts and activity declined gradually. About 84% of residual activity remained for BFFE and 69 % for CBFE after the 6^{th} run. During the 7^{th} run CBFE could retain only 57% of its initial activity, whereas, BFFE still performed better with 76% of residual activity. The results are given in figure: 4.38.

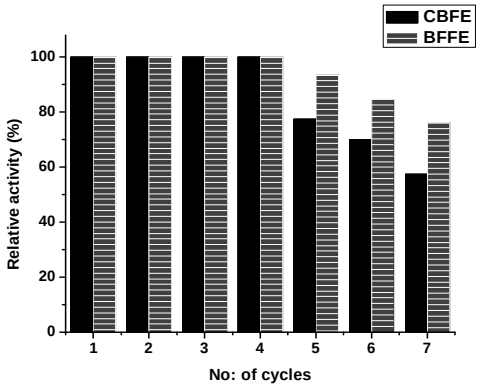

Figure: 4.38 Reusability studies of immobilized enzymes on sugarcane bagasse

4.4 Conclusion

Natural fibers from Coconut and sugarcane bagasse were found to be promising supports for α-amylase immobilization. Both of the supports were functionalized via APTES coupling and found to be having enhanced efficiency for the immobilization of enzyme compared to unfunctionalized forms. All the supports and their immobilized forms were characterized via various analytical techniques which includes FT-IR, TG, SEM, BET and EDS. The properties of immobilized enzymes are compared with that of free enzyme. The main observations can be summarized as follows:

- ✓ Pretreatment of coconut fibers and bagasse fibers with H_2SO_4 and NaOH removed waxes, hemicelluloses and other impurities from the surface and makes cellulose more exposed and available for functionalization.
- ✓ The immobilization efficiency on CCF was found to be 64% whereas that for CFF was found to be 71%.
- ✓ The optimum pH for immobilized enzyme on CCFE was found to be at pH 5 which is same as that of free enzyme. In the case of CFFE the optimum pH was at pH6.

- ✓ It was found that the optimum temperature for both the free and the immobilized enzyme was 50-55°C. But the relative activity retained by immobilized enzyme in the range of 55-70°C was about 85-44% for CCFE and 90-67% for CFFE, whereas, for free enzyme retained only about 78-15%.
- ✓ It was observed that thermal stability of the immobilized enzymes was much better than that of soluble enzyme at 40-70°C. Among CCFE and CFFE, thermal stability after immobilization was higher for CFFE.
- ✓ Among CCFE and CFFE, the higher value of V_{max} is for CFFE, which corresponds to enzyme activity.
- ✓ Free enzyme loses, almost completely, its activity within 10 days of storage under identical conditions as that for immobilized enzymes. CCFE could retain 52% of its initial activity after 25 days, whereas, CFFE could retain 58% of its initial activity.
- ✓ When reusability was checked immobilized preparations CCFE lost 75% its initial activity after 7 cycles, whereas, CFFE lost only 30% of its initial activity after 7 cycles during the same period.
- ✓ In the case of sugarcane bagasse as support, immobilization efficiency for CBF was about 54% and that for BFF was about 80%.
- ✓ The optimum pH for bagasse after chemical pretreatment and after functionalization with APTES was at pH6.
- ✓ The optimum temperature for CBFE was attained at 50°C whereas, for BFFE it was at 40°C.
- ✓ At 60°C there was a sudden decline in activity for CBFE from 71% to 35%, whereas, for BFFE it was about 55% at this temperature. Free enzyme could have only 11% of the residual activity at this elevated temperature.

- ✓ After pre-incubation for about 100 minutes at 40°C, 61% of activity was exhibited by CBFE and 87% by BFFE.
- ✓ K_m value for CBFE was about 3.89 ± 0.05 mg/ml whereas for BFFE it was about 2.32 ± 0.02 mg/ml. Corresponding V_{max} values were 2.88 ± 0.06 mg/ml/min and 4.57 ± 0.03 mg/ml/min for CBFE and BFFE respectively.
- ✓ Storage stability for BFFE was much more enhanced when compared with CBFE. The activity was not altered much for the first five days but decreased to 45% for CBFE and 57% for BFFE after 30 days of storage. Free enzyme stored at 4°C in buffer under similar conditions lost almost its activity within 10 days.
- ✓ The results obtained from reusability studies showed that after 7 cycles CBFE could retain only 57% of its initial activity, whereas, BFFE still performed better with 76% of residual activity.

4.5 References

[1] D. Chandramohan, K. Marimuthu, A Review on natural fibers, IJRRAS 8 (2011).

[2] L.A. Pothan, S. Thomas, G. Groeninckx, The role of fiber/matrix interaction on the dynamic mechanical properties of chemically modified banana fiber/ polyester composites, Compos. Part A: Appl. Sci. Manuf. 37 (2006) 1260-1269.

[3] L. Sene, A. Converti, M.G. Felipe, M. Zilli, Sugarcane bagasse as alternative packing material for biofiltration of benzene polluted gaseous streams: a preliminary study, Bioresour Technol. 83 (2002) 153-157.

[4] S. Samanta, M. Jana, C. Maity, S. Kar, P.K.D. Mohapatra, B.R. Pati, K.C. Mondal, The potential of immobilized bacterial α-amylase on coconut coir, a smart carrier for biocatalysts, Biocatal. Biotransform. 27 (2009) 131-135.

[5] B.B. Bhowmick, C.R. Debnath, Coir fibre, Part I: Properties of coir fibre, Indian Coconut J. 15 (1984)11-14.

[6] S. Varavinit, N. Chaokasem, S. Shobsngob, Covalent immobilization of a glucoamylase to bagasse dialdehyde cellulose, World J. Microbiol. Biotechnol. 17 (2001) 721-725.

[7] T. Branyik, A.A. Vicente, J.M.M. Cruz, J.A. Teixeira, Spent grains - a new support for brewing yeast immobilization, Biotechnol. Lett. 23 (2001) 1073-1078.

[8] J.G. Gwon, S.Y. Lee, G.H. Doh, J.H. Kim, Characterization of Chemically Modified Wood Fibers Using FTIR Spectroscopy for Biocomposites, J. Appl. Polym. Sci. 116 (2010) 3212-3219.

[9] G. Dey, B. Singh, R. Banerjee, Immobilization of α-amylase production by Bacillus circulans GRS 313, Braz. Arch. Biol. Technol. 46 (2003) 167-176.

[10] A.I. Brıgida, A.D. Pinheiro, A.L. Ferreira, G.A. Pinto, L.R. Goncalves, Immobilization of Candida antarctica lipase B by covalent attachment to green coconut fiber, Appl. Biochem. Biotechnol. 137-140 (2007) 67-80.

[11] G Dey, V. Nagpal, R. Banerjee, Immobilization of α-amylase from Bacillus circulans GRS 313 on coconut fiber, Appl. Biochem. Biotechnol. 102-103 (2002) 303-13.

[12] Y. Zhao, N. Yan, M. Feng, Characterization of phenol- formaldehyde resins derived from liquefied lodge pole pine barks, Int. J. Adhes. Adhes. 30 (2010) 689-695.

[13] R.M. Siverstein, G.C. Bassler, T.C. Morril, "Identificacao Espectrometrica de Composite Organicos",5 ed., Guanabara Koogan S.A, Rio de Janeiro 1994, 93.

[14] R.G. Marchessault, P.R. Sundararajan, Cellulose. In: Aspinall GO, editor. The Polysaccharides. Ed 2. New York: Academic Press; (1983) 11-95.

[15] M.M. Rahman, A.K. Mallik, M.A. Khan, Influences of various surface pretreatments on the mechanical and degradable properties of photografted oil palm fibers, J. Appl, Polym. Sci. 105 (2007) 3077-3086.

[16] J. Rout, S.S. Tripathy, S.K. Nayak, M. Misra, A.K. Mohanty, Scanning electron microscopy study of chemically modified coir fibers, J. Appl. Polym. Sci. 79 (2001) 1169-1177.

[17] P.J.-F. Herrera, A.-G. Valadarez, A study of the mechanical properties of short natural-fiber reinforced composites, Composites: Part B 36 (2005) 597-608.

[18] M.F. Rosa, B.-S. Chiou , E.S. Medeiros, D.F. Wood, T.G. Williams , L.H.C. Mattoso, W.J. Orts, S.H. Imam, Effect of fiber treatments on tensile and thermal properties of starch/ethylene vinyl alcohol copolymers/coir biocomposites, Bioresour. Technol. 100 (2009) 5196-5202.

[19] E. Ukaji, T. Furusawa, M. Sato, N. Suzuki, The effect of surface modification with silane coupling agent on suppressing the photo-catalytic activity of fine TiO_2 particles as inorganic UV filter, Appl. Surf. Sci. 254 (2007) 563-569.

[20] A.-G. Valadez, J.M. Cervantes-Uc, R. Olayo, P.J.-F. Herrera, Chemical Modification of Henequen Fibers with an Organosilane Coupling Agent, Compos Part B-Eng. 30 (1999) 321-31.

[21] M.A. Mondragon, V.M. Castano, M.J. Garcia, S.C.A. Tellez, Vibrational Analysis of Si $(OC_2H_5)_4$ and Spectroscopic Studies on the Formation of Glasses Via Silica Gels, Vib. Spectrosc. 9 (1995) 293-304.

[22] A. Bismarck, A.K. Mohanty, I.-A. Aranberri, S. Czapla, M. Misra, G. Hinrichsen, J. Springer, Surface characterization of natural fibers; surface properties and the water up-take behavior of modified sisal and coir fibers, Green Chem. 3 (2001) 100-107.

[23] D.S. Varma, M. Varma, I.K. Varma, Thermal behaviour of coir fibres, Thermochim. Acta 108 (1986) 199-210.

[24] R. Ibbett, D. Domvoglou, D.A.S. Phillips, The Hydrolysis and Recrystallisation of Lyocell and Comparative Cellulosic Fibres in Solutions of Mineral Acid, Cellulose 15 (2008) 241-254.

[25] Y. Liu, H. Hu, X-ray Diffraction Study of Bamboo Fibers Treated with NaOH, Fibers and Polymers 9 (2008) 735-739.

[26] J. Gassan, A.K. Bledzki, "Possibilities for improving the mechanical properties of jute/epoxy composites by alkali treatment of fibers", Compos. Sci. Technol. 59 (1999) 1303-1309.

[27] H. Gu, "Tensile behaviours of the coir fiber and related composites after NaOH treatment", Mater. Des. 30 (2009) 3931-3934.

[28] A.I.S. Brigida, V.M.A. Calado, L.R.B. Goncalves, M.A.Z. Coelho, "Effect of chemical treatments on properties of green coconut fiber", Carbohydr Polym. 79 (2010) 832-838.

[29] K.C.C. Carvalho, D.R. Mulinari, H.J.C. Voorwald, M.O.H. Cioffi, Chemical modification effect on the mechanical properties of hips / coconut fiber composites, Bioresources 5 (2010) 1143-1155.

[30] A. Choudhury, S. Kumar, B. Adhikari, Recycled milk pouch and virgin lowdensity Polyethylene/linear low-density polyethylene based coir fiber composites, J. Appl. Polym. Sci. 106 (2007) 775-785.

[31] M.M. Rahman, M.A. Khan, Surface treatment of coir (Cocos nucifera) fibers and its influence on the fibers' physico-mechanical properties, Compos. Sci. Technol. 67 (2007) 2369-2376.

[32] J.M. Kisler, G.W. Stevens, A.J. O'Connor, Adsorption of proteins on mesoporous molecular sieves, Mater. Phys. Mech. 4 (2001) 89.

[33] J.F. Dıaz, K.J. Balkus Jr, "Enzymes immobilized in MCM-41 molecular sieves", J. Mol. Catal. B: Enzym. 2 (1996) 115-126.

[34] V.O.S. Neto, A.G. Oliveira, R.N.P. Teixeira, M.A.A. Silva, P.T.C. Freire, D.D. Keukeleire, R.F. Nascimento, Use of Coconut Bagasse as alternative

adsorbent for separation of copper (II) ions from aqueous solutions: isotherms, kinetics and thermodynamic studies, BioResources 6 (2011) 3376-3395.

[35] C.J. Tien, B.H. Chiang, Immobilization of α-amylase on a zirconium dynamic membrane, Proc. Biochem. 35 (1999) 377-383.

[36] J. -P. Chen, Y. -M. Sun, D.-H. Chu, Immobilization of α-amylase to a composite temperature-sensitive membrane for starch hydrolysis, Biotechnol. Prog. 14 (1998) 473-478.

[37] A. Emine, T. Leman, Characterization of immobilized catalases and their application in pasteurization of milk with H_2O_2, Appl. Biochem. Biotechnol. 50 (1995) 291-303.

[38] U.-H. Renate, A. Ulrich, M. Johanna. The concept of the unfolding region for approaching the mechanism of enzyme stabilization, J. Mol. Catal. B: Enzym. 7 (1999) 125-131.

[39] A.S. Maria Chong, X.S. Zhao, Design of large-pore mesoporous materials for immobilization of penicillin G acylase biocatalyst, Catal. Today 93-95 (2004) 293-299.

[40] Y. Zhao, J. Qiu, H. Feng, M. Zhang, The interfacial modification of rice straw fiber reinforced poly (butylene succinate) composites: Effect of aminosilane with different alkoxy groups, J. Appl. Polym. Sci. 125 (2012) 3211-3220.

[41] D.J. Lartigue, Basic Enzymology. In: Immobilized Enzymes for Industrial Reactors,: R.A. Messing eds., Academic Press, New York (1975).

[42] S. Varavinit, N. Chaokasem, S. Shobsngob, Immobilization of a thermostable α-amylase, Science Asia 28 (2002) 247-251.

[43] M.Y. Arica, H. Yavuz, S. Patir, A. Denizli, Immobilization of glucoamylase onto spacer - arm attached magnetic poly (methyl methacrylate) microspheres :

characterization a11d application to a continuous flow reactor, J. Mol. Catal. B. Enzymatic 11 (2000) 127 -138.

[44] L. Cao, R.D. Schmid, Carrier-bound Immobilized Enzymes: Principles, Application and Design, Wiley-VCH Verlag GmbH & Co. Weinheim, (2005) 578.

[45] J. Zhou, Immobilization of alliinase and its application: Flow injection enzymatic analysis for alliin, Afr. J. Biotechnol. 8 (2009) 1337-1342.

[46] A. Parmar, H. Kumar, S. Marwaha, J.F. Kennedy, Advances in enzymatic transformation of penicillins to 6-aminopenicillanic acid (6- APA), Biotechnol. Adv. 18 (2000) 289-301.

[47] N. Jaiswal, O. Prakash, Immobilization of Soyabean α-amylase on Gelatin and its Application as a Detergent additive, Asian J. Biochem. 6 (2011) 337-346.

[48] G.J.V. Betancur, N. Pereira Jr, Sugar cane bagasse as feedstock for second generation ethanol production. Part II: Hemicellulose hydrolysate fermentability, Electron. J. Biotechn. 13 (2010).

[49] J.C. Santos, Í.R.G. Pinto, W. Carvalho, I.M. Mancilha, M.G.A. Felipe, S.S. Silva, Sugarcane Bagasse as Raw Material and Immobilization Support for Xylitol Production, Appl. Biochem. Biotechnol. 121-124 (2005) 673-684.

[50] C. G. Mothe, I. C. de Miranda, "Characterization of sugarcane and coconut fibers by thermal analysis and FTIR," J. Therm. Anal. Calorim. 97 (2009) 661-665.

[51] H. Sayilkan, S. Erdemoglu, S. Sener, F. Sayilkan, M. Akarsu, M. Erdemoglu, Surface modification of pyrophyllite with amino silane coupling agent for the removal of 4-nitrophenol from aqueous solutions, J. Colloid Interface Sci. 275 (2004) 530-538.

[52] J.G. Gwon, S.Y. Lee, S.J. Chun, G.H. Doh, J.H. Kim, Effect of chemical treatments of wood fibers on the physical strength of polypropylene based composites, Korean J. Chem. Eng. 27 (2010) 651-657.

[53] A. Guinier, X-Ray Diffraction in Crystals, Imperfect Crystals, and Amorphous Bodies, Dover Publications, New York, NY, USA, 1963.

[54] T. Williams, M. Hosur, M. Theodore, A. Netravali, V. Rangari, S. Jeelani, Time effects on morphology and bonding ability in mercerized natural Fibers for composite reinforcement, Int. J. Polym. Sci. 2011 (2011) 9.

[55] V. Vilay, M. Mariatti, T. Mat, M. Todo, "Effect of fiber surface treatment and fiber loading on the properties of bagasse fiber - reinforced unsaturated polyester composites," Comp. Sci. Tech. 68 (2008) 631-638.

[56] Z. Zhang, L. Moghaddam, I.M. O'Hara, W.O.S. Doherty, Congo Red adsorption by ball-milled sugarcane bagasse, Chem. Eng. J. 178 (2011) 122-128.

[57] H. Khademieslam, M. Kalagar, E.M. Moridani, R. Hosienpoor A. Tavakkoli, The Influence of Rice Straw Flour Silane Treatment on the Physical and Mechanical Properties Composite, World Appl. Sci. J. 27 (2013) 663-666.

[58] B. Arkles, Silanes and surfaces : Hydrophobicity, Hydrophilicity and Coupling Agents, Gelest, Inc.170.

[59] C.A. Rezende, M.A. de Lima, P. Maziero, E.R. deAzevedo, W. Garcia, I. Polikarpov, Chemical and morphological characterization of sugarcane bagasse submitted to a delignification process for enhanced enzymatic digestibility, Biotechnol. Biofuels. 4 (2011) 54.

[60] P. Kumar, D.M. Barrett, M.J. Delwiche, P. Stroeve, Methods for Pretreatment of Lignocellulosic Biomass for Efficient Hydrolysis and Biofuel Production, Ind. Eng. Chem. Res. Article ASAP 2009.

[61] Y. Zhao, J. Qiu, H. Feng, M. Zhang, The Interfacial Modification of Rice Straw Fiber Reinforced Poly (butylene succinate) Composites: Effect of Aminosilane with Different Alkoxy Groups, J. Appl. Polym. Sci. Wiley Periodicals, Inc. (2012) 2-10.

[62] K. Bilba, M.-A. Arsene, Silane treatment of bagasse fiber for reinforcement of cementitious composites, Compos. Part A 39 (2008) 1488-1495.

[63] K. Buchholz, V. Kasche, U.T. Bornscheuer, Biocatalysts and Enzyme Technology. Wiley-VCH, Weinheim 2005.

[64] H.M. El-Shora, M.M. Youssef, Identification of Catalytically Essential Amino Acid Residues and Immobilization of Glutamate Dehydrogenase from Rumex Cotyledons, Asian J. Biochem. 3 (2008) 320-329.

[65] K. Sangeetha, T.E. Abraham, Preparation and characterization of cross-linked enzyme aggregates (CLEA) of subtilisin for controlled release applications, Int. J. Biol. Macromol. 43 (2008) 314-319.

[66] C. Mateo, J.M. Palomo, G.-L. Fernandez, J.M. Guisan, R.-L. Fernandez, Improvement of enzyme activity, stability and selectivity via immobilization techniques, Enzyme Microb. Technol. 40 (2007) 1451-1463.

[67] H. Tumturk, S. Aksoy, N. Hasirci, Covalent immobilization of α - amylase onto poly (2 -hydroxyethyl methacrylate) and poly (styrene -2- hydroxyl ethyl methacrylate) microspheres and the effect of Ca^{2+} ions on the enzyme activity, Food Chem. 68 (2000) 259-266.

[68] J.M.S. Cabral, In: Thermostability of Enzymes, editor: M.N. Gupta, Berlin: Springer-Verlag, (1993) 162-181.

[69] T. Bahar, A. Tuncel, Immobilization of invertase onto crosslinked poly (*p*-chloromethylstyrene) beads, J. Appl. Polym. Sci. 83 (2002) 1268-1279.

[70] G.F. Drevon, Enzyme immobilization into polymers and coatings, BS, Chimie Physique Electronique Lyon, Submitted to the Graduate Faculty of School of Engineering in partial fulfillment of the requirements for the degree of Doctor of Philosophy 1997.

[71] D. Kumar, M. Muthukumar, N. Garg, Kinetics of fungal extracellular α-amylase from Fusarium solani immobilized in calcium alginate beads, J. Environ. Biol. 33 (2012) 1021-1025.

[72] N. Jaiswal, O. Prakash, Immobilization of Soyabean α-amylase on Gelatin and its Application as a Detergent additive, Asian J. Biochem. 6 (2011) 337-346

[73] P. Tripathi, A. Kumari, P. Ratha, A.M. Kayastha, Immobilization of α-amylase from mung beans (Vigna radiata) on Amberlite MB 150 and chitosan beads: A comparative study, J. Mol. Catal. B: Enzym. 49 (2007) 69-74.

****

Chapter 5

Summary and Conclusion

Contents

5.1 Introduction

Immobilized enzymes have proved as very useful tools in the areas where there is more demand for applications that have biological impact. The major objective being the economic reuse of enzymes, it is gaining more importance in various fields of chemical and pharmaceutical industries. The availability of different types of supports ranging from synthetic to natural ones, both inorganic and organic, makes immobilization an easy task and thus an excellent process choice. The vast literature available underlines the fact that the researchers are still putting in tremendous efforts to improve this technique and thus to extend its application in a wider area.

In this work we have pointed out the possibility of using chemically prepared polypyrrole and its variable forms as support for diastase α-amylase immobilization. Also, because of the emerging human concerns and environmental awareness there is an increasing trend towards use of natural polymers as support for immobilization. We have successfully immobilized Diastase α-amylase onto natural polymers from coconut fiber and sugarcane bagasse and their APTES functionalized forms

5.2 Summary

The thesis work is presented in six chapters. A chapter wise summary is given below.

Chapter 1. The chapter begins with a brief introduction to biocatalysis and its relevance in the emerging world scenario. This is followed by description of the enzyme, its structure, classification and application. A description of enzyme catalysis and factors affecting enzyme activity has also been included. Enzyme immobilization, its need, methods of immobilization, choice of support, properties and characteristics of immobilized enzyme, benefits and limitations of enzyme immobilization are also described. Relevance of synthetic polymer polypyrrole and natural polymers: coconut fiber and sugarcane bagasse, as supports for enzyme immobilization are discussed. Different pretreatment methods are briefly discussed. Then advantages and disadvantages of natural polymers are mentioned. Description of diastase α-amylase, the model enzyme of our study was also included. And finally the objectives of the study adopted are given in this chapter.

Chapter 2. This chapter provides the experimental procedures adopted for the preparation of immobilized enzymes. This is followed by enzyme activity studies, optimization of immobilization parameters for free and immobilized enzymes and physico-chemical techniques used to characterize the supports and immobilized enzymes.

Chapter 3. This chapter describes immobilization of diastase α-amylase on to different polypyrrole supports. Significance of polypyrrole as the support for enzyme immobilization was discussed in brief. Significance of Diastase α-amylase as model enzyme for the study is then mentioned in detail. The immobilization parameters were optimized so as to obtain stable biocatalysts that can retain maximum activity. The activity, pH & thermal stability, reusability and storage stability of free and immobilized enzymes were compared. Kinetic study was also

performed and compared with that of free enzyme. Kinetic parameters were evaluated using Line weaver - Burk plots and Hanes-Woolf plots.

Chapter 4. The immobilization of Diastase α-amylase on to natural polymers is presented in this chapter. The immobilization parameters like pH of the immobilization medium, time needed for immobilization, concentration studies are all optimized using activity as the main measured variable. Thermal stability, reusability and storage stability were also analyzed. Kinetic parameters were evaluated using Lineweaver - Burk plots and Hanes-Woolf plots.

Chapter 5. Summary of the work done along with major outcomes are briefly described in this chapter.

5.3 Conclusions

The major findings of the study are outlined below:

5.3.1 Synthetic polymers as support for enzyme immobilization.

Polypyrrole was successfully synthesized in different forms via chemical polymerization method.

The study reveals that chemically prepared Polypyrroles can behave as excellent supports for immobilization of enzymes which was proved by the model enzyme diastase α-amylase retaining appreciable activity after being immobilized on to these supports.

Both supports and immobilized enzymes were characterized using FT-IR spectroscopy and was found that all prepared polymers showed characteristic peaks of polypyrrole irrespective of the method of preparation but had shift in the peak either to higher or lower wave number based on the modification applied and due to difference in nature of dopants that have influenced the ring vibrations of polypyrrole. After immobilization peaks corresponding to the organic structure of

enzyme were also present which confirmed that immobilization had occurred on to these supports.

SEM images were taken to characterize the morphology of the polymers prepared. Depending on the method of preparation there were significant differences in the surface morphology of all samples. This difference was found to have a profound influence on enzyme loading as surface area get varied, which subsequently affect the activity of the resultant immobilized enzymes.

TG-DTG analysis showed that the polymers formed were stable up to 188°C and there was increase in thermal stability as synthesis procedure was varied with Polypyrrole composites having high thermal stability. After immobilization decomposition temperature gets lowered as enzyme could not withstand such high temperature.

EDS was used to characterize functionalization using APTES and was able to ensure the coupling of APTES by the increase in intensity of N and decrease in intensity of Cl (chloride ion) present on the surface.

Optimization of biochemical parameters showed that for free α-amylase the optimum pH for starch hydrolysis is in the range 5-5.5 and optimum temperature 50°C.

After immobilization both pH and temperature get shifted depending upon supports and methods used for modification of supports.

The pH was shifted due to change in dissociation equilibria of charged groups on the enzyme and the support as the pH of medium changes. This results in change in intra-molecular forces holding conformation at the active site thus bringing about alterations in the optimum pH.

The optimum temperature was either shifted or remained the same which solely depended on the activation energy needed for bringing about necessary

conformational changes at the active site of the immobilized enzyme so as to induce fit the substrate. This in turn depended on the nature of the support. The greater the rigidity of the immobilized enzyme greater will be its resistance to unfolding at higher temperatures than the soluble enzyme.

After immobilization thermal stability gets enhanced. It might be due to reduced conformational flexibility at the active site that was induced by the immobilization procedure.

All the free and immobilized enzyme systems followed Michaelis Menten kinetics. For free enzyme the K_m value was found to be 0.50 mg/ml and that of V_{max} is about 7.40 mg/ml/min.

After immobilization kinetic parameters get altered in such a way that K_m increased and V_{max} decreased which is the consequence of conformational effects and micro environmental effects that was imposed on immobilized enzyme.

The immobilized enzyme showed excellent stability for storage and reuse. When stored at 4°C in wet buffered media most of them retained more than 50% of their initial activity even after 4 months which was much better than free enzyme which lost its entire activity after 7 days of storage.

All the immobilized enzymes were recyclable for more than 10 cycles.

5.3.2 Natural polymers as support for enzyme immobilization

Pretreatment steps were carried out so as to clean the fiber surface and make the surface hydroxyl groups more exposed which thus made it amenable to surface modification with chemical reagents.

Coconut and Sugarcane bagasse fibers thus cleaned were modified via coupling reaction with APTES.

Treated, untreated and modified fibers were characterized by FT-IR spectroscopy. It was confirmed from the decrease in intensity or disappearance of peaks that pretreatment methods carried out were effective in removing the cementing materials like hemicelluloses, lignin, waxes and other water soluble substances. The additional peaks corresponding to that of siloxane bonds confirmed APTES coupling on to natural polymers.

SEM images showed clearly the morphological changes that occurred after pretreatment were carried out.

TG-DTG curves clearly depicted the degradation temperatures of hemicelluloses, celluloses, and lignin. After pretreatment thermal stability was found to get enhanced this underlined the fact that cementing materials get removed after the chemical treatments were carried out. After functionalization there was a slight decrease in the degradation temperature which might be due to the decomposition of silane group introduced during coupling procedure.

EDS spectra also showed presence of Si atom at the surface indicating the successful coupling of APTES with natural fibers.

XRD curves showed variation in the degree of crystallinity and 2θ values with respect to each chemical treatment carried out and immobilization procedure applied.

Diastase α-amylase was successfully immobilized on natural fibers that were chemically pretreated and also modified with APTES.

Immobilization parameters were optimized and immobilization yield, activity yield and immobilization efficiency were found out.

The immobilized enzymes showed a wider pH and temperature profile when compared to free enzyme. Increased stability of immobilized α-amylase over

a wider range of pH is an indication of stability attained after the immobilization procedure which thus provides ability to withstand changes in environmental pH.

Thermal and storage stabilities of all immobilized enzymes were found to improve after immobilization when compared to free enzyme.

All the immobilized forms were able to be reused successfully for more than 3 cycles retaining about 50% of its initial activity in the case of chemically treated ones and 80% activity for fibers modified with APTES. The silane coupling treatment enhanced the hydrophobicity of cellulose fibers and thereby enabled the APTES activated supports to exhibit high catalytic efficiency and reusability.

All these observation throws light to the fact that amino groups introduced to the support can act as an efficient base catalyst. Hence modified supports are promising materials for practical use in catalytic and other application.

****

Curriculum Vitae

Navya Antony

Address:	*Mundanchery house,*
	S.N. Junction
	Cheranellore P.O- 682034
Telephone number	*09961303567*
E-mail:	*navyalg@gmail.com*
Date of birth	*1st April 1983*
Sex:	*Female*
Religion	*Christian*
Caste	*Latin Catholic*
Marital status:	*Married*
Nationality:	*Indian*

Academic profile

- *B.Ed (Bachelor of Education) in Physical science (2005-2006), Mahatma Gandhi University, Kottayam, Kerala, India; (First class).*
- *M.Sc in Pure Chemistry (2003-2005), Mahatma Gandhi University, Kottayam, Kerala, India; (First class).*
- *B.Sc in Chemistry (Physics and Mathematics as subsidiary) (2000-2003), Mahatma Gandhi University, Kottayam, Kerala, India; (First class).*
- *Plus- Two (Physics, Chemistry, Mathematics, Biology) (1998-2000) Board of public examination, (First class).*
- *SSLC (Secondary School Leaving Certificate) (1998) Board of public examination, Kerala Government (First class).*

International / National conference papers

- *Immobilization of α-amylase on polypyrrole, Navya Antony, P.V. Mohanan, Presented at International Conference MatCon-2010, Cochin University of Science and Technology, Kerala, India [2010].*
- *Immobilization of diastase α-amylase on to polypyrrole polymer prepared by chemical oxidative polymerization, Navya Antony, P.V. Mohanan, Presented at International seminar held at M.G. University Kottayam [2010].*
- *Immobilization of α-amylase on nano zinc oxide, Navya Antony, Remya Nair, P.V. Mohanan., Presented at K.V. Thomas Endowment National seminar organized by Sacred Hearts College, Thevara [2010].*
- *Immobilization of diastase α-amylase on to polypyrrole polymer Navya Antony, P.V. Mohanan, S. Balachandran, U.G.C sponsored national seminar, M.G. college Thiruvananthapuram [2010].*
- *Immobilization of diastase α-amylase on to polypyrrole prepared in presence of colloidal silica as templates, Navya Antony, P.V. Mohanan, Presented at National conference CTriC 2011, Cochin University of Science and Technology, Kerala, India [2011].*
- *Immobilization of α-amylase on to polypyrrole prepared in presence of sodium dodecyl sulphate, Navya Antony, P.V Mohanan, Presented at National conference CTriC 2012, Cochin University of Science and Technology, Kerala, India [2012].*
- *Immobilization of α-amylase on to pyrrole - aniline copolymer, Navya Antony, P.V. Mohanan, Presented at National conference CTriC 2013, Cochin University of Science and Technology, Kerala, India [2013].*

International / National workshop & Symposium

- *National Symposium in chemistry organized by the department of chemistry, St Paul's College Kalamassery in collaboration with M.G. University Kottayam, 2008*
- *The application of X-Ray Fluorescence Spectroscopy in analytical science and Technology, Organized by Indian Society of Analytical scientists [2009].*
- *Analytical Science for Advanced Materials Processing and Environmental Impact Assessment, International Analytical Science congress [2010].*
- *Participated in 1st Kerala Women's Science Congress -2010 held at St Teresa's college, Ernakulam [2010].*

Journal Papers

1. *A. Navya, P.V. Mohanan, Synthesis of polypyrrole nanoparticles in surfactant gel, Research Lines, ISSN 0975-8941, 3 (2010) 84-89.*
2. *A. Navya, S. Balachandran, P.V. Mohanan, Effect of Surfactants on catalytic activity of diastase α- amylase, J. Surfact. Deterg. (2013) 1-3.*